THE DESIGN OF A CATALYTIC OXIDATIVE DIMERIZATION-CYCLIZATION SYSTEM

by

LEONARD ALLAN DOERR, B.E.Sc.

A thesis submitted for

the Degree of Doctor of Philosophy

in the Faculty of Engineering of

The University of London

ABSTRACT

This thesis describes the discovery and the development of a catalyst for the oxidative dimerization and cyclization of propylene to benzene. The combination of dimerization and cyclization in an oxidative system is completely novel. During the course of the studies, catalysts which are active for oxidative dimerization (thallic oxide), for oxidative cyclization (bismuth molybdate) and for oxidative dimerization-cyclization (indium oxide) have been examined. The kinetics and mechanism of the latter system have been studied in some detail.

Methods of catalyst design are outlined in the introduction, and chemical and chemical engineering aspects of the problem are correlated within an overall framework. The importance of the reaction kinetics and their dependence on heat and mass transfer effects was considered in terms of possible chemical mechanisms. The catalyst design methods were applied to the reaction systems (a) oxidative dimerization and (b) oxidative cyclization and used to identify possible catalysts.

Methods of testing the catalytic activity of these solids and the results obtained are described in the experimental and results sections. Successful catalyst design is a progressive process, and potential catalysts identifed in the introduction form only a basis of the testing programme.

The preliminary testing programme is discussed in the final section. An analysis is presented of the failure of some predicted catalysts, and possible catalysts for the dimerization and cyclization reactions are identified. The initial development studies were completed with the thallic oxide catalyst suitable for dimerization. Although a suitable reaction mechanism and some reaction kinetics were obtained, the system deactivated very rapidly, due to the thermal instability of the thallous oxide. In an attempt to identify an alternative catalyst, indium oxide was found to be an efficient oxidative dimerization/cyclization catalyst, and the development of the cyclization catalyst (bismuth molybdate) was not extended.

The effect of reaction parameters on the yields of acrolein, hexadiene, benzene and carbon dioxide obtained over the indium oxide catalyst were examined in some detail. A reaction mechanism has been suggested that explains most of the observed results and the kinetics of the reaction - both initially and at longer contact times - have been found to be consistent with the mechanism. Application of the Langmuir-Hinshelwood theories show that inhibition by products plays as important role in the process.

It has been found possible to present a mathematical model of the process, based on the proposed reaction mechanism and kinetics. The usefulness of this in extending the mechanistic studies and in further design of the catalyst is discussed.

ACKNOWLEDGMENTS

I wish to express my sincere gratitude to Dr. D.L. Trimm for his guidance and encouragement during the course of this research.

I am also indebted to other members of the department for their valuable assistance, especially my colleagues in the Catalyst Research Laboratory who provided an interesting and friendly atmosphere.

My thanks are also due to the Athlone Fellowship and to Shell Canada Limited who generously donated financial support.

I wish to extend special recognition to my wife, Donna, for her excellent typing and for her continuous encouragement during the course of my work.

LEONARD ALLAN DOERR,
Department of Chemical Engineering
and Chemical Technology,
Imperial College,
London, S.W. 7.

CONTENTS

SECTION I.

INTRODUCTION

1. Introduction

The production of chemical feedstocks from crude oil has become increasingly important in recent years (1). Petrochemicals now account for 36% of the chemical output of the United States and 65% of the total chemical sales dollars, and the demand is predicted to quadruple in the next 10 to 15 years. Within the industry, the production of useful compounds by oxidation is perhaps most desirable since oxygen is freely available. Oxidation reactions are, however, notoriously difficult to control and attention has been centred largely on reactions carried out over solid catalysts. The demand for partial oxidation products such as ethylene oxide, maleic anhydride and acrolein has involved the development of selective oxidation catalysts that can promote a desired reaction in as high a yield as possible.

More recently, considerable effort has been devoted to the study and the application of oxidative dehydrogenation processes. These reactions involve the removal of hydrogen by oxygen without any addition of oxygen to the fuel molecule. As compared to conventional dehydrogenation, the thermodynamics and the equilibrium constants of the reactions are much more favourable if hydrogen is removed as water. Thus, the oxidative dehydrogenation of butene to butadiene over bismuth molybdate (2) has largely replaced conventional catalytic dehydrogenation (3) over nickel-calcium-phosphate as the conventional route to

butadiene.

It has been the intention of this research to recognise and develop a novel system based on an oxidative dehydrogenation reaction combined with a dimerization-cyclization process, namely the production of hexadienes and benzene from propylene. At the present time, the price ratio of benzene to propylene would be of the order of 1.5:1 (56). In addition, as a result of the problems of disposal of lead additives for gasoline it would appear highly desirable to develop a process that would convert a product usually available in excess into a fuel of high octane number (benzene, octane no. 99) (4). Complete development of a catalyst system, as described below, is a complex and long term problem, and attention has been focused only on the initial, more academic aspects of the investigation.

It is possible to justify two distinct but related aspects of catalyst development. From a chemical view point it is necessary to identify a catalyst that will promote the desired reaction in as high an activity and selectivity as possible. Traditionally, these aspects of catalyst selection have been considered empirically and to a large extent this is still true. The difficulty arises in that basic information on new catalysts, with which it would be possible to make an empirical choice, is usually not available. However, with recently developed knowledge of the theories of heterogeneous catalysis and chemisorption,

it is becoming possible in some cases to use the principles of catalyst selection to determine a group of potential catalysts, one of which might prove experimentally to be both active and selective for the desired reaction. In these arguments, which are reviewed in some detail below, results obtained for other catalytic oxidations (both homogeneous and heterogeneous) aid in the understanding and the prediction of the chemistry and mechanism of the desired reaction.

The position with respect to the structure and the physical properties of the catalysts is much less empirical. The factors which influence catalyst properties such as porosity or thermal conductivity have been established theoretically, and are reviewed at a later stage. However, once it has been possible to identify optimal physical parameters it is still necessary to prepare the catalysts. Within a given frame work (see below) such preparations often remain the last citadel of alchemy in modern science!

Once a catalyst has been identified, a detailed investigation of the kinetics and mechanism of the reaction over the solid is necessary for the optimization of the process, which in turn leads to further development of the catalysts. In many cases, it is rewarding to express the results in terms of a mathematical model, in that considerable saving in time and expenditure can be achieved over experimental studies by simulating the effect

of given changes with the aid of a computer. In this respect it is possible to use two types of models. In a purely chemical model the system is considered in the total absence of heat or mass transfer effects. This type of approach is particularly valuable in connection with scale-up of reactors, where at the present time no satisfactory method exists of predicting the actual influence of heat and mass transfer effects in large reactors. For a given reactor it is possible, however, to use a complete model which describes the reaction as it actually occurs in situ. Such a model is obviously complex and is generally not developed except under special conditions where a given reactor is expected to be on stream for some considerable time.

2. The design of heterogeneous catalysts

Largely in the context of the desired oxidation of propylene to benzene it is rewarding to consider the genesis of a catalytic process. The development of a catalytic process to the point where industrial operation is feasible is a complex and long term problem, involving several inter-related stages which are complex in themselves. Generally the development can be considered as involving three sections: the exploratory stage (Table 1) in which a suitable catalysts is designed, the semi-technical stage (Table 2) involving kinetic testing of the catalyst and

TABLE 1

The genesis of a catalytic process

The exploratory stage

1. The idea
2. The description of the idea
3. Compile the relevant information
4. Design suitable catalysts
5. Specify methods of preparation
6. Make the catalysts
7. Test the catalysts
8. Select Mark I

TABLE 2

The genesis of a catalytic process

Large scale laboratory & semi-technical stage

9. Make Mark I. Feed back information to 3-7

10. Retest Mark I exhaustively

11. Determine kinetics on Mark I

12. Specify the composition and preparation of the catalyst

13. Design semi-technical plant to make and test the catalyst

14. Design full scale plant to make and use catalyst

Feed back and communicate

design of both the pilot and full scale plants, and full scale construction and start-up of the catalytic process (Table 3). Successful development requires the interaction of knowledge gained in the previous stages before moving on with the design. Academically, of course, it is possible only to confine attention to the first and part of the second stage. The problems involved in scale-up of reactors, although of great interest, fall outside the immediate scope.

2A. The chemical basis for catalyst design

Perhaps the most successful design methods have been developed by a combination of an empirical approach with the application of information from a wide variety of scientific disciplines. The technique, which has been described by Dowden (5), can be summarised in terms of the virtual mechanism shown in Table 4.

A list of equations (the stoichiometric statement) containing all the possible reactions between molecules is compiled, and by utilizing the experience of systematic chemistry the number of equations is reduced to manageable proportions. These reactions are expressed in terms of the target reaction and various types of competing undesirable reactions.

The plausibility of these reactions is tested by application of thermodynamic data (exact, approximate or

TABLE 3

The genesis of a catalytic process

Full scale

15. Build plant to make the catalyst

16. Test the plant product exhaustively

17. Bring the catalytic process on line

18. Examine good, spoilt and spent catalysts inside and outside the reactor

19. Improve the catalyst with feedback to 7

Feed back and communicate

TABLE 4

The virtual mechanism

1. The stoichiometric statement
   a) The target reaction
   b) The characteristic chemistry

2. The thermodynamic theme

3. The mechanistic model
   a) The basic reactions

4. The chemisorbed complexes

5. The kinetic considerations
   a) Slow and fast steps
   b) The rate controlling step

guessed) over various ranges of temperature, pressure and concentrations; the undesirable reactions are then examined by the same methods but only over those ranges where the target reaction is feasible. Any reactions that can make major contributions to the process can now be given a mechanism, in the form of a series of simple molecular reactions (dehydrogenation, decarbonylation, etc.) arranged in a logical succession.

At this stage it is possible to recognise provisionally those solid components that could accelerate the target reaction and inhibit any undesired reactions, and to translate the mechanistic model in terms of possible reactions that could occur on the surface. Although this transposition requires the use of empirical data, the theories of adsorption and catalysis can now be usefully employed. The nature of possible chemisorbed complexes can be established and the electronic configuration of the oxide catalyst for each step of the mechanism can be derived using either empirical knowledge or rough ligand field theory. A few closely related electronic configurations will be possible for each overall mechanism.

The most appropriate electronic configuration for the probable rate controlling step can now be selected and shown to be compatible with the requirements of all other surface complexes. An oxide system that is capable of sustaining the appropriate properties (valency states,

acidities, etc.) is chosen and the necessary valency states are induced by various devices (altervalent additives, adjustment of acidity and basicity, compound formation).

The physical form of the solid must also be considered. Thus, for example, the amount of heat that can be generated during the reaction is of prime importance in determining the type of catalyst bed and the size and shape of the catalyst pellet. Again, the nature of the target reaction and the kinetics of the reaction can influence the desired porosity of the catalyst. If, as is often the case, a product intermediate to a consecutive reaction is desired, over-reaction would be favoured if the catalyst is highly porous. On the other hand, high activity demands the use of a high surface area (and hence high porosity) catalysts. Obviously the optimum porosity will depend upon the individual system.

These latter effects have been largely handled by chemical engineers, and the principles governing selection are outlined in section B. In order to start the process, however, it is necessary to establish the nature of the chemical components. The basic science used in the "chemical" design is outlined below. Necessary "empirical" data, obtained from observations previously reported in the literature, is reviewed in section 3.

(i) Adsorption

Since it is not possible to change the thermodynamics of a reaction, a catalyst can only alter the rate at which the process attains equilibrium. The particular type of reaction promoted depends upon the nature of adsorbed species possible on the surface of a given solid, as can be illustrated by a comparison of the energetics of a reaction occurring both in the homogeneous and the heterogeneous phase. The barriers to chemical reaction, with and without a catalyst, are shown in Figure 1. Since the rate of the gas phase reaction might be expressed as

$$-\frac{d(R)}{dt} = k(\text{Reactants})^{x} \qquad \ldots.1$$

where $k=A\exp(-\Delta E_{hom}/RT)$, the reaction velocity at a given temperature will be increased by reducing ΔE_{hom} or by increasing A. In the presence of a catalyst one or more of the reactants is chemisorbed, and the system may follow a new reaction path with a lower energy of activation (ΔE_{het}). For example, in the reaction

$$C_2H_4 + H_2 \rightleftarrows C_2H_6 \qquad \ldots.2$$

ethane is produced in the absence of a catalyst in equilibrium amounts after 30 minutes at 600°C. In contrast, in the presence of a platinum catalyst, equilibrium can be attained in 30 minutes at ambient temperature (6).

As can be seen from Figure 1, the value of ΔE_{het}

FIGURE 1

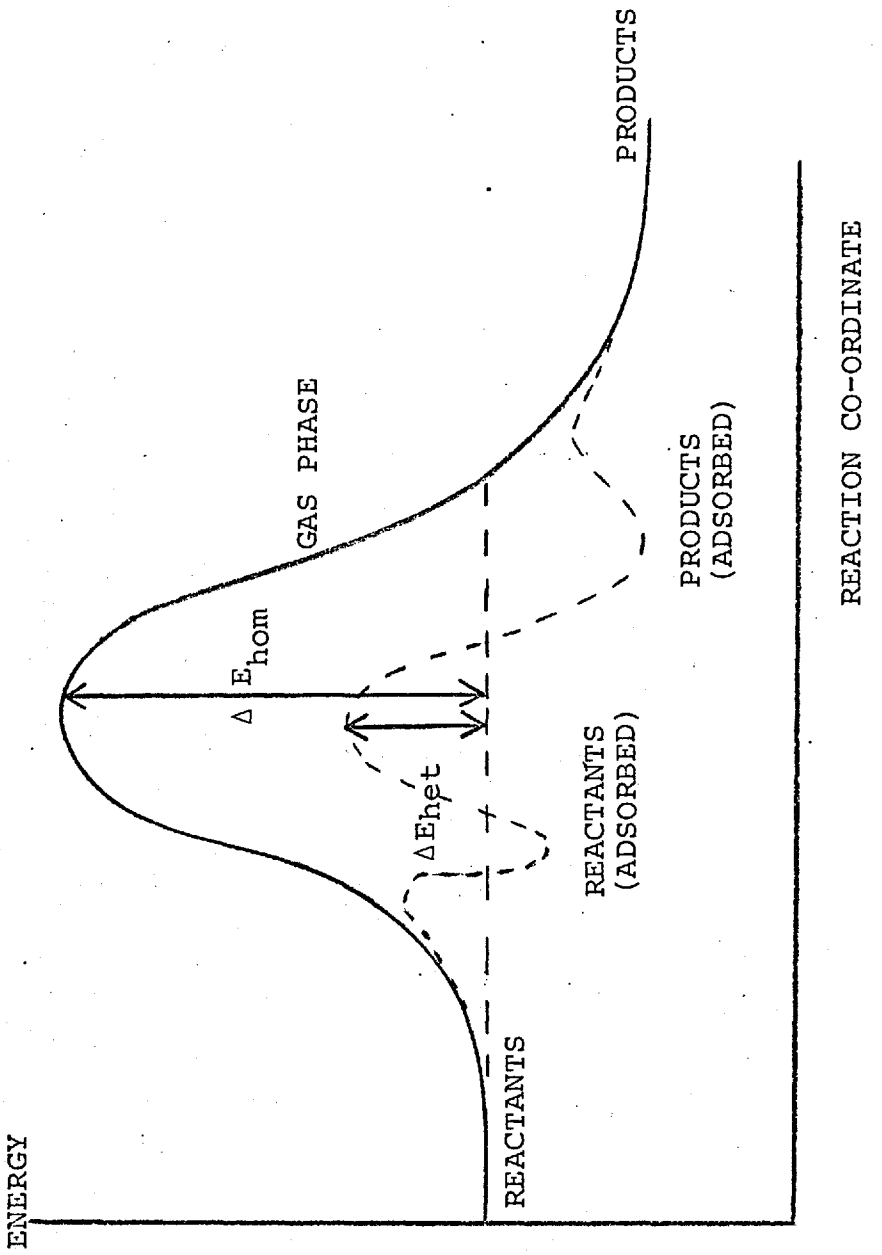

Comparison of potential energy curves for a homogeneous or heterogeneous reaction path.

is obviously very dependent upon the energy associated with the adsorbed reactants, which in turn depends upon the nature of adsorption at the surface. Both the strength and the extent of adsorption varies widely from system to system, but a general division between physical adsorption and chemisorption is recognisable: physical adsorption is caused by the forces of molecular interaction (often designated as van der Waals adsorption) while chemisorption involves the formation of chemical bonds between the interacting gas and solid. It is usually possible to distinguish the two types of adsorption by the application of four experimental criteria. The magnitude of the heat of adsorption is usually indicative since the heat liberated during physical adsorption is generally in the region of 2-6 kcal/mole as compared to values rarely less than 20 kcal/mole for chemisorption. Second and third criteria involve the rate and the temperature at which the process occurs. Since physical adsorption simulates liquefaction, it should require no activation and should proceed very rapidly but only at temperatures close to the boiling point of the adsorbate at the operative pressure. Chemisorption, like most chemical processes, requires activation but can occur at much higher temperatures. As a result, the temperature range over which adsorption is important often indicates the type of adsorption. The specificity of gas-solid interaction also helps to distinguish adsorption types.

Physical adsorption, being similar to liquefaction, is non-specific while chemisorption is a chemical reaction and is specific. As a result, however, adsorption can never exceed more than one or two layers whereas physical adsorption usually extends to multilayers.

The inter-relationships that can exist between physical adsorption and various forms of chemisorption are perhaps best brought out by means of a Lennard-Jones plot of energy in the systems (7). Such plots can be evaluated with considerable precision from a knowledge of some basic parameters such as the activation energy of either adsorption or desorption. As chemisorption involves the formation and rupture of chemical bonds, it will require an activation energy as is depicted for the example of chemisorption of hydrogen on copper depicted in Figure 2. Sufficient energy must be supplied to "atomize" molecular hydrogen before adsorption of atomic hydrogen can occur, and the system will follow curve A (Figure 2) as the atom approaches the surface. The necessary energy of atomization is shown as E_α and this energy will be the activation energy of adsorption. The curve is characterised by a deep and narrow minimum quite close to the surface, in such a position that the metal-hydrogen centres are separated by the appropriate bond length.

The energetics of physical adsorption (curve P) are very different, in that the curve has a broad and shallow minimum at distance D_p from the surface. This distance is approximately the sum of the covalent radii of the copper and

FIGURE 2

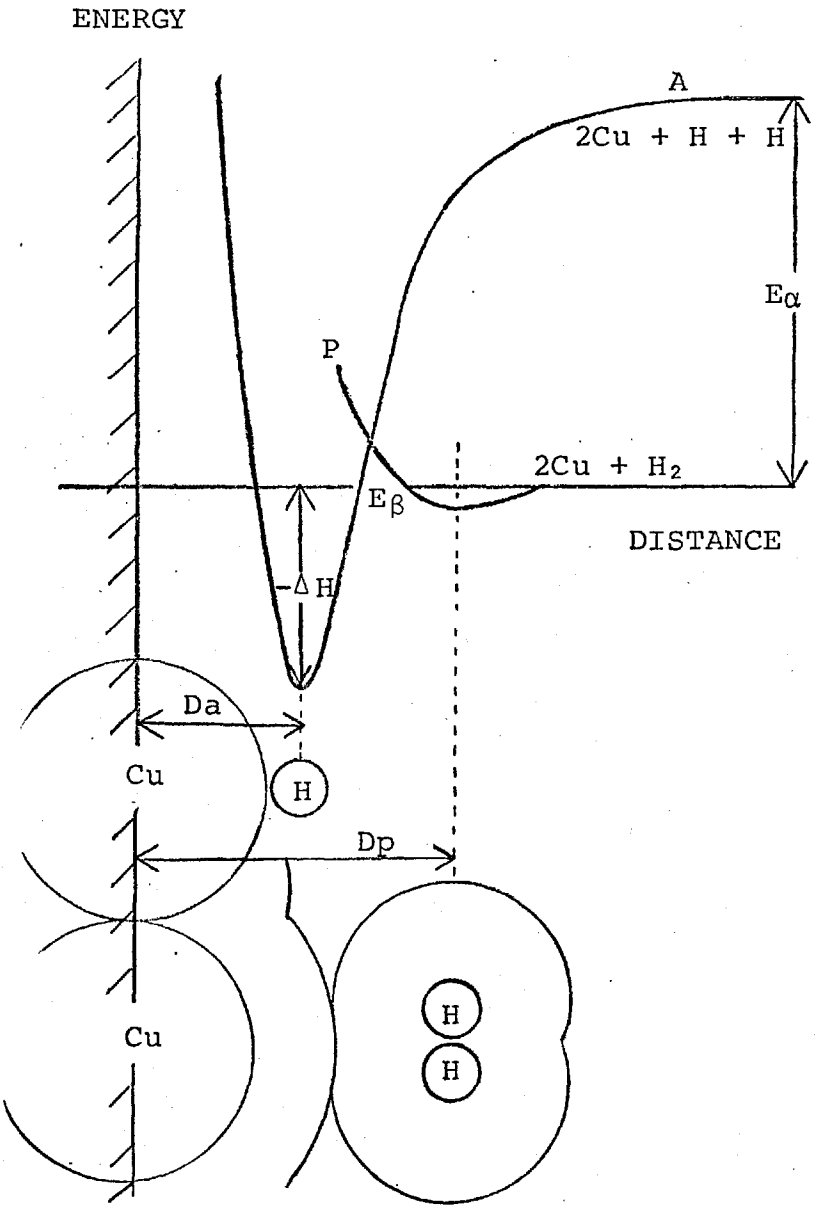

Potential energy curves for the adsorption of hydrogen on copper (8) and a diagrammatical representation of the adsorbed states.

hydrogen molecules plus the additional thicknesses of the two van der Waals envelopes. As a result of this type of adsorption hydrogen can be dissociatively adsorbed by copper without the prior dissociation of the molecule in the gas phase, as can be seen from Figure 2. If the hydrogen molecule is physically adsorbed, the molecule only requires sufficient energy to reach the intersection of curve P and curve A before it can transfer to curve A and become chemisorbed in the dissociated state. Thus the phenomenon of physical adsorption has reduced the energy of activation for chemisorption from the high value, E_α, to the much lower value, E_β.

It is interesting to note that provided that the transfer from physical to chemical adsorption is fast, physically adsorbed species may be important intermediates even if present in only small amounts. However, intermediate chemisorbed species may be more important in the adsorption process at high temperatures. Thus, for example, the associately bonded form of adsorbed oxygen is an intermediate in the formation of dissociatively adsorbed atoms (9)

$$M\text{-}M + O_2 \rightarrow \overset{O\text{-}O}{M\text{-}M} \rightarrow \overset{O\ O}{M\ M} \qquad \ldots.3$$

and similar species exist for hydrogen, although there is no general agreement as to whether the physical state of the intermediate adsorbed state is molecular (10) or atomic (11) (12). The importance of this type of adsorption is seen in Figure 3 where curve C represents the intermediate adsorbate.

FIGURE 3

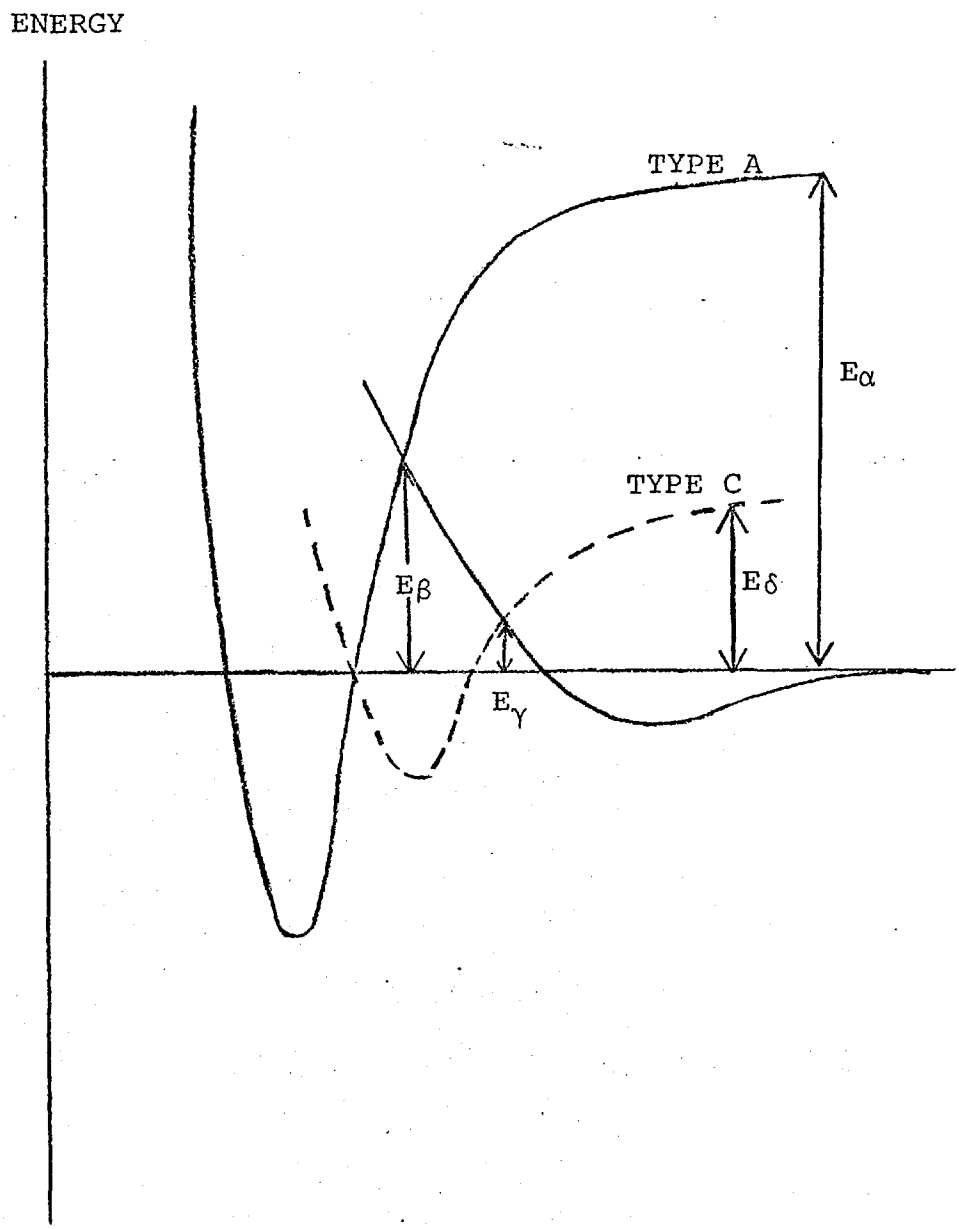

Type c potential energy curve after Dowden (12).

In the presence of physical adsorption curve C crosses curve P well below the crossover from P to A. As a result, the energy of activation decreases from E_β to E_γ. In the absence of physical adsorption the energy of activation is again reduced, from E_α to E_δ. At higher temperatures, where physical adsorption is unlikely, sufficient energy to provide E_δ could well be supplied thermally.

The direct relationship between adsorption and catalysis has been recognized for many years. The importance of such factors as strength of adsorption in determining the nature and importance of a catalytic reaction is easily seen, for example, by reference to the decomposition of formic acid. In the extreme cases, formic acid molecules may be very strongly adsorbed, when they will be unreactive and may constitute a catalyst poison, or may be adsorbed so weakly that there is a very low concentration on the surface and the rate of decomposition will again be low. Thus it would be expected that the rate of decomposition should pass through a maximum when expressed as a function of the strength of adsorption, as has indeed been found to be the case experimentally (Figure 4). Metals such as gold are poor catalysts as very little formic acid is adsorbed while the amount and strength of adsorption on, for example, tungsten is so high as to poison the metal as a catalyst. Metals with intermediate adsorption strengths such as Ru, Pt and Ir are found to be good catalysts.

FIGURE 4

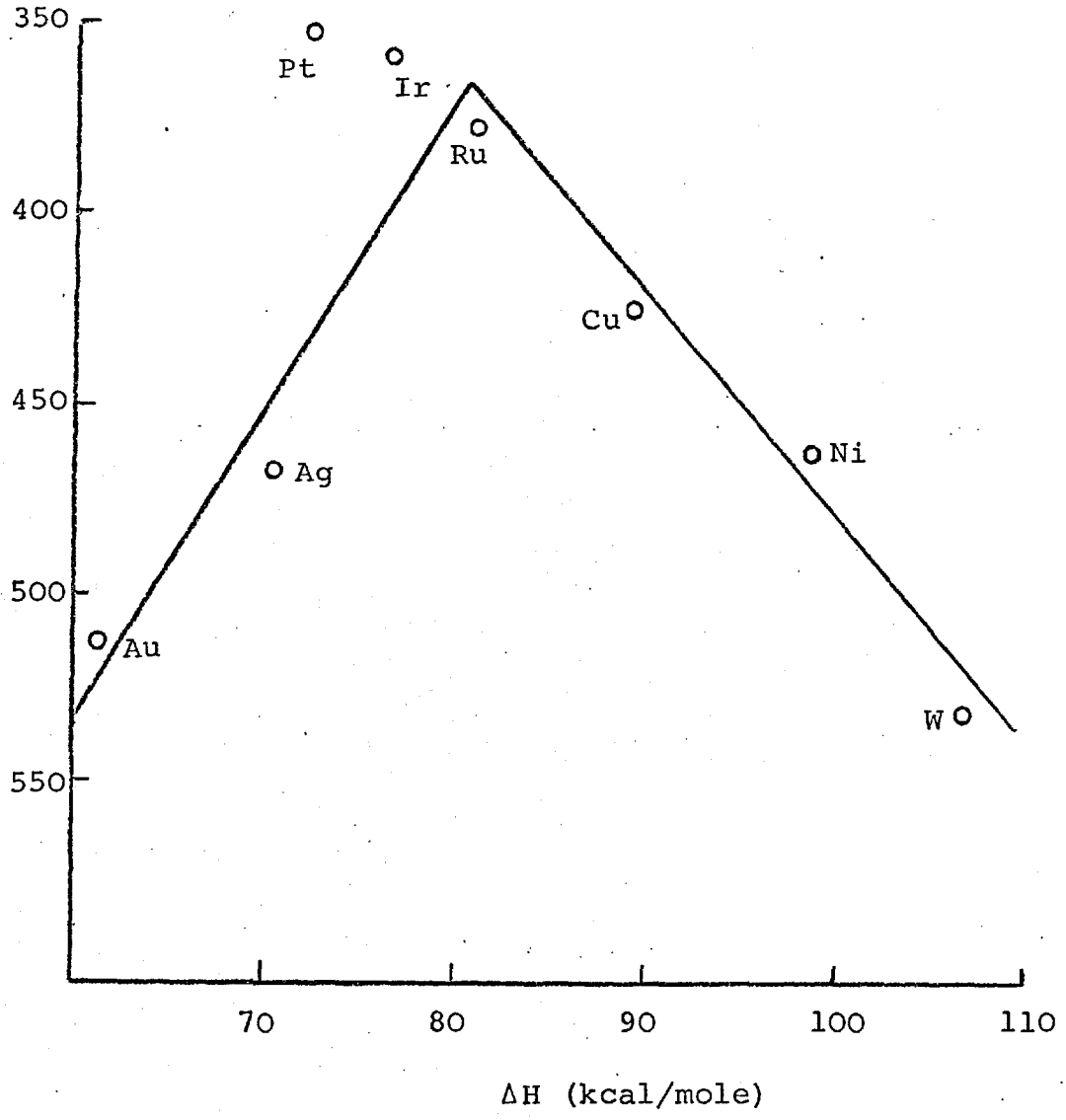

Activity of various metals for the decomposition of formic acid as a function of the heat of adsorption (13).

Although observations such as these confirm the important inter-relationships between adsorption and catalysis, they provide no information as to whether different forms of adsorption may be produced at the surfaces, as to how these alternative forms affect catalysis and as to what processes may be involved in adsorption and reaction. In order to understand more of these effects it is necessary to discuss briefly some more theoretical aspects of catalysis.

(ii) Theories of oxidative catalysis

a) Electronic theories

Catalysts for oxidation reactions have been found to be limited mainly to metal salts, and in particular oxides, together with a few metals. Metallic catalysts are limited in that most metals form and act as oxides when in an atmosphere of oxygen.

One of the earliest theories of catalytic oxidation that explained at least some of the experimental observations, was developed mainly to account for the semiconductivity of many transition metal oxide catalysts. As opposed to the oxides of metals that occur before the transition periods in the periodic table, which are stoichiometric except under extreme cases and are not good oxidation catalysts, transition metal oxides were found either to lose or to gain oxygen when heated in air. The oxides

were found to possess an associated small electrical conductivity, which was either positive or negative with respect to the parent stiochiometric oxide, and were often good oxidation catalysts.

It was found possible to relate the semiconductivity and the oxidative catalysis in terms of the concept that chemisorption or catalysis required the re-distribution of electrons between the solid and the adsorbate. In this case the arrangement of electrons in the adsorbent will be crucial in deciding such properties as the ease and strength of chemisorption. The nature of the bonding can be more clearly seen from a brief review of alternative theories of the solid state, namely the band theory, the boundary-layer theory and the valence bond theory. Their basic ideas are not dissimilar and only their emphasis and terminology differ.

The valence bond theory, due to Pauling (14) describes the properties of metals in terms of covalent bonds between adjacent atoms. The original theory was not concerned with oxidation catalysts to any extent and the application of the simpler Pauling ideas in this area have been incorporated in the crystal field approach (see later). Details of the valence bond theory, particularly in its application to metals, is discussed in detail by Bond (15) and Thomas and Thomas (16).

The band theory is based on the suggestion that although electrons of isolated atoms have sharp, discrete energy values, normally separated from one another by appreciable intervals, the levels broaden when the atoms

form a crystal to give a band of permitted energies. For example, the isolated iron atom, with an electronic configuration of $3d^6\ 4s^2$, changes in the metallic state to a band structure of, on average, $3d^{7.8}\ 4s^{0.2}$. The application of the band theory to metallic catalysts has been described in detail (16), (17), (18); in metal oxides wave functions of neighbouring metal ions do not overlap and the only important concern is the oxygen ion bands. Due to the 2s and 2p states of an isolated O^{2-} ion being full, the sp band in the oxide should be full and separated by some distance from the empty sp band formed from the 3s and 3p state. This is indeed the case for stoichiometric oxides: thermal promotion acorss the large energy gap is difficult below 500°C (19) and virtually no conductivity is observed.

Semiconducting oxides, on the other hand, can either gain or lose oxygen on heating. For an n-type semiconductor such as ZnO, the loss of oxygen on heating may be represented as

$$2Zn^{2+} + 2O^{2-} \rightarrow (2Zn^{2+} + O_{2\uparrow} + 4e) \rightarrow 2Zn + O_2. \quad ....4$$

Electrons, coming originally from an oxide ion are located by the zinc atom but are available in terms of the semiconductivity of the zinc oxide. Conductivity arises when the zinc atoms transfer electrons from their donor levels to the conduction band. As is shown in part (a) of Figure 5 the energy gap between the donor levels (Zn atoms) and the conduction band is small compared to the gap between the full band and the conduction band, and conductivity occurs

FIGURE 5

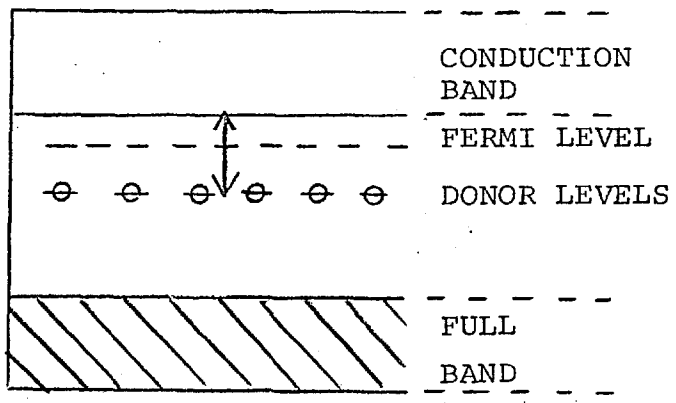

(a)

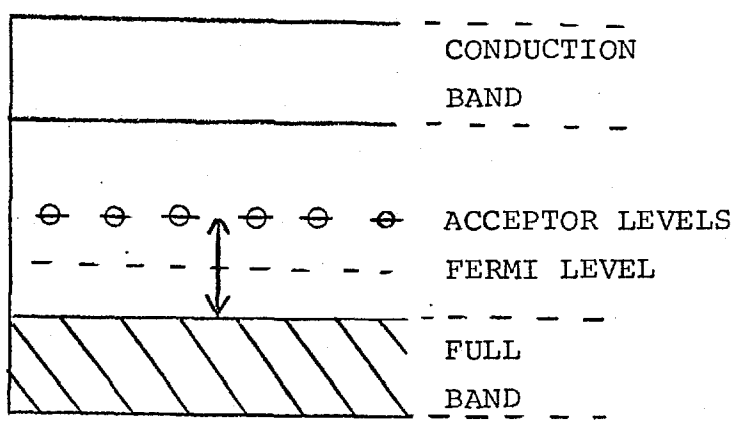

(b)

Arrangement of electrons in (a) a metal-excess (n-type) semi-conductor (b) an oxygen-excess (p-type) semi-conductor.

at moderate temperature. Other methods of treating zinc oxide may also give the same effect: oxide ions may also be removed by reducing gases such as hydrogen and carbon monoxide or the conductivity of zinc oxide may also be increased by direct exposure to zinc vapour, with no loss of oxide ion.

For p-type semiconductors, the gain of oxygen may be represented as

$$4Ni^{2+} + O_2 \rightarrow 4Ni^{3+} + 2O^{2-} \quad \ldots.5$$

and four Ni^{3+} ions, each having an excess of positive charge, result from each oxygen adsorbed. In this case electrical conductivity results from the movement of positive holes, which is equivalent to the migration of electrons in the opposite direction. The arrangement of electrons in an oxygen-excess (p-type) semiconductor is shown in Figure 5 part (b). The rather unstable Ni^{3+} act as acceptors of electrons abstracted from the full band, partly emptying it and therefore giving conditions for conductivity. Again it is possible to change the concentration of positive holes in p-type oxides, either as above or by introducing small amounts of an oxide whose cation is of different valency (doping). If Li^{1+} ions replace Ni^{2+} ions in the lattice there will be an excess of oxide ions, and one Ni^{3+} will be formed for each Li^{1+} present, thereby increasing the concentration of acceptors. Alternatively, if Cr^{3+} ions replace Ni^{2+} ions, there will be a deficiency of oxide ions and additional oxygen will be taken up

without the formation of Ni^{3+} (acceptors).

The correlation between semiconductivity and catalytic behavior can be well illustrated by reference to the oxidation of carbon monoxide:

$$2CO + O_2 \rightarrow 2CO_2 \quad \ldots.6$$

The p-type oxides are the most active and on these oxides the mechanism is probably

$$\tfrac{1}{2}O_2 + e \rightarrow O^- \text{ (ads)} \quad \ldots.7$$

$$O^- \text{ (ads)} + CO \rightarrow CO_2 + e \quad \ldots.8$$

where the first step is the chemisorption of oxygen. The carbon monoxide reacts with the adsorbed oxygen ion to produce CO_2 and to regenerate an electron.

Since direct chemisorption of oxygen is impossible on n-type oxides, it is first necessary to reduce the surface with carbon monoxide:

$$CO + 2O^{2-} \rightarrow CO_3^{2-} + 2e \quad \ldots.9$$

One of the lattice oxide ions is then replaced by interaction of $\tfrac{1}{2}O_2$ with the two electrons thus released.

$$\tfrac{1}{2}O_2 + 2e \rightarrow O^{2-} \quad \ldots.10$$

An oxide ion is regenerated by the reaction which produces the desorbed product:-

$$CO_3^{2-} \rightarrow CO_2 + O^{2-} \quad \ldots.11$$

In this way, the n-type oxides are also active at a low temperature for the oxidation of carbon monoxide.

Whereas the band theory considers electron distribution throughout the whole solid, the boundary-layer theory considers primarily the effect of electron

transfer at the surface or boundary-layer of the catalyst. Thus, for example, when oxygen adsorbs as O^{2-} on zinc oxide, the lectrons for negative ion formation must come from the partly full conduction band. As only a few electrons are available in this band, levels deep in the crystal will have to be employed if appreciable adsorption is to occur. However, the abstraction of electrons from deep levels sets up a potential barrier as it proceeds and this, together with the decrease in conductivity caused by removal of conduction electrons, results in the adsorption of only a small fraction of the monolayer (20) (21) (depletive chemisorption).

On the other hand adsorption of oxygen is not limited on p-type oxides such as nickel oxide or cuprous oxide. The almost full band is capable to providing electrons from levels very near the surface, and conductivity increases as adsorption proceeds due to extra positive holes provided by chemisorption (22) (cumulative chemisorption). Of course, the situation is reversed for an adsorbate which involves formation of positive ions, for example, the adsorption of hydrogen as OH^{-}. In this case, adsorption on n-type oxides is cumulative and on p-type oxides is depletive (23).

Wolkenstein (24) has suggested that in weak, low temperature chemisorption the defects in the oxide do not contribute to the surface bond and the adsorbed radical plus its adsorption centre remains electrically neutral. For the

chemisorption of a particle C on the surface of an oxide, MO, (Figure 6) six types of chemisorption were distinguished. Types (a) and (d) represent weak adsorption and which form is observed depends on the nature of the lattice and the particle C. Type (b), (c), (e) and (f) are strong adsorptions involving interaction with the defects and are within the confines of the electronic theory. Acceptor bonds, types (b) and (c), involve transfer of electrons to the adsorbate while types (e) and (f) (donor bonds) involve transfer of electrons to the solid. In reality, intermediate cases between the purely homopolar types (b) and (e), and the purely ionic, types (c) and (f) are more important.

Although the electronic theory does explain some aspects of catalysis, it is easily shown that there are many situations which cannot be explained only in these terms. Thus, for example, the adsorption of hydrogen on zinc oxide, which is responsible for hydrogen-deuterium exchange at low temperature does not change the conductivity of the solid (25) and thus cannot be considered in terms of the redistribution of electrons. Again, it is well known that certain faces of a given crystal are active catalysts, while other faces are inactive (26). Obviously some further refinement of the theory was necessary and the next advance came from consideration of the geometry of the surface of the catalyst.

FIGURE 6

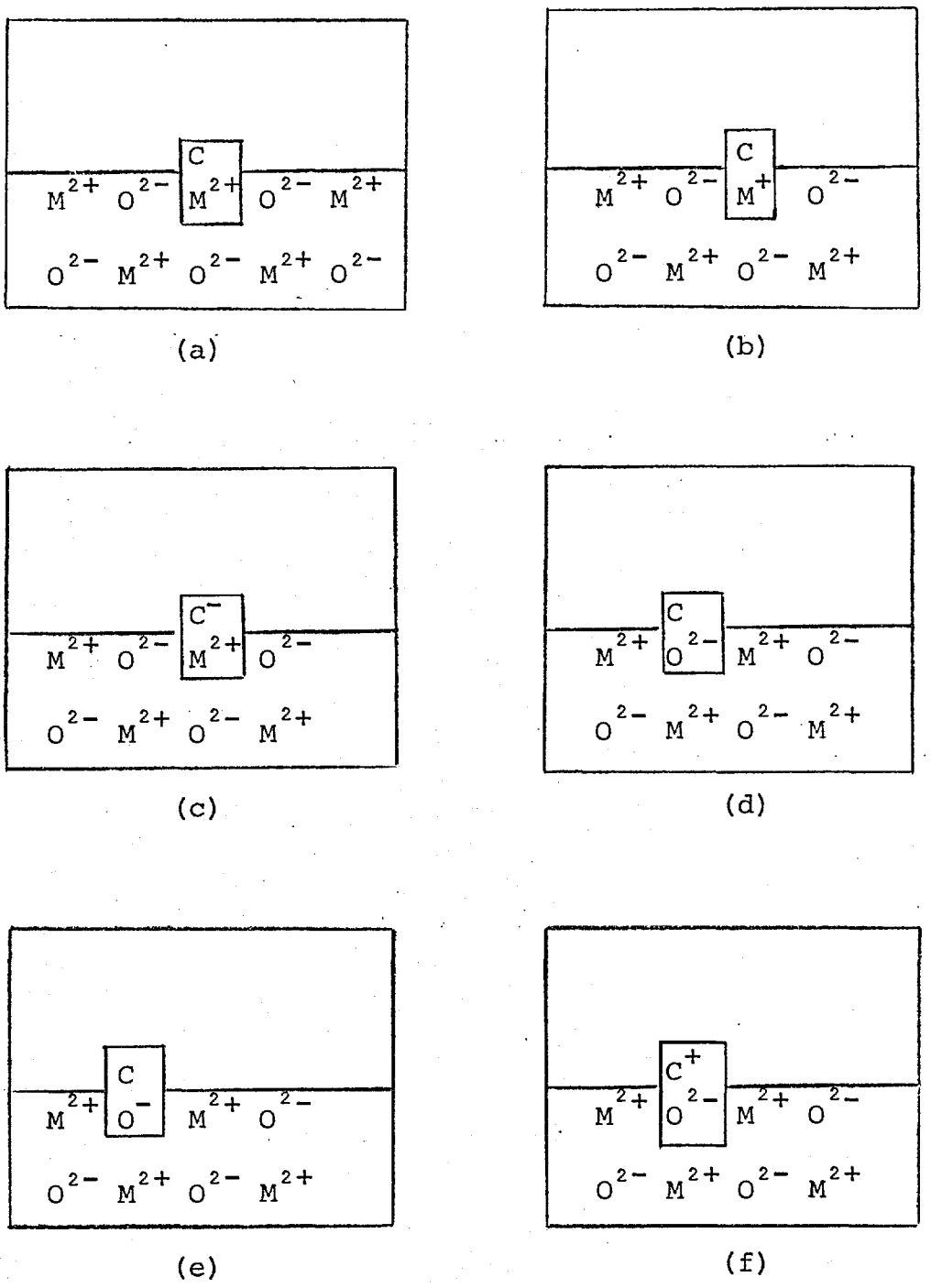

Modes of chemisorption on an oxide (24).

b) Geometric factor

It is well established that the surface geometry can play an important influence in determining the catalytic activity, although such effects seem more important in the context of metallic catalysts. After a very early investigation by Eyring (27), perhaps the most (apparently) complete evidence comes from the work of Beeck and his associates (25), (28) who discovered that the catalytic activity of metals for the hydrogenation of ethylene was apparently related to the lattice distance of thin metallic films (Figure 7) with a maximum in activity at a lattice spacing of 3.75 A^{o}.

The traditional "geometric" approach has been criticized because it was felt that electronic concept could explain and extend the observations. Thus, for example, the Pauling theory of metals showed a direct relationship between the d-character and the single-bond radius of the atoms in a metal crystal (29). It would certainly seem that the predictions must be treated with caution, since recent low energy electron diffraction studies have shown that the interatomic distance of a clean nickel surface is increased by 5% over that in the bulk (30) although this does not, of course, necessarily invalidate relationships of the type found by Beeck.

Perhaps the most correct view of geometric effects is that they do play a role in catalysis albeit not necessarily of overall importance. This is shown, for example, by the work of Balandin (31) from which it has been possible to

FIGURE 7

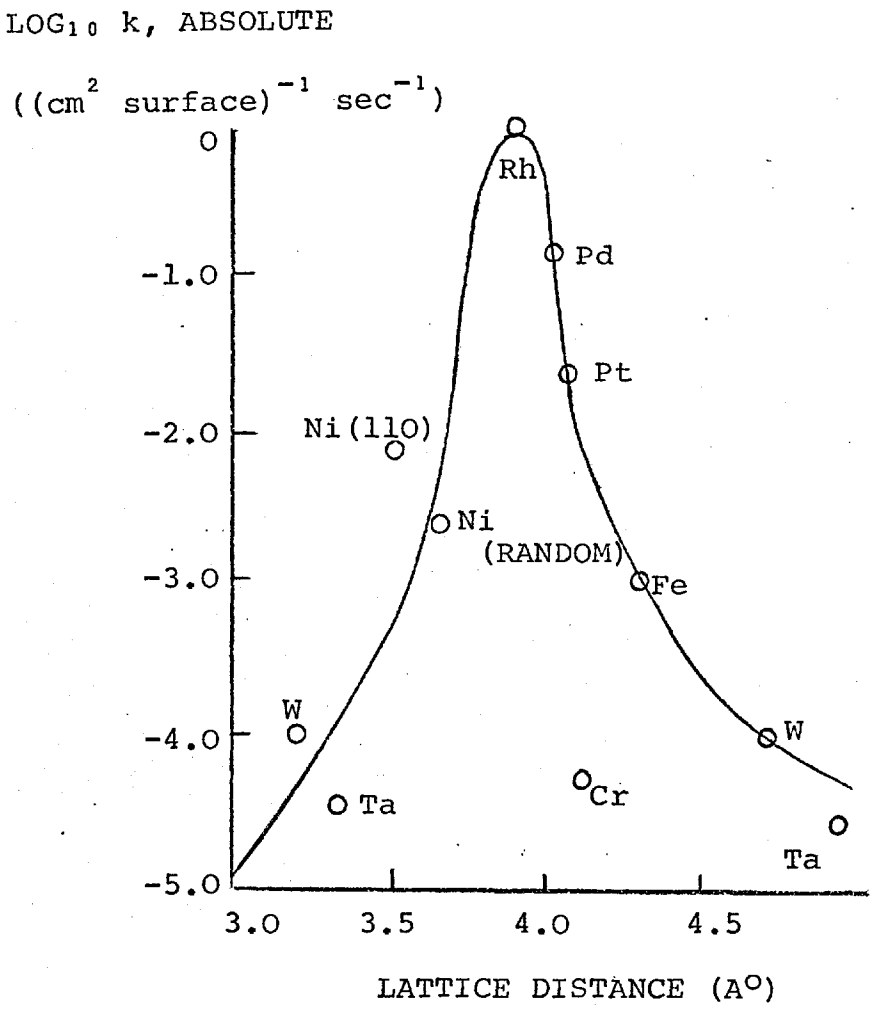

Activity of thin metallic films as a function of lattice distances (25).

suggest that the activity of a catalyst does depend on the presence in the lattice of groups of atoms spaced to accommodate various adsorbed species and to allow reaction between them. Thus, for example, in the benzene ⇄ cyclohexane reaction, it was argued that active metallic catalysts would be expected to show similar geometric characteristics. As is shown in Figure 8, if the distance between the hydrogen atoms of the adsorbed benzene and the metal atoms is plotted against the metal diameter, good catalysts do seem to share common geometrical characteristics.

More recently, the importance of geometric effects has been stressed in an oxidation system involving bismuth molybdate catalysts (32). The comparatively high activity and selectivity of the catalysts has been related to, amongst other things, the particular geometric arrangement of ions in the crystal lattice.

It is clear, however, that no combination of the electronic and the geometric theories of catalysis can explain completely most of the experimental observations. It would appear that electronic effects are primarily concerned with the behaviour of electrons in the bulk of the crystal, while geometric effects may be a secondary manifestation of some primary effect. What is necessary is some theory that can be used to relate and to extend these two factors, and this has largely been provided by the application of the crystal field theory to catalysis.

FIGURE 8

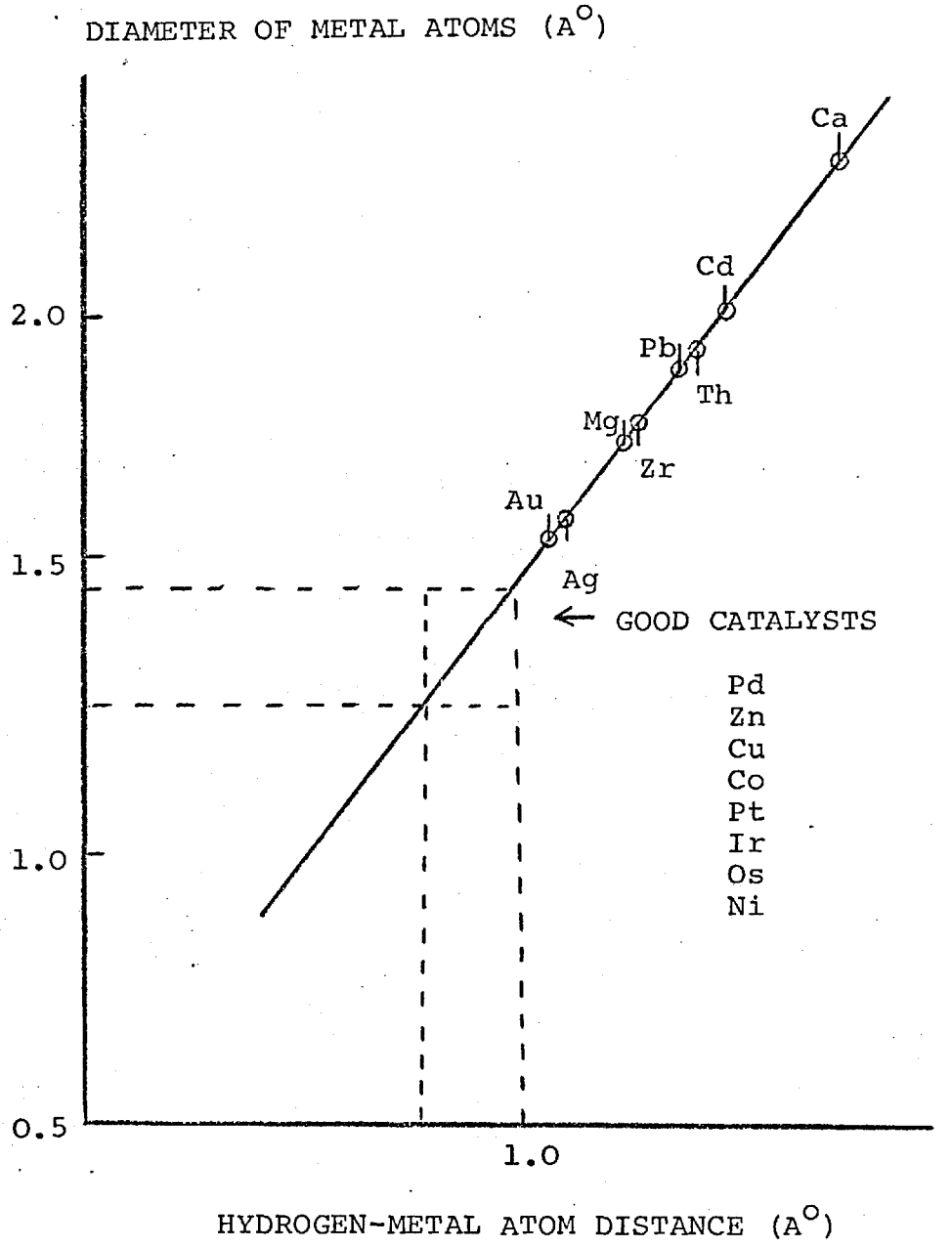

Evidence of geometric factor: metals within square possess requisite spacing and are good catalysts for hydrogenation of benzene (31).

c) Surface complexes

Consideration of this theory is perhaps best started from a statement of the major difficulties facing the early postulates, which can be summarised by the results plotted in Figure 9. In several reactions, the specific activity over various catalysts was found to follow a twin-peaked pattern as is shown in this diagram. In order to explain this pattern it was, in fact, necessary to consider the nature of changes that occurred on formation of adsorbed surface complexes. This, in turn, was possible only from information previously obtained in the study of homogeneous electron transfer reactions.

The energy changes that occur on formation of an adsorbed ionic surface intermediate are described by the crystal field theory (33, 34). The theory suggests that the energy of the electrons in the free ions becomes differentiated in the field of the adsorbate (or, in homogeneous terms, the ligand). As a result the energy level associated with particular orbitals will depend upon the position and relative intensity of the applied field: those orbitals lying towards the applied field will be raised in energy, while those lying away will be lowered. The splitting will obviously depend on the particular complex, as is shown in Figure 10.

If the overall potential energy gained stabilizes the system, the geometry of the complex may change to one of higher crystal field stabilization energy (CFSE) although

FIGURE 9

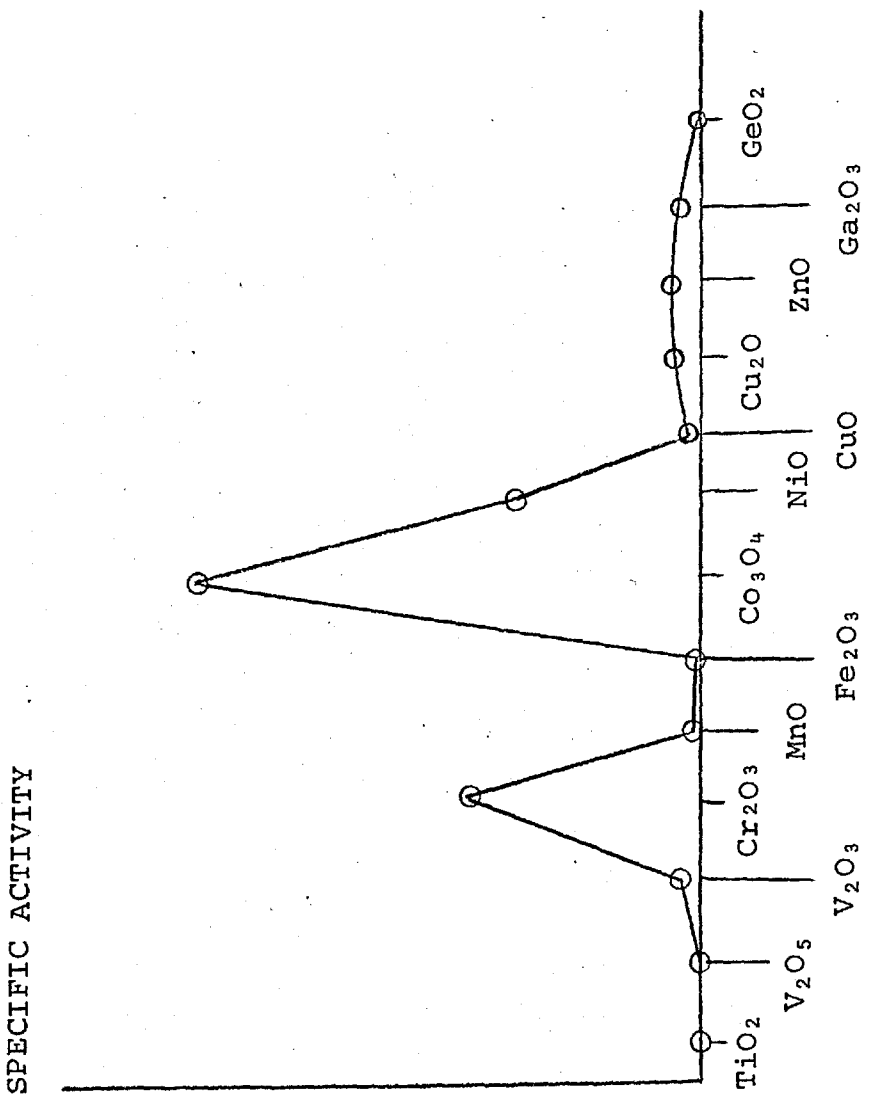

H_2/D_2 exchange on metal oxides of first transition period (26).

FIGURE 10

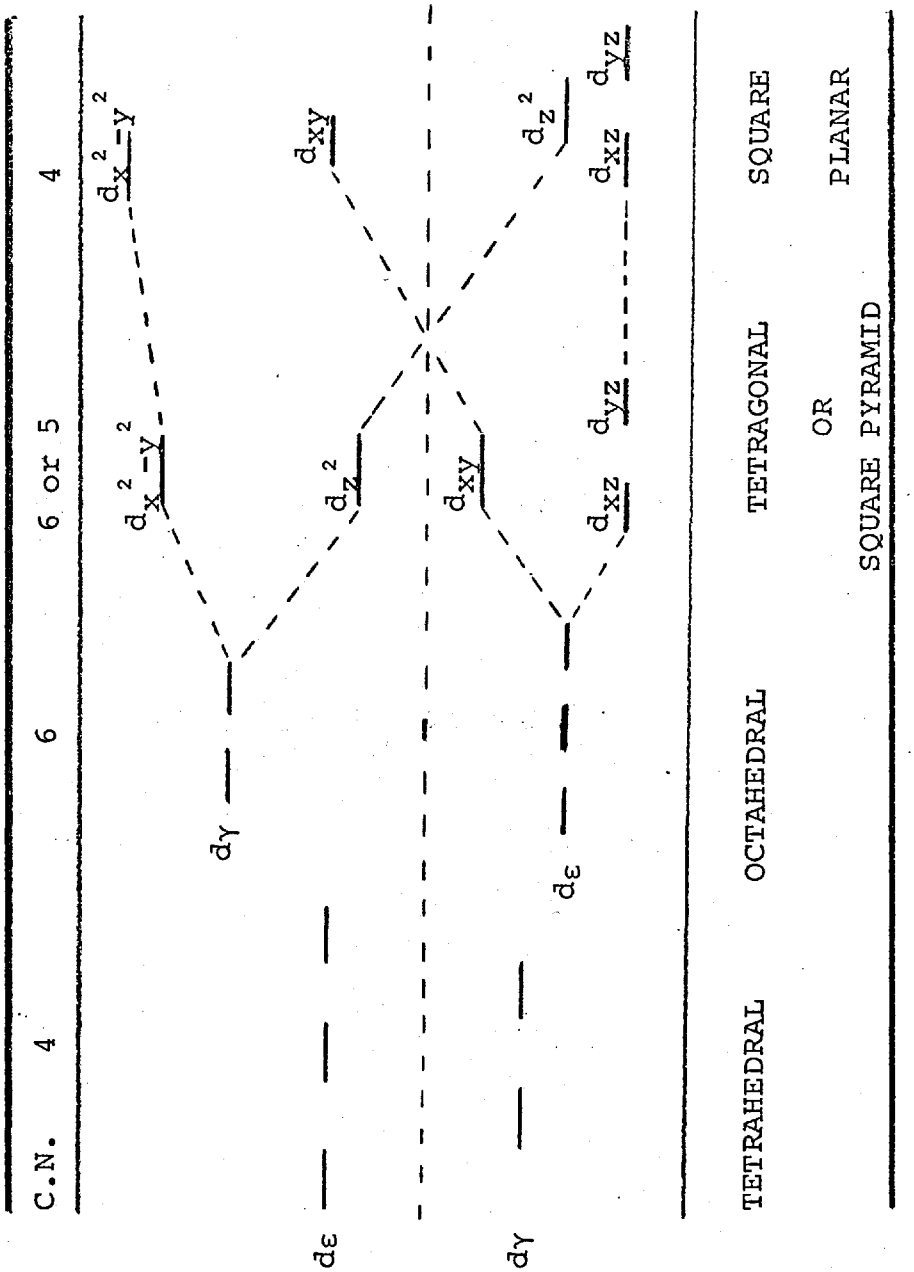

Crystal field splitting of d levels changes with the symmetry of complex.

in the process there may be a loss in bonding energy due to reduction of the co-ordination number. The copper fluoride crystal undergoes a deformation of geometry from an octahedron to a tetragonal structure of higher CFSE:

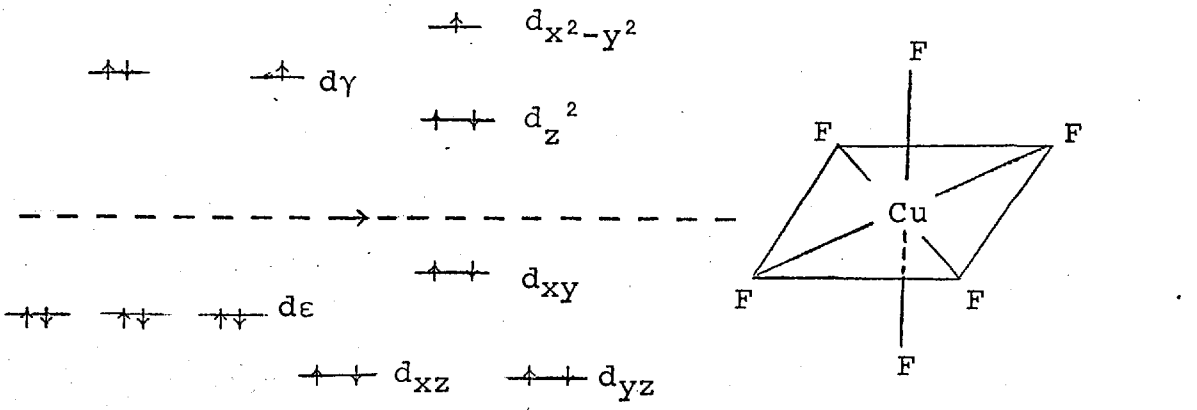

Octahedral Tetragonal

The deformation may lead to square planar complexes if the loss of bonding energy (co-ordination number changes from 6 to 4) is compensated by the gain in CFSE.

In general the difference in CFSE for different symmetrics are small and reversible changes of the complexes may occur. Indeed such changes have been suggested to be the fundamental cause of catalytic activity. Thus, for example, if a metal oxide ion at the surface of the catalyst has a vacant orbital, the ion may well adopt a square pyramid structure, with the point of the pyramid towards the bulk of the solid. On approach of a potential adsorbate, the ion could rearrange to form an octahedral complex; such a complex could then easily revert if the

adsorbate was removed, for example, as the result of a chemical reaction.

This model, because it is based on the ionic nature of the co-ordinate bond, cannot be applied to neutral complexes. In this case, the molecular orbital theory describes the formation of a co-ordinate bond as the combination of the s, p and d electrons of the metal with the s and p electrons of the ligand (absorbate). Two types of metal-ligand bonds have been noted: the σ-type bond and the π-type bond. Thus, for example, in the octahedral complex $Cr(CO)_6$, six σ-type bonds are formed from two d_γ, one s and three p metal orbitals combined with six s or p ligand orbitals. As the three atoms Cr-C-O are co-linear as shown in Figure 11 the empty π^* antibonding orbital of CO overlaps one of the d_ε metal orbitals forming the π bond with the electron pair donated by the metal. A more stable configuration is obtained because the six d electrons occupy the lower-lying π bonding orbitals. Similar complexes are produced by ligands such as olefins, dienes, alkynes and aromatic hydrocarbons.

Using these concepts, it has been possible to explain many aspects of chemisorption and catalysis on semi-conductors. Considering, for example, the semi-conductor, Cr_2O_3, each Cr^{3+} cation is octahedrally surrounded by six O^{2-} anions except at the crystal surface where chromium ions of different oxidation state and co-ordination number may occur. The exact state of the surface will depend on the history of

FIGURE 11

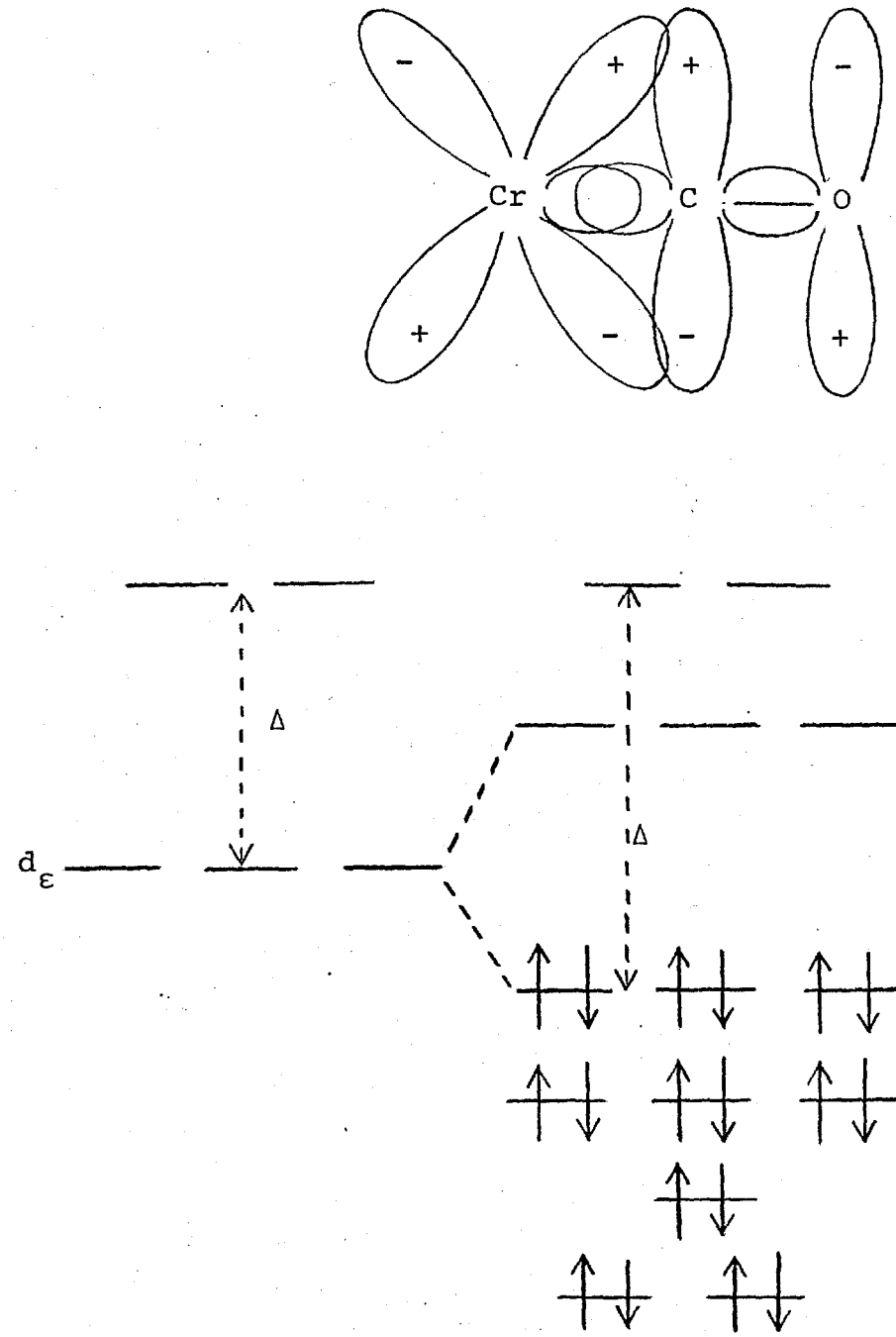

Electronic configuration of a π bonding ligand.

the sample. Thus the negative charge of the anions at the surface of the oxide prepared by dehydration of the hydroxide is compensated for by protons. The surface is catalytically inert but if dehydration is carried out at higher temperatures, incompletely co-ordinated Cr^{3+} cations may be produced by removing part of the hydroxide layer as water (Figure 12a). Oxygen may also be removed by reduction with hydrogen to give chromium ions with co-ordination numbers of four or three (Figure 12b). The electrons released during reduction decrease the oxidation state of an equivalent number of cations from 3+ to 2+, although at high temperatures, where semi-conductivity becomes important, these excess electrons may jump from cation to cation (n type semi-conductivity).

Re-oxidation will cause the co-ordination number and oxidation state of the cations to rise and will produce incompletely co-ordinated Cr^{4+}, Cr^{5+} or Cr^{6+}. The positive charge (holes) produced by transfer of electrons to the oxygen may migrate through the lattice giving rise to p type semi-conductivity.

The incompletely co-ordinated cations of the surface complexes may be satisfied by formation of σ-type or π-type bonds, a transfer of an electron occurring if the resulting complex is more stable. Thus, Cr^{4+} ions have a strong tendency to revert to Cr^{3+} of higher CFSE by capturing an electron from their ligands, the transfer producing a positively charged ligand which may move to a nearly O^{2-} ion (Figure 12c). The adsorbed ligand may then either be

FIGURE 12

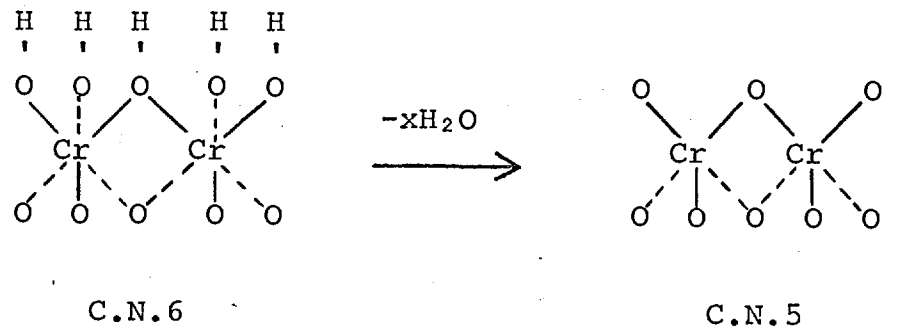

C.N.6 C.N.5

(a) DEHYDRATION

C.N.4 C.N.3

(b) REDUCTION

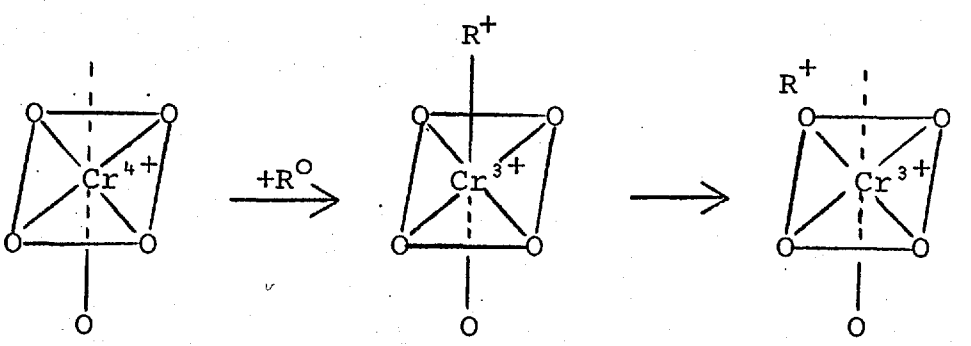

(c) ELECTRON CAPTURE

Change of co-ordination number (a), (b) and oxidation state (c) of chromium oxide surface.

"parked" in a position where subsequent adsorption can lead to easy reaction, or may react with the oxide ion itself to produce the desired product. Reoxidation of the catalyst may then occur and the cycle repeated.

Under these circumstances the inter-ion distance will obviously be of some importance in determining the catalytic activity, and the theory thus supplies some basis for the geometric concept. If chemisorption involves an electronic transfer with the cations, correlation of chemisorption with electrical conductivity will be noted and the electronic theories will apply. If not, chemisorption and catalysis must be caused by changes in co-ordination number and will be independent of semi-conductivity. This type of adsorption, involving changes of co-ordination number, will be dependent on the number of d electrons available in the metal ion.

These ideas have been very successful in explaining many observations, particularly with respect to the pattern of transition metal oxides for hydrogen-deuterium exchange as shown in Figure 9. Thus, optimal catalytic activity occurs over those cations of abnormal co-ordination number and/or oxidation state which are known to try to re-establish the stable configuration of the bulk cations. The theory is the best available although some extension of the arguments is still necessary, since the corresponding patterns of activity over the f-shell metal oxides are not so readily explained in these terms.

Returning to the problem of catalyst design, the theoretical approach does help in translating the virtual

mechanism for any given reaction. Thus, for example, it is possible to predict the nature and extent of adsorbate bond formation over a given solid, and to translate the desired reaction in terms of reactions that can occur on a given surface. It is interesting to see the advantages of this approach in the context of the selection of catalysts.

(iii) Applications

The problem of catalyst selection has, for many decades, been based on a trial and error procedure with minimum guidance from scientific principle. Activity patterns of the type shown in Figure 9 have been used to give a good indication of the solids which will be good catalysts for a similar reaction.

In recent years, however, it has been possible to place catalyst selection on a more quantitative basis, although it is still not possible to predict a good catalyst on a purely theoretical basis. This is partially because of the incomplete understanding of the complex processes that affect catalysis, and partially because of the lack of knowledge of the behaviour of solids that are not normally considered to be catalysts. It is rewarding, however, to consider the grounds on which selection can be made.

a) Electrical properties of solid catalysts

It has been possible to show that a relationship may exist between the catalytic properties and the

semiconductor characteristics of oxides. The prediction of new catalysts on the basis of electrical correlations is not possible, but the possibility of regulating adsorptive and catalytic properties of semiconductors arouses particular interest in the context of modifying known catalysts to higher selectivity and/or activity.

According to the electronic theory, an increase in adsorption of electron donors is expected when the Fermi level is lower. A reaction in which the limiting stage involves the transfer of an electron to the catalyst should thus be accelerated by the lowering of the Fermi level, and reactions whose limiting stage involves transfer of an electron from the catalyst to the reacting substance should be retarded.

These hopes for a simple connection between Fermi level position and the catalytic properties to solids have not been regularly confirmed. Often, in the cases where it was possible to establish a correlation, it has turned out contrary to the predictions of the electronic theory. Thus, for example, experimental data has shown that when lithium oxide in small concentrations (<0.6 atom per cent) is added to nickelous oxide, the electron work function increases as predicted (35) but the rate of oxygen chemisorption actually increases contrary to the predictions of the theory (36). Similarly, while the electron work function of titanium dioxide was increased by promotion with WO_3 (37), the rate of oxygen chemisorption also increases (38) contrary

to prediction. It must be assumed that the introduction of additives into such oxide catalysts causes not only a change in the Fermi level but also creates local chemical changes on the surface which can exert a strong influence on the chemisorptive process (36). From the point of view of catalyst selection, electronic effects may be useful but cannot be considered as reliable.

b) Energy of the intermediate

Catalysis by its nature is a chemical phenomenon and must involve some intermediate interactions of reagents with a catalyst. It is apparent from the previous discussion on surface complexes that one rewarding approach involves the stability of the surface complex. Ideally, a theoretical prediction of a catalyst is based on a calculation of the maximum probability of the active complex formation. Although this is not possible at present, restricted generalizations involving the energies of active complexes, as reflected in reaction rates, on bond energies are of importance in investigating and improving catalysts.

The concept of an optimum value of the energy of intermediate interaction has been developed by Balandin (39) in the form of a principle of energetic conformity of the multiplet theory. The application of this approach is not, however, just limited to the multiplet theory. It has been further developed by the work of Makishima (40), Sachtler (41), Temkin (42), Roiter (43), Tanaka (44) and

Boreskov (45), each approach tending to differ slightly in the method of correlating activation energy to some property of the system and in the means of estimating this property.

Boreskov (46) and fellow workers at the Russian Institute of Catalysis assume that in the course of a single reaction on various catalysts, the change in bond energies of the reacting substances with the solids will exert the main effect on the value of the energy of the active complex. The reaction activation energy on various catalysts is predicted to be a linear dependency with the change in reactant-catalyst bond energy.

$$E = Eo \pm \alpha q \qquad 0 < \alpha < 1 \qquad \ldots.12$$

The plus or minus signs correspond to reactions in which the limiting stage is the breaking or forming respectively of a reactant-catalyst bond. Over the wide range of bond energy where the change in the limiting stage occurs, the relationship becomes more complex (Figure 13 part a), producing a valley where the limiting cases are expressed by the above equation. The variation of activity with the bond energy is shown in Figure 13 (b): these plots are usually referred to as "volcano curves".

The catalytic activity of oxidation catalysts as a function of the value of the bond energy of oxygen with the catalyst has been studied in detail at the Institute of Catalysis. The activation energies for homomolecular oxygen exchange (I) and for the oxidation of methane (II) and hydrogen (III) have been correlated as a function of oxygen

FIGURE 13

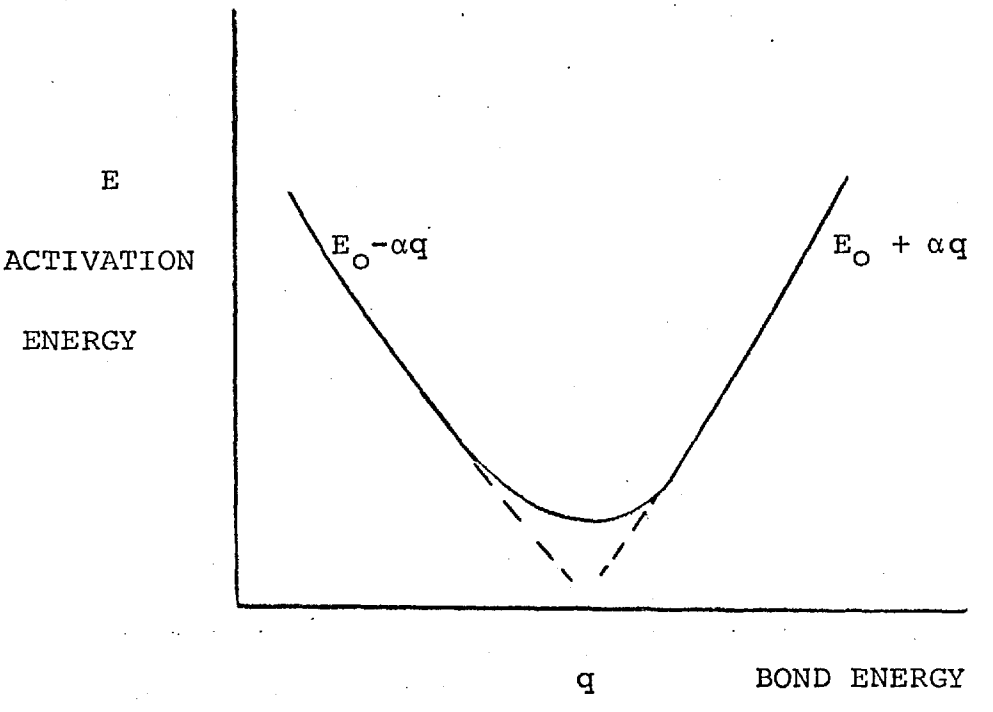

(a)

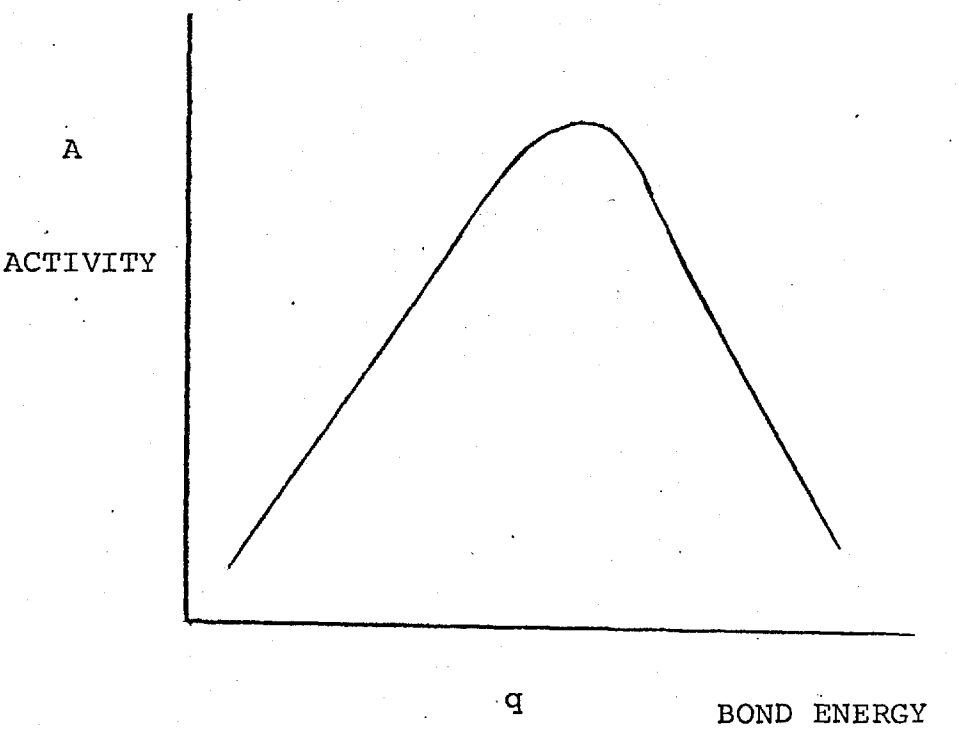

(b)

Relationship between bond energy of reactant-catalyst bond and (a) reaction activation energy (b) activity.

bond energy as is illustrated in Figure 14. The correlation corresponds to the equation:

$$E = E_o + \alpha q \qquad \ldots.13$$

and the catalytic activity of oxides for the reactions considered decreases in the following sequence:

$$Co_3O_4 > CuO \sim NiO \sim MnO_2 > Cr_2O_3 > Fe_2O_3 > ZnO > V_2O_5 > TiO_2 \qquad \ldots.14$$

which coincides with the sequence of increase in oxygen bond energy on the oxide surface (45, 46).

Although it is possible to select a catalyst of moderate or high activity on such a basis, this is not the sole criterion of selection. In addition, the selectivity of complex oxidation reactions is of prime importance. Thus the overall rate of the oxidation of methanol varies in the series of the fourth period oxides in conformity with the above sequence, but the yield of the intermediate oxidative product (formaldehyde) varies in the reverse direction (46). The catalytic activity and selectivity for the oxidation of methanol to formaldehyde is, in fact, mutually exclusive (47) (Figure 15). High activity oxides favour strongly the over oxidation of the aldehyde to unwanted terminal products, and to maximise the production of desirable intermediates, the oxygen bond energy on the catalyst surface must be sufficiently low to obtain a reasonable activity yet high enough that further oxidation of desirable products does not occur.

Japanese (40), Dutch (41) and Russian (39) workers have used the concept that the most suitable catalysts are

FIGURE 14

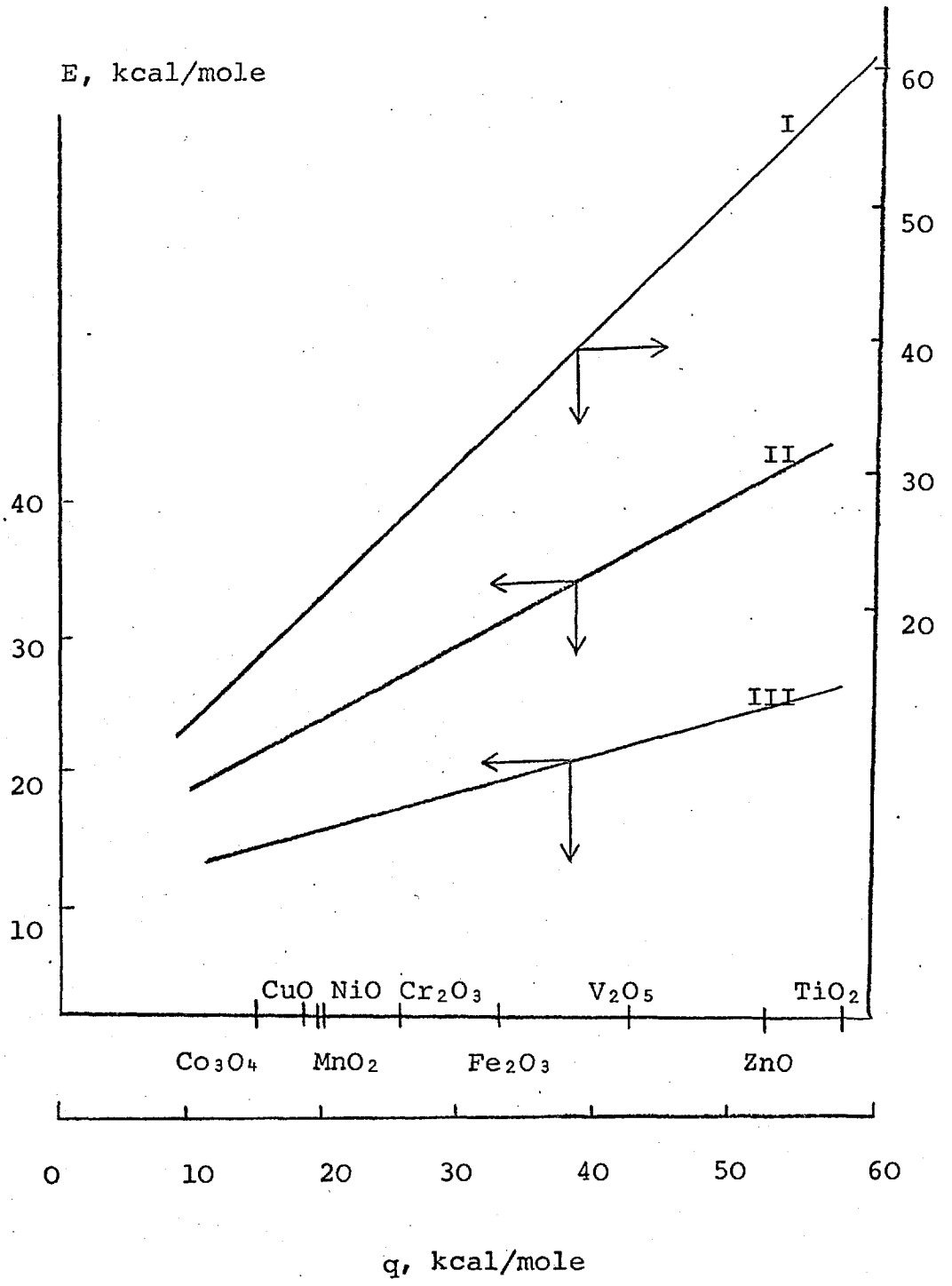

Activation energies of homomolecular oxygen exchange reaction (I), methane oxidation (II), and hydrogen oxidation (III) as a function of oxygen bond energy for the oxides of the fourth period (46).

FIGURE 15

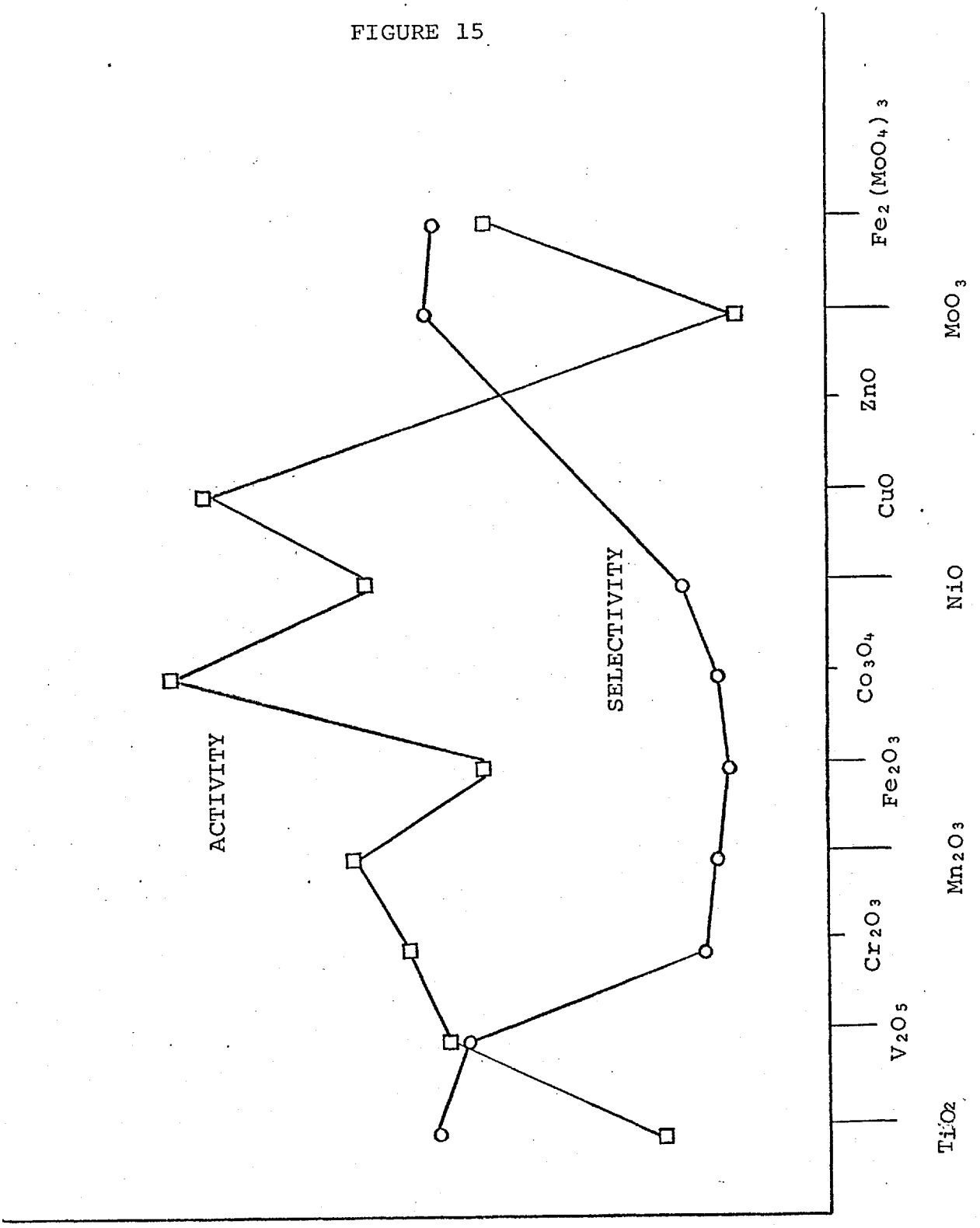

The activity and selectivity for the formation of formaldehyde from methanol (47).

those for which the change in enthalpy of each of the interactions of the catalyst with the components of the reaction catalyzed equals approximately half of the change in enthalpy of the overall process. For example, if the reaction

$$CO + \tfrac{1}{2}O_2 \rightarrow CO_2 \qquad \ldots.15$$

proceeds in two stages

$$\text{catalysts} + \tfrac{1}{2}O_2 \rightarrow O\text{-}X \qquad \ldots.16$$

$$O\text{-}X + CO \rightarrow CO_2 + \text{catalyst} \qquad \ldots.17$$

the best catalyst is that for which the heat of the overall reaction is equally distributed between the partial reactions. Attempts to correlate the change in enthalpy of the hypothetical intermediate and the catalytic activity of oxides has proven generally successful, with an apparent maximum at half the overall enthalpy. Irregularities are apparent, however, with many oxides showing either a much lower or much higher activity than predicted (40) (43).

This concept can also be applied directly to the problem of selectivity. If we take as an example the oxidation of ethylene to ethylene oxide (43), three reactions can occur:-

$$C_2H_4 + \tfrac{1}{2}O_2 \rightarrow C_2H_4O \quad (\tfrac{1}{2}\Delta H^{\circ}_{298} = -12 \text{ kcal/mole}) \qquad \ldots.17$$

$$C_2H_4 + 3O_2 \rightarrow 2CO_2 + 2H_2O \quad (\tfrac{1}{2}\Delta H^{\circ}_{298} = -26 \text{ (kcal/mole)} \qquad \ldots.18$$

$$C_2H_4O + 2\tfrac{1}{2}\,O_2 \rightarrow 2CO_2 + 2H_2O \quad (\tfrac{1}{2}\Delta H^{\circ}_{298} = -29 \text{ (kcal/mole)} \qquad \ldots.19$$

and the first stage is identical in each reaction

$$\text{catalyst} + \tfrac{1}{2}O_2 \rightarrow O\text{-}X \qquad \ldots.20$$

For optimum selectivity, the enthalpy of the first stage

should be approximately half the enthalpy change for the production of ethylene oxide. Silver is known as a selective catalyst for this reaction

$$2Ag + \tfrac{1}{2}O_2 \rightarrow Ag_2O \quad (\Delta H^{o}_{298} = -7 \text{ kcal/mole}) \qquad \ldots.21$$

and, in confirmation, the value of the enthalpy of the first stage is nearly half the value for the reaction producing ethylene oxide over this catalyst.

The approach to prediction of catalysts by correlation of catalytic activity with the energy of the intermediate suffers from two main faults. The estimation of enthalpy from thermodynamics is a coarse approximation, and the results do show irregularities. The correlation with bond energy involves laborious experiments and only predicts maximum activity but not necessarily the selectivity to desirable intermediate products. It is apparent that the above approaches do have merit but can only supply a general prediction.

2B. Chemical engineering aspects of catalyst design

Once it has been possible to define chemically a given catalyst for a chemical reaction, it is necessary to consider the physical form and optimal surroundings of the solid. In the case of oxidation, for example, the reactions are known to give off heat, and this may have a deleterious effect on selectivity. Again, if the reactor temperature is too high or if the catalyst is very porous, over-oxidation may be severe. The design of the catalyst

structure, the catalyst pellet and the catalyst bed must obviously consider the effect of such factors on the reaction yield.

It has been customary for these aspects to be dealt with primarily by the chemical engineer. On the basis of an approximate or an accurate knowledge of the kinetics and thermodynamics of the reaction it is possible to recognise and to minimise problems of heat and mass transfer that may arise. Using the example of catalytic oxidation the approach may be discussed in more detail.

A gas solid catalytic reaction may proceed at a rate controlled by one or more processes. These may be summarised as

(1) The mass transfer of reactants and products to and from the exterior surface of the catalyst.
(2) The diffusion of reactants and products into and out of the pore structure of the catalyst particle.
(3) The activated adsorption of reactants and desorption of products at the catalytic interface.
(4) The surface reaction of adsorbed reactants.

Although all of these processes should be dependent upon the concentration gradients involved, it would be expected that widely different factors should affect each individual step. For example, bulk diffusion should be dependent on the flow characteristics of the system, while pore diffusion should be affected by the degree of porosity of the catalyst, the dimensions of the pores, the size of the particles, the diffusional characteristics of the system,

and the rate at which the reaction occurs at the interface. The rate of adsorption/desorption should be more dependent on the nature of the catalytic surface and the properties of the gases which, together with the catalytic reaction rate, should be largely independent (apart from the amount of available surface) of the geometry of the catalyst.

Considering the movement of gases through a single idealized catalyst pore, and treating the adsorption and reaction as one, the three resistances to mass transfer may be illustrated as in Figure 16. Although the gas film and surface reaction steps are in series relationship with each other, simple methods of combining resistances can not be used as pore diffusion is not related in a simple way to the other steps. As a result film and surface reaction resistances can be treated separately but the pore diffusion resistance can never be treated independently.

(i) The rate of the chemical reaction

Rate expressions for the surface reaction in the absence of significant resistances from film and pore diffusion have been developed largely from the Langmuir-Hinshelwood arguments (48) which, in turn, were developed on the basis of theory first proposed to explain some aspects of adsorption (49). Using a specific model of adsorption, Langmuir was able to develop a mathematical relationship that described one type of adsorption isotherm particularly associated with chemisorption. The assumptions

FIGURE 16

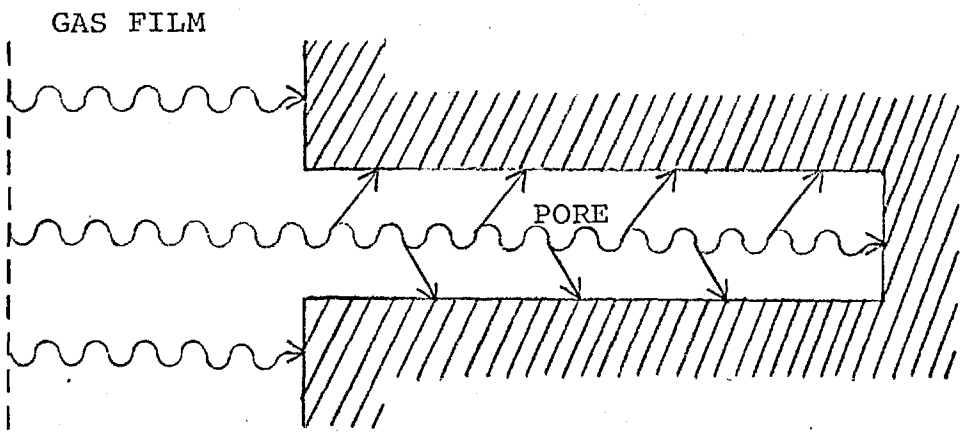

(a) Sketch of a catalyst pore

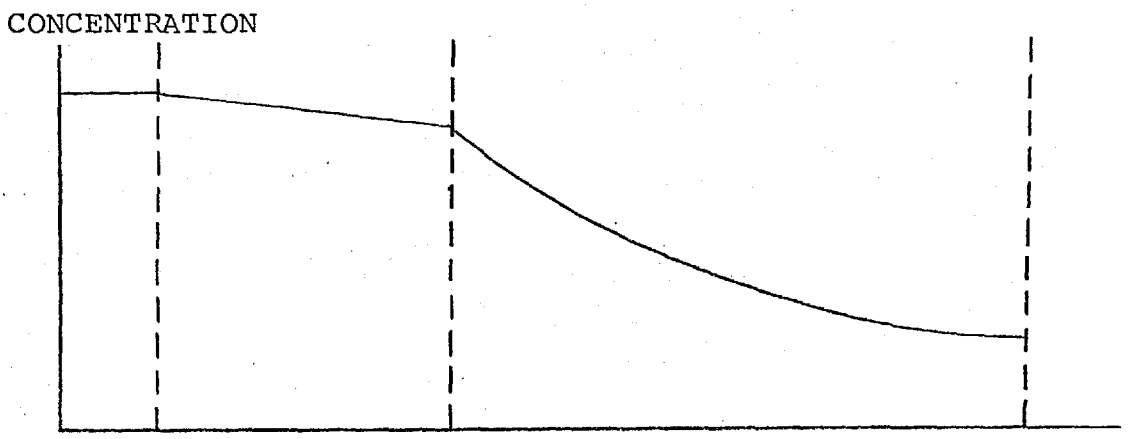

(b) Concentration within a pore

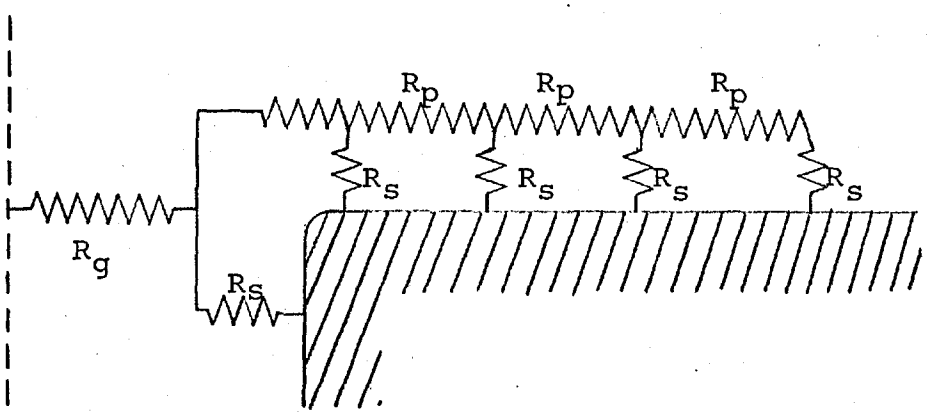

(c) Electrical analog of a pore

Continuous-reaction model for porous catalysts.

of the model, which are open to some criticism, can be listed:

(1) The adsorbed species are in a monolayer i.e. adsorption only takes place through collision of gas molecules with vacant sites.

(2) Adsorption involves only one adsorbed particle per site.

(3) The energy of an adsorbed particle is the same at any site and is unaffected by neighbouring sites.

(4) The adsorbed species are in equilibrium with the gas, the strength of adsorption being a function of the time which a molecule remains on the surface.

Since the rate of adsorption at steady state must equal the rate of desorption, the relationship below must hold:

$$r_{ads} = k_a(1-\theta)P = r_{des} = k_d\theta \qquad \ldots.22$$

whence the surface coverage θ is related to the pressure P by

$$\theta = \frac{bP}{1 + bP} \qquad \ldots.23$$

where b is the adsorption coefficient (k_a/k_d) and k_a and k_d are the rate constants for adsorption and desorption respectively. Similarly, if a molecule splits into n fragments, each occupying one site, the equation becomes

$$\theta = \frac{bP^{1/n}}{1 + bP^{1/n}} \qquad \ldots.24$$

and if two gases A & B compete for the same sites

$$\theta A = \frac{b_A P_A}{1 + B_A P_A + b_B P_B} \qquad \ldots.25$$

and

$$\theta B = \frac{b_B P_B}{1 + b_A P_A + b_B P_B} \qquad \ldots.26$$

Now the rate of a catalytic reaction involving reaction between two adsorbed species must be dependent on the available concentrations

$$\text{i.e.} \qquad r = k\theta_A \theta_B \qquad \ldots.27$$

whence

$$r = \frac{k b_A P_A b_B P_B}{(1 + b_A P_A + b_B P_B)^2} \qquad \ldots.28$$

Alternatively, if B dissociates into two fragments the rate expression becomes:

$$r = \frac{k b_A P_A \sqrt{b_B P_B}}{(1 + b_A P_A + \sqrt{b_B P_B})^2} \qquad \ldots.29$$

The denominator in all of these equations depends basically on the molecules that compete for adsorption on active sites on the solid. The relative importance of any term depends on the adsorption coefficient b. If a product X is formed in the reaction, then this may also compete for sites; in this case the number of available sites is reduced and equation becomes

$$r = \frac{k b_A P_A b_B P_B}{(1 + b_A P_A + b_B P_B + b_X P_X)^2} \qquad \ldots.30$$

This Langmuir-Hinshelwood approach can obviously be applied to a variety of reaction models (52, 53, 54, 55). Two important extensions of the arguments are possible.

The first of these,developed by Rideal and Eley (50), envisages a slightly different model in which reaction between an adsorbed species and a molecule in the gas phase may occur. For a monomolecular adsorbate A, the Rideal-Eley rate expression becomes

$$r = k\theta_A P_B = \frac{k' b_A P_A P_B}{(1 + b_A P_A)} \qquad \ldots.31$$

It is not absolutely necessary for B to be a free molecule in the gas phase: a similar expression would be obtained if B were located near to the surface, for example by physical or weak adsorption.

A second alternative to the original model is also possible, where components A and B do not compete for the same sites: a dual function catalyst is a good example of this type of solid. In this case, the coverage for each reactant can be written as in equation above, and the rate expression becomes

$$r = \frac{k b_A P_A \, b_B P_B}{(1 + b_A P_A)(1 + b_B P_B)} \qquad \ldots.32$$

For the purposes of this introduction it is convenient to use an expression such as Equation 32 above as an illustrative example.

Under certain circumstances Langmuir-Hinshelwood expressions of this type can be reduced to a more simple power rate law. With reference to Equation 32, if $b_A P_A$ and $b_B P_B$ are small compared to unity over a range of conditions, the expression reduces to

$$r = k'P_A P_B \quad \ldots.33$$

while if the reverse is true, i.e. $b_A P_A$ and $b_B P_B$ are large compared to unity, the equation approximates to a zero order plot

$$r = k'' \quad \ldots.34$$

Thus, in the general term, the equation can be approximated to

$$r = k'''P_A^{\,x} P_B^{\,y} \quad \ldots.35$$

where x and y are fractional orders.

These power rate laws are considerably easier to handle than the full Langmuir-Hinshelwood plots, and are often applied in the development of a mathematical model of a reaction. It is rewarding to review the relative advantages of the accurate and approximate rate expressions:

(1) Provided that the full equation is correct, the rates of a reaction can be obtained under all conditions. The power rate law, on the other hand, is only applicable over that range of conditions where, for example, $b_A P_B$ and $b_B P_B$ is less than unity.

(2) The full equation can be used to obtain some idea of the reaction mechanism. If a series of rate expressions are developed for alternative theoretical models, comparison with experimental results can lead to the elimination of some models. As a result of experimental error, it is possible that experimental results may agree with more than one Langmuir-Hinshelwood model, but it will be possible

to reject many cases where the agreement is outside the limits of the error. Thus it is generally accepted that the fitting of the full equation to the experimental data ia a necessary but not sufficient condition for any proposed mechanism. The power rate law, on the other hand, cannot be used to differentiate between other than grossly different mechanisms.

(3) The development and use of a mathematical model of the reaction to be used as a basis of prediction or control of a reaction may be very complex using the full equation. In these cases a power rate law is handled much more easily.

(4) If a reaction is affected by both the chemical reaction and by diffusion, the mathematics becomes very complex using the full equation and it is usual to use the power rate law.

To summarise, then, there are definite advantages to the use of both equations under appropriate conditions, but care must be taken not to apply either expression indiscriminately.

Although the Langmuir-Hinshelwood theories have been widely applied, it is possible to criticise the basis of the theory (51). Under the peculiar conditions of catalysis, some of these criticisms can, however, be refuted. Thus, for example, the model is based on the idea that each adsorption site is associated with the same energy. In the case of adsorption this is known not to be true, the energy of adsorption being a function of coverage (25). During

catalysis, on the other hand, the sites actually involved in the reaction are associated with a very small range of energy as discussed in section 2A(i), and this assumption becomes much more tenable. Again, since catalysis usually involves chemisorbed species, the assumption of monomolecular coverage is justifiable. Certainly it is true to say that the Langmuir-Himshelwood treatments, suitably modified to account for various mechanistic approaches, have been used widely and successfully to explain the rates of catalytic reactions.

a) Selectivity and chemical reaction rates

In considering the design of a catalyst, the selectivity of the reaction is as important as the activity: concurrent or consecutive reactions leading to unwanted products are obviously undesirable. To a large extent the reaction selectivity is a function of the chemical nature of the catalyst, but it is possible to favour a particular reaction path by adjusting reaction conditions. Thus, for example, if the desired reaction is of lower kinetic order and lower activation energy than any other reaction, reactant concentrations and temperatures should be kept as low as possible consistent with the overall activity desired. This overall activity can be increased by increasing the surface area of the catalyst, and provided that this does not introduce any mass transfer limitations, the selectivity will not be affected.

(ii) Gas film diffusion controlling

When the gas film resistance is much larger than the resistances of the surface phenomenon or of pore diffusion, the rate of reaction is limited by the rate of transport of reactants and products to and from the surface, and is controlled by the mass transfer coefficient, k_g, between the gas and the solid. The rate of reaction becomes (57)

$$r = k_g S(C_g - C_i) \quad \ldots.36$$

where C_g and C_i are the concentration of the reactant in the gas stream and at the interface respectively and S is the exterior surface of the particle. The value of k_g depends upon the nature of the diffusion component, the turbulence near the surface and the properties of the entire gas mixture (57). Actual values for the mass transfer coefficient can be claculated from empirical or semi-empirical dimensionless correlations developed by Hougen and Wilkie (58) and by Froessling (59).

a) Selectivity and gas film diffusion

The rate of diffusion through the boundary layer usually only becomes important where the surface reaction is very rapid i.e. generally at high temperatures. Under these conditions, not only will the overall kinetics of the reaction change but the selectivity of the process may also change. Considering, for example, a reaction producing a desired product C which in turn can react further to undesired compounds, D, then the initial reaction will occur as soon

as the reactants reach the surface. The diffusion of products into the gas stream will, however, depend on setting up a concentration gradient i.e. the product C will tend to remain on the surface for longer times. As a result, the production of undesired D will be favoured, and the selectivity of the reaction will decrease.

(iii) Pore diffusion and reaction rates

Pore diffusion resistance acts in parallel with the surface reaction resistance (Figure 16) and both must be treated together; pore diffusion cannot be reaction controlling in the sense that it alone will determine the rate of reaction. Three distinct processes may be identified, namely ordinary bulk diffusion, Knudsen diffusion and surface diffusion (60). When the pores are large and the gas relatively dense, the process can be considered as a special case of bulk diffusion. For reactions carried out at moderate pressures on catalysts with pores greater than 1000A^{o} this process may well be important (60a) but if the pores are smaller or if the gas density is low, gas molecules will collide with the pore wall more frequently than with each other and the factors influencing diffusion change (Knudsen diffusion). If molecules adsorb on the surface, then these can show considerable mobility over the surface in the direction of decreasing surface concentration (surface diffusion).

Of these three, Knudsen diffusion is probably the most influential process during heterogeneous catalysis.

Bulk diffusion, as discussed above, is usually important only at high temperatures, and available data (61, 62) indicates that surface diffusion contributes little to overall transport through a porous mass unless appreciable adsorption occurs.

If pore diffusion is significant, a concentration gradient through the catalyst pellet must be established and the internal catalyst surfaces are exposed to a lower concentration of reactants than the exterior surfaces. As a result, the overall rate decreases and the rate expression must be modified by the use of an effectiveness factor (ε), defined as the ratio of the actual reaction rate obtained to that which would be obtained if all the surface was exposed to the reactants at the same concentrations as that existing at the outside surface. For a reaction

$$A + B \rightarrow C + D \qquad \ldots.37$$

where the chemical reaction rate can be expressed as

$$\text{rate} = kA^m B^n \qquad \ldots.38$$

if pore diffusion becomes important, then the rate expression become

$$\text{rate} = kA^m B^n \varepsilon \qquad o<\varepsilon<1 \qquad \ldots.39$$

The approach generally adopted has been to develop mathematical equations for simultaneous mass transfer and chemical reaction in a porous catalyst where the following assumptions are made (63, 64, 65)

(1) Isothermal conditions

(2) A single overall diffusion coefficient D representing the complicated diffusion

phenomena within the porous structure.

(3) A negligibly small volume change on reaction within the porous structure.

Thus, for example, the effectiveness factor for a first order unimolecular reaction involving a spherical catalyst particle under these conditions has been shown to obey the relationship (66)

$$\varepsilon = \frac{3}{\phi}\left(\frac{1}{\tanh\phi} - \frac{1}{\phi}\right) \qquad \ldots.40$$

where ϕ, the Thiele Modulus is a dimensionless parameter of the form

$$\phi = L\sqrt{k/D} = L\sqrt{2k_s/Dr} \qquad \ldots.41$$

where L is a measure of catalyst pore length (L = 1/3 radius of sphere), k and k_s are the reaction rate constant per unit volume and unit surface area of catalyst respectively, r is the average pore radius and D is the effective diffusion coefficient, defined as the ratio of the flux to the concentration gradient, and is related to Knudsen and bulk diffusion by the following relationship:

$$1/D = 1/D_K + 1/D_B \qquad \ldots.42$$

where D_K and D_B are the Knudsen and bulk diffusion coefficients respectively.

In the Knudsen diffusion regime, gas molecules hitting the wall are momentarily adsorbed and then givenoff in random directions. As a result, the Knudsen diffusion coefficient responds differently to reaction conditions compared with the bulk diffusion coefficient. The Knudsen

diffusion coefficient varies as the square root of temperature and is independent of pressure while the bulk diffusion coefficient varies with temperature to the three-halves and is inversely proportional to pressure. The Knudsen coefficient for diffusion also varies with the average pore radius.

The effectiveness factor is found to depend on the Thiele modulus in a quite characteristic fashion (Figure 17). For values of ϕ less than 0.5 the effectiveness factor is approximately unity, pore diffusion is unimportant and the concentrations of gases does not decrease appreciably within the pore. In the other extreme ($\phi > 5$) the effectiveness factor is found to be inversely proportional to ϕ and the concentration of gas drops rapidly inside the pore. The decrease in concentration along the pore length, as the Thiele modulus increases, is shown in Figure 18.

The relationship shown in Figure 17 is found to be surprisingly insensitive to geometry or to reaction order. The dependence of effectiveness factor on Thiele modulus can be calculated for various geometries (Table 5) and each system gives a very similar result. In fact, provided that the distance parameter L is defined carefully, it is possible to use an average curve to estimate ε within an error of 10% for any geometry.

If pore diffusion is important in a system, many kinetic parameters such as apparent activation energy and reaction order become dependent on the physical properties

FIGURE 17

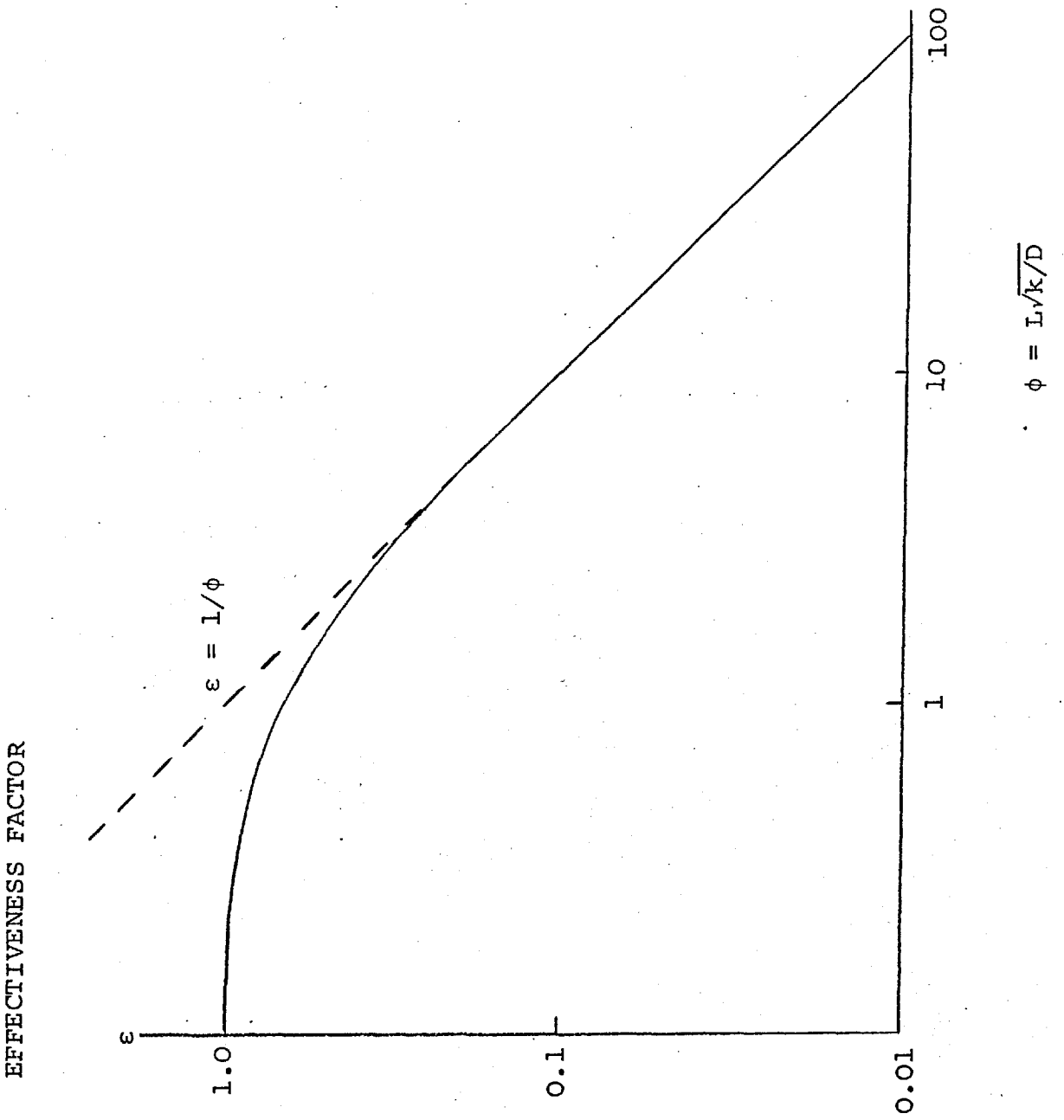

The effectiveness factor as a function of the Thiele modulus, ϕ, for a spherical catalyst and a first order reaction (72).

FIGURE 18

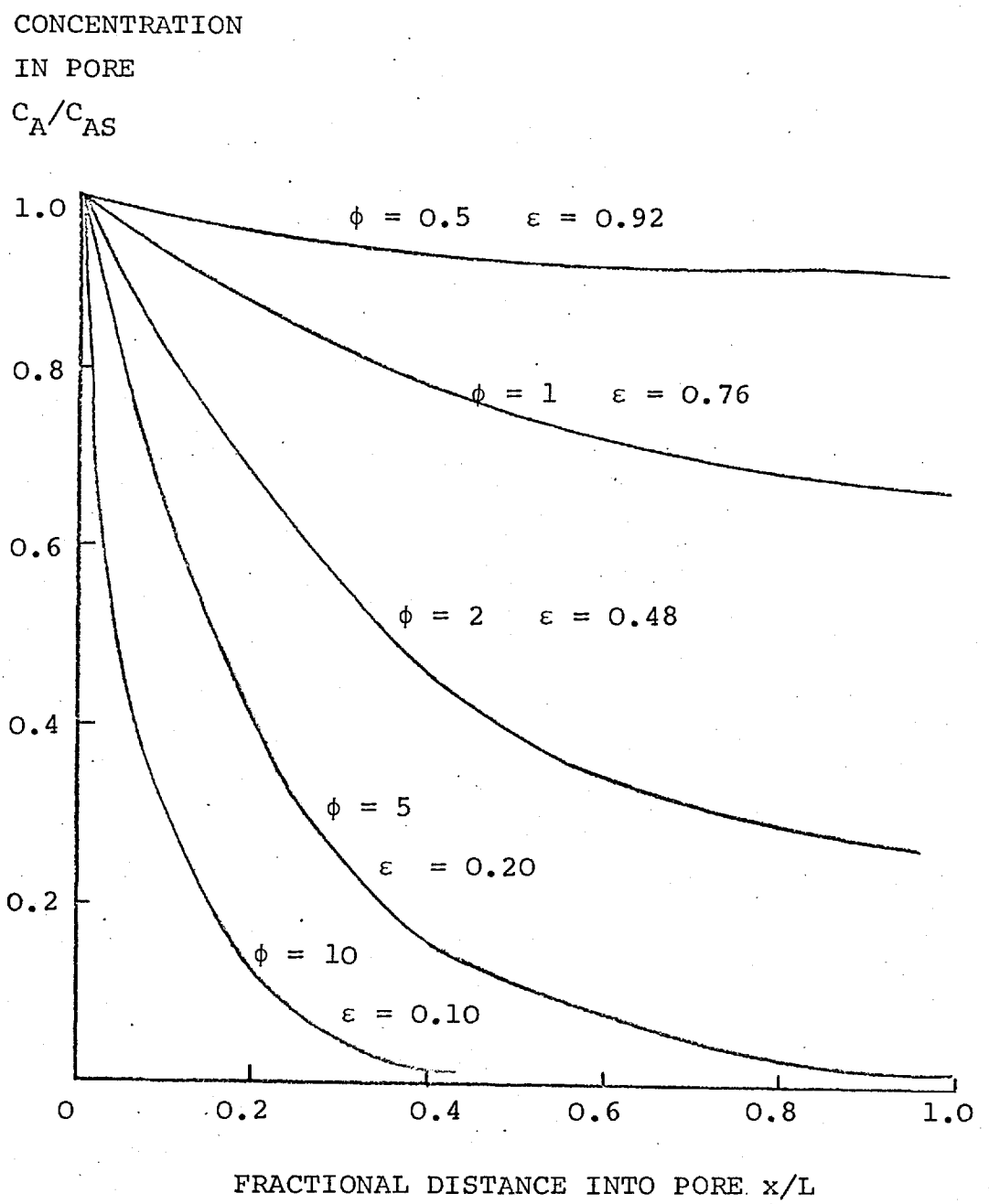

Variation of reactant concentration within a catalyst pore as a function of the Thiele modulus (73).

TABLE 5

Summary of effective factors and length parameters used for various shapes of catalyst pellets where L^1 is the thickness of the plate and I's are modified Bessel functions (72)

Geometry	Single cylindrical catalyst pore	Flat-plate catalyst pellet	Cylindrical catalyst pellet	Spherical catalyst pellet
Length parameter	L	$L = L^1/2$	L = R/2	L = R/3
Effectiveness factor ε	$\frac{\tanh \phi}{\phi}$	$\frac{\tanh \phi}{\phi}$	$\frac{2I_1(2\phi)}{I_o(2\phi)}$	$\frac{3}{\phi}(1/\tanh \phi - 1/\phi)$

of the catalyst. The effect of pore diffusion on the apparent order and activation energy can be derived (66). For a nth order reaction rate:

$$\text{rate} = K\, c^{n}\varepsilon \qquad \ldots.43$$

and for ε less than 0.5, ε becomes inversely proportional to ϕ and

$$\text{rate} = k\, c^{n}/\phi = k\, c^{n}/L \sqrt{k\, C^{n-1}/D} \qquad \ldots.44$$

or

$$\text{rate} = C^{(n+1)/2} \sqrt{k/D}\ /L \qquad \ldots.45$$

As can be observed from the equation the activation energy measured under conditions of strong pore diffusion resistance will apparently be one-half the true value, and the true order will decrease to a $(n + 1)/2$ apparent order, i.e. a true second order becomes a 3/2 order and so forth. The effect of strong pore diffusion on the observable parameters and the relation between the physical properties of the catalyst and the diffusion coefficient is shown in Table 6.

a) Selectivity and pore diffusion

The oxidation of hydrocarbon to a desired intermediate can often be represented by the scheme

$$\begin{array}{ccccc} A & \xrightarrow{k_1} & B & \xrightarrow{k_2} & C \\ & \searrow^{k_3} & & & \\ & & C & & \end{array} \qquad \ldots.46$$

where B is the desired intermediate and C is the undesired

TABLE 6

The effect of strong pore diffusion on the observable parameters and the dependence of the diffusion coefficient on the catalyst properties (74)

	Reaction order	Activation energy	Bulk diffusion			Knudsen diffusion		
			Pore radius	Surface area	Pore volume	Pore radius	Surface area	Pore volume
Slow reactions, large pores	n	E	r	Sg	Inde-pendent	-	-	-
Fast reactions, small pores	$\frac{(n+1)}{2}$	$\frac{E}{2}$	$r^{3/2}$	$\sqrt{Sg}$	$\sqrt{Vg}$	r	Inde-pendent	Vg

product, usually carbon dioxide. The effect of pore diffusion on selectivity is best understood if the reaction sequence 46 is considered as a mixture of concurrent and consecutive reactions.

For concurrent reactions the selectivity is not influenced by the catalyst structure if the order of the reactions to each of the products is the same. At each point in the interior of the catalyst structure, the reactions will proceed at rates proportional to their kinetic rate constants and the selectivity remains unaltered. If the orders are not equal, then small pores ($\phi > 3$) will increase the selectivity of the catalyst towards the product associated with the lower order. Wheeler (67) has pointed out that if a reactor can be operated at low partial pressure of reactants to give greater selectivity, then using the same catalyst containing smaller pores should further increase the selectivity to this product. Of course, the reverse is true, and if the desired reaction is the higher order reaction, then strong pore diffusion will have an adverse effect on the selectivity.

Considering consecutive reactions, the rate of disappearance of A relative to B, for chemical reaction control, becomes

$$-\frac{dB}{dA} = 1 - \frac{1}{S}\frac{B}{A} \qquad \ldots.47$$

where S is the selectivity factor k_1/k_2, and integration gives the conversion of B as a function of A reacted:

$$\alpha_B = \frac{S}{S-1} (1 - \alpha_A) \{(1 - \alpha_A)^{-(1-1/S)} - 1\} \quad ....48$$

where α_B is the fraction of initial A converted to B and α_A is the fraction of A reacted.

If the catalyst is porous, then the intermediate B will take longer to diffuse away from the active surface and the chance of further reaction will increase. The decreased yields can be quantitatively calculated as described by Wheeler (67). For an active porous solid the differential yield of B at a point in the reactor can be expressed by:

$$-\frac{dB}{dA} = \frac{\sqrt{s}}{1 + \sqrt{s}} - \frac{1}{\sqrt{s}} \frac{B}{A} \quad ....49$$

and integration yields:

$$\alpha_B = \frac{S}{S-1} (1-\alpha_A) \{(1-\alpha_A)^{-(1-1/\sqrt{s})} - 1\} \quad ....50$$

A direct comparison between the yield in the presence and absence of pore diffusion is shown in Figure 19. The maximum loss of yield possible for very low effectiveness factors is reported to be approximately 50% (67). The observed selectivity becomes independent of the modulus at values of ε less than 0.3 ($\phi > 3$), and the decrease in selectivity all occurs in the region $1.0 > \varepsilon > 0.3$. In this range, then, it should be possible to increase the yield of a desired intermediate substantially by subdividing the catalyst or altering the pore structure so as to increase the effective diffusivity. If the effectiveness factor is well below 0.3, a large reduction in pellet size or large

FIGURE 19

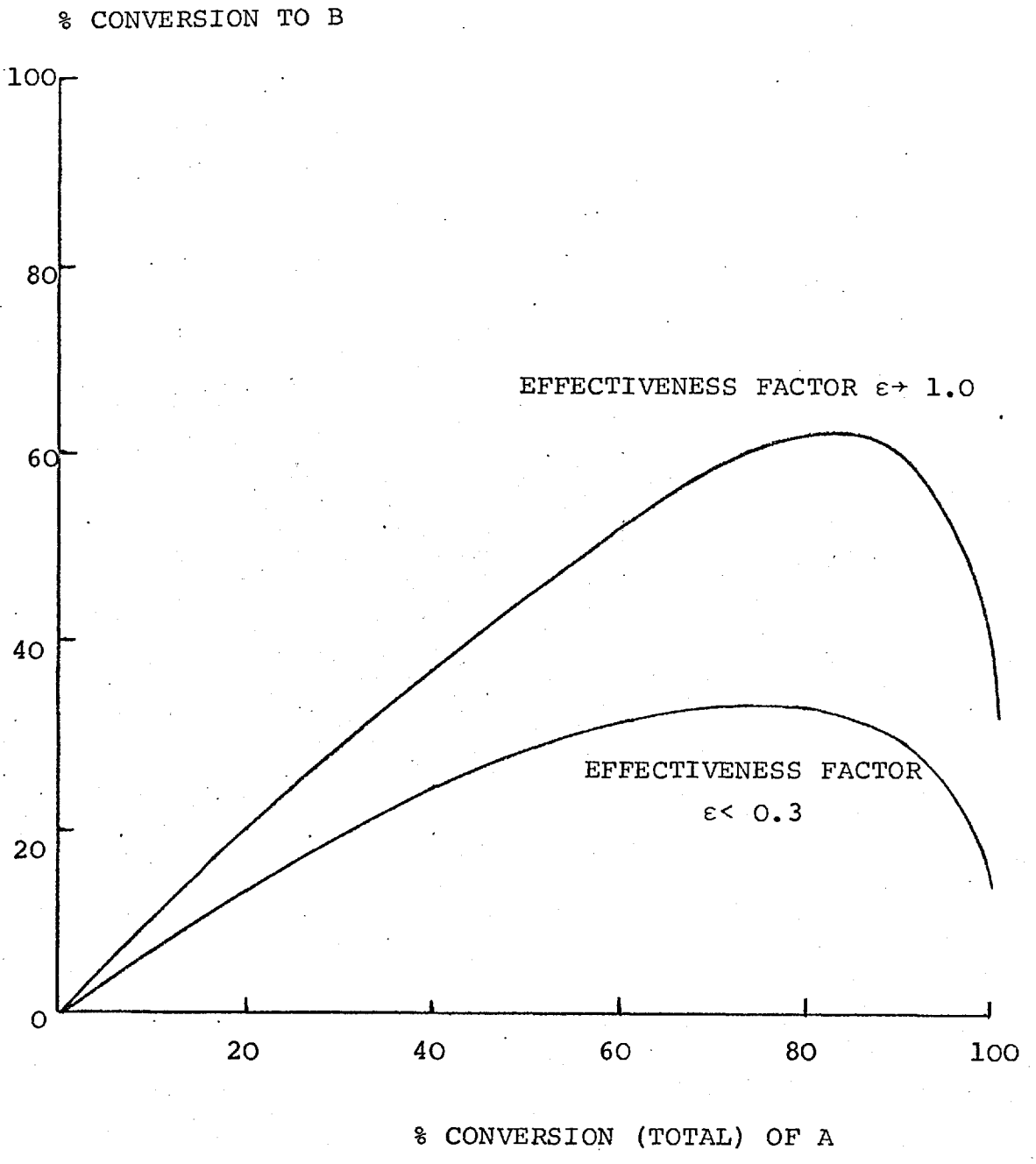

Effectiveness factor and catalyst selectivity for reactions of the type $A \overset{k_1}{\rightarrow} B \overset{k_2}{\rightarrow} C$ $(k_1/k_2 = 4.0)$ (67).

increase in effective diffusivity is required to obtain any significant improvement in selectivity.

(iv) Heat and mass transfer

a) To the catalyst particle

The theory discussed above has been applied mainly to isothermal conditions which, since oxidation reactions are usually very exothermic, is synonymous with low conversions in this instance. If thermal effects do become important, it is possible to assess heat and mass transfer effects in the system using similar techniques since both are transferred between solid and fluid by similar mechanisms. Data on heat transfer in fixed beds are correlated in the same way as data on mass transfer (68) in the form of a dimensionless expression:

$$j_D \equiv \frac{k_c \rho}{G} N_{Sc}^{2/3} \qquad j_H \equiv \frac{h}{C_p G} N_{Pr}^{2/3} \qquad \ldots.51,52$$

$$k_c \equiv \frac{N}{(C_o - C_s)} \qquad h \equiv \frac{q}{T_s - T_o} \qquad \ldots.53,54$$

$$N_{Sc} \equiv \frac{\mu}{\rho D} \qquad N_{Pr} \equiv \frac{c_p \mu}{k} \qquad \ldots.55.56$$

where j_H and j_D represent the dimensionless expressions for heat and mass transfer respectively and may be determined from established correlation with the Reynolds number, h and k_c are the heat and mass transfer coefficients, q and N are the heat and mass fluxes (per unit pellet surface area), N_{Pr} and N_{Sc} are the Prandtl and Schmidt numbers, T_s and T_o

are the temperature of the pellet and the fluid, C_s and C_o are the concentration at the pellet and in the fluid, C_p and k are the heat capacity and the thermal conductivity of the fluid, ρ and μ are the density and viscosity of the fluid, and D and G are the molecular diffusion coefficient and the mass velocity of the fluid respectively.

The relationship between importance of mass transfer control of the reaction and the temperature difference between the pellet surface and fluid may be derived for steady-state conditions, where the heat produced must equal the heat transferred from the surface. Under these conditions,

$$k_c(C_o-C_s)(-\Delta H) = h(T_s-T_o) \qquad ....57$$

which can be substituted for k_c and h (Equations 51, 52) to give:

$$(T_s-T_o) = \frac{j_D}{j_H}\left[\frac{N_{Pr}}{N_{Sc}}\right]^{2/3}\frac{(-\Delta H)}{\rho cp}(C_o-C_s) \qquad ....58$$

Introducing a term f, the extent of mass transfer control, which is defined as the ratio $(C_o-C_s)/C_o$, the equation reduces to

$$(T_s-T_o) = \frac{j_D}{j_H}\left[\frac{N_{Pr}}{N_{Sc}}\right]^{2/3}\frac{(-\Delta H)C_o}{\rho\ cp}\ f \qquad ....59$$

The quotient $(-\Delta H)C_o/\rho C_p$ represents the temperature rise that would be observed for complete adiabatic reaction of the fluid mixture. Since the ratio j_D/j_H is about 0.7 and the ratio N_{Pr}/N_{Sc} (for most gas mixtures) is approximately unity, for a completely mass transfer controlled reaction (f = 1) the temperature difference between the gas and the solid would be expected to be about 70% of the calculated

adiabatic temperature rise for complete reaction. For oxidative reactions, where the reaction is usually exothermic, the temperature rise during mass transfer control will be expected to be large and will tend to lead to more unselective reactions.

b) In the catalyst particle

In practice it has been found that substantial temperature gradients can sometimes occur in a porous catalyst and there have been a number of publications describing mathematical analyses of this effect (69, 70, 71). As a result of this temperature rise the effectiveness factor can become much larger than unity; a typical family of curves relating the effectiveness factor to the Thiele modulus for a given set of operating variables is shown in Figure 20. The definition of effectiveness factor must, of course be referred not only to the concentrations but also to the temperature of the exterior surface.

The system also responds to two characteristic parameters γ and β, where γ is the exponent in the Arrhenius reaction rate expression, E/RT and β is a heat generation function $c_s(-\Delta H)D/\lambda T_s$, where ΔH is the heat of reaction and λ is the thermal conductivity of the porous catalyst. The heat generation function β also represents the maximum temperature difference that could exist in the particle relative to the surface temperature, $(T-T_s)max/T_s$. High temperature differences can occur if ΔH is large and exothermal and the

FIGURE 20

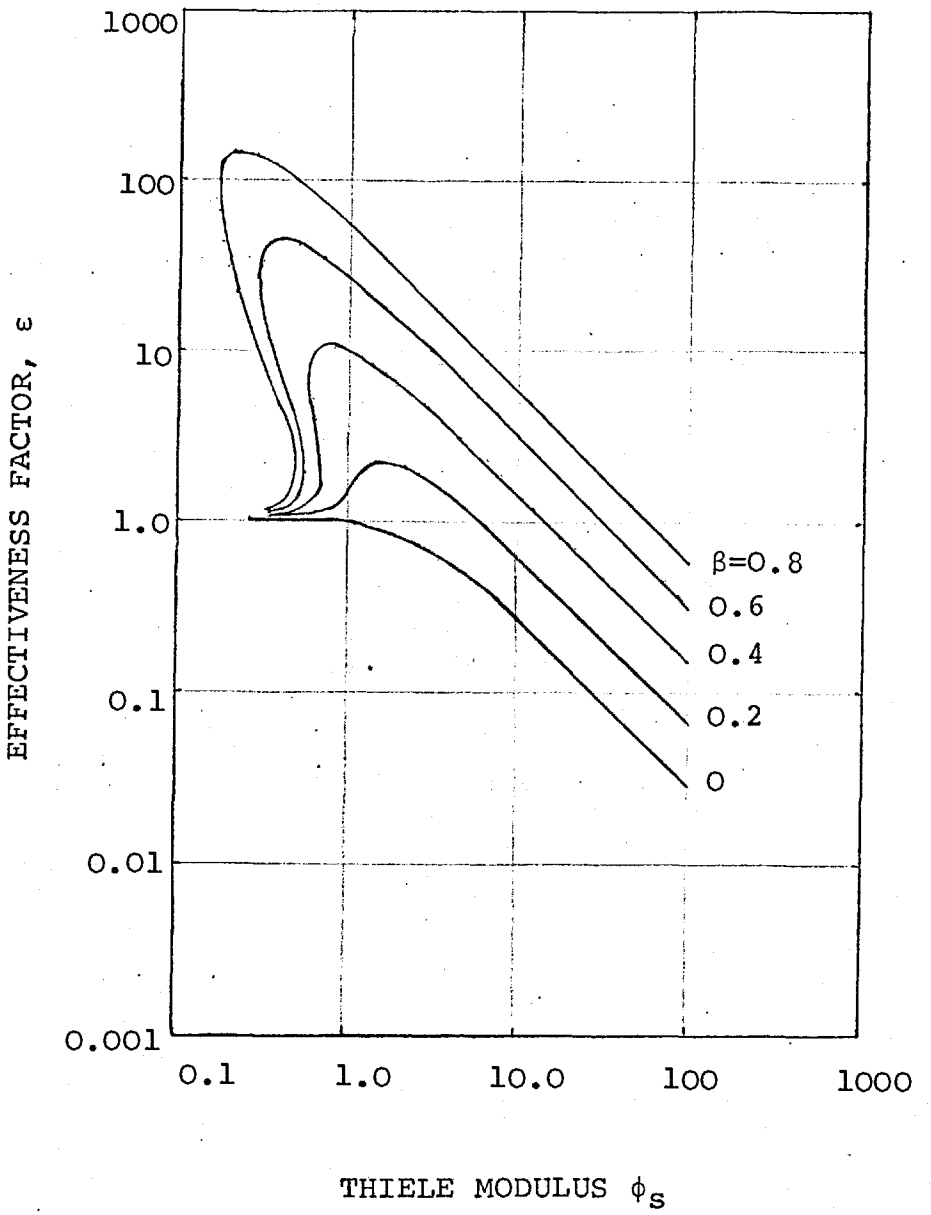

Effectiveness factor ε as a function of Thiele modulus ϕ_s for γ=20. First-order reaction in sphere (70).

thermal conductivity (λ) of the porous catalyst is low, as is common for oxidation catalysts. The results in Figure 20 were evaluated at $\lambda = 20$ (activation energy of 24,000 calories and reaction temperature of 600^{o}K) with the curve $\beta = o$ representing the isothermal case. For exothermic reactions ($\beta > o$), the effectiveness factor ε may exceed unity, since the increase in rate caused by the temperature rise towards the centre of the particle more than offsets the decrease in rate caused by the drop in concentration. In practice, if the temperature becomes too high, the reactants will be consumed near the pore mouth and mass transfer to the surface will become rate controlling.

The effect of this temperature rise on the selectivity of consecutive reactions has not been mathematically analysed because of the complexity of the problem. Considering a physical picture, the intermediate product produced in a pore is known to have a higher probability of reacting further under the influence of pore diffusion. If a higher temperature exists inside the pore, the rates of reaction would be higher and the intermediate product is even more likely to react further. As a result, the selectivity is likely to be reduced.

It is also apparent that, whereas, under isothermal conditions the observed activation energy can be as low as one-half the true value, the opposite effect can occur when $\varepsilon > 1$, i.e., the apparent activation energy can exceed the true value (71). In addition, it is possible to have

effectiveness factors greatly exceeding unity at relatively low observed reaction rates, conditions under which analysis assuming isothermal operation (β = o) would indicate an effectiveness factor of essentially unity.

(v) Summary of the effect of catalyst properties

a) Chemical rate controlling

The physical properties of the catalyst have no effect on the selectivity but the surface area (concentration) of active species controls the activity and heat release.

b) Film diffusion controlling

As mass and heat transfer depends on the fluid properties rather than the catalyst, the rate of chemical reaction must be decreased to make the reaction kinetics independent of diffusion. This will tend to improve selectivity.

c) Strong pore diffusion

The effectiveness factor and the selectivity can be increased by decreasing the particle size or surface area or by increasing the pore radius. The temperature rise in the pores can best be controlled by lowering the heat generated (by decreasing the surface area (porosity)) or by increasing the thermal conductivity of the catalyst (using a support or different pelleting conditions).

3. The development of a mechanism for the production of benzene from propylene

It is clear from the above discussion that the selection of catalysts is not practicable on purely theoretical grounds at present, but that it is possible to recognize possible catalysts by combination of theoretical arguments and experimental observations. It is rewarding to outline this exercise in the context of the production of hexenes and benzene from propylene. The desired reaction sequence should take the form

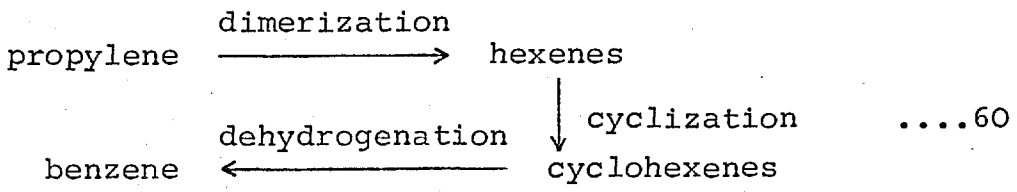

where some dehydrogenation may occur before cyclization.

Consideration of various alternative possibilities showed that there were definite advantages to the use of oxidative atmospheres; although other possibilities are discussed, the subsequent discussion is primarily directed to such systems. Complicating reactions may occur, such as the oxidation of propylene to compounds such as acrolein and the over-oxidation of any product to carbon dioxide.

3A. Dimerization

The thermodynamics of conventional dimerization favour high yields only at temperatures less than 300°C or at high pressures (75). The equilibrium yield expected

for the conversion of propylene to a linear hexene is expected to be always less than conversion to a branch chain hexene (76). For example, dimerization at 600°K would be expected to produce only 36% (relative to propylene) of hexene-1, but 81% of the branched trans-3-methylpentene-2. With increasing temperature the branched chain isomer is staill favoured; at 700°K, 7% conversion to hexene-1 and 38% conversion to trans-3-methylpentene-2 can be expected.

Catalytic polymerization (dimerization) can involve either free radical or ionic intermediates, where "ionic" polymerization may be either cationic or anionic. Acid-catalysed (cationic) polymerization of olefins is easily explained in terms of the classical carbonium theory (Figure 21a). Proton addition to a double bond is followed by the addition of the carbonium ion to the double bond of a second propylene. The dimeric ion may then lose a proton to the catalyst, or to another propylene molecule, or become involved in further addition reactions. The degree of polymerization is related to the realtive case of expulsion of a proton and of further polymerization. The product obtained tends to be a branched chain molecule, and isomerization, together with further polymerization, may lead to a wide variety of products (77).

A corresponding reaction involving anionic intermediates can be observed over alkali metals (Na, K, Li) (78) and their derivatives (hydride, alkyl amide) (79). Propylene can be dimerized to a mixture of double-bond

FIGURE 21

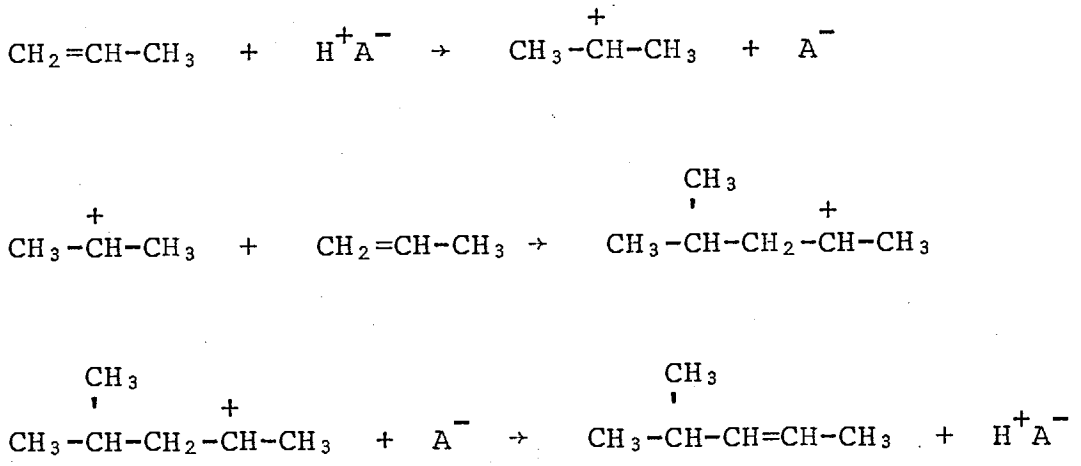

(a)

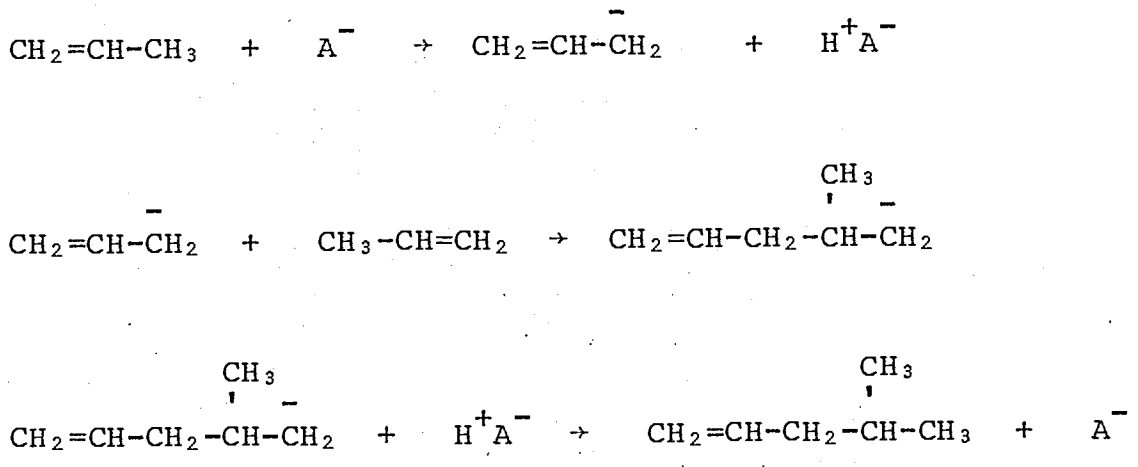

(b)

The mechanism of ionic dimerization of propylene a) cationic and b) anionic.

isomers of the branched 2-methylpentene at 150°-200°C and 70-350 atm with the main product, as expected from the reaction mechanism (Figure 21b), being 4-methylpentene-1. The high yield of the dimer shows that the dimeric carbanion must be short-lived in the presence of other propylene molecules and does not grow to higher polymers.

A very similar reaction has been observed by Ziegler, using alkyl-aluminum catalysts (80). The alkyl groups of $Al-(C_2H_5)_3$ were found to grow by addition of C_2H_4 at about 100°C and 100 atm via a mechanism similar to anionic polymerization. The growth is terminated by an exchange reaction involving the displacement of the polymer by a less substituted olefin. Carefully controlled, this termination step can be used to limit the extent of polymerization. Thus, for example, if the temperature is controlled at 140°C (increase of temperature favours the exchange reaction) the polymerization of propylene can be stopped at the production of 2-methylpentene-1 (80).

Polymerization can also occur as a result of the attack on the double bond of an alkene by a free radical:

$$NC-\overset{CH_3}{\underset{CH_3}{C}}\cdot + CH_2=\overset{H}{\underset{CH_3}{C}} \rightarrow NC-\overset{CH_3}{\underset{CH_3}{C}}-CH_2-\overset{H}{\underset{CH_3}{C}}\cdot \qquad \ldots.61$$

The polymer so formed behaves similarly to an ionic intermediate, being free to attack another double bond

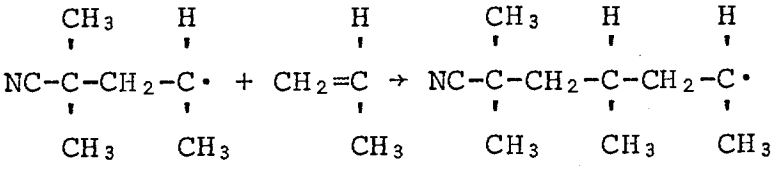

....62

or to exchange with propylene producing a hydrogenated molecule and a monomer radical, or to combine with another free radical to stop the polymer growth. The chain length of the product polymers vary widely in the case of propylene, and the initial radical generating species becomes incorporated into the polymer.

The arguments against the use of any of these processes are similar and can be considered together. One main problem is that the dimer is the required product while, with exception of anionic or Ziegler catalysts, most polymerization catalysts produce a wide spectrum of products. Since the product must be cyclized to eventually produce benzene, linear dimers are necessary but all the above reactions produce branched chain molecules. If higher molecular weight polymers are formed, these tend to poison the catalyst.

To sum up, although dimeric products may be formed by anionic polymerization, the products tend to be branched chain molecules produced non-selectively. In this event it would seem preferable to consider alternative routes of producing linear hexenes.

Consideration of the mechanism of the oxidative dehydrogenation of butene to butadiene led to the suggestion that a similar type of sequence could result in the desired

product. Adsorption of butene on a suitable catalyst leads to the removal of an H entity and the formation of a π adsorbed intermediate, similar to those observed during the oxidation of propylene to acrolein:

$$CH_2=CH-CH_3 \rightarrow \underset{\downarrow\pi}{CH_2-CH-CH_2} \quad ....63$$

The exact mechanism is discussed later in this section. Obviously, if it is possible to produce two such entities adsorbed on adjacent sites, then dimerization may occur:

$$\underset{\downarrow\pi}{CH_2-CH-CH_2} + \underset{\downarrow\pi}{CH_2-CH-CH_2} \rightarrow CH_2=CH-CH_2-CH_2-CH=CH_2 \quad ...64$$

Such processes have been observed in the gas phase, for example, in a free radical reaction in which initial hydrogen was abstracted by hydrogen peroxide (81). No report of such a reaction occurring over a catalyst could be found.

3B. Cyclization

The cyclization of paraffins and olefins over metal oxides (Cr_2O_3,MoO_2) and metal-acidic oxides ($Pt-Al_2O_3$) has been intensively studied, as the reaction is an important part of the reforming process. Both types of catalysts are fairly selective to aromatics at low hydrogen pressures (50% to 60% toluene) but tend to deactivate. The reaction is believed to involve the dehydrogenation and subsequent cyclization of the paraffin, and the rate of cyclization is much faster than dehydrogenation. Since the reactions are

sequential, any factor - such as the presence of a metal component - designed to facilitate dehydrogenation will accelerate the overall reaction.

Both types of catalysts are poisoned quickly at low pressures of hydrogen by coke formation on the surface. Thus, for example, Feighan and David (82) have reported that the yield of toluene over unsupported Cr_2O_3 decreases from 95% to 14% in three hours. The acidic nature of the catalysts seems to promote coke formation but the poison can be removed by hydrocracking in the presence of high pressures of hydrogen. Unfortunately, such high pressures supress the cyclization reaction: for example, over $Pt-Al_2O_3$ reforming catalysts, the yield of toluene from heptene decreases from 58.8% at 100 psig to 11.2% at 500 psig (83). As a result, conventional dehydrocyclization of paraffins and olefins has proven to be uneconomic due to deactivation of catalysts (84).

Under these circumstances, the advantages to be gained if it is possible to operate this type of reaction under oxidative conditions become obvious, and various recent studies of possible reactions have been initiated. Chambers and Boudart compared hydrogen and oxygen atmospheres for the dehydrogenation of cyclohexane to benzene over gold (85). In a hydrogen atmosphere, hydrogenation to cyclohexane reduced the selectivity to benzene, but in the presence of oxygen, the selectivity increased by a factor of 3000. Approximately 10% of the cyclohexene was converted to oxidized products. A similar qualitative study was carried out over $Pt-Al_2O_3$

and Cr_2O_3 catalysts (86) which showed that oxidative dehydrogenation and cyclization of olefins and paraffins is possible in oxidative conditions, although the circumstances of the investigation were such that few generalizations or comparisons of the advantages of an oxygen atmosphere were possible.

Considerable information has been obtained in recent years on the oxidative dehydrogenation of olefins over complex mixtures of oxides. Although these will be reviewed in the next section, it can be noted that Adams (87) has reported evidence of cyclization and dehydrogenation of hexenes over such catalysts. The oxidation of hexene-1 at 460°C over bismuth molybdate (conversion ~ 70%) gave 32% selectivity to benzene and 40% selectivity to hexadiene and hexatriene which could be further reacted to benzene. Hexene-2, heptene-1 and heptene-3 could also be cyclized over the same catalyst, producing good yields of benzene and toluene. The reaction mechanism has not been investigated.

3C. Oxidative dehydrogenation

The use of conventional dehydrogenation catalysts, involving metal oxides or metal-acidic oxides, was not considered suitable for the dehydrogenation of hexenes and cyclohexenes since the equilibrium conditions are unfavourable at high hydrogen pressures and yet the catalysts are poisoned by coke deposition at low pressures. Oxidative dehydrogenation, involving the removal of hydrogen

as water, seemed to offer much more scope. In reviewing the literature, it is necessary to consider not only the oxidation of olefins to diolefins but also the oxidation to aldehydes, since the process involves a similar reaction mechanism and occurs over the same catalysts. The scope of the reaction has been recently reviewed by Skarchenko (88). Other reviews, written by Sampson and Shooter (89) and Voge and Adams (90) emphasize respectively the role of the catalyst and the reactivity of different olefin structures in the reaction.

As a result of radiotracer studies, the reaction mechanism has been elucidated in some detail. Adsorbed intermediates are formed by hydrogen abstraction from the allylic carbon:

$$\begin{array}{l} CH_2{=}CH{-}CH_2{-}R \\ \quad\downarrow\pi \\ \quad M \quad O \end{array} \rightarrow \begin{array}{l} CH_2{-}CH{-}CH{-}R \\ \quad\quad\downarrow\pi \quad\quad H \\ \quad\quad M \quad O \end{array} \qquad \ldots.65$$

with the carbon skeleton losing the identity of the allylic carbon and the furthest vinyl carbon (91).

Using propylene labelled with deuterium in various positions, Adams and Jennings (92, 93) concluded that the allylic intermediate is attacked at a hydrogen atom rather than at a carbon atom. The second abstraction of hydrogen was found to occur if possible at a carbon adjacent to the allylic carbons thereby producing a diene:

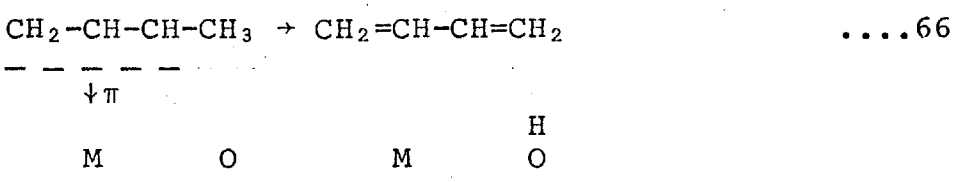

....66

If such an abstraction could not occur, the hydrogen of a terminal carbon of the allylic intermediate was removed and further reaction occurred by oxygen insertion:

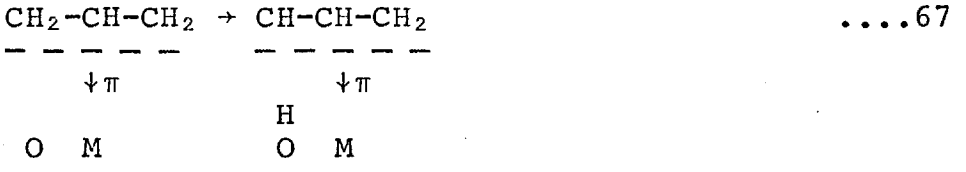

....67

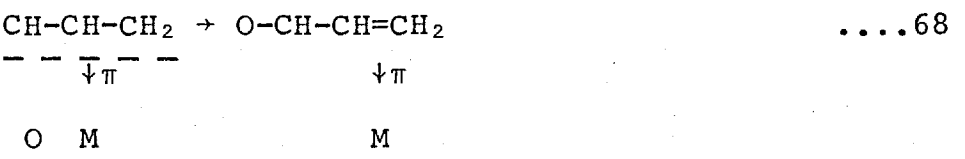

....68

Where the formation of a diene is possible, the reaction is much faster than the formation of an aldehyde (94). The reaction can be very selective: butene-1, for example, reacts to butadiene over bismuth molybdate with 90% selectivity at 80% conversion.

The mechanism for oxidative dehydrogenation can be speculatively applied to oxidative cyclization. Considering a linear six carbon compound, it would seem possible to dehydrogenate an olefin or diolefin to an absorbed hexatriene:

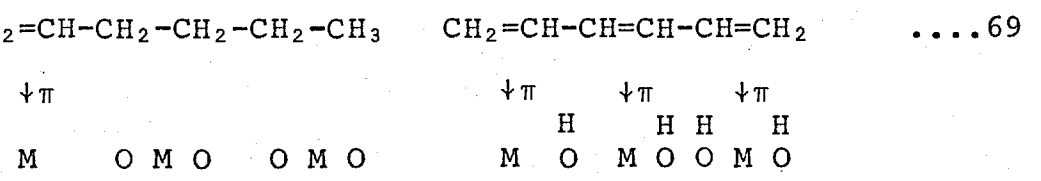

....69

which might be expected to desorb. However the observed inhibition of oxidative dehydrogenation by products of parent olefins of carbon number greater than four (87) indicates that surface coverage by the diolefin should be very high. Under these circumstances the absorbed hexatriene might well be expected to react further to oxygenated products (CO_2) or to cyclize to 1,3 cyclohexadiene:

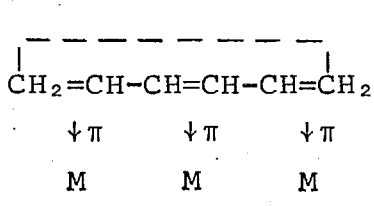

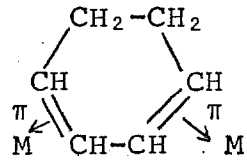

....70

which will probably quickly dehydrogenate to benzene. Benzene is known to be a very stable molecule and should easily desorb.

3D. Proposed mechanistic scheme

From the above, it would appear that there are definite benefits if each stage of the overall mechanism (summarized in Figure 22) is completed in the presence of oxygen. If propylene is initially adsorbed by being π-bonded to a metal site, and a oxygen atom (either lattice or chemisorbed oxygen) abstracts an allylic hydrogen to form a bonded allylic intermediate, then dimerization (step 2) may produce the linear dimer 1,5 hexadiene and as an undesirable side reaction, acrolein (step 6). Preferably the rate of dimerization should be as fast as possible with respect to the second hydrogen abstraction. The adsorbed

FIGURE 22

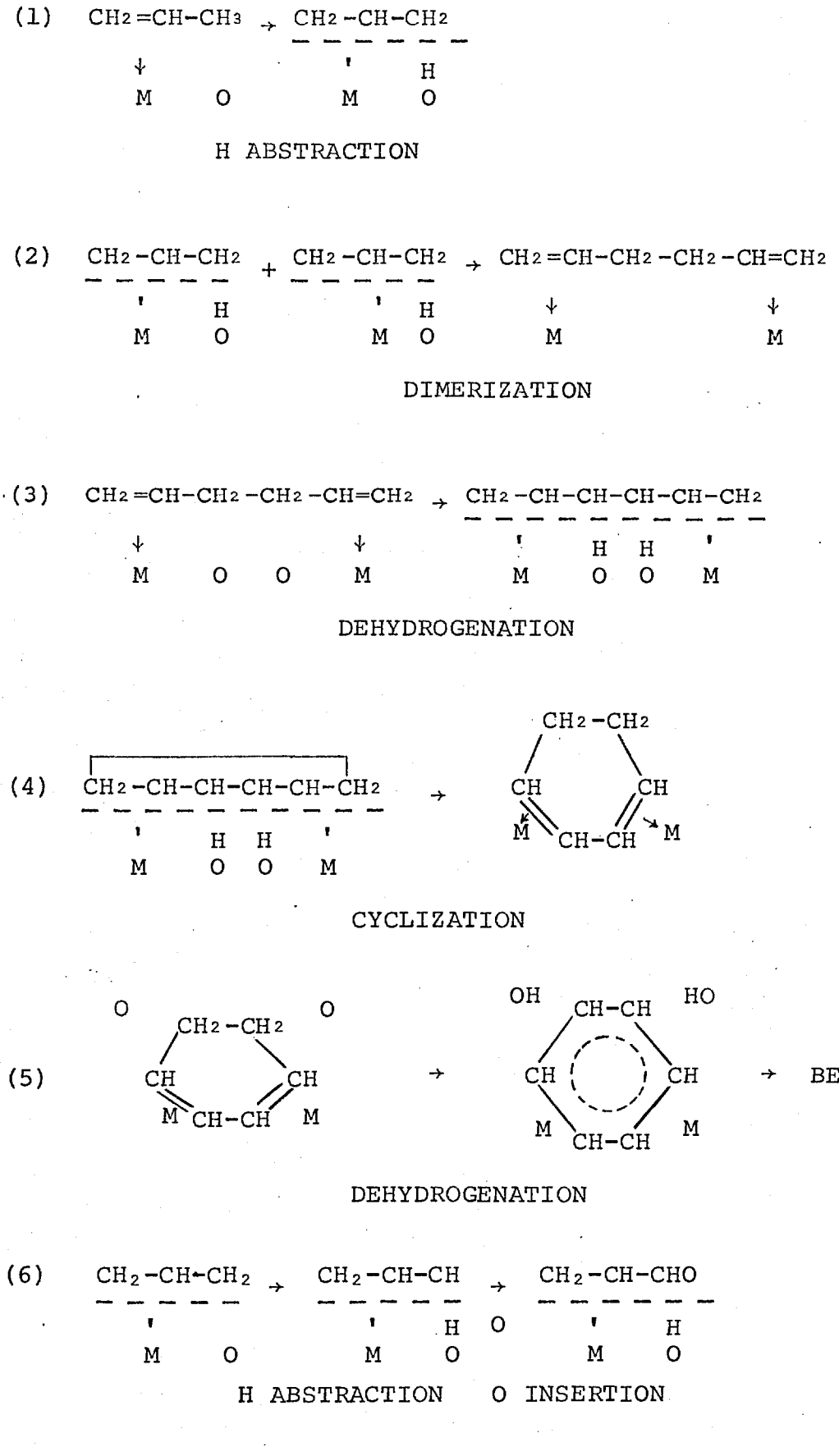

Proposed mechanism for oxidative dimerization-cyclization reaction of propylene.

hexadiene should then be quickly dehydrogenated to the hexatriene which, in turn, can cyclize to 1,3 cyclohexadiene or combust to carbon dioxide. The cyclohexadiene should dehydrogenate to benzene by losing two hydrogen atoms. All intermediate products, 1,5 hexadiene, hexatriene and 1,3 cyclohexadiene together with benzene should tend to desorb to some extent and should appear in the gas phase.

4. The selection of catalyst components

Although the dimerization reaction appears to be very similar to the dehydrocyclization reaction, it is probably best to treat them differently for the purpose of catalyst development. Both sequences have the common initial step of hydrogen abstraction, but it is the processes following the abstraction that control the selectivity, as is discussed below.

4A. Dimerization components

Two approaches to the design of this catalyst component are apparent:

(1) Data available in the literature can be screened for possible oxidative dimerization activity.

(2) A mechanistic approach can be adopted, where the necessary properties are recognised from the mechanism and information is reviewed with a view to finding a solid with the desired characteristics.

In the first approach, the only information available came as a side-result from consideration of non-oxidative reactions, in which the dimerization of propylene was found to occur over a cobalt oxide on carbon catalyst (95). Selectivites of 50% to n-hexenes were reported with an equal amount of branched-chain hexenes produced. The mechanism proposed suggested that at least one molecule of olefin could π adsorb probably at a cobalt hydride site, although the possibility of a reaction producing cobalt hydride and a cobalt π allylic complex at the same time (via hydrogen abstraction by cobalt) was discussed. A similar process could also occur in an oxidative atmosphere resulting in a fast dimerization reaction. By similar arguments, nickel oxide (which on silica-alumina is reported to dimerize propylene to hexene (96)) may also be suitable (97).

It was also rewarding to consider cyclization systems as potential oxidative dimerization catalysts. It has been suggested by Steiner (84) that the possible function of the oxygen anions in a metal oxide cyclization catalyst could be to react with a hydrogen from a hydrocarbon, leaving the residual alkyl radical which can interact with the metallic cation. This role of the lattice oxygen is, in fact, similar to the proposed role of oxygen in the hydrogen abstraction step. Now, all the conventional cyclization catalysts are deactivated by coke production as a result of the polymerization of olefinic compounds on the surface (98). Olefinic compounds are known to be strongly adsorbed on the catalyst (84) and interaction between adsorbed species

is not unexpected. It seems possible then, though not probable, that normal cyclization catalysts such as $Pt-Al_2O_3$, Cr_2O_3, MoO_2 and ThO_2 could prove active for dimerization in an oxidative atmosphere.

The second method of approach necessitates the definition of the desired electronic structure for adsorption and selective reaction. In order to obtain a fast and selective dimerization reaction, the two allylic intermediates must preferably either be very close together (and - at the optimum - on one site) or alternatively should be mobile. In order to obtain a linear molecule, the two intermediates should be π-bonded in order to preserve the double bond intact; solids which satisfy this requirement have the following electronic structure: d^0, d^1, d^2, d^3, d^8, d^9 and d^{10} (5). With the exception of d^{10}, these electronic structures are found in the transition metals. Metal ions such as Sn^{+4}, Sb^{+5}, Tl^{+3}, In^{+3}, Pb^{+4}, Bi^{+5}, etc. have a d^{10} electronic structure.

Referring to the reaction mechanism proposed in Figure 22, it can be seen that the first step involves abstraction of a proton by lattice oxygen ions, leaving a negatively charged allylic intermediate. As has been determined through work function measurements, the adsorbed allylic intermediate has a small positive charge (99) and hence there must be a transfer of an electron to the

catalyst:

$$\underset{\downarrow\pi \quad\quad\quad\quad \downarrow\pi}{\underset{M^{+m} \quad O^{-2}}{CH_2{=}CH{-}CH_3}} \rightarrow \underset{M^{+m-1} \quad H \; O^{-1}}{CH_2{-}CH{-}CH_2} \qquad \ldots.71$$

If the catalyst has a valency state lower by one than the initial state, the allylic-metal complex is stable and can react further with another ion:

$$\underset{\downarrow\pi \quad\quad\quad\quad\quad\quad \downarrow\pi \quad\quad H}{\underset{M^{+m-1} \quad O^{-2} \quad M^{+m}}{CH_2{-}CH{-}CH_2} \rightarrow \underset{M^{+m-1} \quad O^{-} \quad M^{+m-1}}{CH_2{-}CH{-}CH}} \qquad \ldots..72$$

and formation of acrolein should occur rapidly.

Now if the solid only has a valency state two below the initial state, then the ion requires two electrons in quick succession (or even simultaneously). As the second abstraction of hydrogen (Equation 72) is slow, the formation of acrolein would be unfavourable compared with the adsorption of two propylene molecules (Reaction 71), which can supply two electrons very quickly. As a result, two allylic intermediates may be π adsorbed next to each other on the same ion, and dimerization should be favoured. It would seem desirable, then, to use a catalyst component that could π adsorb olefins and yet which has two stable valency forms, 2 units apart.

Transition metals, which will π adsorb, do not meet these requirements, but solids with the d^{10} electronic structure do in some cases. Several such metals have both the d^{10} structure and the required two valency states. Examples

include: Sn^{+2} and Sn^{+4}, Tl^{+1} and Tl^{+3}, Pb^{+2} and Pb^{+4}, Bi^{+3} and Bi^{+5} and In^{+1} and In^{+3} which are members of Groups IIIb, IVb and Vb in the periodic table. Furthermore, in every case the lower valency state involves an "inert pair" of electrons and an electronic structure s^2 which does not π-bond with olefins (5). As a result, if two electrons are transferred to the ion, the resulting electronic structure releases the two allylic intermediates which can then dimerize in order to satisfy their bonding requirements. Since, lower valency state tends to become more stable as the Groups (IIIb, IVb and Vb) are descended (104), and as the desire for the electrons will be proportional to the stability of the lower state, the metal oxides of thallium, lead and bismuth would be expected to be the best catalysts, provided that the ions can be reoxidised to the higher state by molecular oxygen. Bismuth pentoxide is very unstable (100) and the catalytic effects of pure bismuth oxides are not easily studied. Lead dioxide, PbO_2, is also unstable and decomposes at 290°C to PbO via the intermediate oxides Pb_2O_3 and Pb_3O_4 which decompose at 360° and 500°C respectively (106). As a result, the most suitable catalysts would be expected to be the metal oxide of thallium and possibly the oxides of indium and tin.

4B. Dehydrocyclization components

It is known that catalysts comprising mixed oxides such as bismuth molybdate or tin-antimony oxides are capable to converting compounds such as hexadiene to

benzene. Conventional dehydrocyclization catalysts have been shown to exhibit similar properties in an oxygen atmosphere (85, 86, 101). For example, heptene was converted to toluene over $Pt-Al_2O_3$ in an oxygen atmosphere (86) and the oxidative dehydrogenation of cyclohexane has been studied over $Cr_2O_3-Al_2O_3$. Similarly, McHenry and fellow workers (101) found that the rate of cyclization increased by a factor of three while the rates of cracking and isomerization remained constant if a $Pt-Al_2O_3-Cl$ catalyst was treated with air before use. There appeared to be a complex formed between Pt,Al_2O_3 and oxygen which favoured dehydrocyclization; this complex was deactivated by the action of hydrogen produced in the reaction. As a result of these reports, it was thought that it might be possible that normal cyclization catalysts such as $Pt-Al_2O_3$, Cr_2O_3, MoO_3 and ThO_2 could be active and selective for dehydrocyclization in an oxygen atmosphere. Comparison of the activity of these components with bismuth molybdate and tin-antimony oxide catalysts should allow the selection of a suitable catalyst for the dehydrocyclization reaction.

5. The present work

It has been the intention of this research to recognise and to develop a novel system based on an oxidative dehydrogenation reaction combined with a dimerization-cyclization process, namely the production of hexadienes and

benzene from propylene. In order to do this, it has been necessary to develop and to apply a scheme of catalyst design based on existing knowledge, and to use this to make an initial selection of solids that may possibly catalyse the desired reactions. This part of the project, applied to the dimerization of propylene, the cyclization of hexene and the dimerization-cyclization of propylene, all in the presence of oxygen has been described in the introduction in order to follow logically the development of the sequence for catalyst design.

Possible catalysts, as a result of this process, can be examined experimentally, and further design of the catalysts or study of the reactions will be necessary on the basis of these results. The course of this testing and subsequent studies are described in the following sections.

SECTION II.

EXPERIMENTAL

1. Materials

The purity and source of all materials that have been used are reported in Tables 7, 8 and 9. Tables 7 and 8 list the liquid organic materials and gases respectively. All the chemicals used in the catalyst preparations, described in the following section, are tabulated in Table 9. The letters under the column headed catalyst refer to Table 10 in the following section.

2. Catalyst preparations

All catalysts except those obtained from commercial sources were prepared in small amounts by one or more methods as described below. The catalysts were dried on large clock glasses in an electric oven and activation took place either in the reactor or in an electric furnance (Gallenkamp 0-1200^{o}C). The catalysts were always pretreated at reaction temperature in the reactor under a stream of oxygen and nitrogen. The more important preparation variables for each catalyst are listed in Table 10. A more comprehensive description of the preparation of each catalyst follows.

2A. Pt-Al_2O_3-Cl

This general reforming catalyst kindly supplied by Esso Petroleum Company contained approximately 0.3 wt % Pt and 0.6 wt % Cl. The catalyst had a high surface area (~ 200 m/gm) with a metal surface area of approximately

TABLE 7

Organic materials

NAME	PURITY %	USE	SOURCE
hexene-1	97	reactant	R.N. Emanuel
cyclohexene	99.5	identification	"
1,5 hexadiene	98	product-reactant	"
1,4 cyclohexadiene	96	identification	"
1,3 cyclohexadiene	95	product	"
3 methylpentene-2	92	identification	"
3,3 dimethylbutene-1	94	"	"
hexatriene	92	product	"
hexene-2	99	identification	B. Newton Maine
2,3 dimethylbutene-2	99	"	"
2 methylpentene-2	95	"	"
4 methylpentene-1	99	"	"
2 ethylbutene-1	94	"	"
2 methylpentene-1	94	"	"
4 methylpentene-2	95	"	"
1,2 epoxypropane	99	"	B.D.H.
acrolein	99	product	"
acetaldehyde	99	identification	"
hexyne-1	99	"	Phase separations
hexene-3	98	"	"
3 methylpentene-1	99	"	"
benzene	Analar	product-reactant	Hopkin and Williams

TABLE 8

Gases

NAME	PURITY %	USE	SOURCE
oxygen	99	reactant	British Oxygen Corp.
nitrogen	99	diluent	" "
air	-	F.I.D.	" "
hydrogen	99+	chromatographs	" "
1,3 butadiene	99.5	reactant	Air Products
chlorine	99.5	catalyst preparation	" "
carbon monoxide	99.9	identification	" "
propylene	95	reactant	" "
carbon dioxide	99	identification	Distillers Ltd.

TABLE 9

Catalyst materials

NAME	PURITY %	CATALYST	SOURCE
NH_3 solution	35	most	B.D.H.
$Cr(NO_3)_3.9H_2O$	99	B	"
$Th(NO_3)_4.6H_2O$	99	I	"
$Co(NO_3)_2.6H_2O$	99	P	"
$TlNO_3$	98	J,K,L,M	"
NaOH	96	J,K,L,M	"
$Bi_2O_2CO_3$	90% Bi_2O_3	F	"
$Bi(NO_3)_3.5H_2O$	98	G,H	"
H_2MoO_4	90% MoO_3	H	"
$Na_2WO_4.2H_2O$	99	O	"
Tl_2SO_4	99.5	O	"
Tl_2O_3	99	N	"
$In_2(SO_4)_3$	99.5	R,S,T,U,V,W	"
$Al(NO_3)_3.9H_2O$	98.5	B,C,I,J,P,Q	Hopkin and Williams
$(NH_4)_6Mo_7O_{24}.4H_2O$	80% MoO_3	C,F,G	"
$Ni(NO_3)_2.6H_2O$	98	Q	"
$Na_2HPO_4.12H_2O$	99	W	"
pumice	-	T,U,V	"
Al_2O_3 fused	-	L,N	Norton Catalyst Carriers
Al_2O_3 activated	-	K	-

TABLE 10

Important catalyst preparation variables

CATALYST	CONSTITUENTS WT%	PREPARATION METHOD	TEMPERATURE °C DRYING	TEMPERATURE °C ACTIVATION
2A	Pt - 0.3 Al_2O_3 - 99 Cl - 0.6	commercial	-	500 air
2B	Cr_2O_3 - 10 Al_2O_3 - 90	coprecipitation	150	500 air
2C	MoO_3 - 10 Al_2O_3 - 90	coprecipitation	120	500 air
2D	SnO_2 - 20 Sb_2O_5 - 80	commercial	-	500 air
2E	Bi_2O_3 - 50 MoO_3 - 41 P - 1 SiO_2 - 7	commercial	-	500 air
2F	Bi_2O_3 - 62 MoO_3 - 38	coprecipitation	150	500 air
2G	Bi_2O_3 - 62 MoO_3 - 38	self precipitation	150	500 air

TABLE 1o continued

CATALYST	CONSTITUENTS WT%	PREPARATION METHOD	TEMPERATURE °C DRYING	TEMPERATURE °C ACTIVATION
2H	Bi_2O_3 - 77 MoO_3 - 23	boiling	120	500 air
2I	Th O_2 - 33 Al_2O_3 - 67	coprecipitation	130	500 O_2
2J	Tl_2O_3 - 16 Al_2O_3 - 84	coprecipitation	150	500 air
2K	Tl_2O_3 - 80 Al_2O_3 - 20	Tl_2O_3 precipitated and wet-mixed with Al_2O_3	150	500 air
2L	Tl_2O_3 - 60 Al_2O_3 - 40	Tl_2O_3 precipitated and wet-mixed with Al_2O_3	150	500 air
2M	Tl_2O_3	precipitated	dessicated R.T.	500 air
2N	Tl_2O_3 - 60 Al_2O_3 - 40	commerical Tl_2O_3 wet-mixed with Al_2O_3	140	500 air
2O	Tl_2WO_4	precipitated	150	500 air
2P	CoO 50 Al_2O_3 - 50	coprecipitated	150	500 air
2Q	NiO - 50 Al_2O_3 - 50	coprecipitated	150	500 air

TABLE 10 continued

CATALYST	CONSTITUENTS WT%	PREPARATION METHOD	TEMPERATURE °C DRYING	TEMPERATURE °C ACTIVATION
2R	In_2O_3	precipitated	150	560 air
2S	In_2O_3	precipitated	120	240 air 560 air
2T	In_2O_3 Pumice	impregnated	120	820 air
2U	In_2O_3 from 2S Pumice	wet-mixed	130	reaction temp.
2V	In_2O_3 Pumice	impregnated-precipitated	140	500 air
2W	In_2PO_4	precipitated	150	500 air

40 m^2/gm. The catalyst was activated at 500°C overnight in a stream of oxygen-nitrogen.

2B. Cr_2O_3-Al_2O_3

The catalyst was coprecipitated from a solution containing 26.4 grams $Cr(NO_3)_3.9H_2O$ and 336 grams $Al(NO_3)_3.9H_2O$ at a pH of 7.0 by the addition of NH_3 solution. The precipitate was filtered, washed five times, dried at 150°C overnight and activated at 500°C in a stream of O_2 and N_2. The final catalyst contained approximately 10% by weight of Cr_2O_3 and was expected to have a rather high surface area (100-300 m^2/gm).

2C. MoO_3-Al_2O_3

A solution of NH_3 was added to a solution of 6 grams $(NH_4)_6Mo_7O_{24}.4H_2O$ and 336 grams $Al(NO_3)_3.9H_2O$ to coprecipitate the desired catalysts. After filtering, the catalyst was washed four times in a weak ammonia solution; dried at 120°C and activated at 500°C. The surface area of the finished catalyst would be expected to be relatively high due to the Al_2O_3. The final MoO_3 concentration was approximately 10% by weight.

2D. SnO_2-Sb_2O_5

The catalyst was kindly supplied by BP(UK) Ltd. and is normally used as a selective oxidative dehydrogenation

catalyst (102). The surface area is approximately $7m^2/gm$ and the percentage compositions of the two main constituents of the catalyst are 15.4% by weight tin and 61.7% by weight antimony.

2E. Bi_2O_3-MoO_3

The catalyst is generally used for mild oxidation or oxidative dehydrogenation (103). This catalyst was kindly supplied by I.C.I. and had the empirical formula $(Bi_9PMo_{12}O_{52})$ $(SiO_2)_5$. The SiO_2 acts as a support giving the catalyst a higher surface area (~ 90 m^2/gm).

2F. Bi_2O_3-MoO_3 coprecipitation

250 gm $Bi_2O_2CO_3$ were dissolved in an acid solution and to this were added 167 gm $(NH_4)_6$ $Mo_7O_{24}.4H_2O$. A mixture of the hydroxides was precipitated by the addition of an NH_3 solution. The precipitate was filtered, and then washed and filtered five times, dried at 150°C and activated at 500°C. The catalyst contained equal atomic amounts of Bi and Mo and from values reported in the literature (104) the surface area was low (< 10 m^2/gm).

2G. Bi_2O_3-MoO_3 self precipitation

A catalyst of equal atomic amounts of Bi and Mo was prepared by precipitation under the conditions described by Adams (87). 240 gm of $Bi(NO_3).5H_2O$ in solution were mixed with 167 gm $(NH)_6Mo_7O_{24}.4H_2O$ at about pH5. The

resulting precipitate was filtered, dried and activated at 500°C.

2H. Bi_2O_3-MoO_3 boiling (104)

$Bi(OH)_3$ was precipitated from solution by ammonia and thoroughly washed by decanting. To this solution was added H_2MoO_4 to produce a Bi to Mo ratio of 2:1 and the entire solution was well stirred and allowed to boil. The boiling and stirring produced a change of colour from white to yellow and after two days the solids were filtered and dried at 120°C. The dried solid was activated in air at 500°C.

2I. ThO_2-Al_2O_3

ThO_2 and Al_2O_3 were coprecipitated as their respective hydroxides from a solution containing 22 gm $Th(NO_3)_4.6H_2O$ and 130 gm $Al(NO_3)_3.9H_2O$. The hydroxide mixture was filtered and then washed five times. The wash solution contained a small amount of NH_3 to retard peptization. After drying overnight at 130°C, the catalyst was activated at 500°C for two hours in a stream of O_2. The final catalyst contained 33% by weight ThO_2 and 67% by weight Al_2O_3, which would be expected to impart a relatively high surface area.

2J. Tl_2O_3-Al_2O_3 coprecipitation

A solution of thallic ion was prepared by bubbling Cl_2 gas through a solution of 11.2 gm $TlNO_3$ at a temperature near 0°C. After the addition of a solution

containing 133 gm $AlCl_3$, both Tl_2O_3 and $Al(OH)_3$ were coprecipitated by the addition of a 2N NaOH solution. Due to the fact that $Al(OH)_3$ was precipitated as a gel while the Tl_2O_3 precipitated was granular, a non-homogeneous catalyst was obtained. The precipitate was filtered and then washed and filtered five times and then dried and activated. The yield of the catalyst, 16% by weight Tl_2O_3 on Al_2O_3, was approximately 60 gm.

2K. Tl_2O_3 (precipitation)-Al_2O_3 (activated) wet-mixed

The Tl_2O_3 was prepared by bubbling Cl_2 gas through a 30 gm $TlNO_3$ solution and precipitating the oxide with the addition of 2N NaOH. The precipitated Tl_2O_3 was filtered, washed and mechanically mixed with activated Al_2O_3. The resulting catalyst (80% by weight Tl_2O_3) was dried at 150°C overnight. Great difficulty was encountered in forming the catalyst into a suitable pellet and eventually the granular lumps were just sized by sieving. The catalyst was activated in a stream of O_2 and N_2 at 500°C. The surface area would be expected to be fairly low as the Tl_2O_3 was precipitated in a granular form.

2L. Tl_2O_3 (precipitation)-Al_2O_3 (fused) wet-mixed

The Tl_2O_3 was prepared from a solution of $TlNO_3$ by the method outlined for catalyst 2K. The precipitated Tl_2O_3 was filtered, washed and mechanically mixed with fused Al_2O_3. The catalyst was dried overnight at 150°C and activated at 500°C in a stream of O_2 and N_2. The resulting

catalyst contained approximately 60% by weight Tl_2O_3 and had a relatively low surface area.

2M. Tl_2O_3

The thallous ion in a $TlNO_3$ solution was oxidized to the thallic state by Cl_2 gas bubbling through the solution. The granular Tl_2O_3 was precipitated by a 2N NaOH solution. The excess solution was decanted off and the precipitate was washed by successive slurrying and decantations. The wet precipitate was allowed to dry for one week in a dessicator filled with silica gel. The catalyst was activated in the reactor at 500°C in a stream of O_2 and N_2.

2N. Tl_2O_3 (commercial)-Al_2O_3 (fused) wet-mixed

Commercial Tl_2O_3 was wet-mixed with fused Al_2O_3 to yield a catalyst containing 60% by weight Tl_2O_3. The catalyst was dried and activated.

2O. Tl_2WO_4

The preparation of Tl_2WO_4 as an active catalyst has been described in a Japanese patent (105). A solution of 48 gm Tl_2SO_4 was water-cooled continuously and a solution of 250 gm $Na_2WO_4.2H_2O$ was added dropwise. The solution was stored at room temperature until a white precipitate of Tl_2WO_4 was completely formed (1 hour). After decanting and washing several times, the catalyst was dried at 150°C and activated at 500°C overnight in a stream of O_2 and N_2.

2P. $CoO-Al_2O_3$

The hydroxides of CoO and Al_2O_3 were coprecipitated from a solution containing 125 gm $Co(NO_3)_2.6H_2O$ and 190 gm $Al(NO_3)_3.9H_2O$. A final catalyst containing 50% by weight CoO would be expected from these concentrations. The precipitate was filtered, washed five times, dried overnight and activated at 500°C. The surface area would be expected to be relatively high as both constituents were prepared from their hydroxide.

2Q. $NiO-Al_2O_3$

Great difficulty was encountered in preparation of this catalyst as $Ni(OH)_2$ is soluble in acid and in NH_4OH, and is also slightly soluble in water (106). A careful control of pH was necessary to precipitate the desired product. The $Ni(OH)_2$ is light green and the colour of the precipitate is an indication of the amount of $Ni(OH)_2$ precipitated. An NH_3 solution was added to a solution containing 336 gm $Al(NO_3)_3.9H_2O$ and 200 gm $Ni(NO_3)_2.6H_2O$ until the colour of the precipitate reached its maximum. The coprecipitated hydroxides were filtered, then washed and filtered five times. After drying overnight at 150°C, the catalyst was activated at 500°C in a stream of O_2 and N_2. The final concentrations were 10% by weight NiO and 90% by weight Al_2O_3. The high concentration of Al_2O_3 would impart a high surface area to the catalyst.

2R. In_2O_3 high temperature activation

A solution of NH_3 was added to a solution of

$In_2(SO_4)_3$ to precipitate the hydroxide. The precipitate was filtered and then washed and filtered three times, dried at 150°C overnight and activated at 560°C in a muffle furnace. The surface area was found to be 60 m^2/gm.

2S. In_2O_3 low temperature activation

It is known that $In(OH)_3$ is dehydrated sharply to In_2O_3 at 170°C (107). In order to have a better control of the pore-size distribution $In(OH)_3$, prepared as in the previous section, was activated at 240°C in a muffle furnace. After the catalyst changed colour from whitish-grey to a strong yellow, the temperature was raised above the expected reaction temperature to 560°C.

2T. In_2O_3 Impregnation

Pumice, 20-30 mesh, was soaked in a solution of $In_2(SO_4)_3$ for two hours. The excess liquid was removed by filtration and the impregnated pumice was dired overnight at 120°C. The dissociation pressure of $In_2(SO_4)_3$ varies with temperature as follows: (108)

T (°C)	771	780	803	815	820
P (mmHg)	250	315	600	790	900

and activation temperatures of approximately 820°C were used to decompose the sulphate. The concentration of In_2O_3 on the final catalyst was proportional to the concentration of the initial solution. The concentrations were very low as the pumice would only soak up a small amount of solution due to its low porosity.

2U. In_2O_3-pumice wet-mixed

Pure In_2O_3 was prepared as in section S and T. After activation at 240°C and at 500°C the catalyst was ground to a fine powder and made into a slurry by adding water. Pumice, 20-30 mesh, was added to the slurry and the mixture well stirred. As the slurry dried (due to the added pumice), more water and more pumice were added until all the In_2O_3 was on the pumice. The resulting catalyst was lightly yellow. It was dried overnight at 130°C and then activated at reaction temperature under a stream of air. The catalyst could contain from 14% to 70% In_2O_3 by weight but a non-homogeneous catalyst could easily result. The removal of catalyst dust before use, especially at the higher concentrations of In_2O_3, was found to be important.

2V. In_2O_3-pumice impregnation-precipitation

A catalyst, with a concentration less than could be obtained by wet-mixing, was required and the method of impregnation (2T) requiring high temperatures for decomposition, produced a brown In_2O_3 which seemed to be inactive (see following section). A method, combining impregnation and precipitation, was developed.

Pumice, 20 to 30 mesh, was soaked in a solution of $In_2(SO_4)_3$ and the excess solution was filtered off. Ammonia vapour was passed through the wet pumice in order to react with the $In_2(SO_4)_3$ and precipitate $In(OH)_3$. The solid was then dried overnight at 140°C and activated for one week at

500°C in a muffle furnace. Any concentration of In_2O_3 could be produced by varying the concentration of the initial solution or by recoating if necessary.

2W. $InPO_4$

20 grams of $In_2(SO_4)_3$ were dissolved in distilled water and added to an aqueous solution containing 28 grams $Na_2HPO_4.12H_2O$. Immediately a white precipitate formed which was then filtered and washed. After drying overnight at 150°C, the catalyst was activated at 500°C in a stream of air. The final catalyst was pure $InPO_4$ and had a low surface area.

3. Apparatus

All experiments were completed in a conventional "flow" system show schematically in Figure 23. The system was designed to allow heterogeneous catalytic reactions involving either gaseous or liquid reactants to be studied under isothermal and plug flow conditions. The system consists basically of three parts: the reagents delivery and measurement system, the reactor and furnace, and the analytical system.

3A. Reactant delivery and measurement

Gases flowing to the reactor were metered at constant pressure (measured by open ended manometers) through rotameters at a flow rate (2 cc/min upwards) which was controlled by fine control needle valves (Edwards/OS1D). The flow meters were calibrated for each gas used by the soap

KEY TO FIGURE

COMPONENT	DESCRIPTION
1	pressure regulators
2	manometers
3	rotameters
4	soap bubble flow meters
5	needle valves
6	vapourizor
7	micro-pump
8	reactor and furnace
9	sample valve
10	selector valve
11	flame ionization chromatograph
12	katharometer chromatograph

FIGURE 23

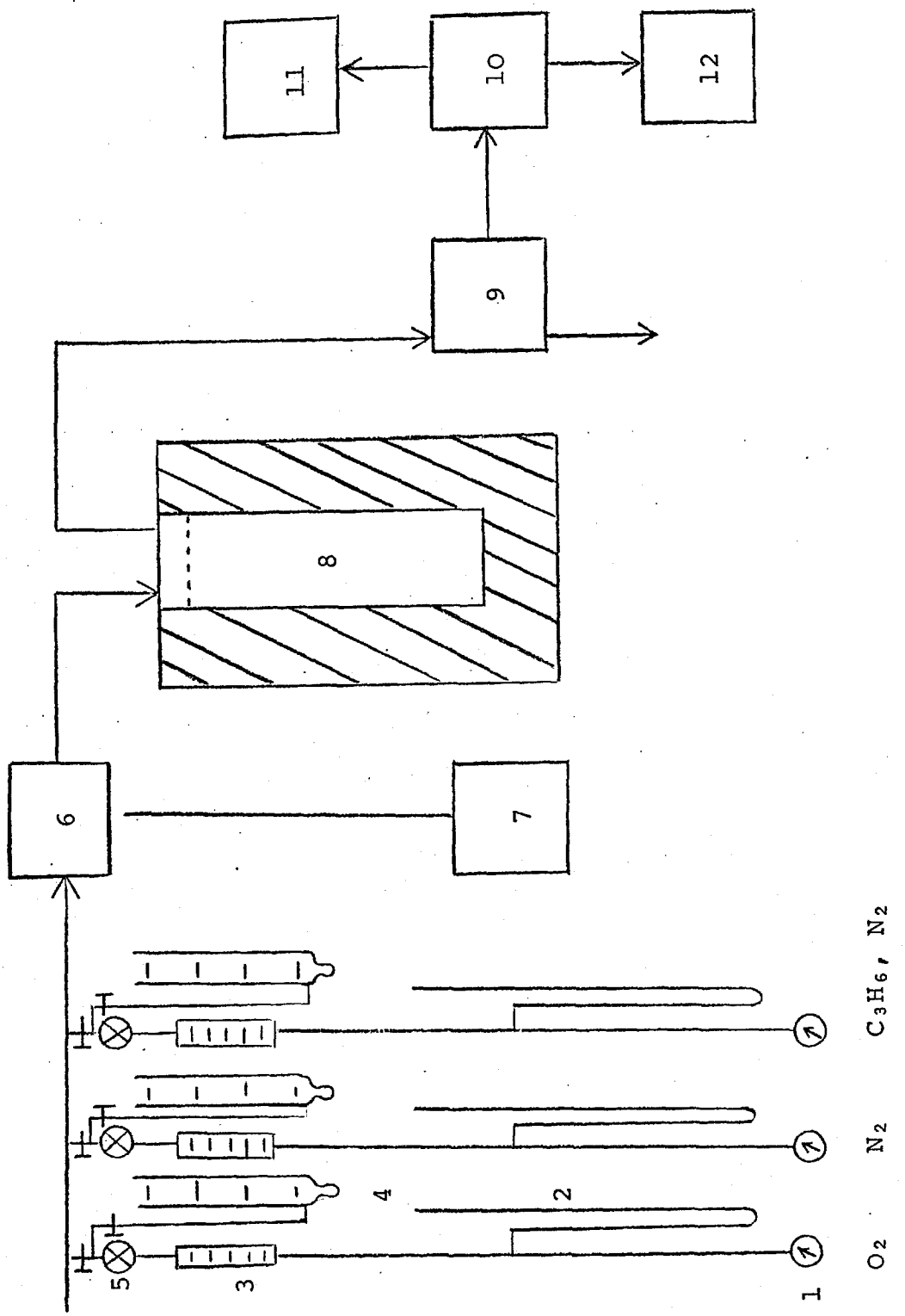

Schematic diagram of the catalytic experimental system.

bubble flow meters shown in Figure 23. By maintaining the identical pressure on the manometer during both calibration and normal use, there was no need to apply pressure correction factors to the rotameter readings. Constant and accurately known flow rates were obtained by using good needle valves and flow meters and by careful calibration.

Several different systems were used for the vaporization of the liquid reactant in an attempt to satisfy the two criteria of constancy and accuracy. The first system used was a series of bubblers, designed to saturate the gas stream, as shown in Figure 24. The liquid was contained in three modified drechsel bottles (capacity 500 ml each), connected in series and suspended in a constant temperature water bath (± 0.5^{o}C) controlled by a contact thermometer and an electronic relay. Gas passing through all the bottles was dispersed efficiently at the glass sinter in the base of each bottle. The bubbles were prevented from reforming by filling the drechsel bottles with glass raschig rings. This system was discarded after preliminary experiments since it was very difficult to determine accurately and reproducibly the rate of vapour pick-up, each determination of the rate being time consuming (at least one hour). The instability of the rotameter measuring the flow rate of the pick-up gas indicated that the flow rate of gas, and therefore the flow rate of the organic vapour, were not constant. This was confirmed by visual examination of the saturator bottles.

The second system involved a micro vaporizer and feed system using gravity or pressure flow. The micro-

KEY TO FIGURE

COMPONENT	DESCRIPTION
1	stirrer
2	drechsel bottles
3	organic liquid
4	water bath
5	temperature controller

FIGURE 24

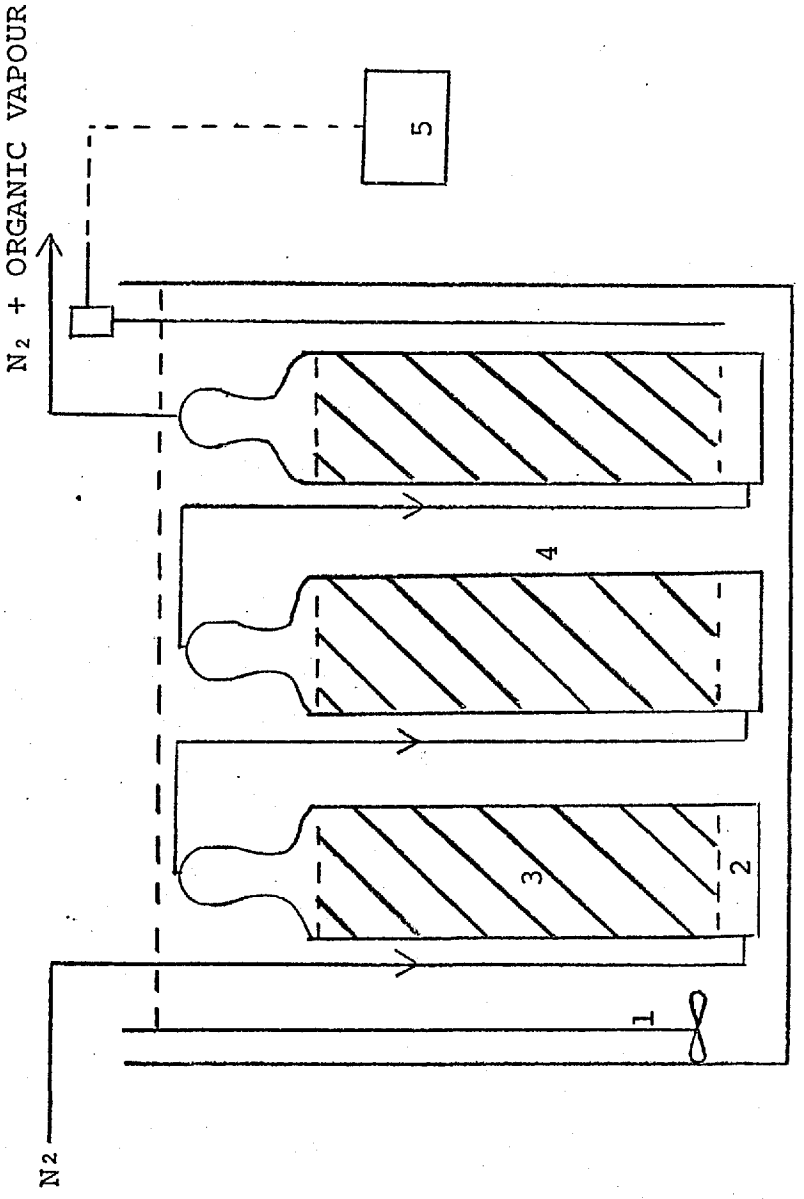

Saturator system for delivery of liquid organic reactant.

vaporizer is shown in detail in part a of Figure 25. The organic liquid flowed from a reservoir under the force of gravity or nitrogen pressure through a restriction or a needle-valve to the vaporizer. The liquid passed up a vertical capillary and was vaporized by hot gases; this arrangement was designed to avoid pulsations caused by the formation of drops. The feed system was quickly discarded as a suitable restriction or needle valve could not be found to regulate the low flows required (as low as 2.0 cc/hr).

The micro-vaporizer was found to perform very satisfactorily and it was retained as the basis of the successful design in conjunction with a micro-pump used to deliver the low flows required. By using a peristaltic pump with a variable speed motor and different tubing sizes, it was possible to design a pumping system capable of delivering 0.5 cc/hr. and upwards. From Figure 25b it can be seen that the pump could be fed by either the large reservoir and/or by the small graduated reservoir (0.02 cc divisions) through the T-stop cock. At any given time the levels were equilibrated and the pump was switched to the measuring reservoir to measure the amount pumped per unit time. A problem of selecting the proper tube was encountered when both silicon and neoprene tubing proved unservicable due to absorption of hydrocarbon, but viton was finally proved to be suitable even over very long periods. A slight pulsation caused by the tube expanding as the roller left the track was overlooked as the system was capable of delivering a relatively constant, accurately known flow.

KEY TO FIGURE

COMPONENT	DESCRIPTION
1	heated coil
2	vaporizer
3	measuring reservoir
4	main reservoir
5	glass T-stop cock
6	peristaltic pump
7	d.c. constant speed motor
8	transistorized rectifier
9	variac
10	brass T-connector
11	capillary, 0.020"i.d.
12	copper tubing

FIGURE 25

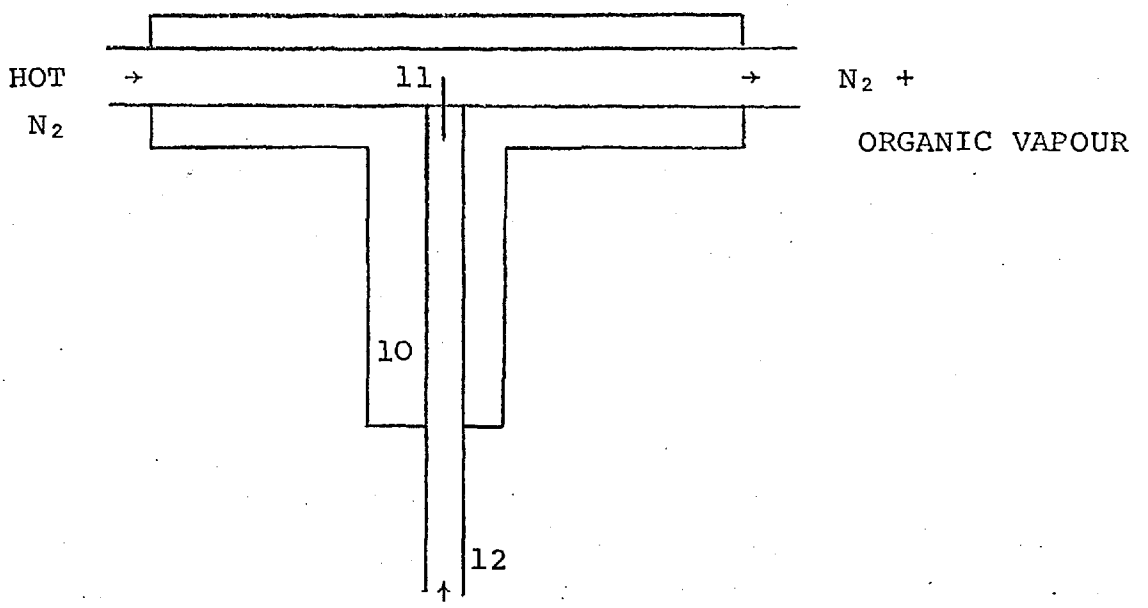

(a)

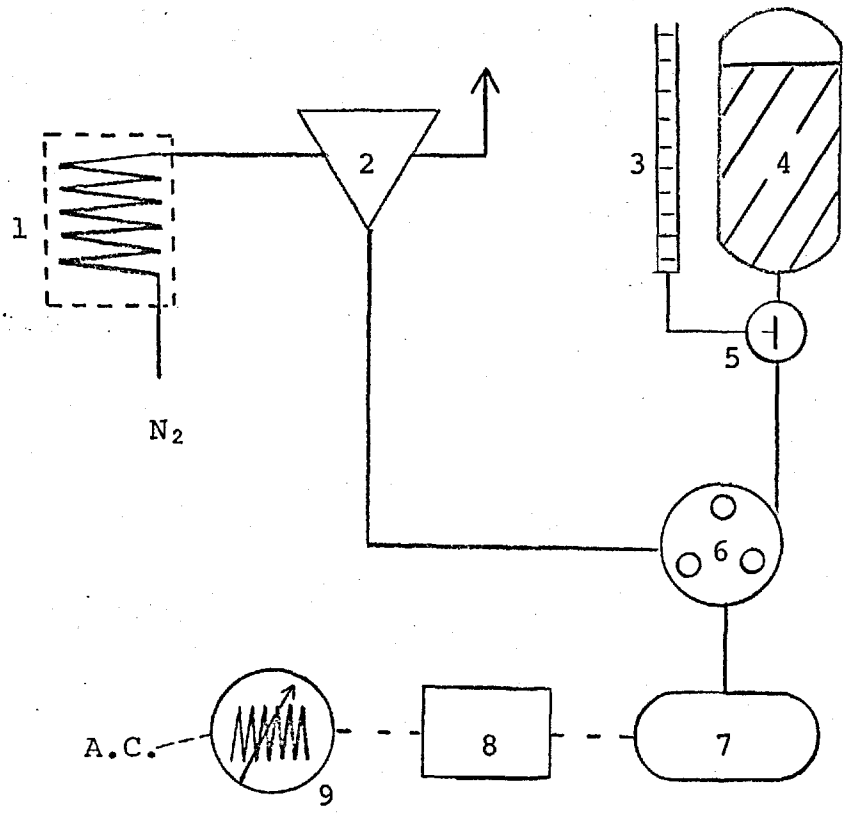

(b)

Detail of micro vaporizer (a) and peristatic pump system for vaporization of the liquid organic reactant (b).

3B. Reactor and furnace

The several designs used for the reactor-furnace system at various stages can be divided into two main areas: metal reactors used with an air furnace and glass reactors used in a tin bath. The initial studies were carried out in a large metal tubular reactor with a thermalwell running down the centre. After the preliminary tests were completed, a micro metal reactor with an internal volume of 5 ml was designed and constructed.

As illustrated in Figure 26 sintered metal discs were used to support the catalyst and distribute the gases. Three small (1/16") iron-constantan thermocouples were inserted along the reactor length to measure the temperature profile. The furnace used consisted of a fused silica tube coiled with nichrome wire (resistance 3 Ω/yd) and placed in an insulated box. The furnace temperature was controlled to ±0.5°C by a controller designed and fabricated in this department.

The instrument incorporated proportional, integral and derivative modes of control, using an iron-constantan thermocouple as the temperature sensing device. A meter displayed the difference of the actual temperature from the set temperature and this value would normally be less than 0.5°C. The temperature in the reactors and in the furnace were measured by iron constantan thermocouples and the resulting e.m.f. measured on a Pye potentiometer capable of discerning 0.001mV.

KEY TO FIGURE

COMPONENT	DESCRIPTION
1	iron-constantan thermocouples
2	stainless steel connector 1/16"
3	stainless steel tube
4	stainless steel sintered discs
5	stainless steel plugs
6	stainless steel tubing
7	catalyst bed

FIGURE 26

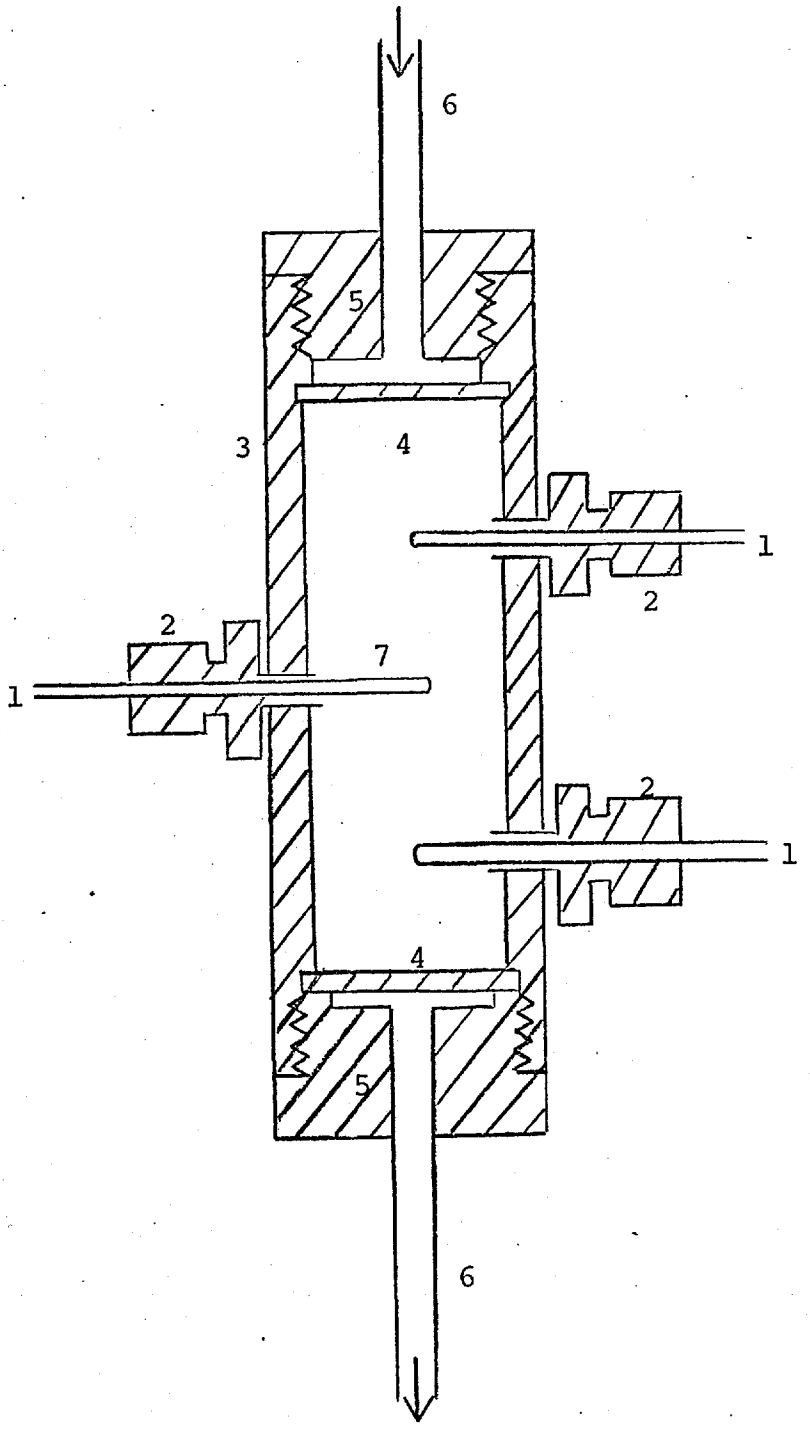

Micro metal reactor.

Because of homogeneous oxidation, also noted by Adams (94), the micro-metal reactor had to be replaced by a glass or silica reactor and at this stage, due to the known problem of a large amount of heat being released during oxidation and the low heat transfer coefficient between glass and air, a tin bath was employed in place of the air furnace. This proved very successful and an indication of the system's ability to transmit heat is the fact that a temperature rise of 150^{o}C in the first part of the bed resulted in a temperature rise of only 5^{o}C at 2 cm downstream and was undetected at 4 cm downstream. The tin at high temperatures (400^{o}C to 600^{o}C) tended to oxidize and this was increased by bubbling nitrogen through the bath. Such stirring was necessary to maintain a suitable temperature profile (Figure 27). The oxidation problem was minimised by placing on top of the tin a layer of carbon dust.

The bath was constructed from thick mild steel, which was replaced (due to corrosion) every six-twelve months. Careful construction was necessary to avoid electrical short circuits: the metal pipe was carefully wrapped in several layers of asbestos paper before it was wound by nichrome wire, a layer of asbestos cement was applied to insulate the windings and the entire form was wrapped in asbestos cloth before being placed in an asbestos box insulated by vermiculite.

The glass or silica reactors were designed with two constraints in mind: fast heat transfer and minimization of any homogeneous reaction. In order to maintain the

FIGURE 27

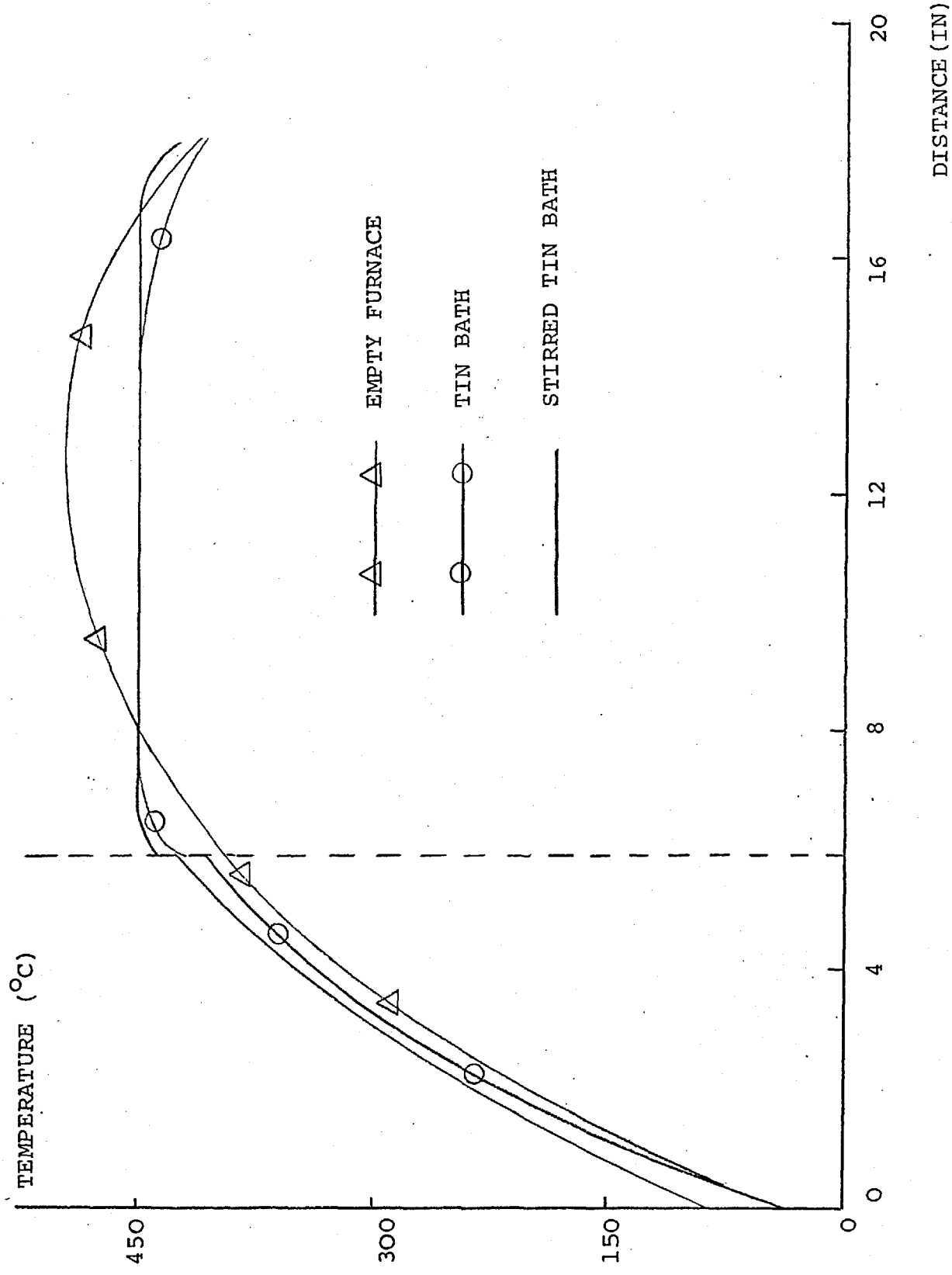

Temperature profiles along the furnace tube.

heat transfer as high as possible and to minimize any temperature profiles, small diameter tubing (5-6 mm I.D.) was normally used. The reactor volume was designed to be only slightly larger than the volume required by the catalyst to minimize possible homogeneous reactions. For studies requiring catalyst volumes between 2 ml and 10 ml, U-tube reactors (Plate 1a) were constructed with thermocouple points at the beginning, middle and at the end of the catalyst volume. Helical reactors were used for catalyst volumes of 16 to 40 ml. These reactors (Plate 1c) contain a thermowell running down the centre of the outlet with the end projecting into the catalyst bed. In exceptional cases it was necessary to use a double helical reactor of 8 mm I.D. (Plate 1b). Each reactor was immersed in the liquid tin to a minimum distance compatable with the gases reaching the reaction temperature but allowing minimal free space at reaction temperature. The inlet and the outlet of the reactor were connected to the line by means of two small pieces of silicone rubber capable of withstanding 200^{o}C.

3C. Analysis of reactants and products

In addition to the reactants, propylene, oxygen and nitrogen, possible products will involve the hexadienes and maybe hexynes. Further dehydrogenation reactions could be possible producing hexatrienes, together with the cyclization products cyclohexene, cyclohexadienes and benzene. Hexene isomers could also be present. Oxidation products

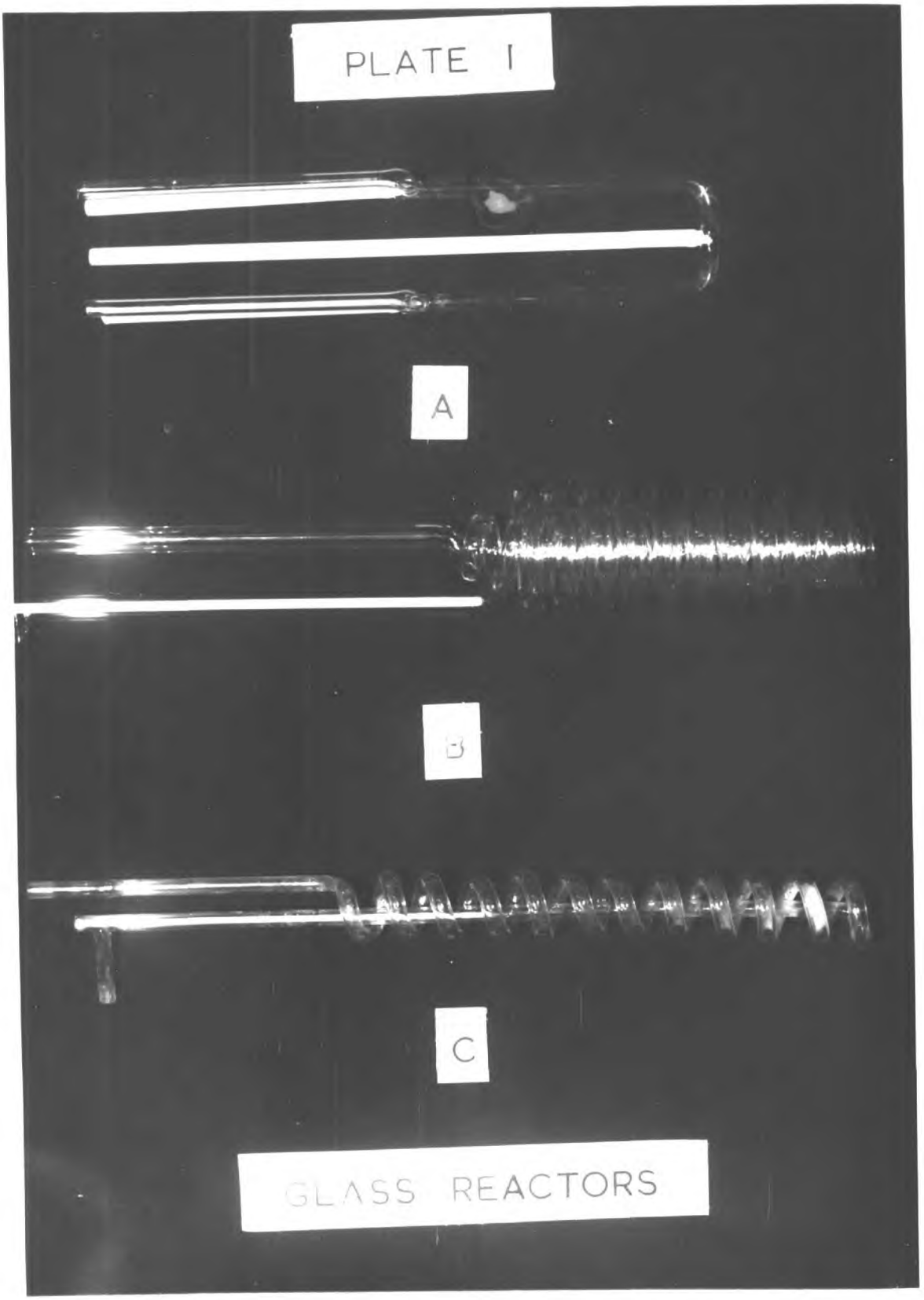
PLATE I
A
B
C
GLASS REACTORS

such as carbon dioxide, water, carbon monoxide, acrolein, etc. could also be produced.

(i) The flame ionization chromatograph

The flame ionization detector (F.I.D.) was chosen for detection of the organic products due to its high sensitivity. As the organic was already diluted by oxygen and nitrogen, the low conversions necessary to study initial kinetics resulted in very low concentrations of products. The detection limit of a normal katharometer detector is 10^{-7} gm of sample (109) but the flame ionization detector is able to detect concentrations as low as 0.001 ppm (110) although compounds such as oxygen, nitrogen, water are not detectable.

The F.I.D. chromatograph (Figure 28) shared with the katharometer a sampling system comprising a sample valve, injector and selector valve. The purpose of this system was to deliver an accurate volume of the product stream to either the F.I.D. chromatograph or the katharometer chromatograph. The operation of the two rotary gas sampling valves, fabricated in the department, is illustrated schemetically in Figure 29. The first valve directed either the carrier gas or the product stream through the sample loop (volume 4.95 cc). The purpose of the second valve was to select the direction the sample is to take. In order to inject a sample to the F.I.D. column, the selector valve was set to pass the F.I.D. hydrogen carrier gas to the

KEY TO FIGURE

COMPONENT	DESCRIPTION
1	product stream
2	sample valve
3	injector
4	selector valve
5	hydrogen carrier gas
6	katharometer chromatograph
7	air-stirred oven
8	column
9	flame ionization detector
10	hydrogen for detector
11	air for detector
12	ionization amplifier
13	recorder

FIGURE 28

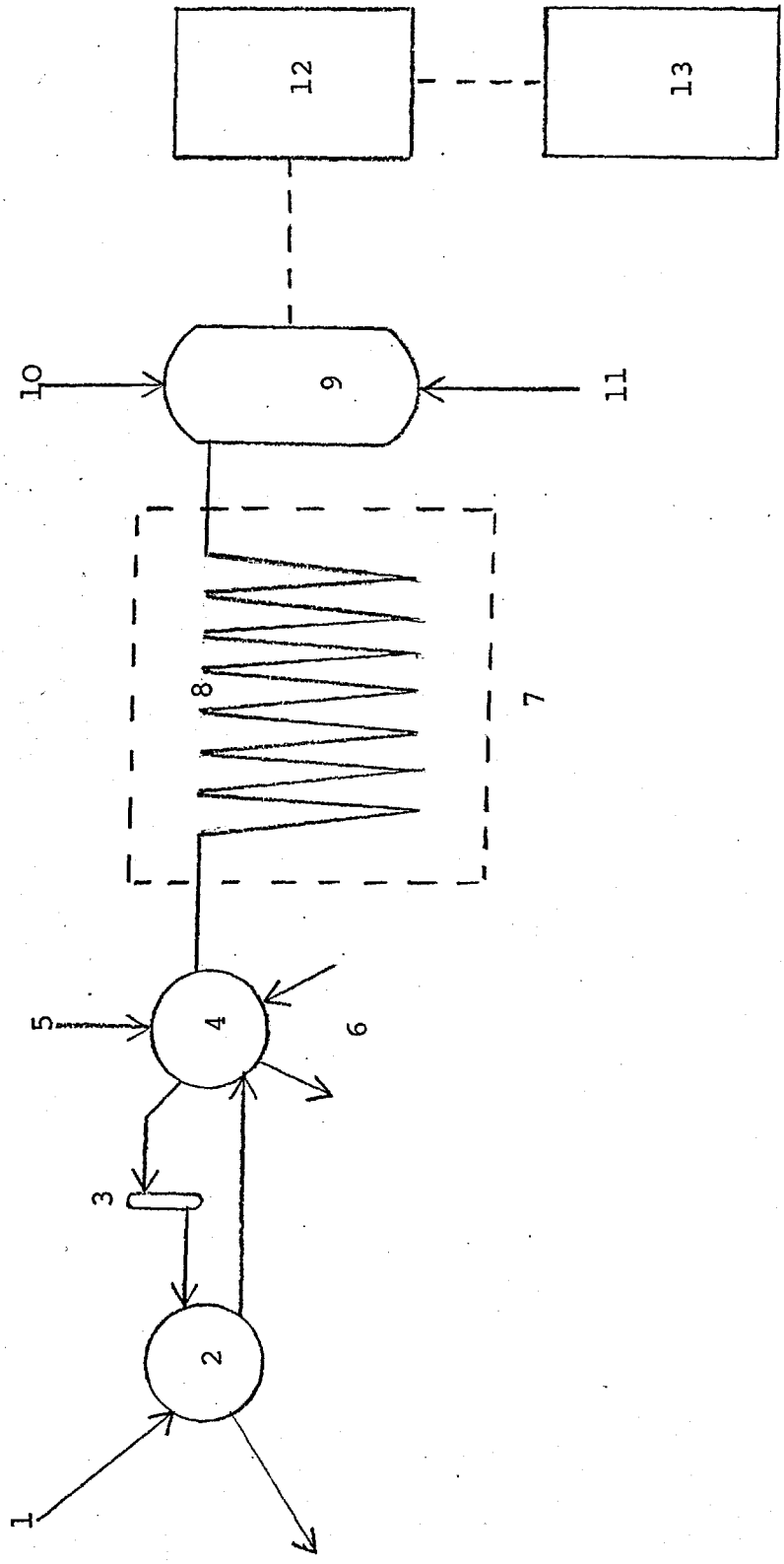

Flame ionization chromatograph.

FIGURE 29

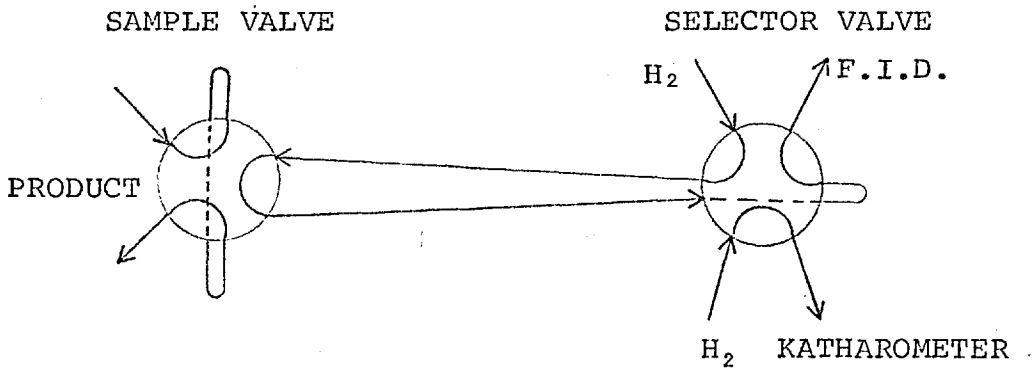

(a) Sampling from product stream

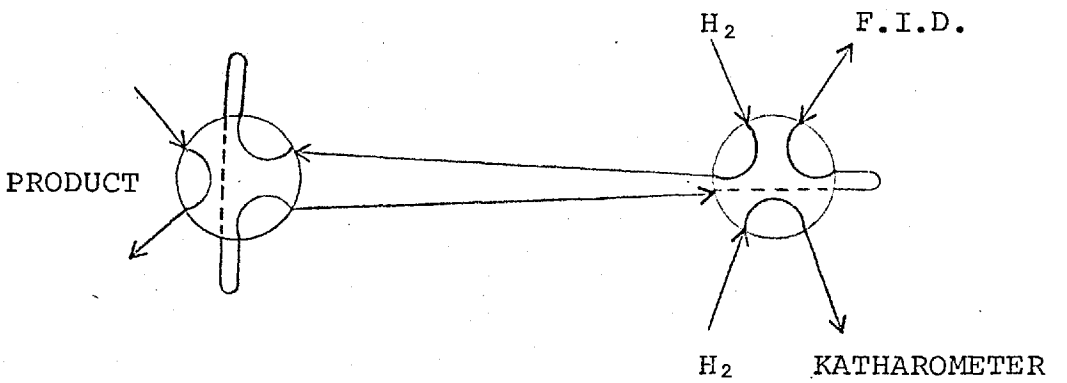

(b) Injection of sample to F.I.D.

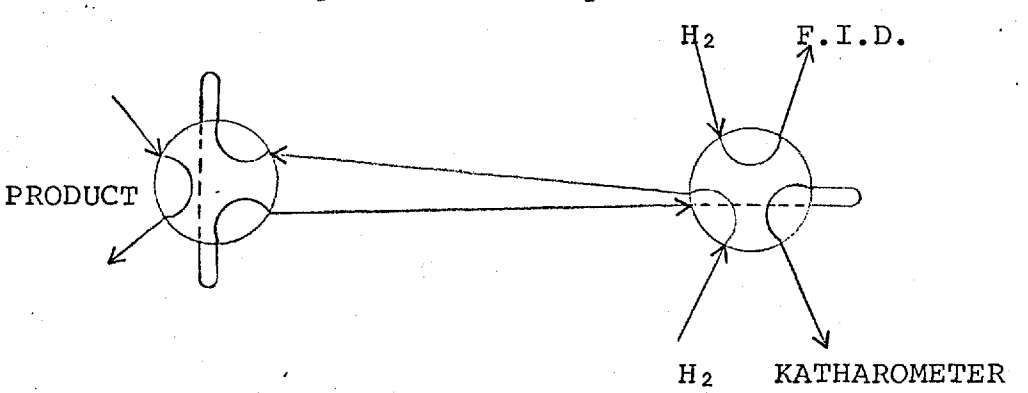

(c) Injection of sample to katharometer

The operation of the gas sampling system.

sampling valve which was in the sampling position thereby allowing the sample loop to fill. The valve was then quickly turned and the hydrogen carrier gas swept the sample to the selector valve and then to the F.I.D. column. The column temperature was controlled to 0.5°C by a stirred air oven. The peaks were eluted directly into the detector where a small current proportional to the concentration was generated. This current was amplified and attentuated by a Pye ionization amplifier and recorded by a sunvic one millivolt recorder. The detector normally requires 35-50 ml/min of hydrogen and 500 ml/min air to support combustion and to remove the heat produced. As the F.I.D. is insensitive to temperatures, flow rate and fluctuation (111) it is an ideal research chromatograph with its high sensitivity.

For purposes of identification and calibration an injector port was placed between the sample valve and the selector valve. The design of the injector port (Figure 30), constructed from a brass Simplifix 1/8" T-connector, allowed the sample to be injected into a hot, fast-moving stream of carrier gas, thereby producing sharp, narrow injection peaks. The injector, sample valve, selector valve and all tubing in contact with a liquid sample were heated by glass cloth sheathed nichrome wire electically heated to a temperature controlled by a variac.

(ii) The katharometer chromatograph

The detection of non-combustible compounds is not possible with a flame ionization detector and these compounds

KEY FOR FIGURE

COMPONENT	DESCRIPTION
1	copper tubing
2	septum
3	heated brass T-connector
4	syringe

FIGURE 30

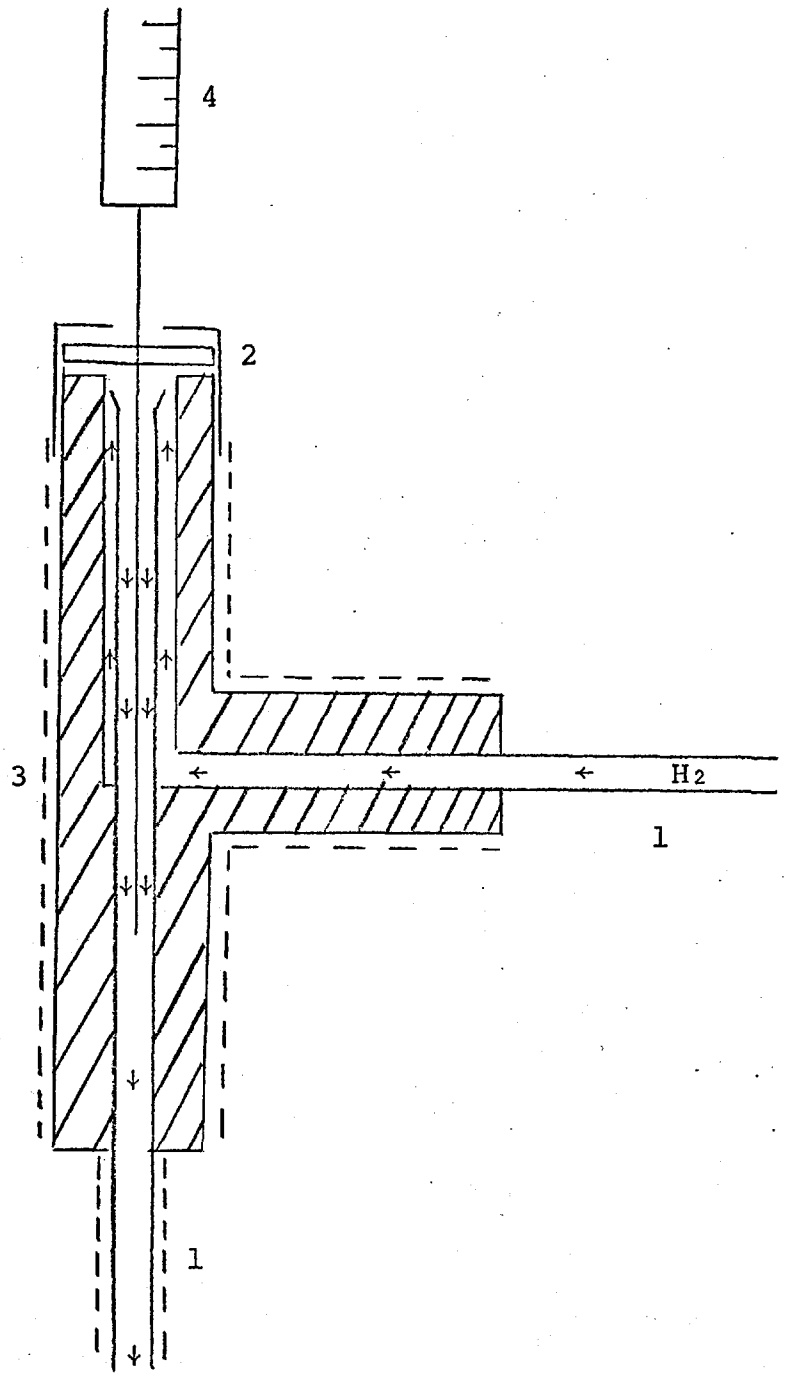

Injector for liquid and vapour samples: dashed lines indicate heating.

are normally detected by use of a katharometer, designed around the necessary column separation. This required three columns, placed in parallel and connected to the same katharometer detector and the same sampling system resulting in the complicated flow diagram as shown in Figure 31. The hydrogen carrier gas passed over the reference filaments and through the selector valve and injector port to the sampling valve where a sample was picked up. The carrier gas and sample returned through the selector valve to the columns where the flow was directed through either the molecular sieve 5a column or the silica gel columns by a double oblique glass tap. In the silica gel columns the flow was directed either for analysis of carbon dioxide at room temperature or for propylene analysis at 80°C: when the silica gel column for carbon dioxide analysis was isolated from the carrier gas, a flow of hydrogen was passed through it to flush any compounds of long retention time from the column.

The peaks were eluted from the column into the sampling side of the katharometer where a voltage change was generated across the bridge. The detector output was attentuated by the decade arrangement shown in Figure 32. before being recorded on a one millivolt Vitatron recorder. The katharometer filaments were normally operated at 300 milliamps with a flow rate of 45 cc/min hydrogen.

KEY TO FIGURE

COMPONENT	DESCRIPTION
1	sample from sampling system
2	double oblique glass stop cocks
3	insulated box
4	molecular sieve 5A column
5	silica gel carbon dioxide column
6	hot oil bath
7	silica gel propylene column
8	stirrer
9	temperature controller
10	needle valves
11	pressure regulator (hydrogen)
12	four filament katharometer
13	to sampling system
14	to vent
15	power supply and attentuator
16	recorder

FIGURE 31

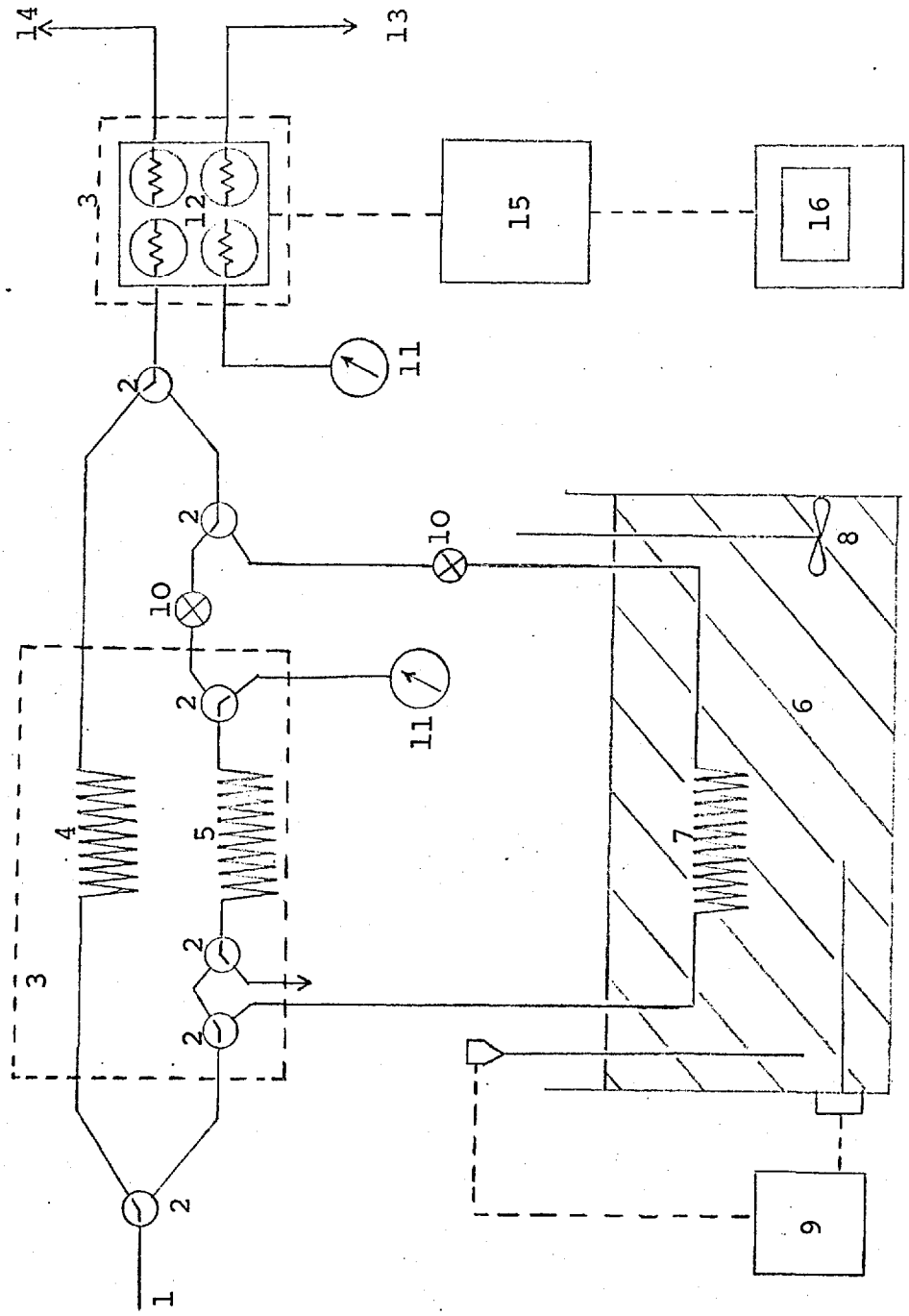

The katharometer chromatograph.

KEY TO FIGURE

COMPONENT	DESCRIPTION
1	katharometer
2	4 Ω potentiometer
3	0.1 Ω resistor
4	5 Ω potentiometer
5	decade resistance box (10 x 1 Ω)
6	decade resistance box (10 x 10 Ω)
7	decade resistance box (10 x 100 Ω)

FIGURE 32

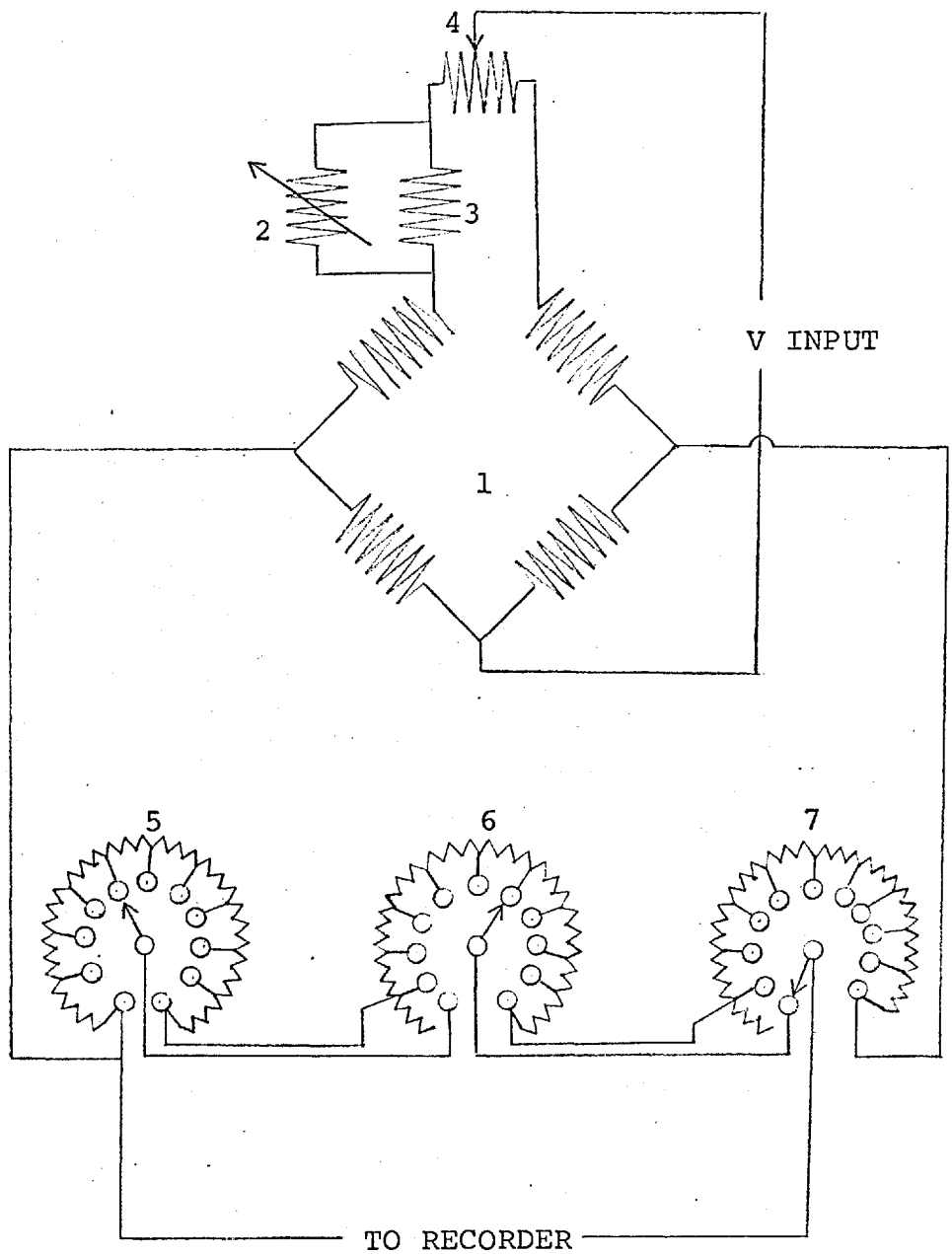

Balance and attentuator circuit for katharometer.

(iii) Choice of columns

Both gaseous and liquid products were produced in the reaction. The separation of the gases was accomplished by the following columns. A 3 ft column of molecular sieve was known to separate oxygen, nitrogen and carbon monoxide at room temperatures but to absorb carbon dioxide and propylene (112). A 2.5 ft silica gel column was therefore used to separate carbon dioxide and propylene from the others. The separation of the propylene on the silica gel on room temperature resulted in a broad peak with a very long tail. Due to the inaccuracy of determining the area of such a peak the propylene was separated on another silica gel column (3 ft) maintained at 80°C in an oil bath. It was found necessary to minimize time of analysis by back flushing the propylene from the carbon dioxide column. Typical chromatograms obtained during analysis of the gases, are shown in Figure 33.

The separation of the liquid products in the flame ionization chromatograph was approached in two ways. Relative retention times of the possible products over polar liquid phases were accumulated. Table 11 lists the relative retention times at 25°C of the possible products over dimethylsulpholane (DMS), β,β' oxydipropionitrile (ODP) and diethylene glycol-silver nitrate (AgEG). The long retention times of benzene and the cyclohexadienes on DMS and ODP made the use of both columns impracticable without temperature programming. The separation of the possible products on the AgEG column appeared satisfactory and a 4 m, 1/8" o.d. column was purchased from

KEY TO FIGURE

PEAK	COMPOUND
1	oxygen
2	nitrogen
3	carbon monoxide
4	air
5	carbon dioxide
6	propylene

FIGURE 33

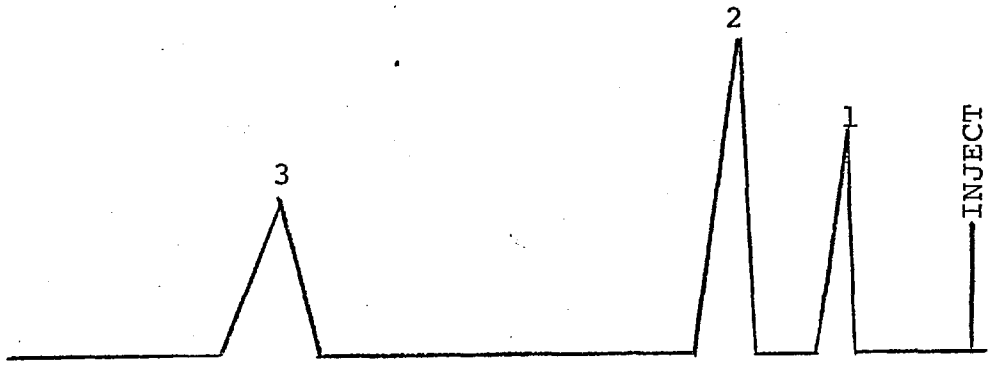

(a) Molecular sieve 5a 20°C

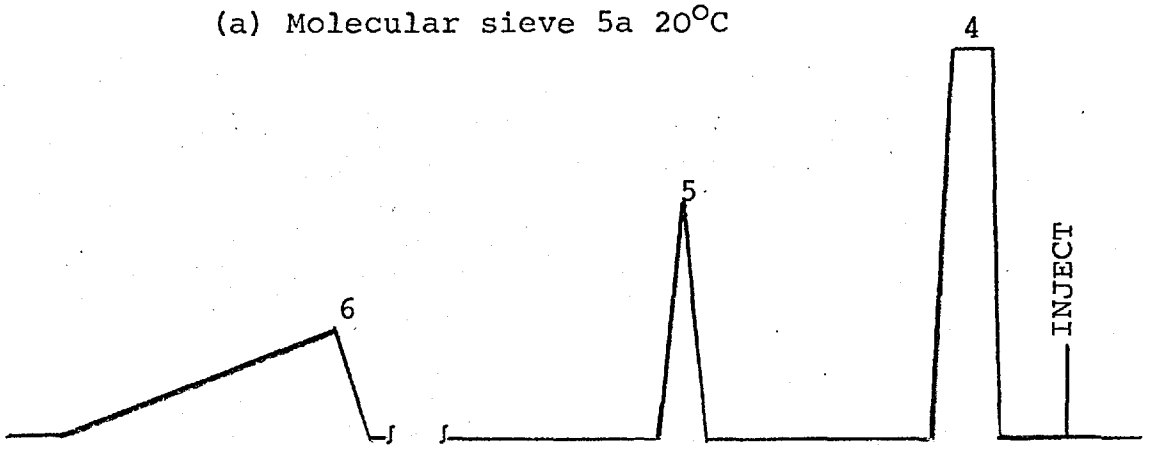

(b) Silica gel 20°C

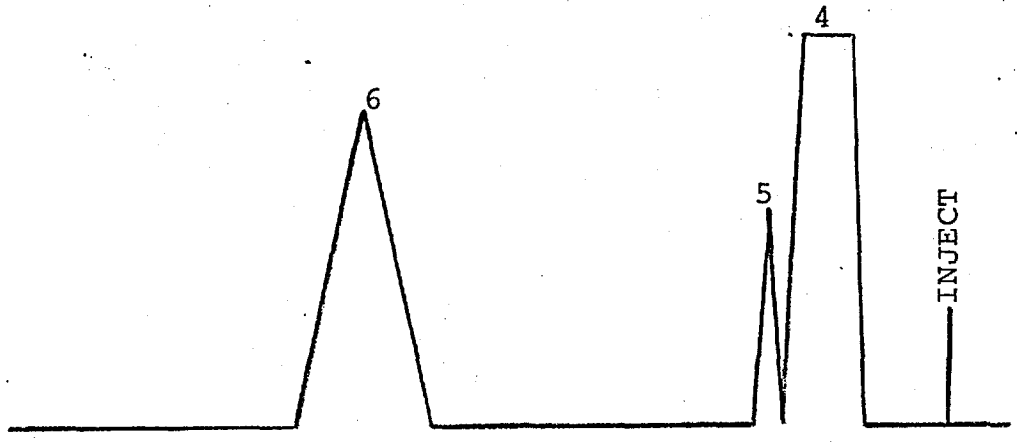

(c) Silica gel 80°C

Typical chromatograms.

TABLE 11

Relative retention times of possible products at 25°C (113)

Hydrocarbon	DMS	ODP	Ag-EG (114)	Sq
Propylene	0.21	0.48	1.04	0.09
Pentane	1.00	1.00	0.07	1.00
trans Pentene-2	1.88	2.25	1.00	1.13
Hexene-1	4.30	4.15	5.65	2.83
1,5 Hexadiene	6.28	7.80	32.2	2.52
1,3 Hexadiene	12.9	15.0	20.0	4.27
Cyclohexene	13.5	16.5	26.6	7.30
1,3 Cyclohexadiene	23.4	35.3	31.9	6.50
1,4 Cyclohexadiene	35.7	52	-	9.90
Benzene	52	83	6.91	5.85

Perkin Elmer. The packing was diethylene glycol + silver nitrate on 60-80 mesh Chromosorb P (30:70). Testing by injecting pure and mixed samples of the possible product indicated that the products could be separated.

A general non-polar column should also be used to check the results. Retention times over squalane, the column chosen are also given in Table 11. Both columns were normally used separately but occasionally both were used in series. During the kinetic studies a short (6") column of polyethylene glycol was used to move the acrolein peak away from the 1,5 hexadiene peak.

(iv) Identification of products

The products were separated on an appropriate column and the retention times were compared with retention times of known compounds. When a tentative identification was made, a sample of the pure compound was injected and the retention times compared. Before an identification was accepted, the retention times had to match on both the columns (polar and non-polar). The identification on the squalane column was aided by a correlation between the boiling point and the retention time. As can be observed in Figure 34 the boiling point of an unknown compound can be estimated to within a few degrees by its retention time. This correlation not only held for members of the same family but also for different compounds such as acrolein and acetone. A sample of the pure compound was then added to the product mixture, and the appropriate peak was checked to increase in the

FIGURE 34

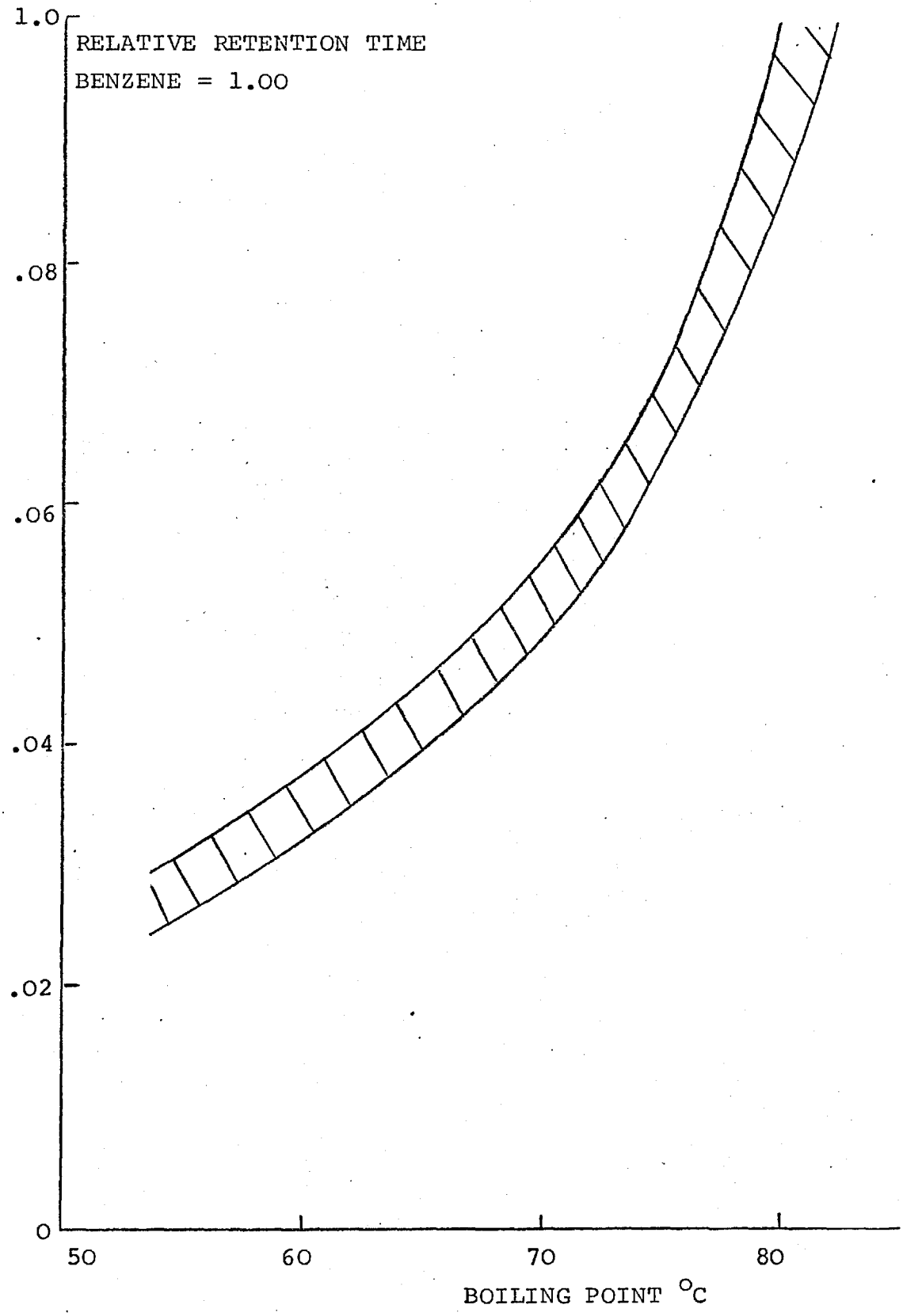

Correlation of relative retention time with the boiling point of a compound.

product chromatograph.

Other methods such as ultraviolet and mass spectrometry were used to confirm identifications. A mass spectrogram of the product stream was also recorded to check that no major product was overlooked.

(v) Calibration

The gaseous products were calibrated by measuring the peak area obtained from injecting samples of the pure gas at different pressures. The sample loop of the gas sampling valve was evacuated and filled with pure gas to a certain pressure as measured by an open end manometer. The sample was injected and swept by the carrier gas through the column to the katharometer. The number of moles was calculated by the ideal gas law ($n = PV/RT$) knowing the pressure, volume (by mercury weight) and temperature. For calibrations at very low concentrations where the pressure readings became unreliable, a known mixture of the gas with hydrogen was prepared and used in place of the pure gas. The concentration of the mixture was checked by overlapping the calibration range with the pure sample.

For the calibration of liquid products a 0-5 µl Hamilton high pressure syringe was used to inject a measured volume of liquid into the heated injection port. As the calibration ranged from 5 ηl to 1 µl, it was generally necessary to dilute the pure liquid with any liquid that would vaporize quickly and would not interfere with the desired peak. The number of gram moles was calculated by

multiplying the volume of liquid injected by its density and dividing by its molecular weight. The calibration curves were checked at regular intervals, normally monthly, unless the system was altered in any way which could effect the calibration.

3D. Procedure

The flowmeters (Figure 23) were first calibrated with soap-bubble meters at a constant up-stream pressure of 40 cm Hg. The furnace was switched on and, having introduced sticks of tin metal into the furnace tube, time was allowed for the tin to melt and for the temperature to reach the desired value. If a liquid organic reactant was to be used, the reservoir of the pump and the line to the vaporizer were filled with the liquid. All lines, including the sample valves, that could come in contact with condensable products were heated to approximately 100^{o}C.

The catalyst to be used was sized by grinding, using a procelain motor and pestle, and by sieving the resultant powder with nylon mesh sieves. The required weight of sized catalyst (normally 20 to 30 mesh) was placed in one of the reactors and any excess volume was minimized by diluting the catalyst with pumice of the same mesh. The reactor was then placed in the molten tin very slowly so as to minimize thermal strain in the reactor and connected to the flow system by silicone tubing. The top of the furnace was plugged with asbestos wool in order that the part of the reactor above the tin remained hot, thereby, preheating the reactants and

preventing condensation of products.

With the reactor-furnace system at reaction temperature a stream of nitrogen, and then, oxygen plus nitrogen was passed over the catalyst for one hour. If the required concentrations of oxygen and fuel were below the explosive limit, the oxygen and nitrogen flow rates were adjusted to the required value before the fuel was slowly introduced. On the other hand, if the reaction mixture was above the explosive limit, the flows of N_2 and fuel were set before the O_2 was brought on stream. The flows to both chromatographs were set and after a period of time the instruments were turned on. The temperature of the catalyst bed was measured periodically during the run by two iron-constantan thermocouples connected to a potentiometer. After all systems were equilibrated, samples were taken for analysis as described above. After the run was completed, the flows of reactants were cut-off in the reverse sequence to the start-up. This prevented an explosive reaction mixture from entering the reactor.

3E. The gas adsorption apparatus

A conventional B.E.T. gas adsorption rig (Figure 35), based on the constant volume principle (115) was used to measure the B.E.T. surface area and to estimate the pore size distribution of the pure In_2O_3 catalysts by nitrogen absorption at $-195^{o}C$.

The system was capable of attaining a vacuum of 10^{-5} torr using a rotary vacuum pump in series with a

KEY TO FIGURE

COMPONENT	DESCRIPTION
1	cold trap
2	McLeod guage
3	null point manometer
4	storage globe (N_2)
5	storage globe (He)
6	adsorption burette
7	sample bulbs
8	saturation vapour pressure manometer

FIGURE 35

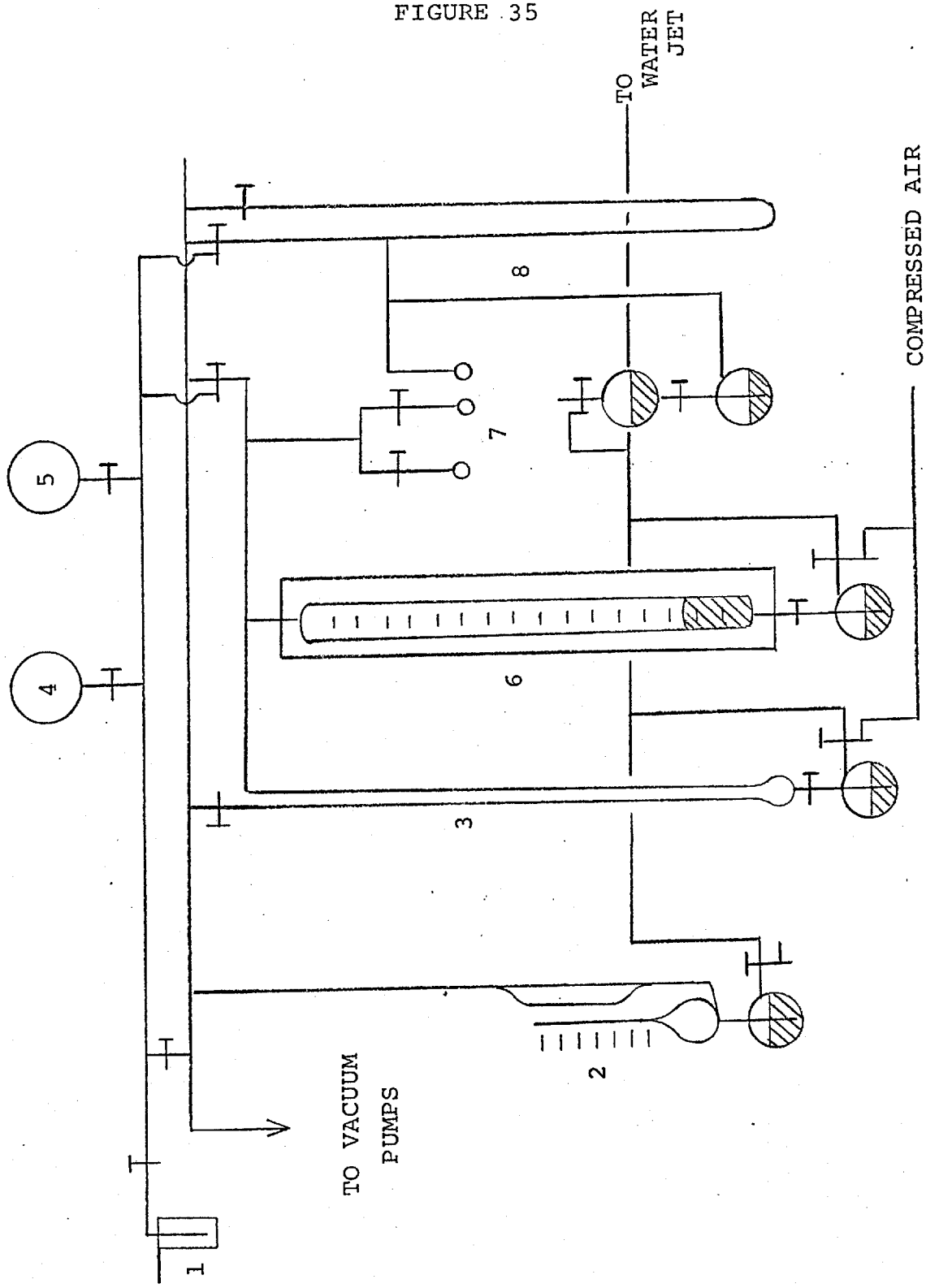

The B.E.T. gas adsorption rig.

mercury diffusion pump. Condensable vapours were trapped out at -195°C between pumping stages. Dead space in the adsorption section was reduced to a minimum by using 2 mm I.D. capillary tubing of pyrex glass. All taps used in the apparatus were high vacuum pyrex glass stopcocks lubricated with silicone grease. The important parts of the apparatus are:

(i) The saturation vapour pressure manometer

This was used to measure the saturation vapour pressure (S.V.P.) of nitrogen at -195°C. The S.V.P. bulb was immersed together with the sample bulbs in the liquid nitrogen and the pressure was increased by mercury displacement in the lower bulb until the pressure returned each time to the same value. The S.V.P. was then read from the manometer. It was necessary to repeat the measurement several times during a long experiment as the S.V.P. varies with the liquid nitrogen temperature.

(ii) The adsorption burette

This was used to alter the volume of the adsorption section and to determine the dead space volume. The 50 ml burette was kept in a constant temperature water bath at a temperature of 25°C ± 0.2°C.

(iii) The null point manometer

The pressure in the adsorption section was measured by the null point manometer. When the pressure

changed, the level of mercury in the arm connected to the adsorption section was maintained at the zero point by by varying the amount of mercury in the manometer. This was accomplished by the pressure in the bulb below the manometer, either forcing more mercury into the manometer or withdrawing mercury. The adsorption pressure was measured as the difference in the two arms, the one arm being maintained at vacuum. A mirror glass scale was fitted to the adsorption manometer and readings to an accuracy of ± 0.05 mm Hg could be obtained.

Other parts of the adsorption apparatus included the sample bulbs, the McLeod gauge to measure the vacuum, the high vacuum line, the low vacuum line and the storage globes for nitrogen and helium.

3F. Procedure for physical adsorption studies

The basic steps in obtaining an isotherm for a catalyst were:

a) outgassing of the surface at high temperature (300°C) and at high vacuum.

b) determination of the dead volume (D.S.) of the adsorption section minus the sample bulb by helium expansion $\left[P_1(\text{D.S.} + \text{Burette}) = P_2(\text{D.S.} + \text{Burette})\right]$

c) determination of total dead volume (T.D.S.) by helium expansion with the sample at liquid nitrogen temperature $\left(P_1(\text{D.S.} + \text{Burette}) = P_2(\text{T.D.S.} + \text{Burette})\right)$

d) admission of a known volume (STP) of nitrogen to

the burette

e) admission of nitrogen to the sample at liquid nitrogen temperature

f) variation of burette volume and measurement of pressure

g) measurement of the saturated vapour pressure (S.V.P.)

h) determination of the weight of the clean sample

The volume of gas adsorbed at S.T.P. was calculated at any pressure, P, by subtracting the volume of nitrogen (based on S.T.P. conditions) in the adsorption section at that pressure P from the volume of gas (at S.T.P. conditions) initially admitted. An isotherm (volume adsorbed (V) versus relative pressure (P/S.V.P.)) was then plotted. The surface area was determined by plotting the left-hand side of the Brunauer-Emmett-Teller equation (116) against the relative pressure (P/S.V.P.)

$$\frac{P/S.V.P.}{V(1-P/S.V.P.)} = \frac{1}{VmC} + \frac{(C-1)\ P/S.V.P.}{VmC}$$

The volume of a monolayer (Vm ml S.T.P.) was determined from the values of the slopes and intercept and the surface area was calcualted by using the value of 16.2×10^{-20} m^2 for the cross-sectional area of a nitrogen molecule i.e.

Surface area = $Vm \times 6.02 \times 10^{23} \times 16.2 \times 10^{-20}/22414 \times wt.$ m^2/gm

The pore size distribution was calculated from the complete isotherm by a method outlined by Gregg and Sing (115), based on the application of the Kelvin equation.

SECTION III.

RESULTS

1. Definitions

$S\alpha$ selectivity to hexadiene: $\frac{2 \text{ hexadiene} \times 100}{2 \text{ hexadiene} + CO_2/3}$

$S\beta$ selectivity to benzene: $\frac{B\alpha \times 100}{100 - H\alpha}$

$S\delta$ selectivity to hexadiene: 6 hexadiene/CO_2

$S\rho$ selectivity to benzene: 6 benzene/CO_2

$S\lambda$ selectivity to hexadiene and benzene: 6(hexadiene + Bz)/CO_2

Bz benzene

Hexd hexadiene

CO_2 carbon dioxide

Hex hexene

C_H hexadiene concentration: moles/litre

Cp propylene concentration: moles/litre

Co oxygen concentration: moles/litre

area area of the chromatographic peak

$H\alpha$ hexene unconverted area %: $\frac{\text{area hexene}}{\Sigma \text{ area}}$

$B\alpha$ benzene yield area %: $\frac{\text{area benzene}}{\Sigma \text{ area}}$

E_A activation energy: kcal/mole

A frequency factor

conversion hexene: $100-H\alpha$

contact time: volume catalyst/flow rate

or weight In_2O_3/flow rate

2. The selection of catalysts

Initial studies of the activity of possible catalysts were carried out with respect to their dimerization and cyclization activity under oxidative conditions. Dehydrogenation-cyclization activity was examined by passing a mixture of hexene-1, oxygen and nitrogen over the catalyst at a range of contact times, temperatures and concentrations, the analysis of the liquid products being completed in each case. The dimerization activity of catalysts was examined by passage of different concentrations of oxygen and propylene over a range of contact times and temperatures. The initial results reported are expressed as a percentage of total area, which eliminated the need for identification and calibration of the isomerization and cracking products.

2A. Dimerization activity

(i) CoO, NiO, Pt, Cr_2O_3, MoO_3 and ThO_2 on Al_2O_3

The catalysts were tested for dimerization activity. No dimerization products were detected over a wide range of temperature, concentration and contact time.

(ii) Tl_2O_3-Al_2O_3

This catalyst was found to be active for the oxidative dimerization of propylene, and hexadiene was detected in significant amounts (Figure 36a). The effect

FIGURE 36

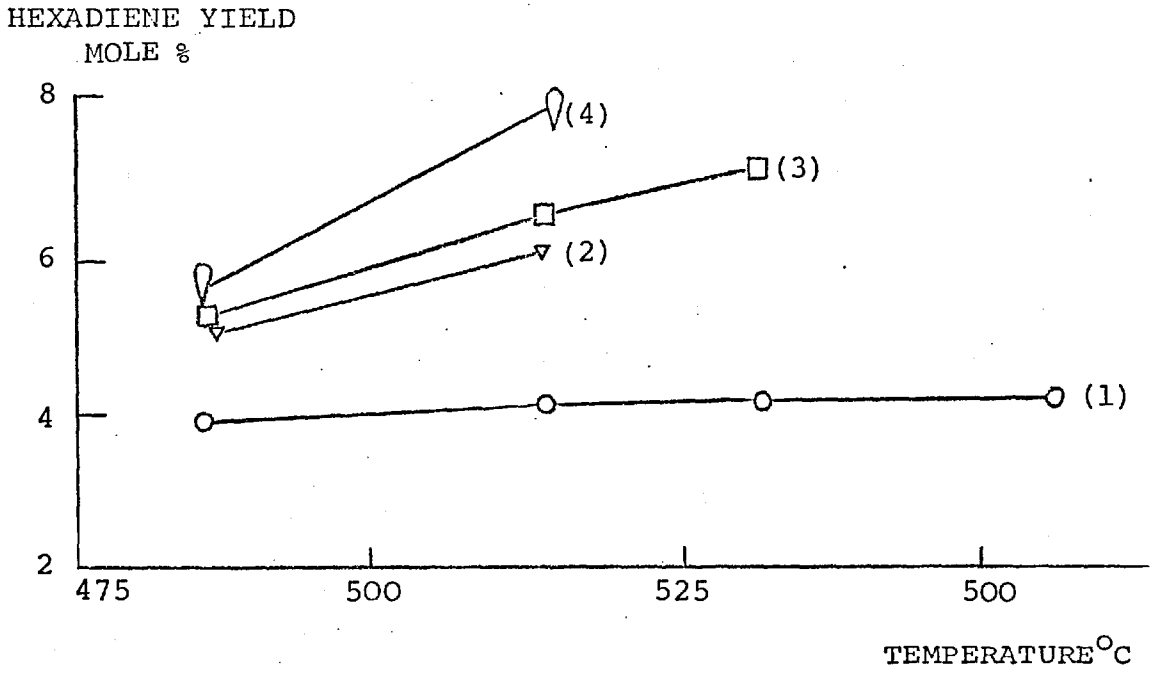

(a)

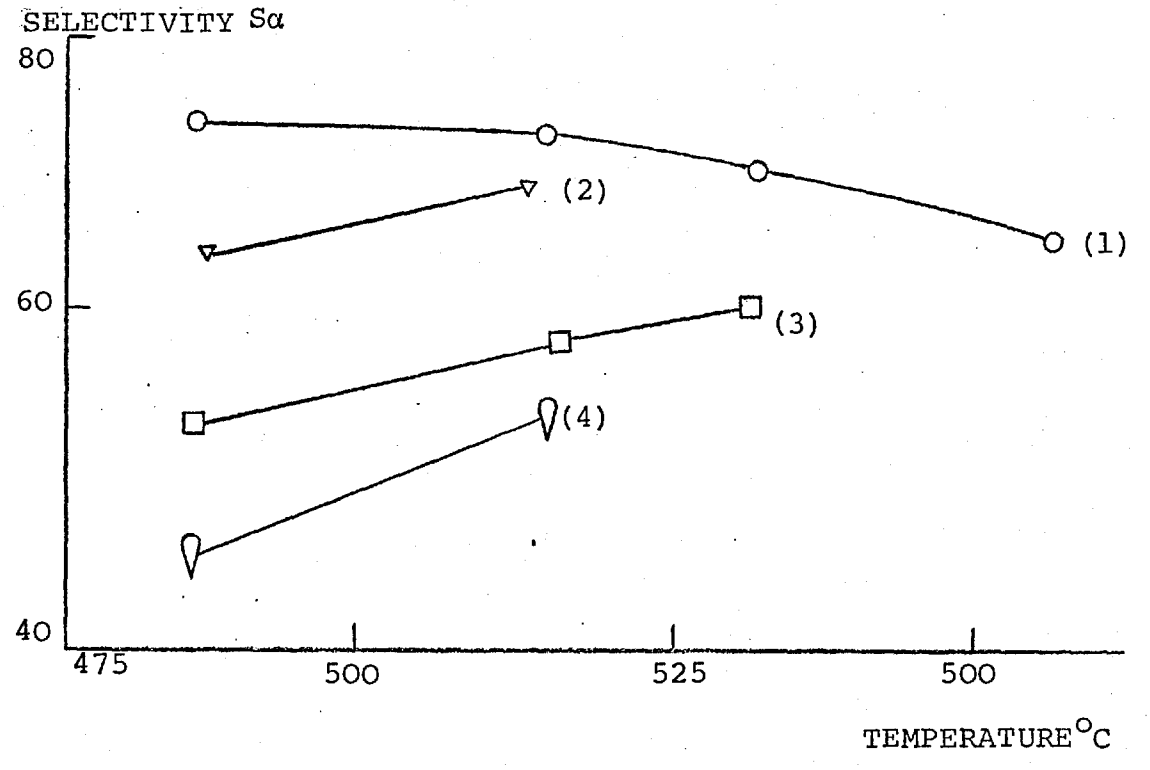

(b)

Effect of temperature variation on (a) hexadiene yield and (b) selectivity, Sα of propylene dimerization over Tl_2O_3-Al_2O_3.

contact time: 10 cc/cc/sec
oxygen to propylene ratio: (1) 0.1, (2) 0.22, (3) 0.5, (4) 1.0

of an increase in temperature on the amount of hexadiene produced varied with the oxygen to propylene ratio, a ratio of 0.1 showing little change (3.8% to 4.1%) while the highest ratio (1.0) showing increasing amounts from 5.5% to 8% over only 40% of the temperature change. Increase in the oxygen to propylene ratio increased the yield of hexadiene especially at higher temperatures.

The only other major product that was produced was carbon dioxide and this varied very little with temperature but showed a large response to increases in the oxygen to propylene ratio. For example, the yield of carbon dioxide at 485°C increased quickly from 7.9 mole % at a ratio of 0.1 to 15.4, 25.6 and 38.2 mole % at ratios of 0.22, 0.5 and 1.0 respectively. The largest change in yield of carbon dioxide (from 7.9 to 12.2 mole %) with respect to temperature (485 to 557°C) occurred at a ratio of 0.1. The amount of carbon dioxide produced was many times larger than hexadiene but, in terms of the selectivity to hexadiene ($S\alpha$) the Tl_2O_3-Al_2O_3 catalyst was found to be very selective (Figure 36b).

The selectivity to hexadiene ($S\alpha$) decreased with a temperature rise at an oxygen to propylene ratio of 0.1 but increased with other ratios. The selectivity ($S\alpha$) also decreased with an increase in the oxygen to propylene ratio, due to the large increases in carbon dioxide production. This catalyst is active for dimerization at higher temperatures than the catalysts described below which were active only

for cyclization.

2B. Cyclization activity

(i) Bi_2O_3-MoO_3

Both the conversion of hexene and the yield of benzene passed through a maximum as the temperature increased from 400°C to 500°C (Figure 37). The rise in temperature resulted in a decrease in the selectivity to benzene (Sβ) from 98% to 87.5% at an oxygen to hexene ratio of 2:1. Decrease of the oxygen/fuel ratio to unity resulted in a decrease in the conversion and in the yield of benzene, particularly at 450°C where both decreased by 25%. The selectivity to benzene (Sβ) showed a larger decrease with temperature at an oxygen to hexene ratio of 1:1 than at 2:1.

(ii) Sb_2O_5-SnO_2

This catalyst was of moderate activity but high selectivity for cyclization (Figure 38). The conversion of hexene and the yield of benzene increased slowly with an increase in temperature (15% in 100C°, O_2:fuel = 2:1) and the selectivity remained fairly constant, varying only between 80 and 90%. The effect of a change in the oxygen to hexene ratio was not observed over the entire temperature range, but from the points available (Figure 38) it appears that the conversion and yield of benzene at the lower oxygen to hexene ratio (1:1) was more affected by increasing temperature, while the selectivity to benzene (Sβ) was the

FIGURE 37

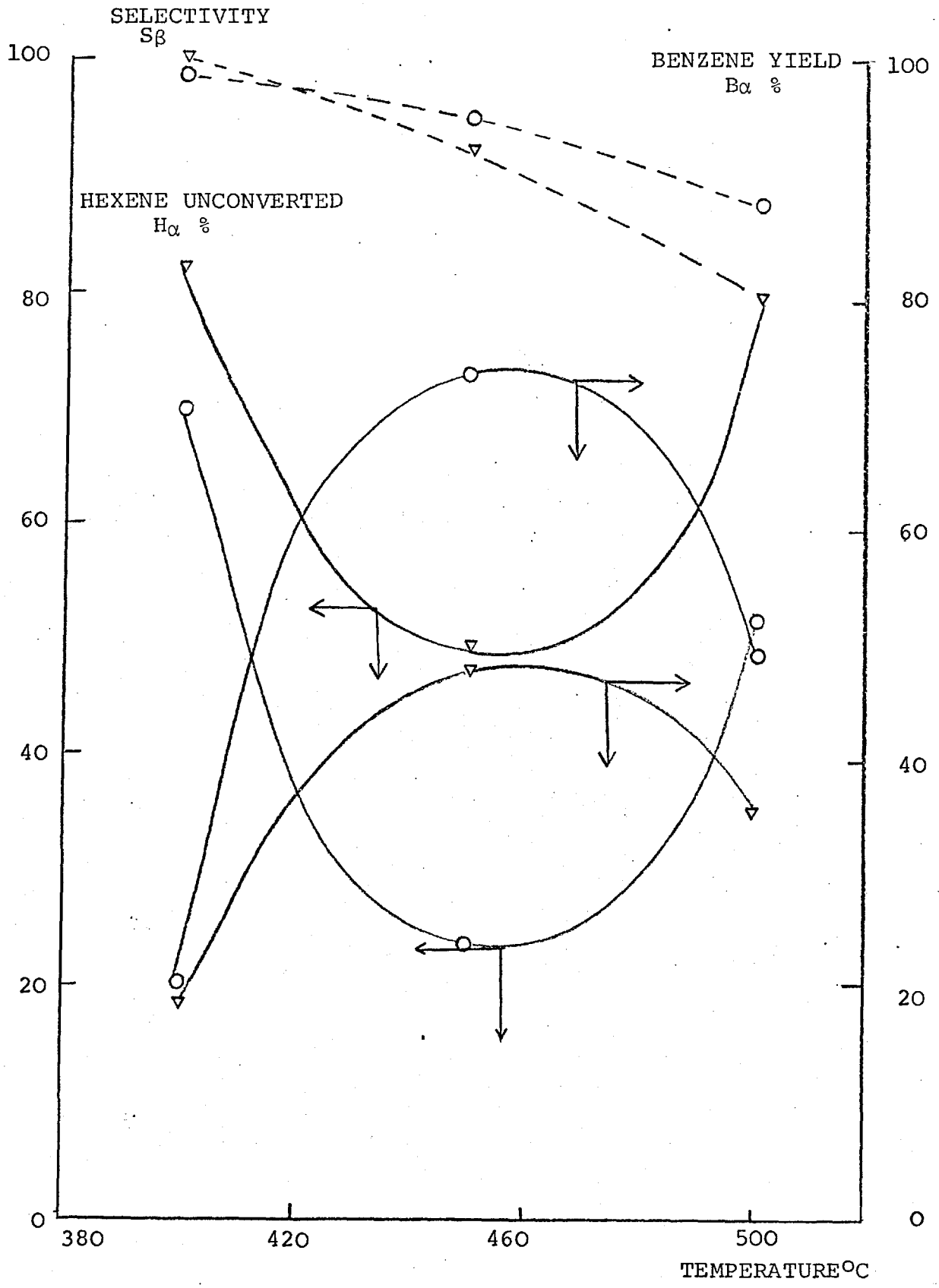

The effect of temperature on the conversion, yield and selectivity of cyclization of hexene over Bi_2O_3-MoO_3.

contact time: 24 cc/cc/sec

hexene concentration:
4.0×10^{-3} moles/litre

oxygen to hexene ratio:
2/1 -O-O-
1/1 -▽-▽-

FIGURE 38

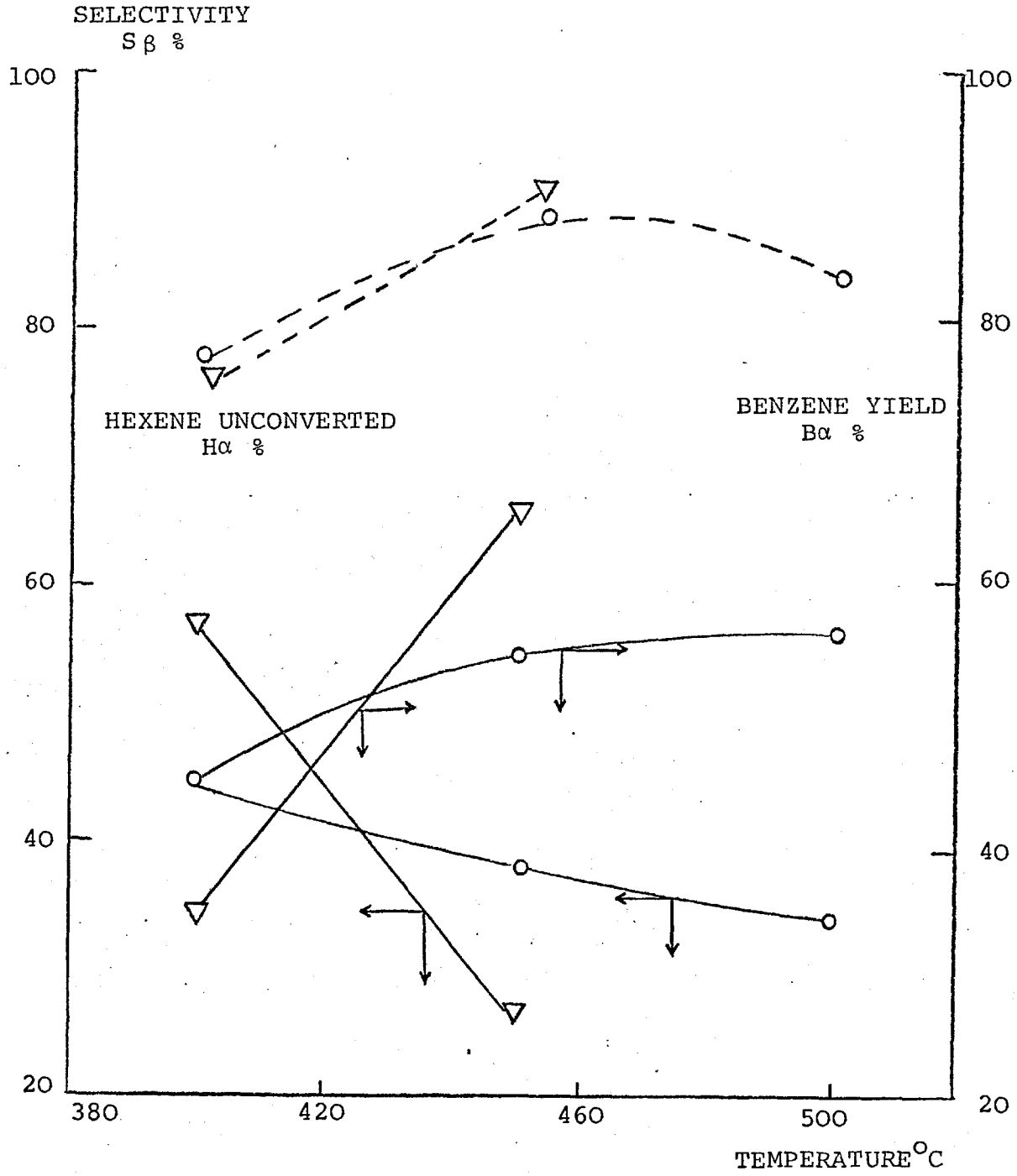

The dependence of conversion, yield and selectivity for the cyclization of hexene over Sb_2O_5-SnO_2 as a function of temperature.

contact time: 24 cc/cc/sec

hexene concentration:
4.0×10^{-3} moles/litre

oxygen to hexene ratio:
2/1 -O-O-
1/1 -▽-▽-

same in all cases.

(iii) $\underline{Pt\text{-}Al_2O_3}$

The conversion of hexene and the yield of benzene was found to increase with a temperature increase from 400°C to 500°C (Figure 39). An increase in the oxygen to hexene ratio at any temperature resulted in an increase in the yield of benzene, while the conversion remained relatively constant. A maximum in the selectivity to benzene, Sβ, (Figure 40) was found at a temperature of 450°C and at an oxygen to hexene ratio of 2:1. Selectivity (Sβ) was increased at all conditions by a decrease in contact time (Table 12).

(iv) $\underline{Cr_2O_3\text{-}Al_2O_3}$

The conversion of hexene increased sharply with temperature but was relatively unaffected by a change in oxygen to fuel ratio (Figure 41). The yield of benzene was found to increase steadily with temperature and showed a marked response to oxygen to hexene changes. The selectivity to benzene, Sβ, was independent of temperature under 460°C but decreased quickly from 47% to 33% over the range 460 to 500°C (O_2:hexene = 2/1). When the oxygen to hexene ratio was increased from 1:2 to 1:1 and 2:1, the selectivity increased markedly from 18% to 31 and 47% respectively at 450°C.

(v) $\underline{MoO_3\text{-}Al_2O_3}$

As the reaction temperature was varied from 400°C

FIGURE 39

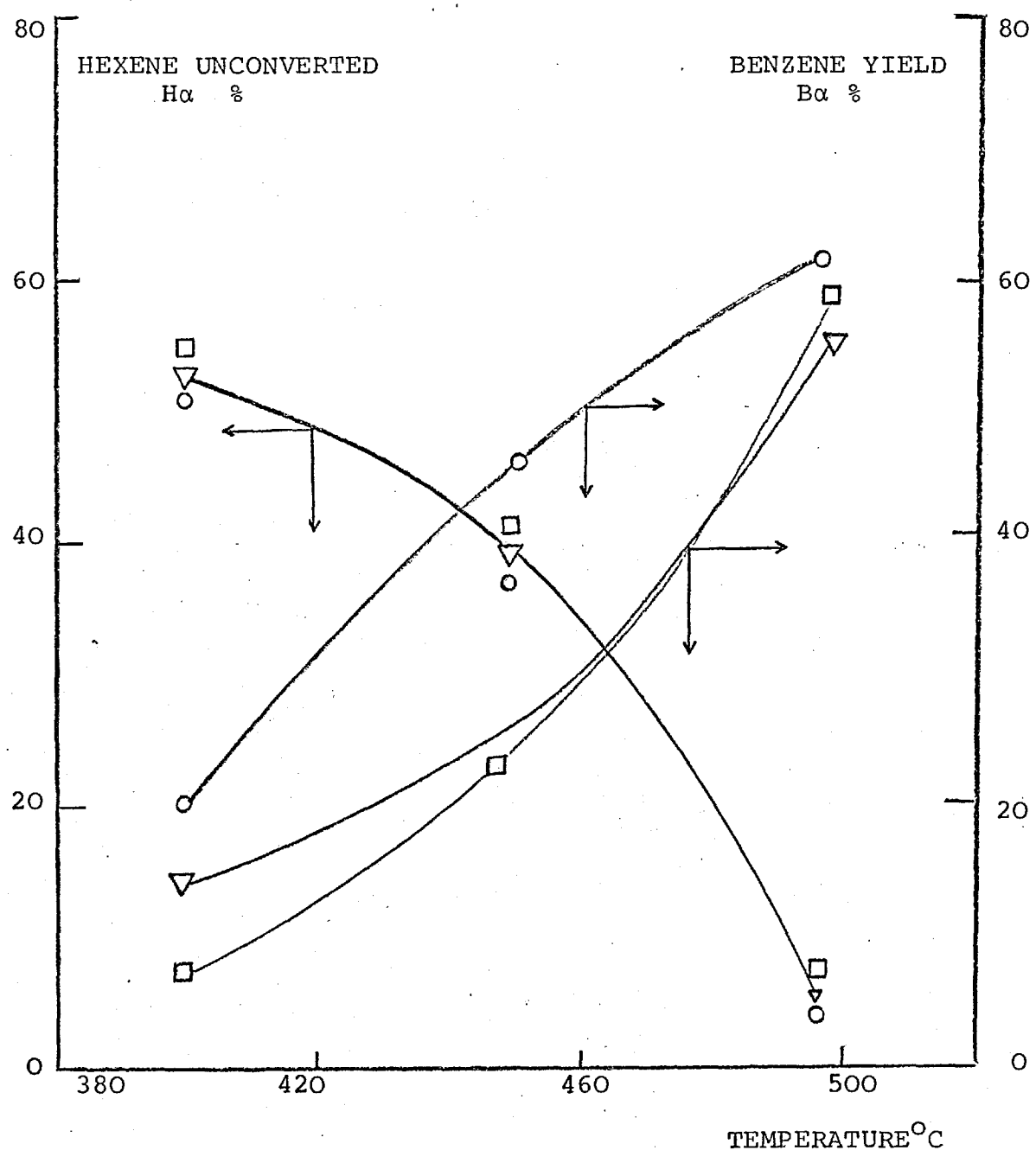

The variation of conversion and yield of benzene from hexene with temperature: $Pt\text{-}Al_2O_3$ catalyst.

contact time: 24 cc/cc/sec

hexene concentration: 4.0×10^{-3} moles/litre

oxygen to hexene ratio: 2/1 -O-O-
1/1 -▽-▽-
1/2 -□-□-

FIGURE 40

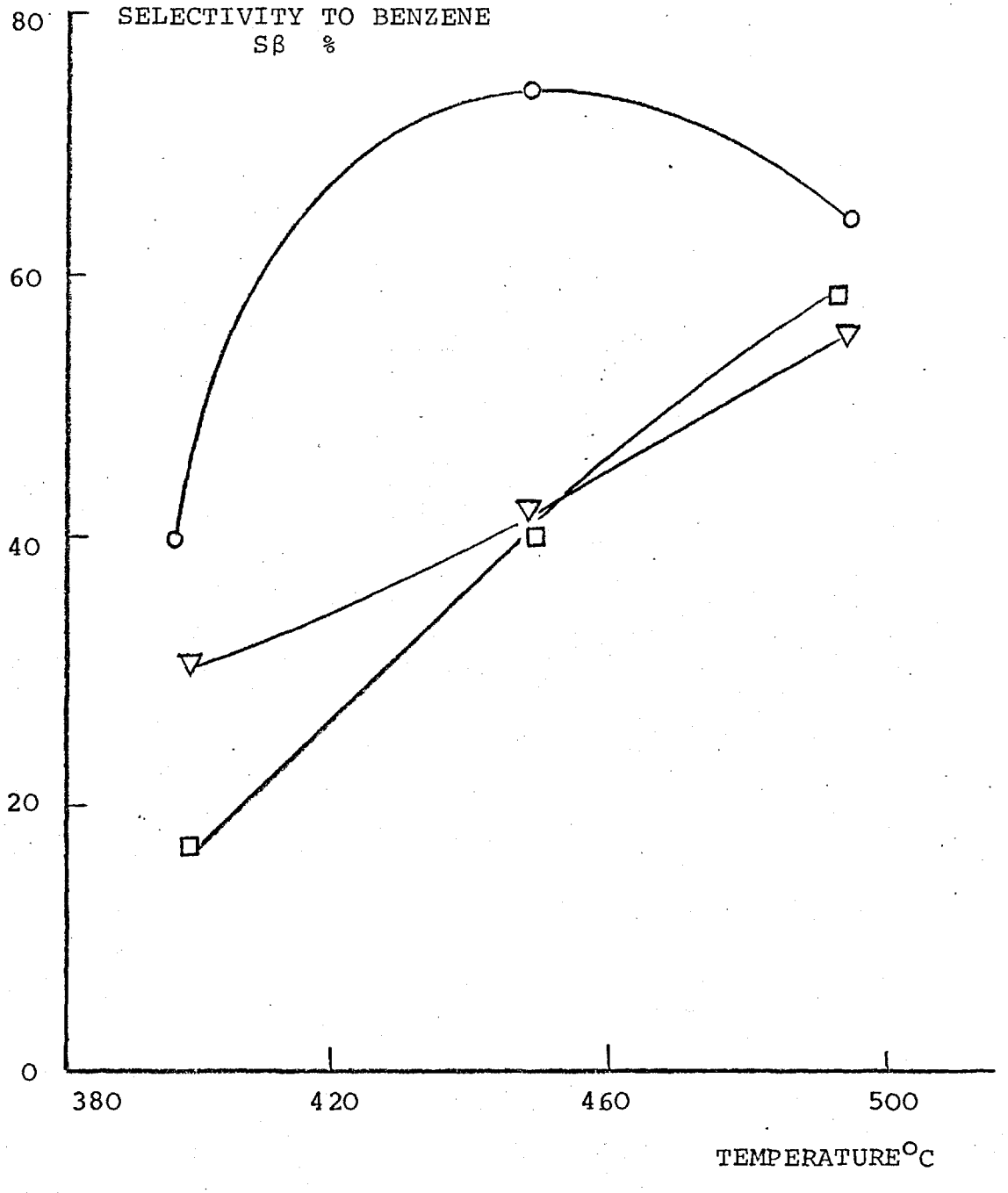

Variation of selectivity to benzene (Sβ) with temperature over a $Pt-Al_2-O_3$ catalyst.

contact time: 24 cc/cc/sec

hexene concentration:

4.0×10^{-3} moles/litre

oxygen to hexene ratio:

2/1 -○-○-

1/1 -▽-▽-

1/2 -□-□-

TABLE 12

The effect of temperature and of oxygen to hexene ratio on the oxidative dehydrocyclization of hexene over $Pt-Al_2O_3-Cl$

Temperature °C	Oxygen/Hexene*	Contact time cc/cc/sec	Yields % Hexene Hα	Benzene Bα	Selectivity Sβ %
399	2.0	24	51	19.7	40.9
		12	67	21.3	64.0
	1.0	24	52	14.3	30.0
		12	59	13.5	33.0
	0.5	24	54	7.4	16.0
		12	72	6.8	24.1
451	2.0	24	37.1	45.9	73.0
		12	39.6	44.0	72.8
	1.0	24	35.8	26.6	41.4
		12	54.5	24.5	53.8
	0.5	24	41.3	24.0	40.9
		12	57.3	26.1	61.1
497	2.0	24	2.6	61.6	63.2
	1.0	24	3.3	56.5	55.0
	0.5	24	4.6	58.4	57.7

*Hexene concentration constant at 4.0×10^{-3} moles/litre

FIGURE 41

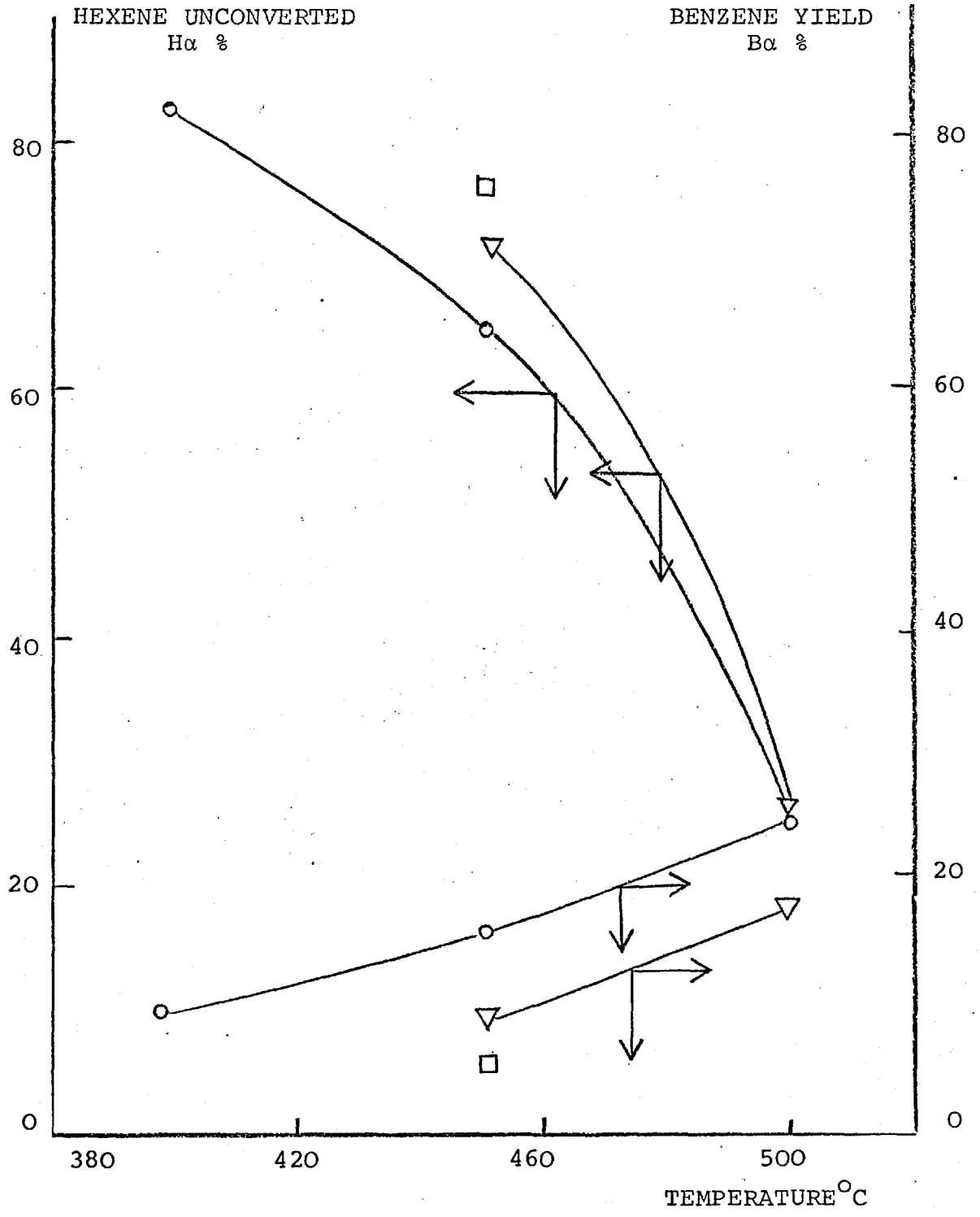

The conversion of hexene and the yield of benzene as a function of temperature over Cr_2O_3-Al_2O_3

contact time: 24 cc/cc/sec

hexene concentration:

4.0×10^{-3} moles/litre

oxygen to hexene ratio:

2/1 -O-O-

1/1 -▽-▽-

1/2 -□-□-

to 550°C (Figure 42) the conversion of hexene increased sharply, but the yield of benzene increased significantly only over 500°C. These two effects resulted in the selectivity to benzene decreasing as the temperature rose, for example, at an O_2:hexene of 2:1:

Temperature	°C	400	450	500	550
Selectivity	Sβ%	60	47	36	32

A change in the oxygen to hexene ratio resulted in little change in conversion especially at the higher temperatures, but the yield of benzene was directly affected. The selectivity to benzene at an oxygen to hexene of 1:1 was 15% lower than the 2:1 value at all temperatures.

(vi) ThO_2-Al_2O_3

Significant conversion of hexene to benzene was only observed at high temperatures, and the selectivity was low (less than 30%), as a result of the high rates of isomerization and cracking.

3. Development studies

As a result of the preliminary studies, one catalyst (Tl_2O_3-Al_2O_3) seemed to offer reasonable activity for a dimerization reaction, while the Bi_2O_3-MoO_3 catalyst was selected as the cyclization catalyst. As a precaution, homogeneous reaction studies were carried out in the metal integral reactor and the metal differential reactor. Significant homogeneous combustion was detected in both

FIGURE 42

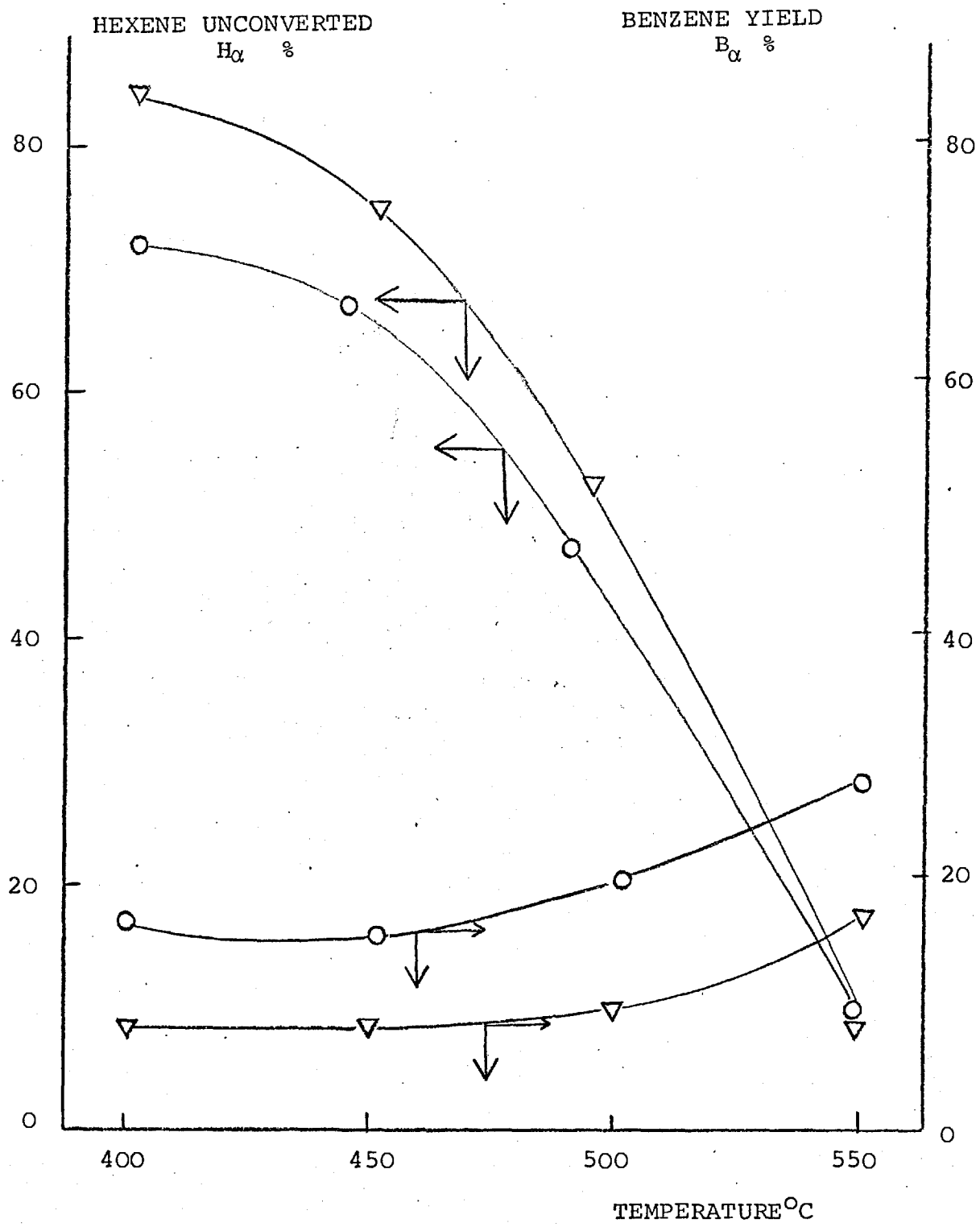

The variation of the conversion of hexene and the yield of benzene with temperature over MoO_3-Al_2O_3.

contact time: 24 cc/cc/sec

hexene concentration:
4.0×10^{-3} moles/litre

oxygen to hexene ratio:
2/1 -o-o-
1/1 -▽-▽-

reactors and a large temperature profile was observed in the metal differential reactor. Very little homogeneous reaction was observed in glass or silica reactors and the development studies for cyclization and dimerization were carried out in these reactors. The effects of temperature, concentration and contact time were examined and in each case all the major products were analysed.

3A. Dimerization

(i) Tl_2O_3-Al_2O_3

Further studies of the dimerization of propylene were initiated at 500°C. The effect of the concentration of reagents and of contact time are reported in Table 13, from which it can be seen that an increase of oxygen concentration decreased selectivity but that an increase in propylene had the opposite effect. The selectivity of the reaction increased with contact time.

The response of the reaction to temperature was studied over a range from 410°C to 518°C at two contact times. Both the yields of hexadiene and carbon dioxide increased with increasing temperature (Figure 43), but as the yield of hexadiene at both contact times increased faster with temperature than did the yield of carbon dioxide, the net effect was to increase the selectivity to hexadiene (Figure 44).

Increase of contact time increased the conversion and both the yield of hexadiene and of carbon dioxide. The

TABLE 13

The effect of the oxygen to propylene ratio and the contact time on the oxidative dimerization to hexadiene over Tl_2O_3-Al_2O_3 at 500°C

Concentration ^{3} moles/litre x 10^{-}		Contact time	Hexadiene*	CO_2*	Selectivity, Sδ
O_2	C_3H_6	cc/cc/sec	moles x 10^{-7}	moles x 10^{-7}	
2.0	18.2	1.0	0.33	1.05	1.88
4.0	40.5	1.33	0.52	2.4	1.30
4.5	40.0	2.2	1.0	3.15	1.90
8.1	36.4	2.0	0.81	3.8	1.30
1.9	34.8	1.9	1.0	2.1	2.86
3.2	29.6	3.1	1.26	3.15	2.4
1.6	36.4	4.0	1.1	1.47	4.5
2.1	33.9	5.1	1.54	2.56	3.6

*sample volume is 4.9 cc

FIGURE 43

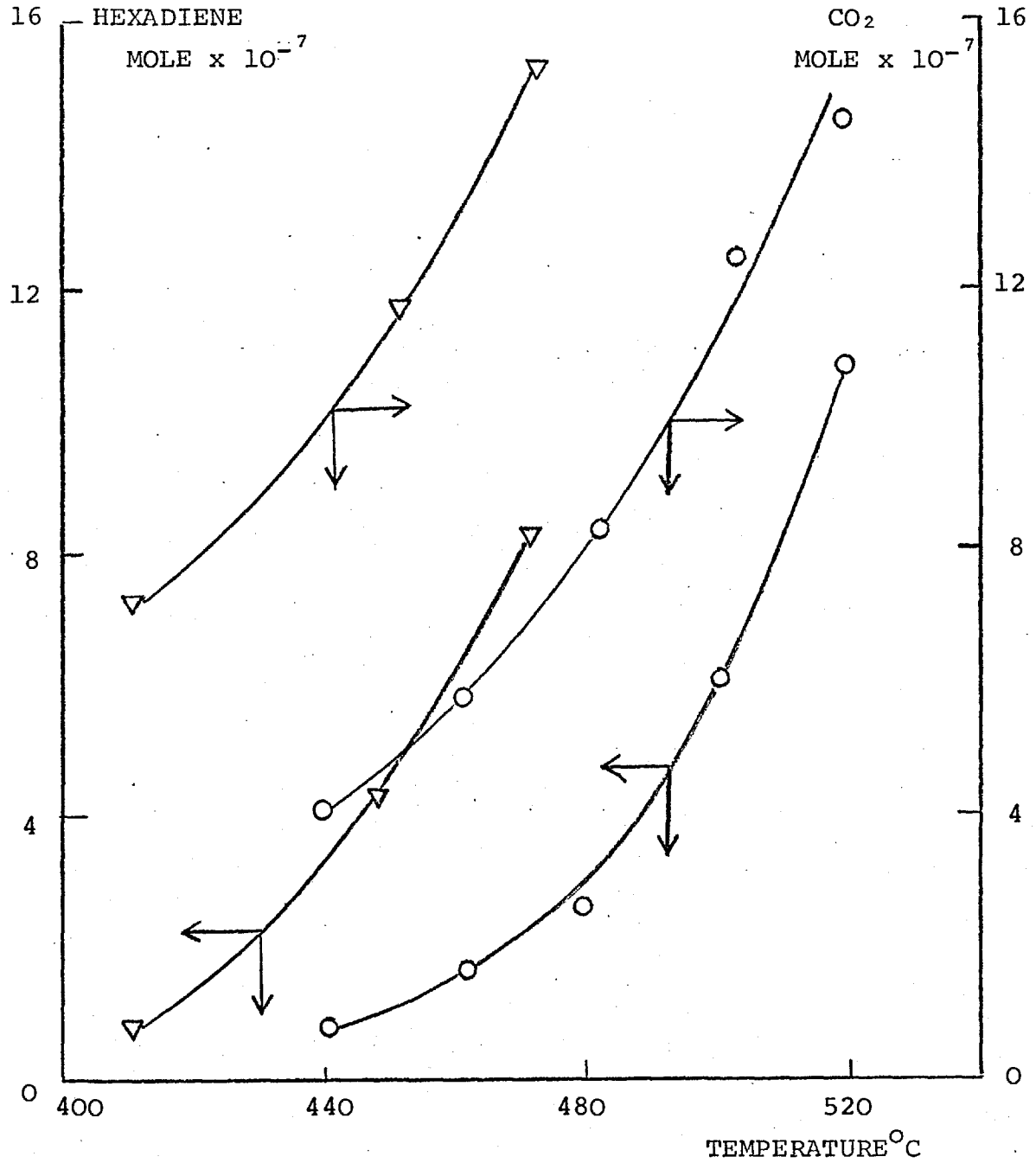

The effect of temperature on the yields of hexadiene and carbon dioxide from propylene over Tl_2O_3-Al_2O_3.

contact time: 4 cc/cc/sec -O-O-
8 cc/cc/sec -▽-▽-
propylene concentration: 40.0×10^{-3} moles/litre
oxygen concentration: 4.5×10^{-3} moles/litre

FIGURE 44

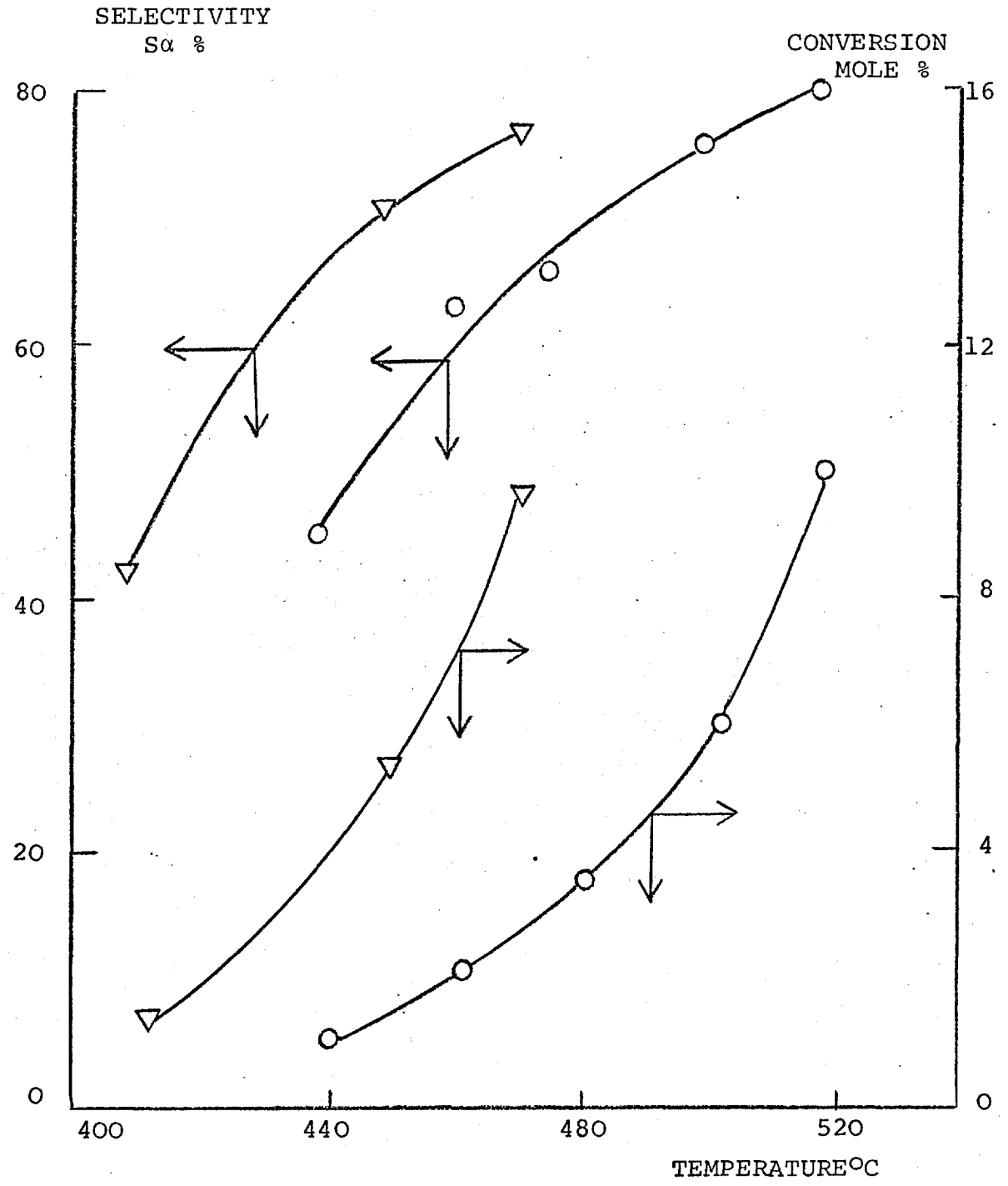

The variation of the conversion of propylene and the selectivity to hexadiene as a function of temperature over Tl_2O_3-Al_2O_3.

contact time: 4 cc/cc/sec -○-○-
8 cc/cc/sec -▽-▽-

propylene concentration: 40.0×10^{-3} moles/litre

oxygen concentration: 4.5×10^{-3} moles/litre

selectivity also increased at the longer contact time.

The deactivation of the supported Tl_2O_3 catalyst under a stream of pure propylene was investigated in some detail (Figure 45). At time zero, a stream of 10 cc/min air which had been mixed with 32 cc/min of propylene and passed over the catalyst at 500°C was stopped; the reaction to hexadiene continued but slowly deactivated the catalyst. After a hour and a half, when the yield had decreased to 40% of the initial value, the contact time was doubled and the concentration of hexadiene increased from 0.6% to 1.6%. The deactivation continued and the yield dropped to 0.6% after a total of three hours. Only a very small amount of carbon dioxide was produced during the deactivation.

(ii) Tl_2WO_4

This solid was tested as a dimerization catalyst over a range of oxygen to fuel ratios and contact times at a temperature of 500°C. The results, reported in Table 14, show that the selectivity was low but improved with contact time. An increase in oxygen concentration increased selectivity at the longer contact times.

3B. Cyclization

(i) Homogeneous reaction

The preliminary selection studies were completed without facilities for monitoring the carbon dioxide production.

FIGURE 45

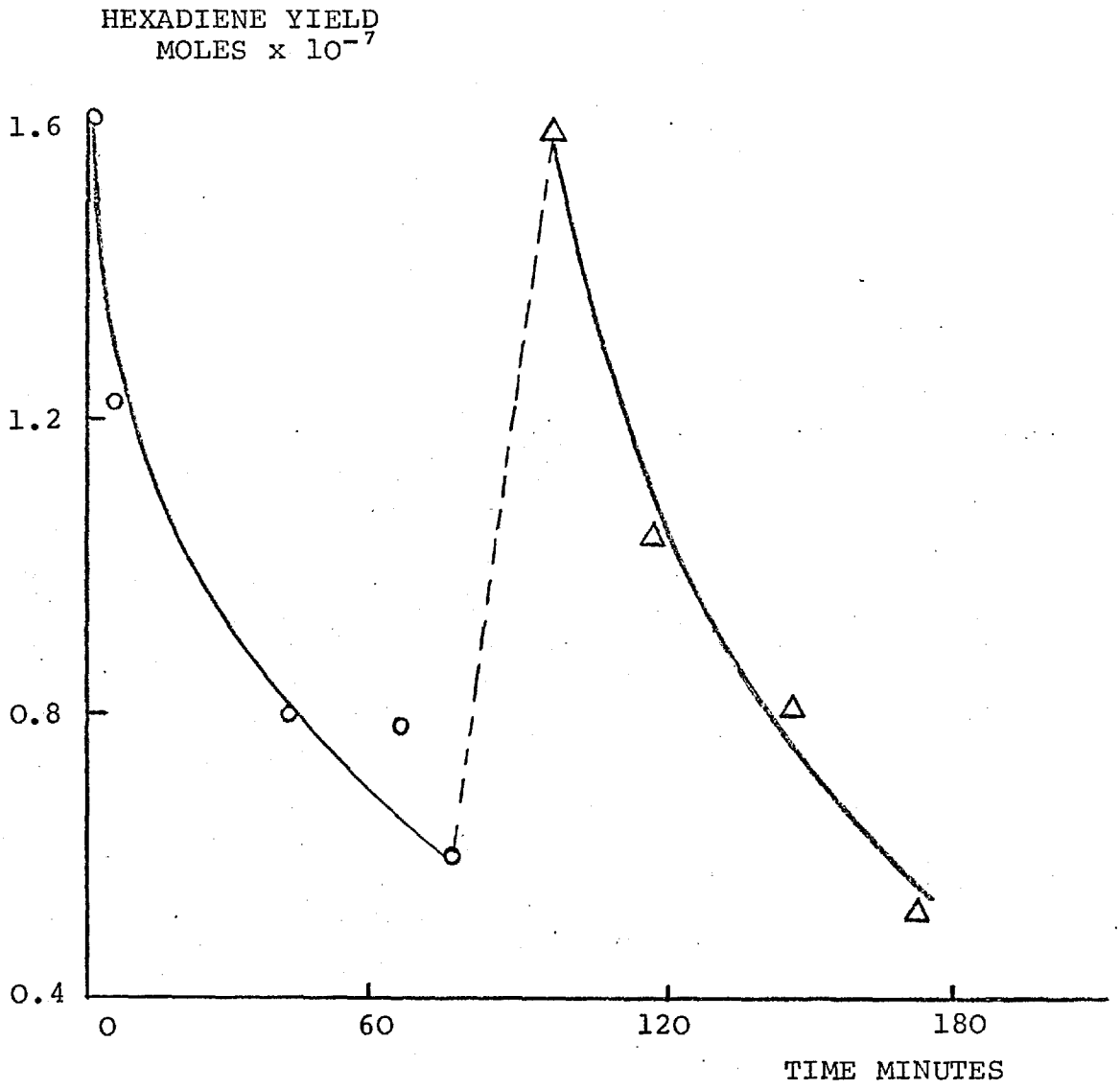

The deactivation of Tl_2O_3-Al_2O_3 by pure propylene at 500°C.

contact time: 6 cc/cc/sec -O-O-
12 cc/cc/sec -▽-▽-

TABLE 14

The effect of the oxygen to propylene ratio on the oxidative dimerization to hexadiene over Tl_2WO_4 at 500°C

O_2 Concentration moles/litre x 10^{-3}	C_3H_6	Contact time cc/cc/sec	Hexadiene* moles x 10^{-7}	CO_2* moles x 10^{-6}	Selectivity, Sα
4.5	40	3	0.38	1.77	10.9%
9.0	35.5	3	0.77	4.1	10.2%
9.0	35.5	1.5	1.6	2.4	28.6%
4.5	40	1.5	0.67	1.7	19.2%
9.0	35.5	0.8	1.8	2.5	30.2%
4.5	40	3	0.40	2.2	10.1%

*sample volume 4.9 cc

As it has been reported that metal reactors can effect selectivity by initiating homogeneous combustion (94), the homogeneous reaction of hexene and oxygen was studied in the metal integral reactor filled with ceramic pieces, over the same conditions as the previous studies (Table 15). Carbon dioxide, the main product, was found to increase with temperature and with the oxygen to hexene ratio. Small amounts of isomerization and cracking products together with benzene were detected.

A metal differential reactor (Figure 26), designed for initial rate studies, was tested for homogeneous reaction over a temperature range from 350°C to 550°C. A temperature profile along the reactor (filled only with pumice stone) of up to 40C° was observed. Carbon dioxide, the main product from the homogeneous reaction, more than doubled with each 100C° rise in temperature (Table 15). An increase in the oxygen concentration also increased the yield of carbon dioxide.

A differential glass reactor was tested for homogeneous combustion of hexene over a range of temperature at a fixed concentration of reactant. The results, reported in Table 15, show that the homogeneous combustion is small and relatively constant over the temperature range where the dehydrocyclization of hexene has been studied.

(ii) Pt-Al_2O_3-Cl

0.44 gm Pt-Al_2O_3-Cl were made up to 4 cc with pumice stone and used as a catalyst at 350°C for a mixture

TABLE 15

Homogeneous reaction of oxygen and hexene

Reactor	Temperature	Concentration O_2 moles/litre	Concentration Hexene $\times 10^{-3}$	CO_2 moles $\times 10^{-7}$
integral (metal)	400	1.8	1.8	0.9
		3.6	1.8	1.4
		7.2	1.8	2.6
	455	1.8	1.8	2.9
		7.2	1.8	4.7
	485	3.6	1.8	5.6
	535	1.8	1.8	3.3
		3.6	1.8	6.8
		7.2	1.8	11.6
differential (metal)	350	13.3	13.3	6.5
	450	13.3	13.3	15.5
		26.6	13.3	26.0
	555	13.3	13.3	40.0
differential (glass)	356	6.7	6.7	0.0
	443	6.7	6.7	2.9
	500	6.7	6.7	2.8

of 30 cc/min O_2, 30 cc/min hexene and 120 cc/min N_2. The oxygen was completely consumed and a 500°C temperature profile was set up along the reactor. The reactor was removed from the tin bath but left with the reaction mixture passing through. Even with a temperature profile of 70°, 220°, 125° at the beginning, middle and end of the catalyst bed respectively, the oxygen was almost completely consumed producing carbon dioxide. The same reactor was then filled with pumice stone and used under the same conditions at a temperature of 425°C. A small, unmeasurable amount of carbon dioxide was produced.

(iii) Sb_2O_5-SnO_2

A very brief study of the effect of contact time on the oxidation of hexene over Sb_2O_5-SnO_2 was carried out at 455°C and at a 1:1 oxygen to hexene ratio. The yield of benzene increased by a factor of three (1.5 to 4.6 x 10^{-7} moles) when the contact time was doubled, while the carbon dioxide increased only from 9.4 to 10.7 x 10^{-7} moles. As a result the selectivity to benzene, Sp, increased from 0.95 to 2.58. A high concentration of intermediate dehydrogenation products (such as hexadiene, hexatriene and cyclohexadiene) was detected at both contact times.

(iv) Bi_2O_3-MoO_3

The effect of an increase in the oxygen concentration on the yield of benzene and carbon dioxide is reported in

Figure 46. The yield of benzene passed through a maximum at a 2:1 oxygen to hexene ratio, but the yield of carbon dioxide increased continuously resulting in a maximum for the selectivity to benzene between a 1:1 and a 2:1 ratio (Figure 46). Decreasing the contact time had little effect on selectivity (Table 16), and the selectivity to benzene was found to be higher at the same conditions at 450°C than at 380°C.

A Bi_2O_3-MoO_3 catalyst was prepared by a different method (self-precipitation) in order to compare preparation methods. The results (Table 17) indicate that there may be differences, especially with respect to selectivity, between the two preparations. However, the results extend the above conclusions concerning the effect of various reaction variables.

The effect of an increase in the hexene concentration on the yield of benzene and carbon dioxide and on the selectivity to benzene is reported in Figure 47. The yield of benzene decreased sharply when the hexene concentration was doubled but appeared eventually to approach a value independent of the hexene concentration. The yield of carbon dioxide appears to be inversely dependent on the hexene concentration while the selectivity, at 450°C, passed through a steep minimum at a fuel:oxygen ratio of 3:1. Other observations at different conditions support this pattern of selectivity (Table 17).

The effect of concentration can not be expressed solely in terms of a hexene to oxygen ratio since when the ratio was kept constant at 1:1 at 450°C and the concentration

FIGURE 46

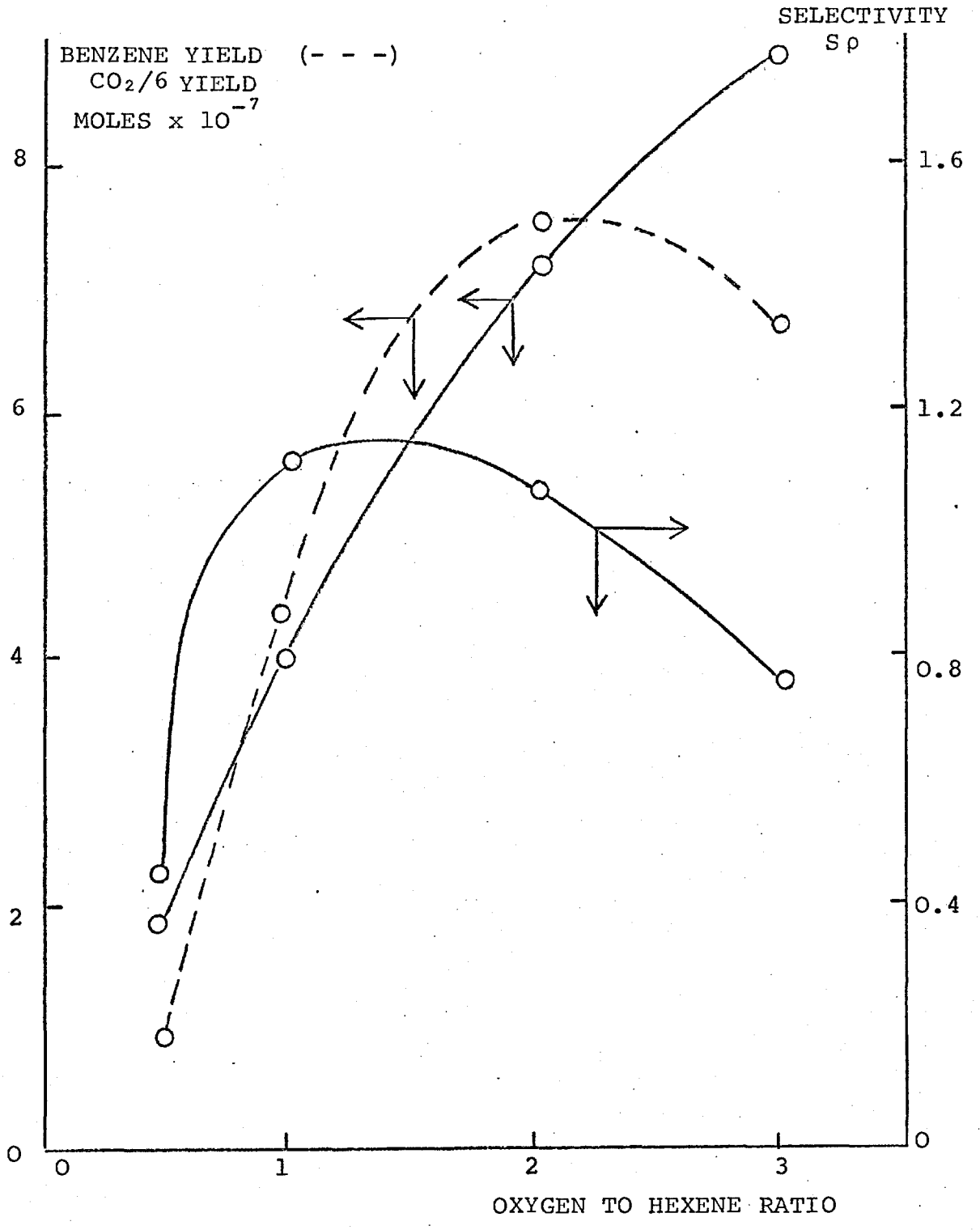

The yield of benzene and carbon dioxide and the selectivity as a function of oxygen concentration (oxygen to hexene ratio) at 450°C over Bi_2O_3-MoO_3.

contact time: 1.5 cc/cc/sec
hexene concentration: 7.0×10^{-3} moles/litre

TABLE 16

The effect of temperature, oxygen to hexene ratio and contact time on the oxidative dehydrocyclization of hexene to benzene over Bi_2O_3-MoO_3

Temperature °C	O_2 moles/litre x 10^{-3}	Hexene moles/litre x 10^{-3}	Contact time cc/cc/sec	Bz moles x 10^{-7}	Co_2 moles x 10^{-7}	Selectivity, Sp
380	7.4	7.4	1.7	0.75	6.5	0.69
420	4.1	8.1	0.9	0.61	4.1	0.89
450	4.1	8.1	1.8	0.84	10.6	0.48
	7.4	7.4	1.7	4.3	23.6	1.12
	12.8	6.4	1.4	7.5	43.0	1.05
	16.8	5.6	1.3	6.6	53.0	0.75
	7.4	7.4	0.8	2.8	15	1.12
	12.8	6.4	0.7	4.9	33.6	0.88

TABLE 17

The effect of temperature and of hexene and oxygen concentrations on the oxidative dehydrocyclization of hexene to benzene over Bi_2O_3-MoO_3

Temperature °C	O_2 moles/litre x 10^{-3}	Hexene moles/litre x 10^{-3}	Contact time cc/cc/sec	Benzene moles x 10^{-7}	CO_2 moles x 10^{-7}	Selectivity, Sρ
400	3.7	3.7	0.8	0.4	5.4	0.44
	6.8	3.4	0.8	1.9	27.4	0.41
	6.4	6.4	0.7	0.8	12.8	0.37
	3.4	6.8	0.8	-	6.7	-
	1.7	6.8	0.8	-	2.1	-
	3.4	13.6	1.5	-	8.2	-
	6.4	12.8	1.4	-	16.4	-
450	3.7	3.7	0.8	3.43	15.4	1.34
	1.9	3.7	0.8	1.53	7.7	1.19
	1.8	7.2	0.8	1.28	6.0	1.28
	3.4	6.8	0.8	3.5	18.1	1.16
	2.0	2.0	0.9	3.0	9.1	1.98
480	2.0	2.0	0.9	2.3	6.4	2.16
	1.9	3.7	0.8	1.7	5.7	1.79
	3.7	3.7	0.8	2.3	-	-

FIGURE 47

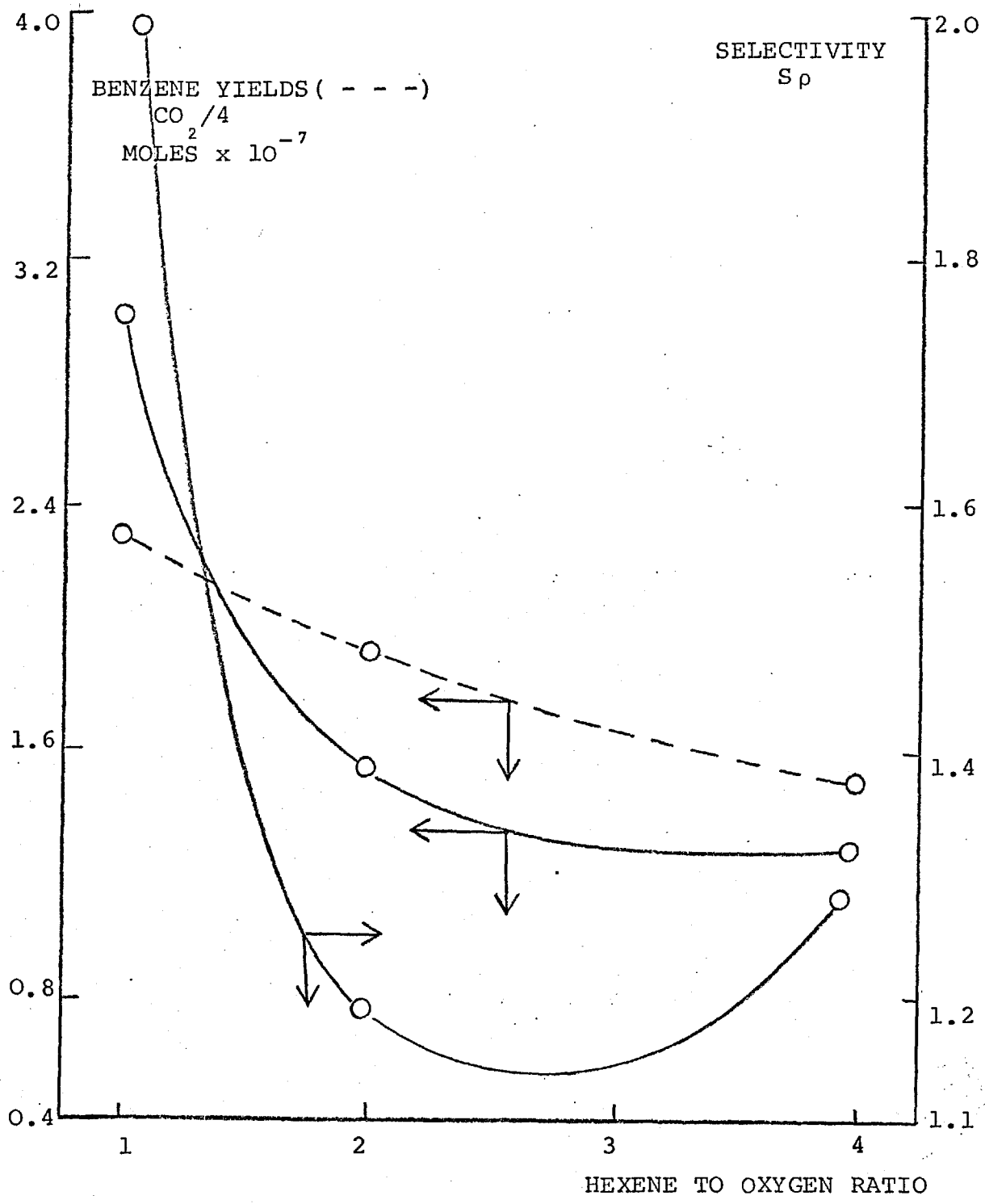

The yield of benzene and carbon dioxide and the selectivity to benzene as a function of hexene to oxygen ratio at 450°C over Bi_2O_3-MoO_3.

contact time: 0.8 cc/cc/sec

oxygen concentration: 1.9×10^{-3} moles/litre

of both reactants was doubled, the selectivity decreased significantly from 1.98 to 1.34. The selectivity to benzene was found to increase with temperature, confirming the observations from Table 16.

4. Detailed studies: Tl_2O_3

Preliminary results showed that the dimerization of propylene did not occur at temperatures less than ca 350°C, and that the activity of the catalyst decayed fairly rapidly, particularly in the absence of oxygen. Initial experiments were designed to investigate the effect of oxygen and fuel on the catalyst activity.

With the temperature of the reactor set at 500°C, the oxygen to propylene ratio was varied between 0.012 and 0.25. The total flow rate and contact time was constant, but the concentration of both propylene and oxygen was varied (Table 18). The results show that the production of 1,5 hexadiene was inversely proportional to, and the production of carbon dioxide directly proportional to the oxygen to propylene ratio (Figure 48). The selectivity dropped quickly as the oxygen to propylene ratio increased from 0.01 to 0.05 but stayed reasonably constant at oxygen to propylene ratios greater than 0.1. The sum of the hexadiene concentration plus the concentration of carbon dioxide divided by 6, was independent of the oxygen to propylene ratio.

The rate of deactivation of the catalyst under various conditions was checked against a "standard" mixture of 1:9

TABLE 18

The effect of the oxygen to propylene ratio and the contact time on the oxidative dimerization of propylene to hexadiene over Tl_2O_3-Al_2O_3 at 500°C

Propylene moles/litre	Oxygen x 10^{-3}	Contact time cc/cc/sec	Hexadiene moles x 10^{-7}	Carbon dioxide moles x 10^{-7}	Selectivity Sρ
44.0	0.45	1.5	2.7	1.1	13.1
43.4	1.1	1.5	2.5	2.0	6.6
42.3	2.2	1.5	2.2	4.2	3.1
40.1	4.4	1.5	2.2	6.2	2.2
35.7	8.8	1.5	1.8	8.0	1.4
40.1	4.4	3.0	4.6	12.0	2.3
35.7	8.8	3.0	3.6	17.0	1.3
40.1	4.4	6.0	6.8	15.1	2.7
35.7	8.8	6.0	5.4	27.2	1.2

FIGURE 48

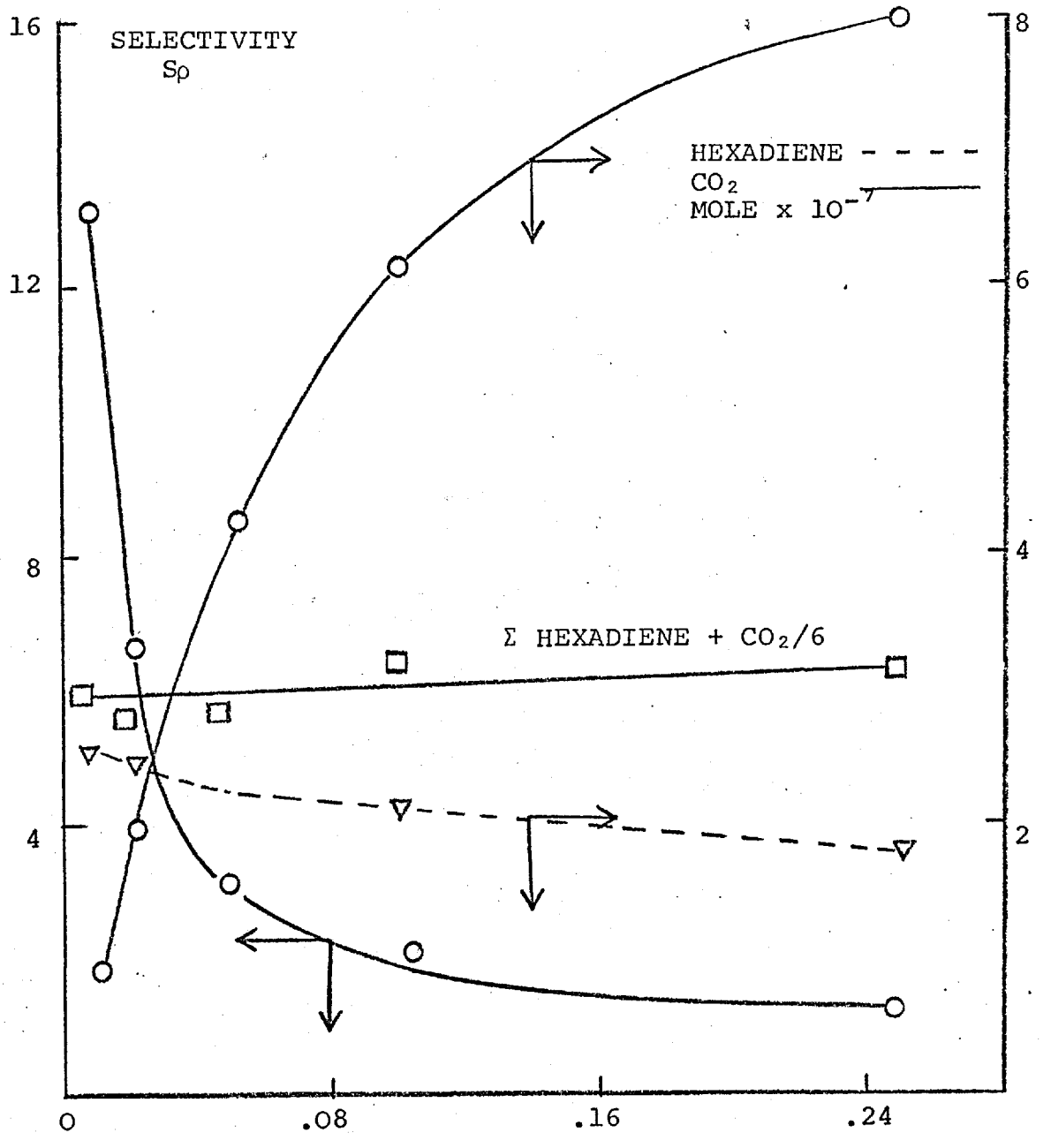

The effect of the oxygen to propylene ratio on the yield of carbon dioxide and hexadiene and the selectivity to hexadiene at 500°C over Tl_2O_3-Al_2O_3.

contact time: 1.5 cc/cc/sec

Σ oxygen and propylene concentrations: 44.5×10^{-3} moles/litre

oxygen:fuel ratio at the same contact time and temperature. With this mixture deactivation was slow over a fresh catalyst and the selectivity (the ratio of 6 x hexadiene to carbon dioxide) remained about the same for comparatively long reaction times.

A freshly prepared catalyst was deactivated by passage of pure propylene for one hour (Figure 49). After this time, the flow of propylene was stopped and replaced by nitrogen (5 min.) and then pure oxygen. After treatment for 30 minutes, oxygen was replaced by nitrogen and then by the standard mixture. The reactivated activity of the catalyst was found to be the same as the original activity. The catalyst was then deactivated once more, the activity following the previous curve. Reactivation using oxygen for times of between 30 min. and 24 hours returned the activity to the original level. Although no oxygen was introduced into the reactor, the products of the deactivation reaction always included small amounts of oxygen (ca 1%) and carbon dioxide (ca 1%). No hydrogen could be detected among the reaction products at any stage.

In one series of experiments, the catalyst was reactivated, treated with hydrogen for fifteen minutes, rinsed with nitrogen, and pure propylene was passed over the solid in the usual manner. The results (Figure 49) show that the activity of the reduced catalyst is much lower than the normal catalyst. Nitrogen was passed over the oxidized catalyst for an equivalent period of time and no change of deactivation pattern was noted.

FIGURE 49

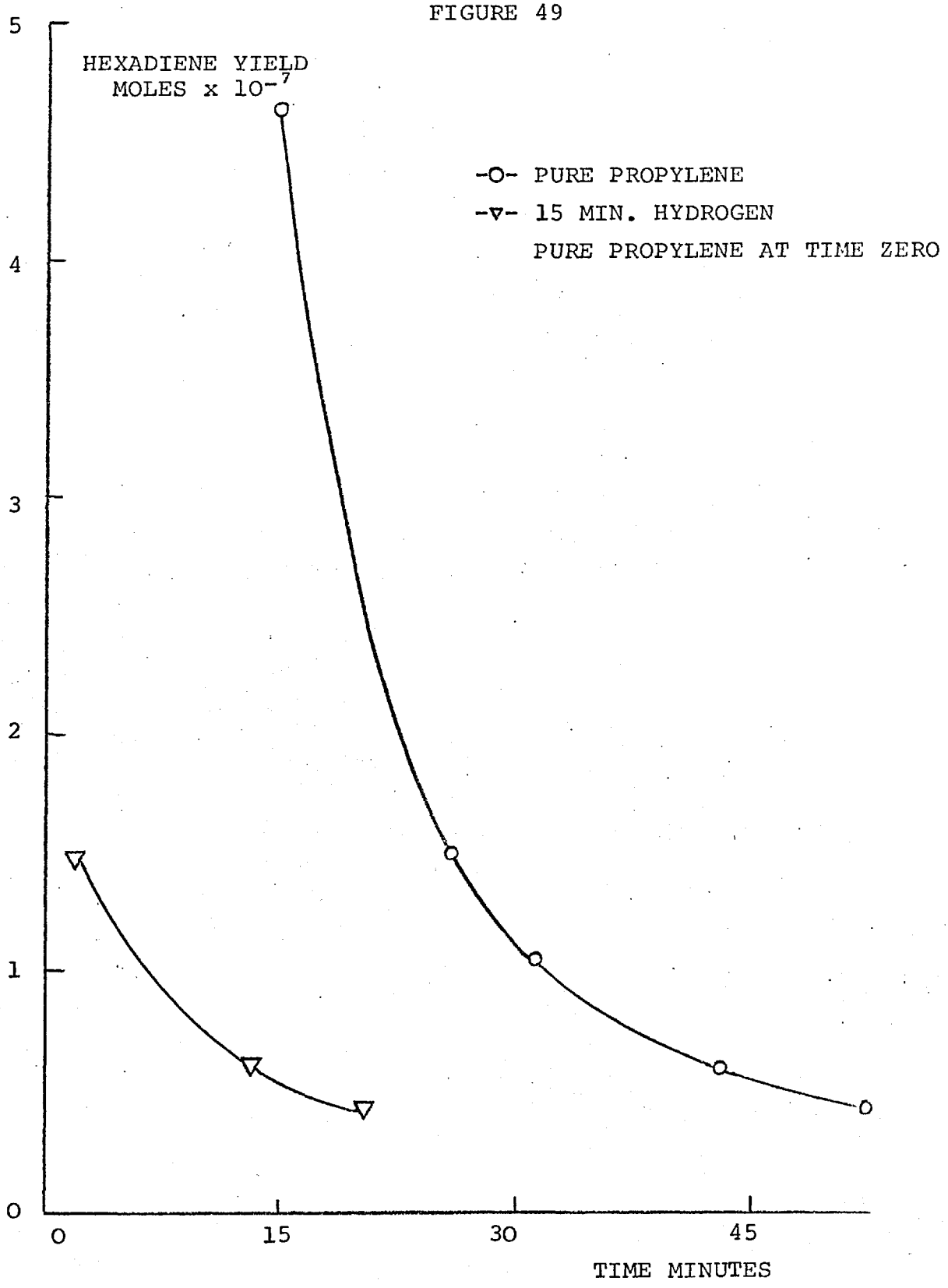

Effect of reduction of Tl_2O_3-Al_2O_3 by hydrogen on the propylene deactivation yield of hexadiene at 500°C.

contact time: 0.8 cc/cc/sec

During these deactivation studies, it was occasionally necessary to replace the catalyst because solid had been carried out of the reactor. This effect was much more noticeable with the reduced catalyst; the solid remaining in the reactor was found by chemical analysis to consist of a mixture of thallic and thallous ion while the solid in the exit line contained primarily thallous ion. Experiments were completed to test whether the volatile thallium compounds were catalytically active, by using a reactor which contained the same amount of catalyst but in which it was possible to vary the heated catalyst free volume after the bed. Under no normal conditions was the product spectrum different from that obtained in a conventional reactor. The homogeneous reaction was examined over pumice stone and little reaction was observed.

All subsequent experiments were completed under conditions such that deactivation was minimised. The standard feed was used as a test of the catalyst activity.

The dependence of the product spectrum on temperature has been investigated at an oxygen mole fraction of 0.1 (Figure 50). The rate of formation of hexadiene increases rapidly over ca 500^{o}C, while that of carbon dioxide increases only slowly. The selectivity of the reaction increases from 1.0 to 3.4 on increasing the temperature of the reaction from 500 to 540^{o}C. The apparent activation energies (Figure 51) were found to be 52 kcal/mole (propylene to hexadiene) and 21 kcal/mole (propylene to carbon dioxide). At higher

FIGURE 50

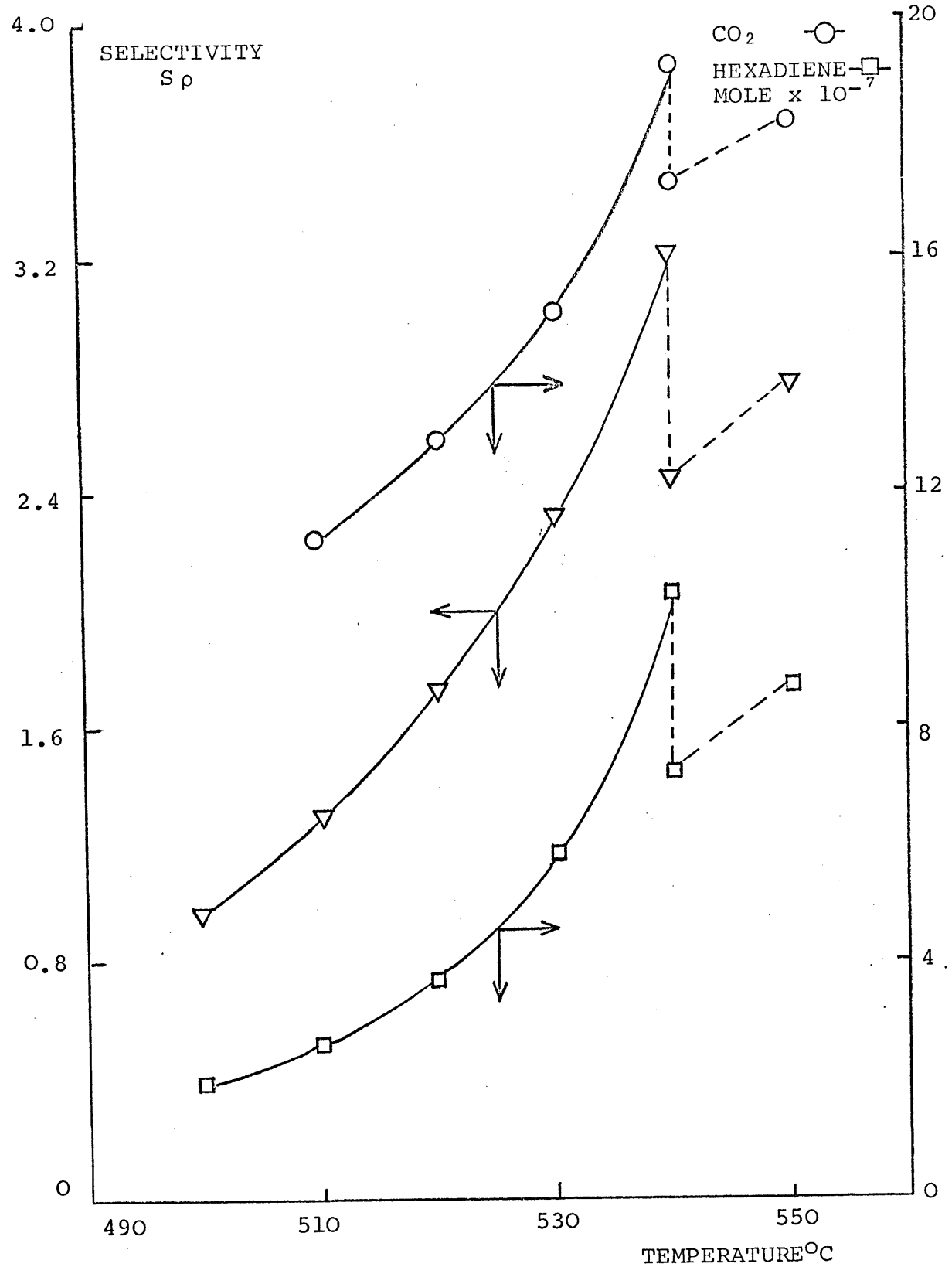

The effect of temperature on the yield of carbon dioxide and hexadiene and the selectivity of reacted propylene over Tl_2O_3-Al_2O_3.

contact time: 1.5 cc/cc/sec
oxygen concentration: 4.45×10^{-3} moles/litre,
propylene concentration: 40.0×10^{-3} moles/litre
- - - - deactivation

FIGURE 51

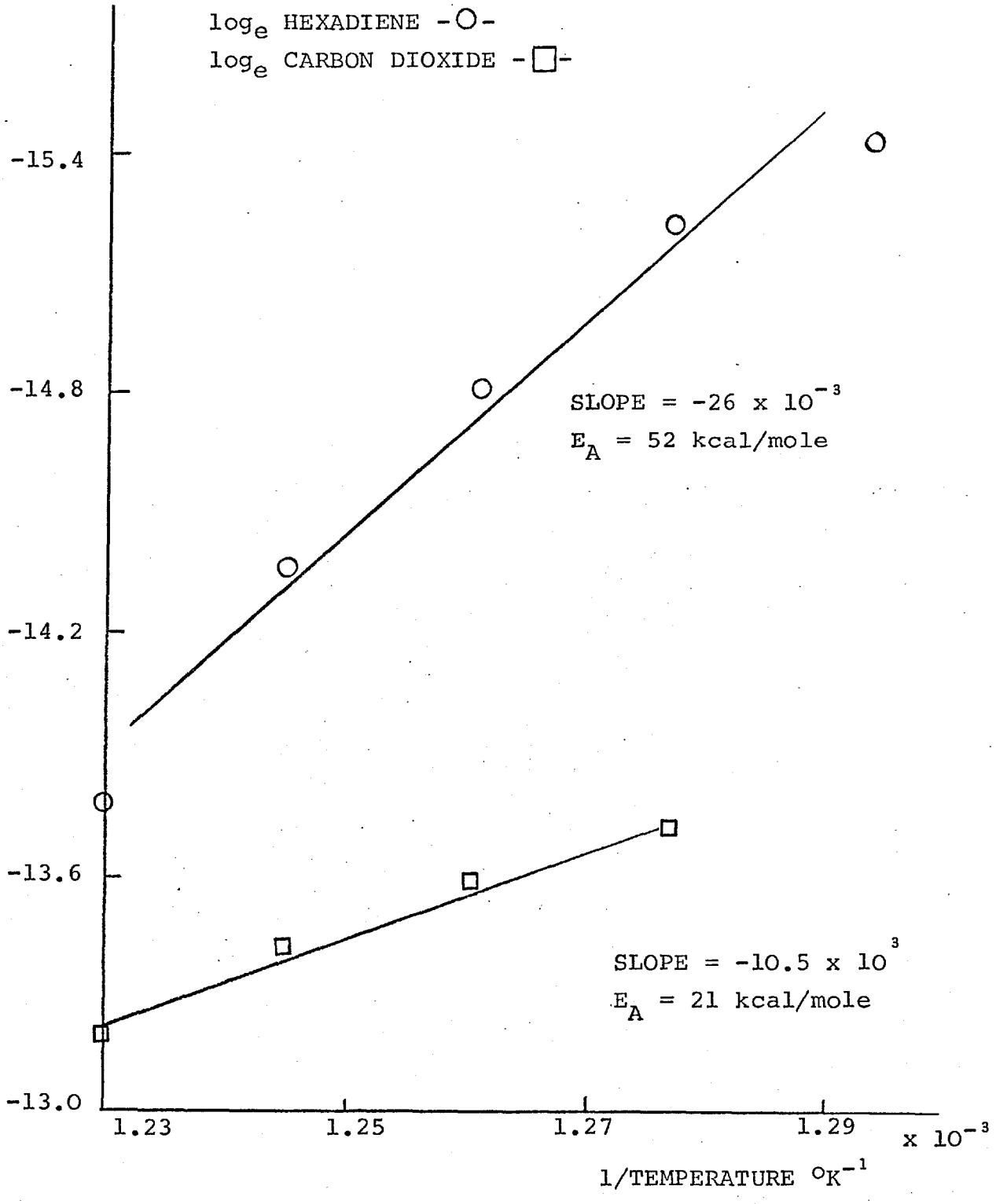

Arrhenius plot of data from Figure 50 to determine the activation energies of hexadiene and carbon dioxide production over Tl_2O_3-Al_2O_3.

temperatures, even in the presence of oxygen, the deactivation of the catalyst was found to occur at a faster rate as can be observed in Figure 50. The effect of contact time upon the concentration of products was examined at oxygen to propylene ratios equal to 0.1 and 0.25. The results shown in Table 18, indicate the selectivity was relatively independent of contact time with the amount of hexadiene or carbon dioxide slightly depending upon the oxygen to propylene ratio.

5. Development studies: In_2O_3

5A. The effect of reactant concentration

The effects of changing the oxygen concentration on the production of benzene and hexadiene from propylene were studied over a pure In_2O_3 catalyst at 444°C by varying the oxygen concentration from 0 to 17.8 x 10^{-3} moles/litre while maintaining the propylene concentration and contact time constant at 26.7 x 10^{-3} moles/litre and 1.2 cc/cc/sec respectively. With no oxygen present in the reacting system, no production of hexadiene or benzene was apparent. A marked maximum in the yield of benzene and hexadiene was observed as the mole fraction of oxygen was increased (Figure 52). The yield of carbon dioxide increased linearly with the mole fraction of oxygen and the selectivity of reacted propylene to benzene and hexadiene passed through a maximum of 0.83 at an oxygen mole fraction of 0.2 (Figure 53).

The effects of a change in the propylene concentration were studied over a pure In_2O_3 catalyst at 445°C at the

FIGURE 52

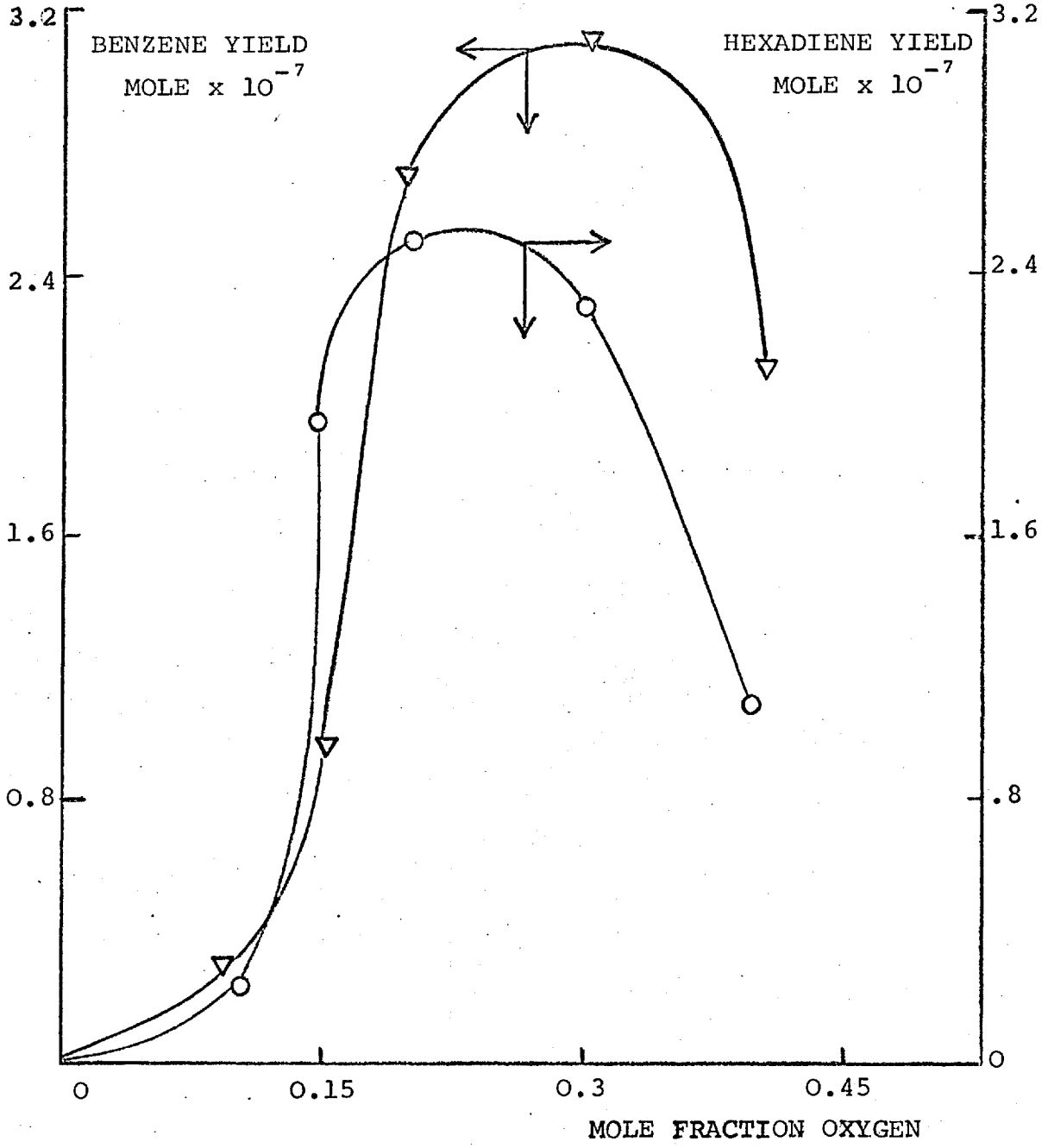

The yield of benzene and hexadiene from propylene over In_2O_3 at 444°C as a function of the concentration of oxygen.

contact time: 1.2 cc/cc/sec

propylene concentration: 0.60 mole fraction = 26.7×10^{-3} moles/litre

FIGURE 53

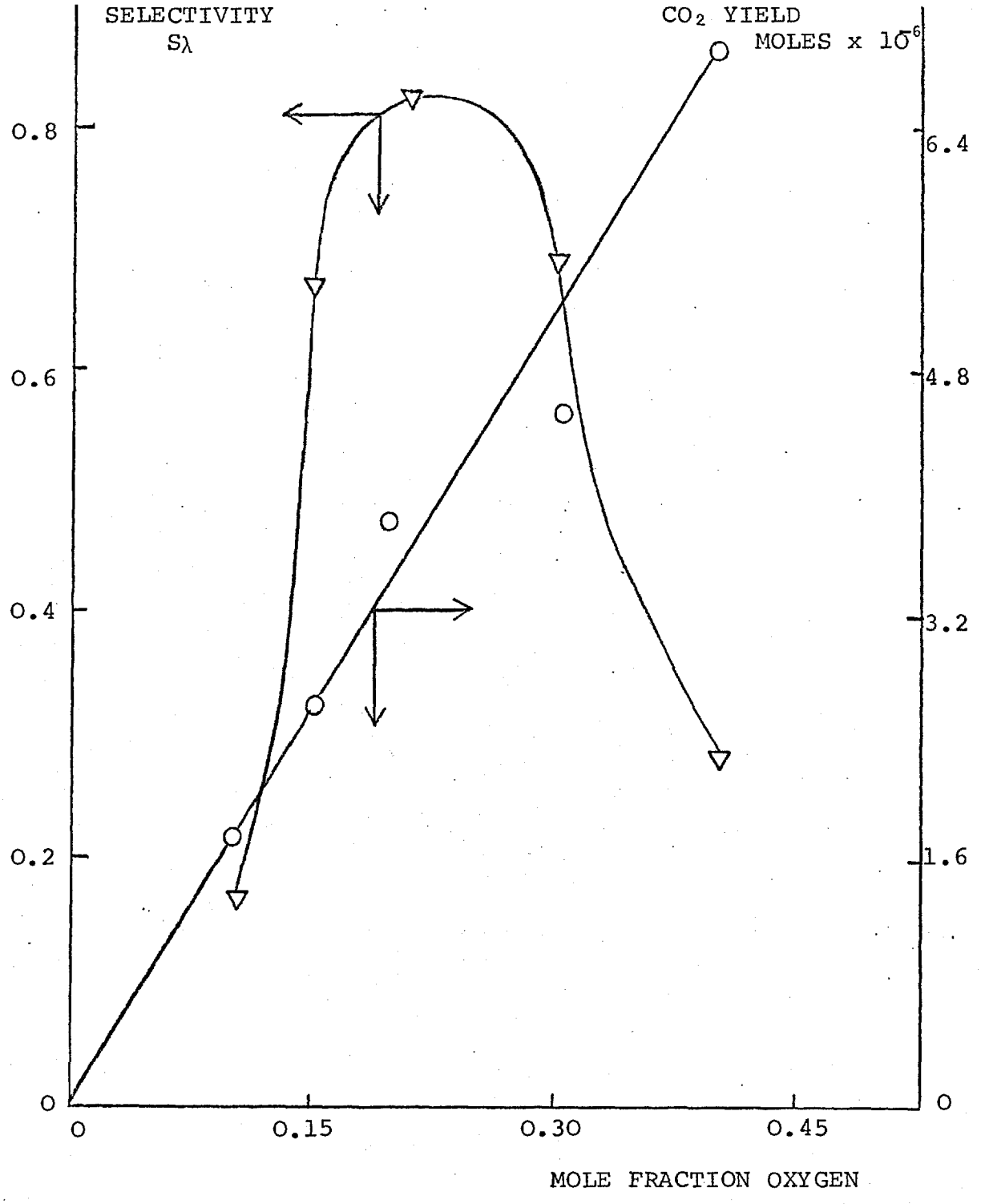

The yield of carbon dioxide and the selectivity of reacted propylene over In_2O_3 at 444°C as a function of oxygen concentration.

contact time: 1.2 cc/cc/sec

propylene concentration: 0.60 mole fraction = 26.7×10^{-3} moles/litre

optimum mole fraction of oxygen of 0.2. The propylene concentration was varied from 13.4 to 35.6 x 10^{-3} moles/litre with the oxygen concentration maintained at 8.9 x 10^{-3} moles/litre and the contact time at 1.2 cc/cc/sec. The yield of benzene slowly increased with an increasing mole fraction of propylene and passed through a maximum at a mole fraction of 0.6 (Figure 54). The carbon dioxide yield, mirrored the change in the yield of benzene (Figure 54). The yield of hexadiene increased with the concentration of propylene as did the selectivity to desirable products (Figure 55).

5B. The effect of temperature

The temperature was varied from 397°C to 505°C with the propylene and oxygen concentrations adjusted to 35.6 x 10^{-3} and 8.9 x 10^{-3} moles/litre respectively and at a contact time of 1.2 cc/cc/sec. The resultant changes in the product spectrum were complex as can be seen in Figure 56. The yield of hexadiene passed through a small maximum before plunging to a deep minimum at 460°C, while the yield of benzene moved in the opposite direction, raising to a maximum between 460°C and 480°C. The yield of carbon dioxide remained fairly constant but passed through a small minimum as temperature increased, while the selectivity mirrored the yield of hexadiene (Figure 57).

FIGURE 54

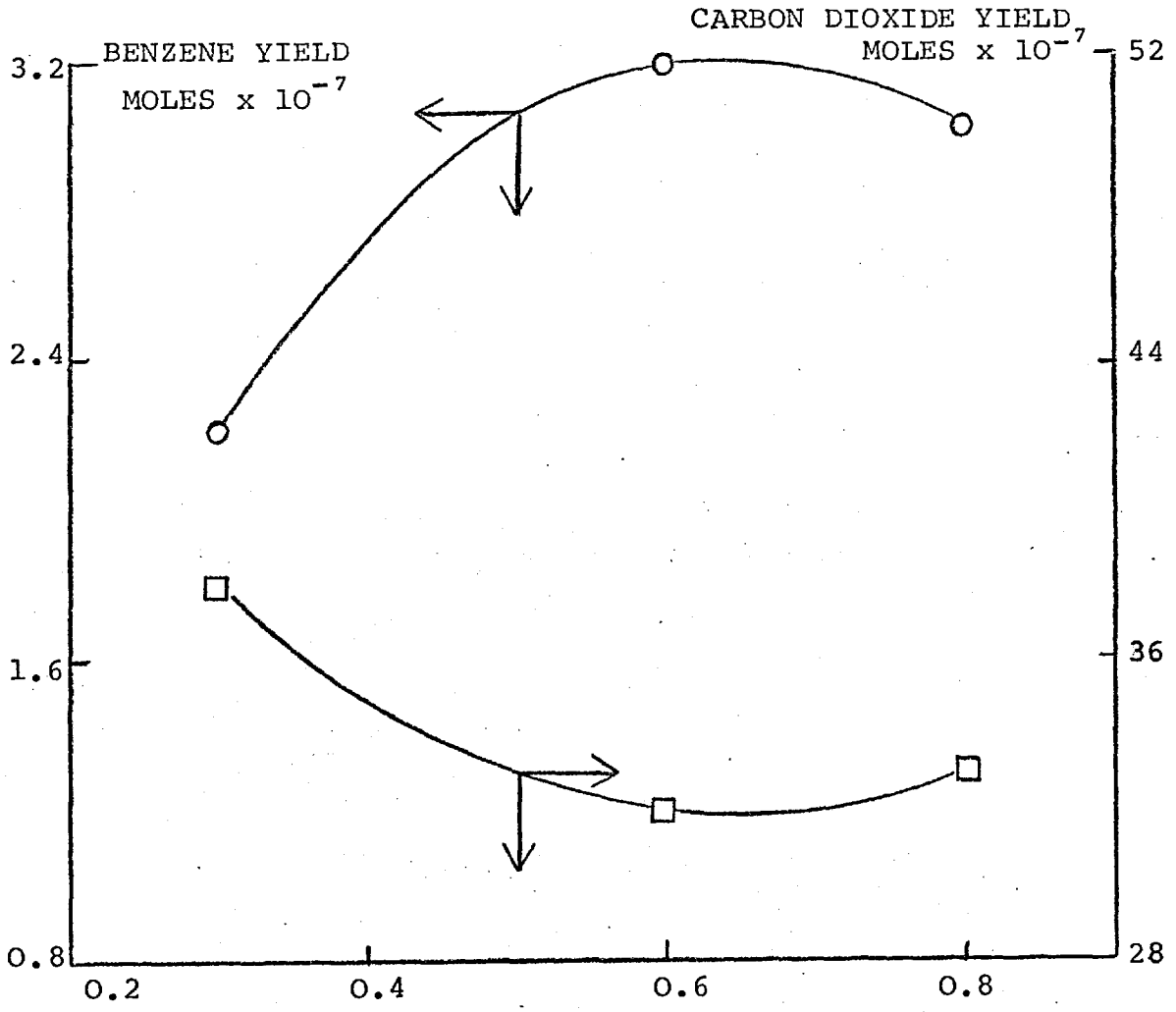

The yields of benzene and carbon dioxide from propylene over In_2O_3 at 445°C as a function of propylene concentration.

contact time: 1.2 cc/cc/sec

oxygen concentration: 0.2 mole fraction = 8.9×10^{-3} moles/litre

FIGURE 55

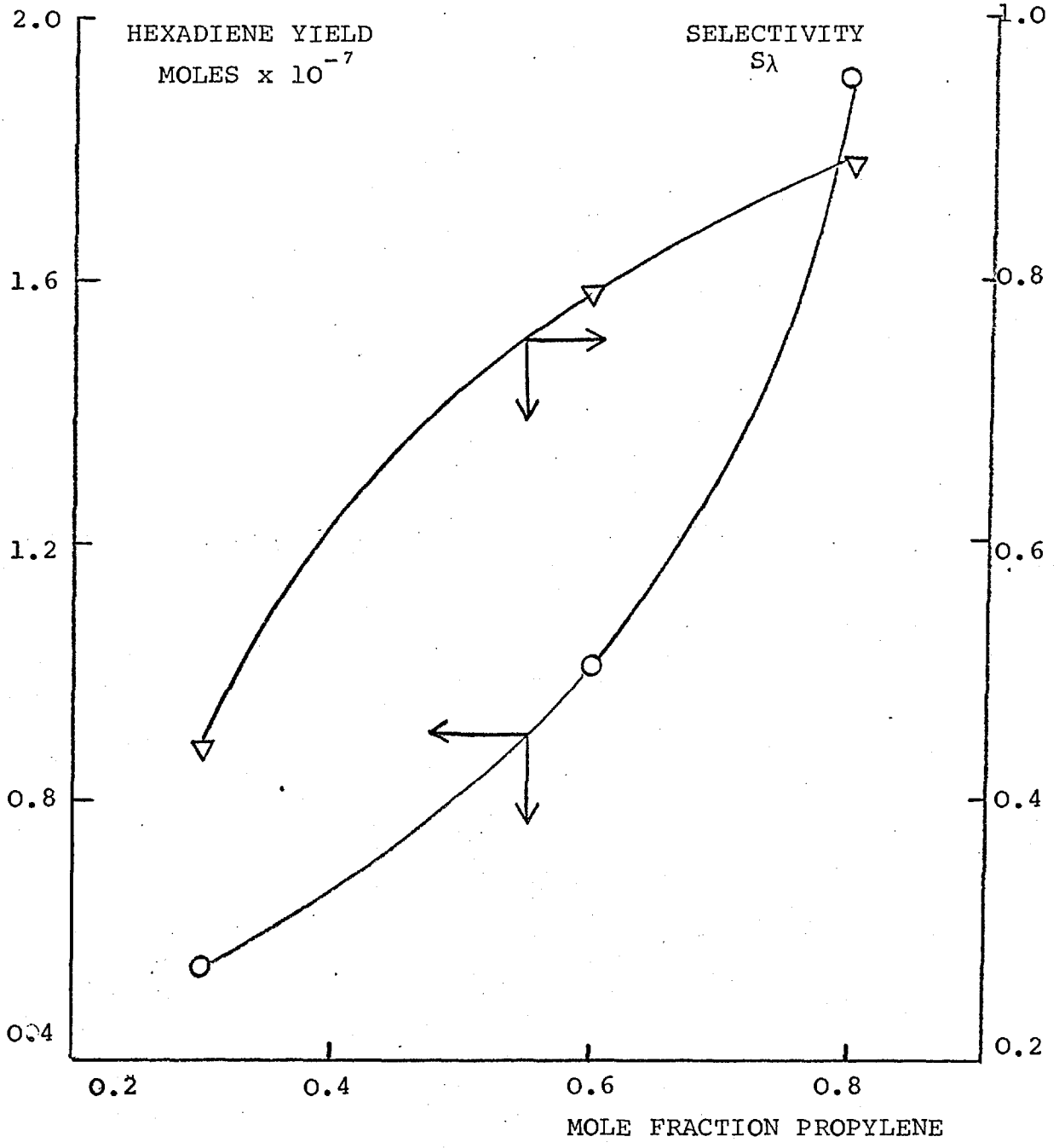

The yield of hexadiene and the selectivity of reacted propylene over In_2O_3 at 445°C as a function of propylene concentration.

contact time: 1.2 cc/cc/sec

oxygen concentration: 0.2 mole fraction = 8.9×10^{-3} moles/litre

FIGURE 56

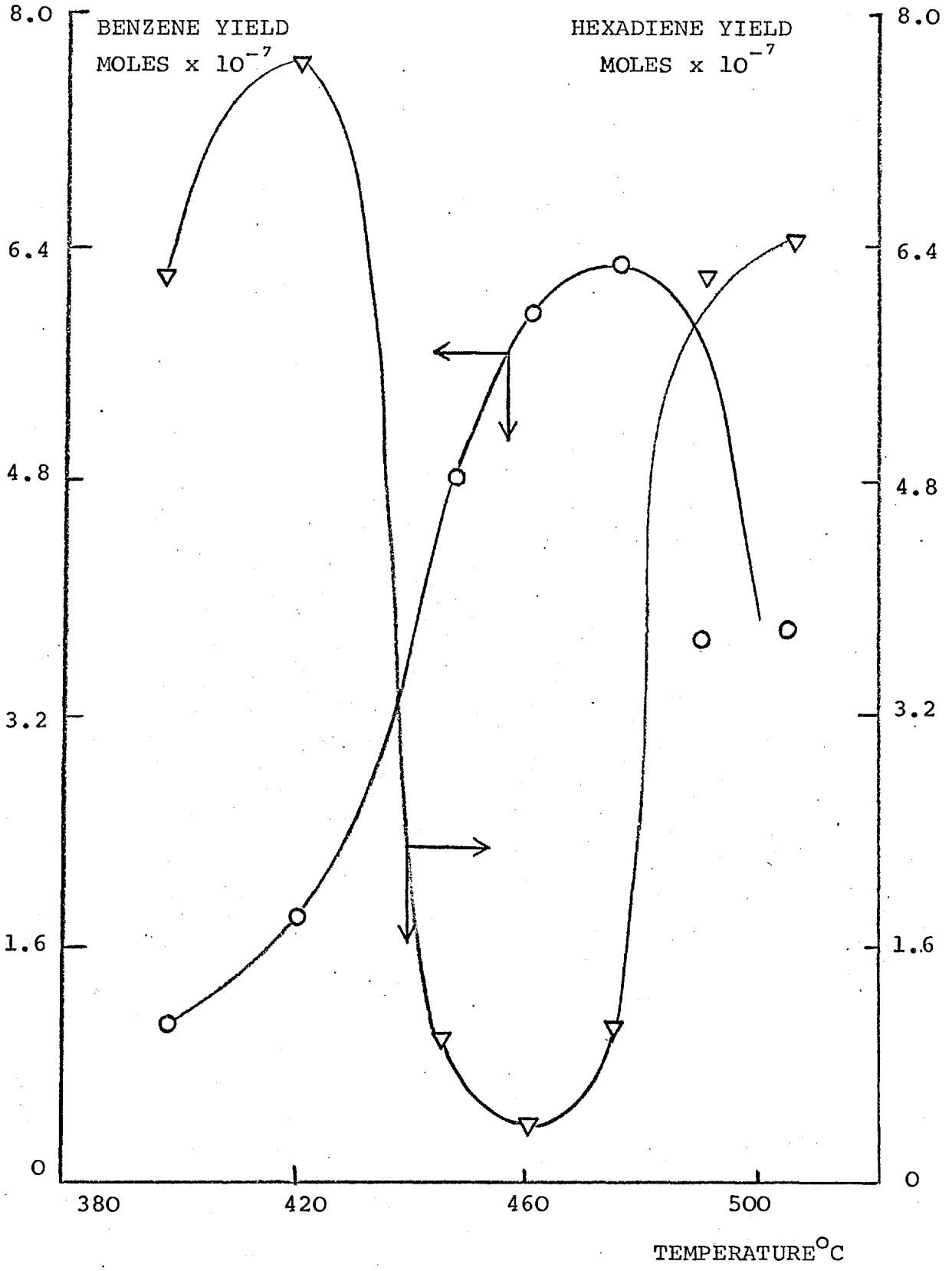

The yields of benzene and hexadiene as a function of temperature over In_2O_3.

contact time: 1.2 cc/cc/sec

concentrations: oxygen = 0.2 mole fraction
propylene = 0.8 mole fraction

FIGURE 57

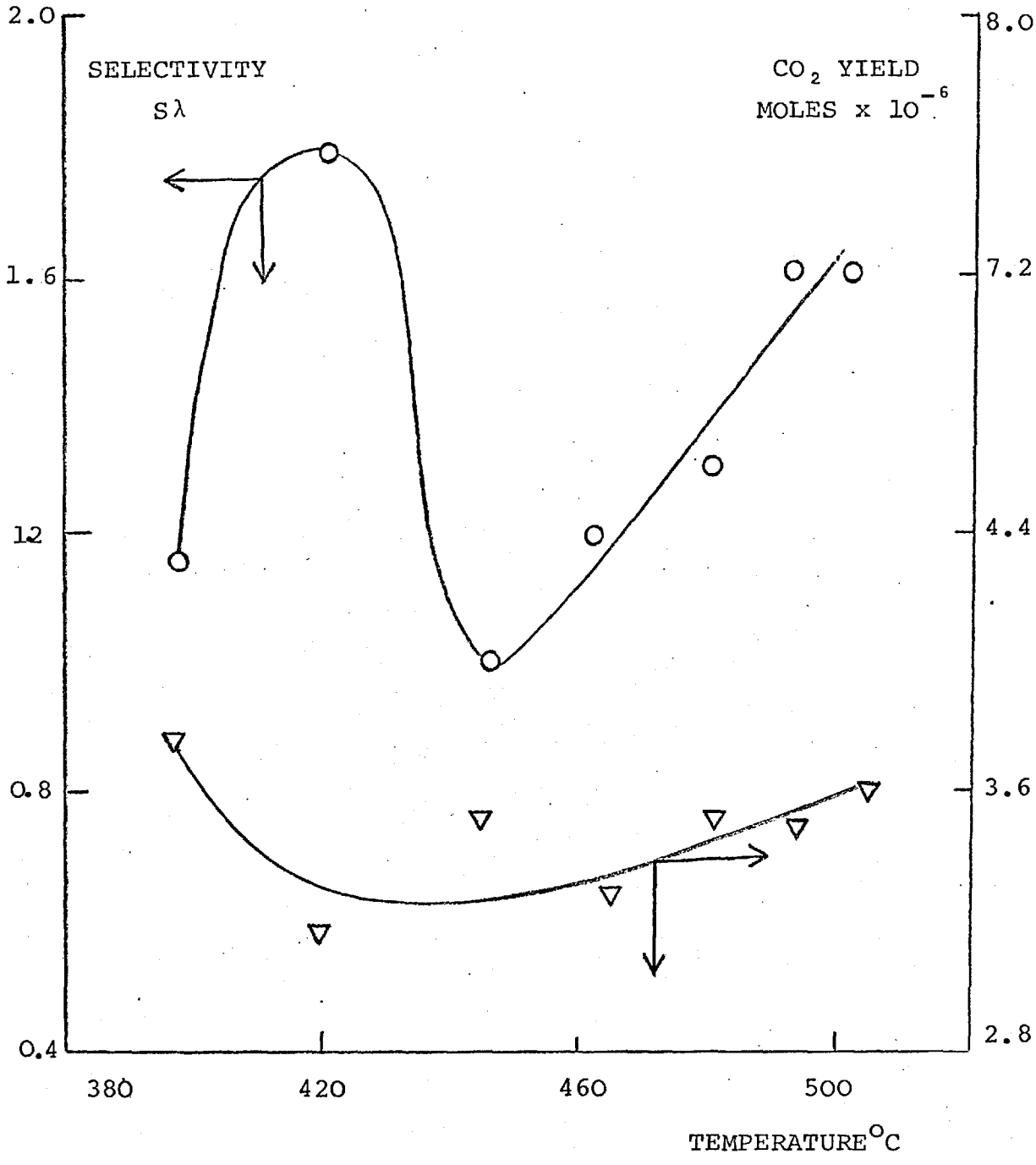

The variation of the yield of carbon dioxide and the selectivity of reacted propylene with temperature over In_2O_3.

contact time: 1.2 cc/cc/sec

concentrations: oxygen = 0.2 mole fraction
propylene = 0.8 mole fraction

5C. Contact time

The effect of contact time on the product distribution was studied at 445°C over pure In_2O_3. The yield of benzene (Figure 58) increased sharply from zero to a value of 5.4×10^{-7} moles at a contact time of 1.0 cc/cc/sec. However, the concentration of benzene quickly fell again at longer contact times. The yield of carbon dioxide remained relatively constant (Figure 58) but passed through a small maximum. The yield of hexadiene (Figure 59) rose quickly at low contact times, but the rate of increase slowed above a contact time of 1.2 cc/cc/sec. The selectivity of the reaction reflected the maximum in the benzene yield by passing through a maximum of 0.92 at a contact time of 1.0 cc/cc/sec (Figure 59).

5D. The physical structure of the catalyst

The effects of the temperature of activation on the surface area and pore radius of the pure In_2O_3 catalyst were studied. A typical isotherm at -195°C for In_2O_3, obtained in a conventional gas adsorption apparatus, is shown in Figure 60 and appears to be a typical "Type IV" isotherm (115). It is generally accepted that "Type IV" isotherms will only appear in a solid which possess pores in the "transitional" range, i.e. having diameters ranging from tens to hundreds of Ångstrom units.

The effect of the initial temperature of activation on the pore size distribution was studied by treating

FIGURE 58

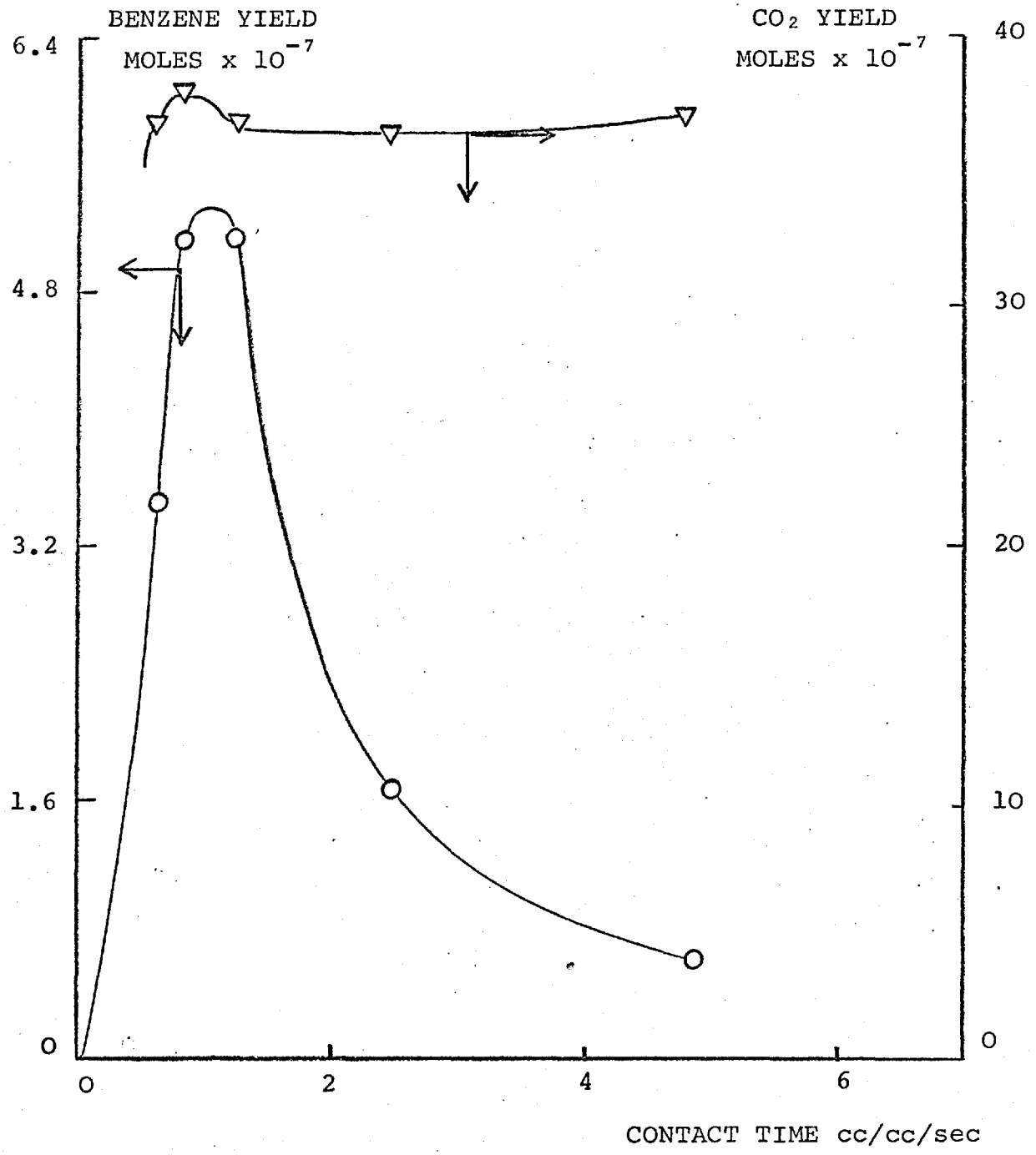

The yield of benzene and carbon dioxide at 445°C as a function of contact time over In_2O_3.

concentrations: oxygen = 0.2 mole fraction
propylene = 0.8 mole fraction

FIGURE 59

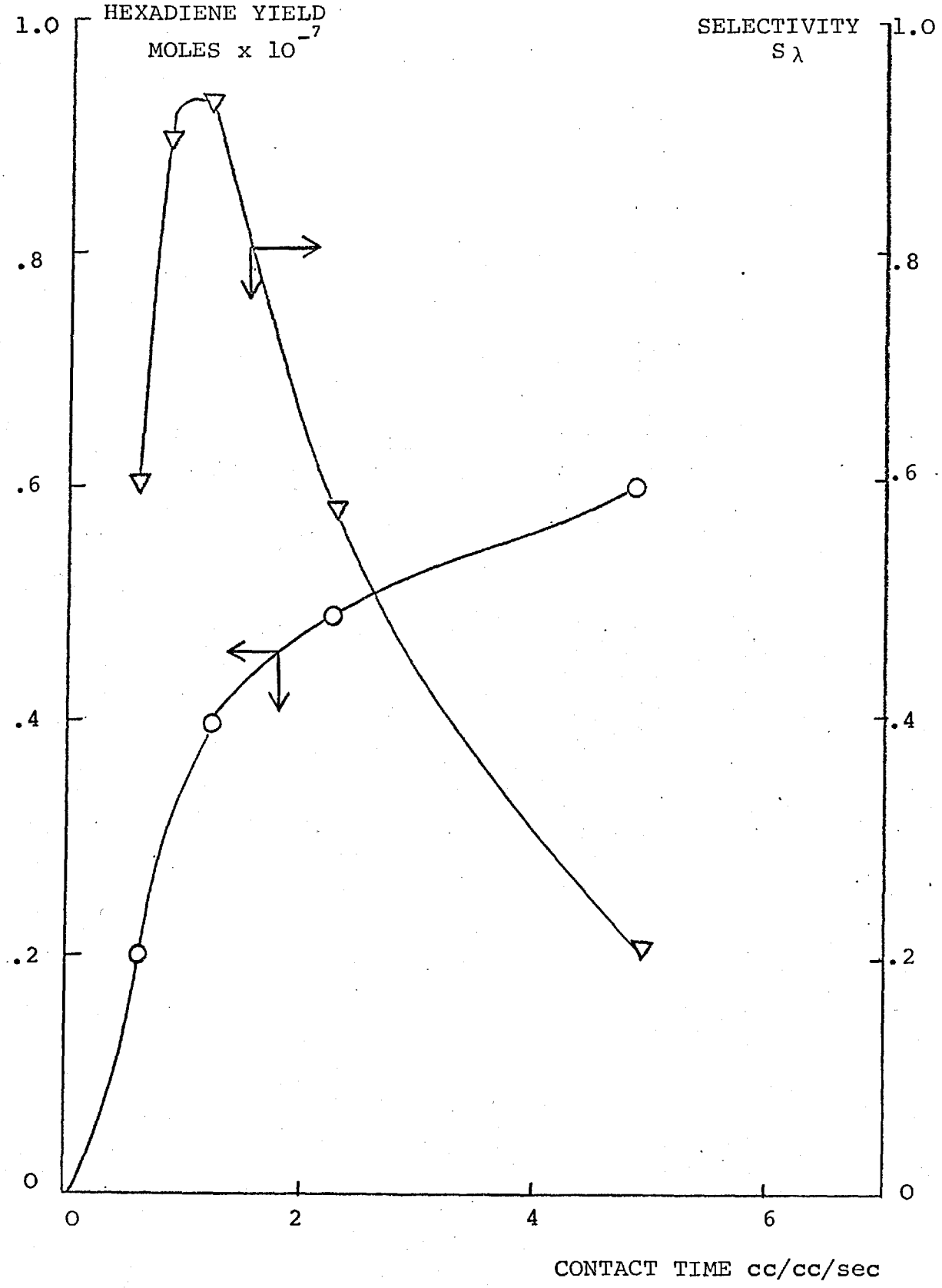

The yield of hexadiene and the selectivity of reacted propylene at 445°C as a function of contact time over In_2O_3.

concentrations: oxygen = 0.2 mole fraction
propylene = 0.8 mole fraction

FIGURE 60

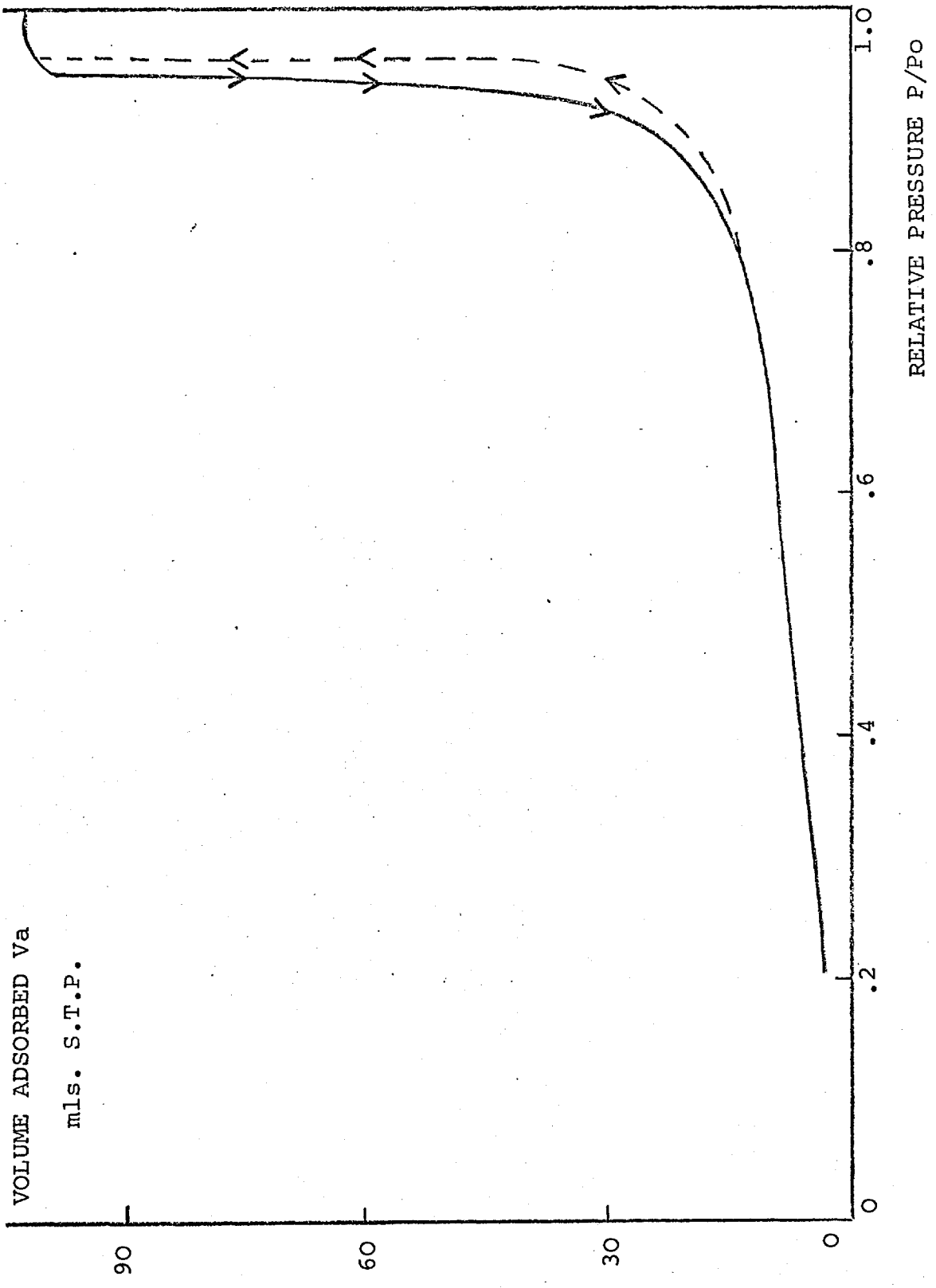

Typical nitrogen adsorption isotherm for In_2O_3 at -195°C.

identical samples of $In(OH)_3$ at two different activation temperatures. One sample was activated at 560°C in air while the other sample was treated first at 240°C in order to decompose the $In(OH)_3$ to In_2O_3 under controlled conditions and then the temperature was raised to 560°C as for sample one. This was necessary for comparison as the final temperature had a significant effect on the surface area. For example, the B.E.T. surface area (section 3F, Experimental) for an activation temperature of 540°C was 62.5 m^2/gm while if the same sample was heated to 740°C, the surface area decreased to approximately 25 m^2/gm. The resulting pore size distributions, calculated by a method based on the Kelvin equation and described in detail by Gregg and Sing (115), are shown in Figure 61. As can be seen, the low temperature activation is greatly superior in providing a catalyst with a characteristic pore radius (150-200 A°). A plot of the cumulative surface area versus pore radius (Figure 62) confirms that the lower activation temperature produces a better catalyst. Over any range of pore radius there was a larger increase in surface area for the lower temperature of activation. In addition the low activation temperature has reduced the surface area available in the small pores. For example, the pores smaller than 70 A° account for only 20% of the total area for the 240°C activation while for the 560°C activation this region accounts for over 40% of the total area.

FIGURE 61

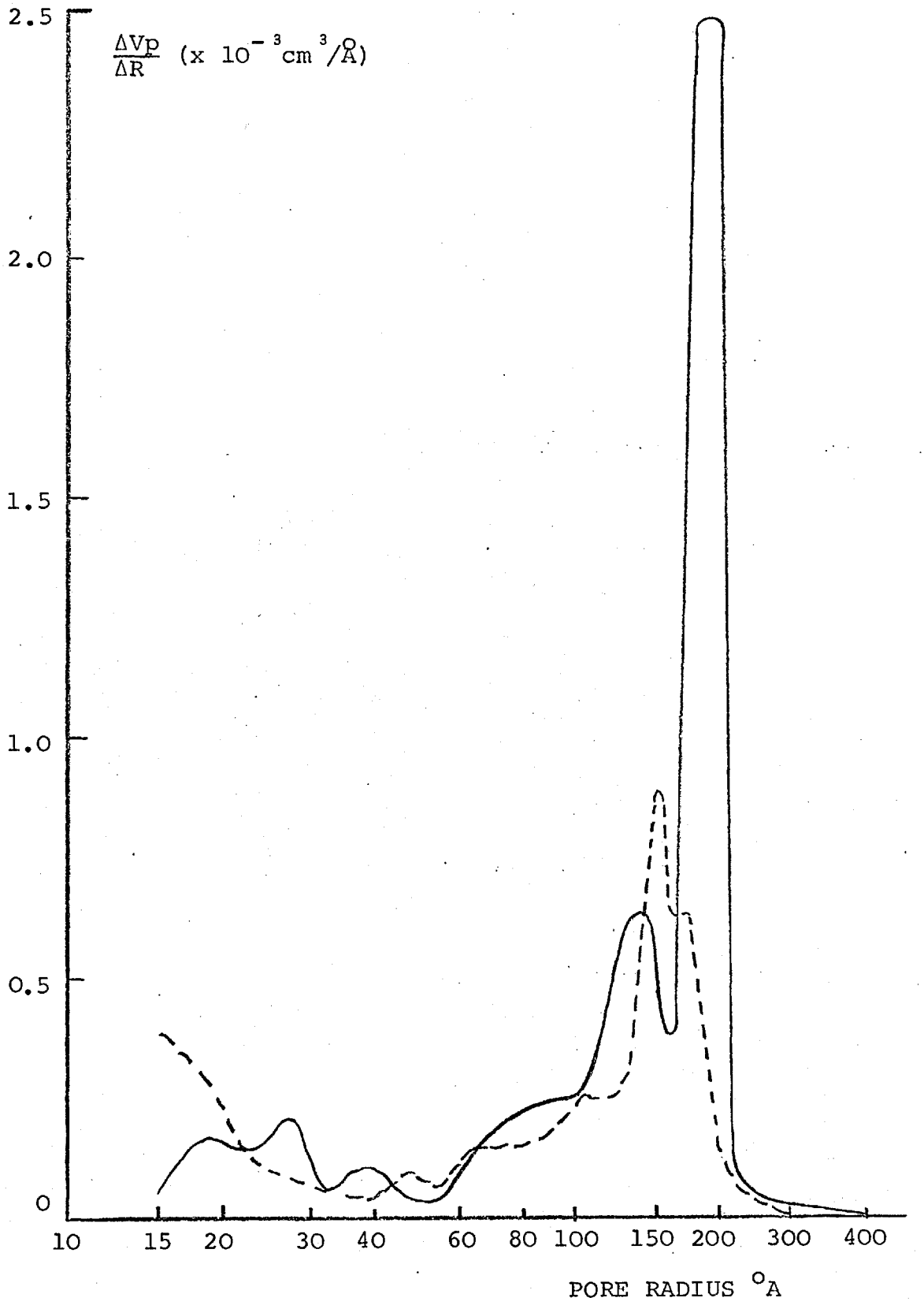

Pore size distribution of In_2O_3 for different temperatures of activation.

_____ catalyst activated at 240° then 560°C

- - - - - catalyst activated at 560°C

FIGURE 62

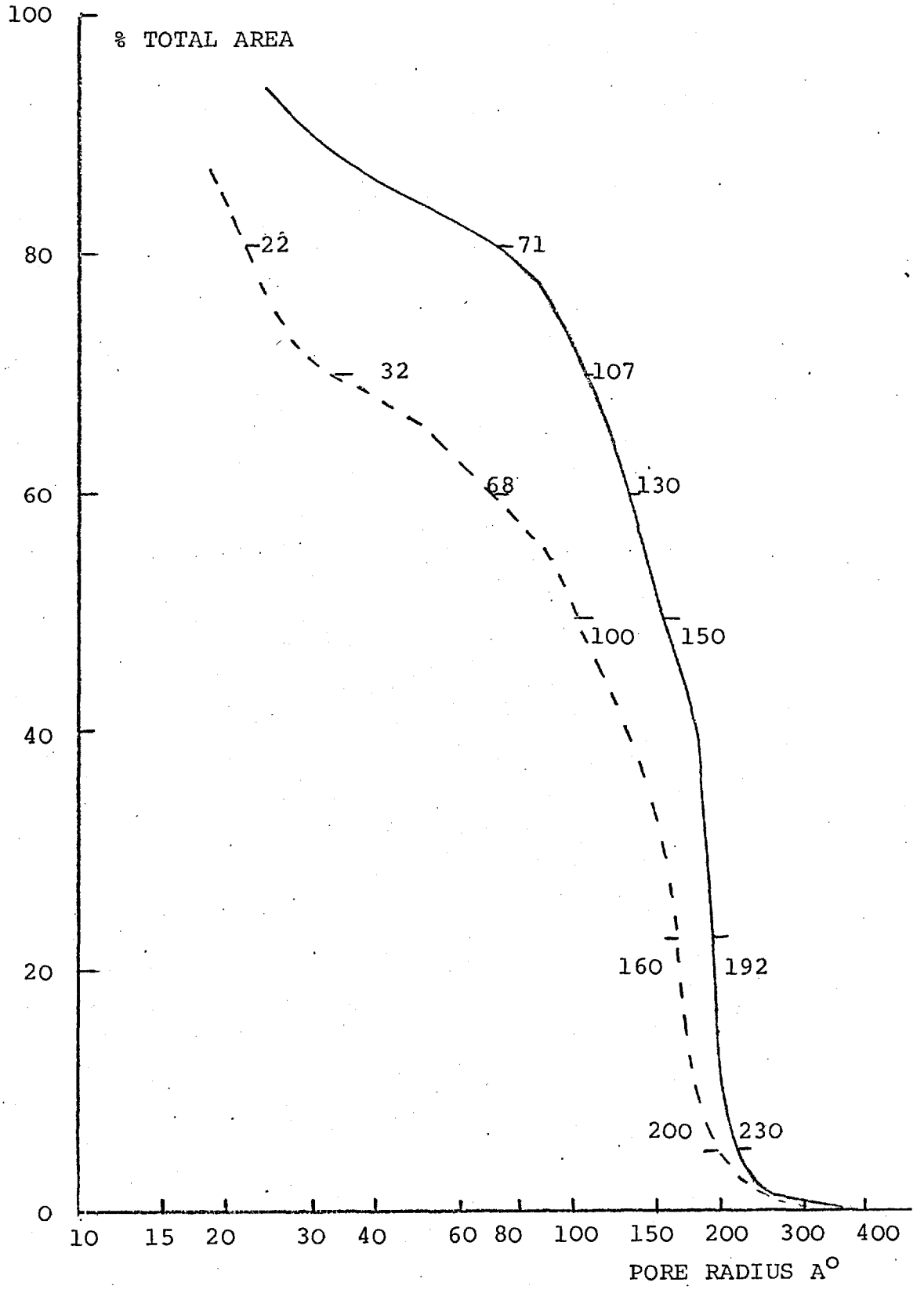

Surface area distribution of In_2O_3 for different activation temperature.

- - - - catalyst activated at 560°C

_____ catalyst activated at 240 than 560°C

5E. Homogeneous reaction

The homogeneous reaction of propylene and oxygen was studied initially over a temperature range of 440°C to 540°C at the reaction conditions of 1:2:7 oxygen:propylene: nitrogen at two flow rates of 800 cc/min and 400 cc/min: the results are reported in Figure 63. As can be observed for both flow rates, the rate of change of hexadiene with temperature increases very quickly. The homogeneous reaction was studied in greater detail below 480°C as is reported in Figure 64. The concentrations were the same as above but the flow rate was reduced to 200 cc/min. The response of the homogeneous dimerization was linear with a temperature increase until over 450°C when the rate of change with temperature quickly increased. There was no detectable trace of carbon dioxide (katharometer sensitivity 10^{-7} moles).

5F. Catalyst preparation and concentration

The pure form of In_2O_3 was found to be too active for studies requiring controlled conditions. From the data in Table 19 it can be seen that a rise in temperature in the catalyst bed occurred very easily even in a 2 cm. long catalyst bed. Two observations can be made from this data. The measured temperature was found to be proportional to the flow rate when one expects the opposite to be true. Thus the temperature of the first part of the bed was probably 450°C or higher under all conditions but only at the shorter contact times was this heat spread down the bed

FIGURE 63

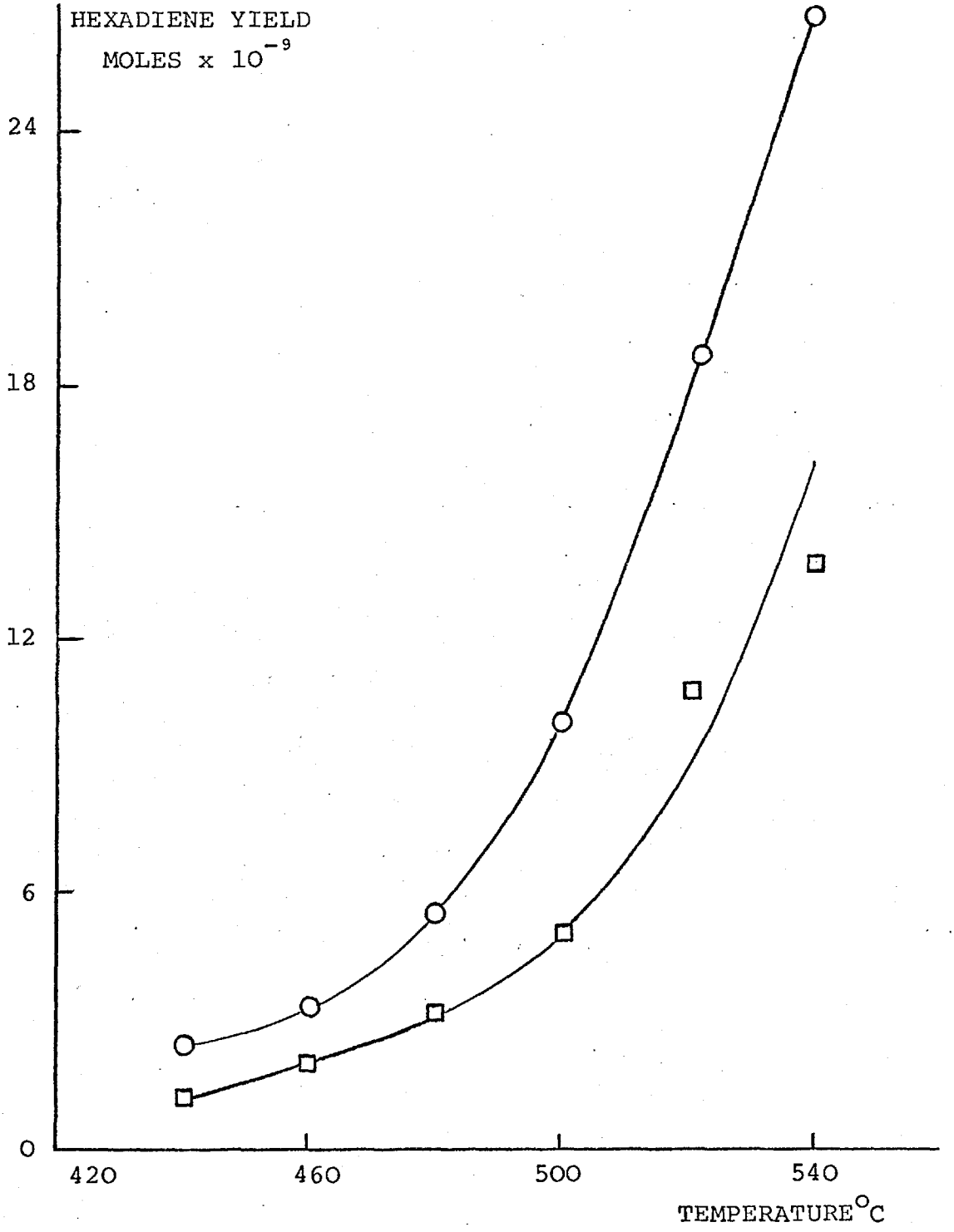

Effect of temperature on the homogeneous oxidation of propylene to hexadiene at concentrations of 1:2:7 oxygen, propylene and nitrogen.

Flow rates: 400 cc/min -○-
800 cc/min -□-

FIGURE 64

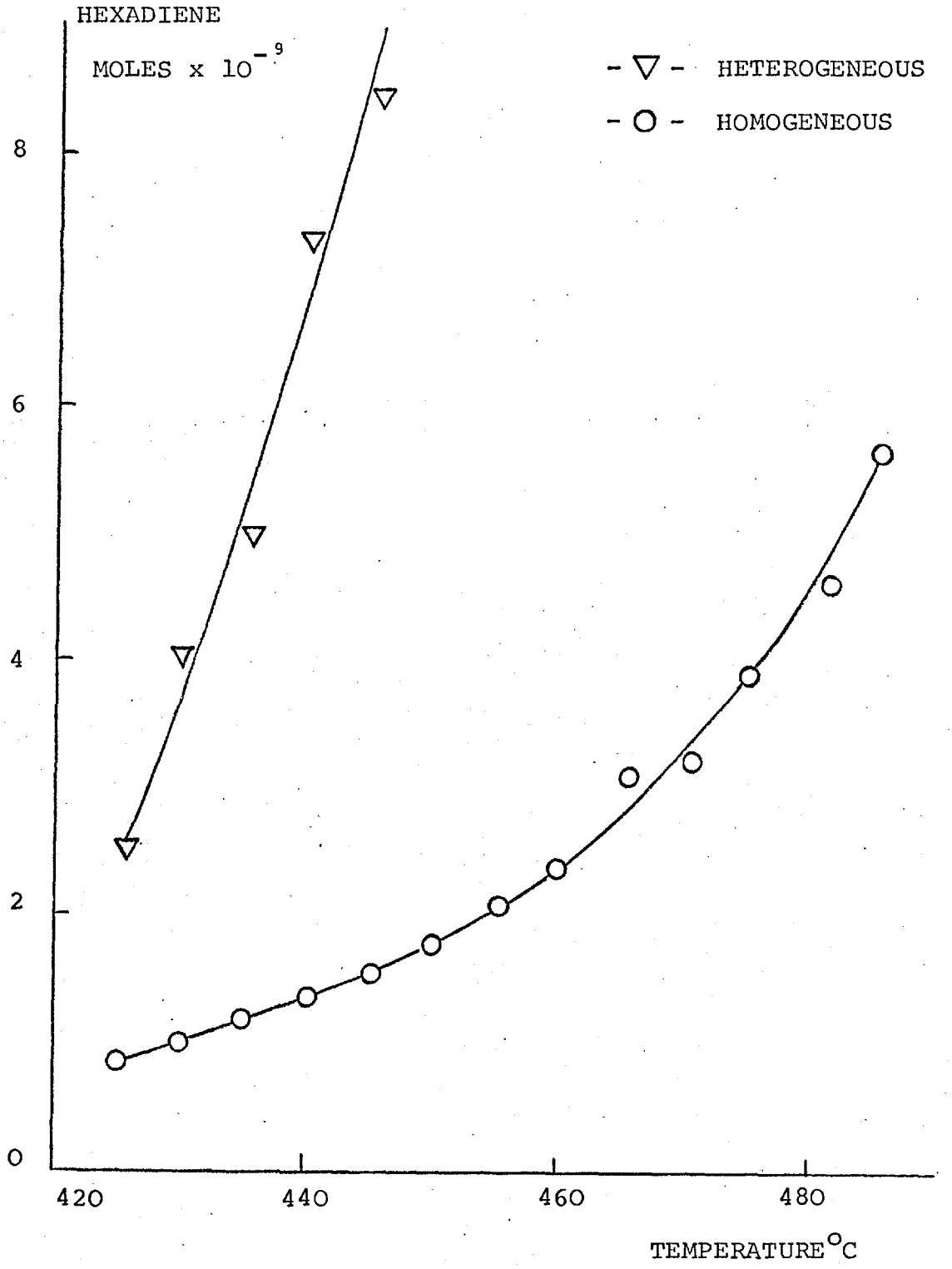

Comparison of heterogeneous (1.5 gm 0.15 wt % In_2O_3 on pumice (2V)) and homogeneous reactions over a range of temperatures.

Conditions: 400 cc/min of 1:2:7 oxygen:propylene:nitrogen (contact time 0.6 cc/cc/sec for heterogeneous)

TABLE 19

The effect of flow rate on conversion and temperature of catalyst bed

Temperature in catalyst bed	Flow rate cc/min	Contact time cc/cc/sec	CO_2 moles x 10^{-7}	Hexadiene moles x 10^{-7}	Benzene moles x 10^{-7}	Cyclohexadiene moles x 10^{-7}
450	900	0.27	50	3.2	1.09	0.45
435	800	0.3	50	2.65	1.04	0.39
405	400	0.6	52	2.0	0.94	0.32
400	200	1.2	47	0.6	0.30	0.15

Temperature of tin bath 395°C; concentrations $O_2/C_3/N_2$ = 1/2/7; pure In_2O_3 catalyst = 0.95 gm.

to the thermocouple (1 cm.). This is certainly an indication of the high efficiency of heat removal of the tin bath. Secondly it should be noted that the carbon dioxide, which consumes over 95% of the oxygen, was independent of contact time. Oxygen was also totally consumed when the same mixture was passed over a catalyst prepared by thermal decomposition of $In_2(SO_4)_3$ impregnated on pumice stone even when only one-tenth of a gram was used. The results obtained (Table 20) can be compared with the pure In_2O_3 results (Table 19). The catalyst was also a different colour, reddish-brown compared to the normal yellow.

A method of catalyst preparation consisting of impregnation and precipitation on the support was then developed as is described above. Catalysts containing 0.15 wt %, 0.029 wt % and 0.009 wt % In_2O_3 on pumice were prepared. The importance of the homogeneous reaction was first compared with the heterogeneous reaction using 1.5 gm of 0.15 wt % In_2O_3 of pumice at the same conditions (Figure 64). The heterogeneous reaction increases much faster with temperature than the homogeneous reaction, and an Arrhenius plot (Figure 64a) can be used to show that the apparent activation energies for the homogeneous and heterogeneous reactions are 40 and 60 kcal/mole respectively. At short contact times, only traces of benzene were detected from the heterogeneous reaction but substantial amounts of acrolein were observed.

Pure $InPO_4$, the preparation of which was described above, was tested as a dimerization catalyst. At 500°C

TABLE 20

Product distribution as a function of contact time over In_2O_3 on pumice catalyst (2T)

Contact time Wt cat/Flow rate	CO_2	Hex	Benzene
	moles x 10^{-7}		
0.546/800	53	3.2	0.9
0.546/400	52	4.4	0.94
0.546/200	49	3.4	0.55
0.546/100	49	1.8	0.28
0.101/800	50	-	0.88
0.101/400	50	2.5	0.93
0.101/200	42	2.9	0.77
0.101/100	36	2.3	0.65

Catalyst, In_2O_3 on pumice (SO_4 decomposed); temperature, 500°C; concentration oxygen, 4.5 x 10^{-3} moles/litre; concentration propylene, 8.9 x 10^{-3} moles/litre.

FIGURE 64a

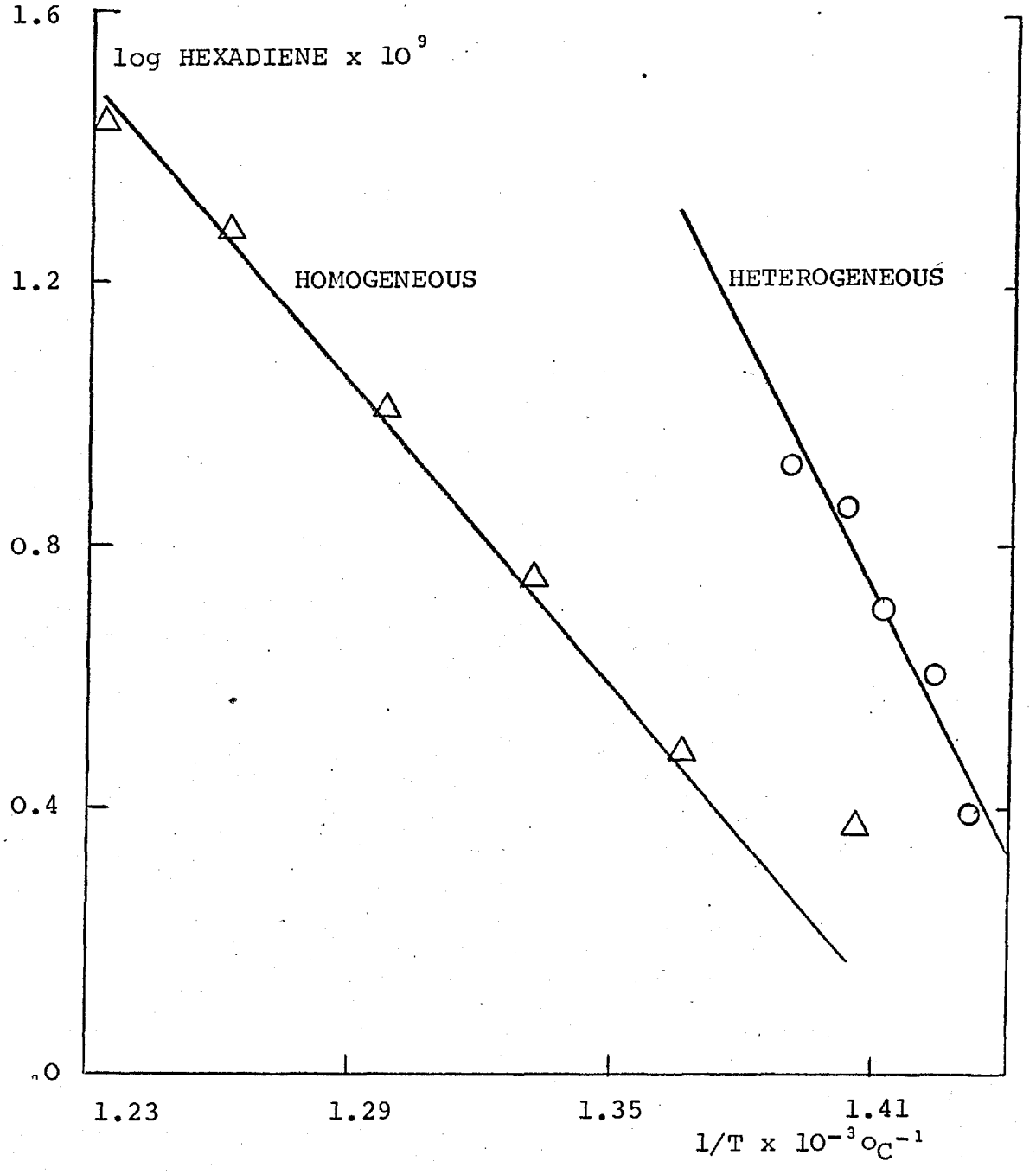

Arhennius plot for homogeneous and heterogeneous reaction to hexadiene; homogeneous data from Figure 63 and heterogeneous data from Figure 64.

and a flow rate of 400 cc/min of a 1:2:7 oxygen, propylene and nitrogen mixture the catalyst produced 3.4×10^{-6} moles carbon dioxide and 5.25×10^{-9} moles hexadiene. The catalyst was thus very unselective and no further work was attempted.

6. Kinetic studies: In_2O_3 on pumice stone

6A. Initial rate studies

The kinetics of the reactions were investigated at various oxygen and propylene concentrations. A catalyst containing 0.40 wt % In_2O_3 on pumice stone was used at 440°C, a temperature near which the homogeneous reaction was not appreciable but where the heterogeneous reaction produces concentrations that are easily measured. At low conversions benzene and carbon dioxide were not identified and hexadiene together with acrolein were the only two products that could be detected.

The order of the reaction with respect to oxygen was investigated by varying concentration of oxygen from 2.23×10^{-3} moles/litre to 8.9×10^{-3} moles/litre while maintaining the propylene concentration at 8.9×10^{-3} moles/litre. The contact time was varied by varying the total flow rate and the results for hexadiene and acrolein are shown in Figure 65 and 66 respectively. The logs of the respective initial rates were plotted against the logs of oxygen concentrations (Figure 67 and 68) from which the rate of production of hexadiene was found to depend on the oxygen concentration to the power 0.39, and of acrolein as oxygen

FIGURE 65

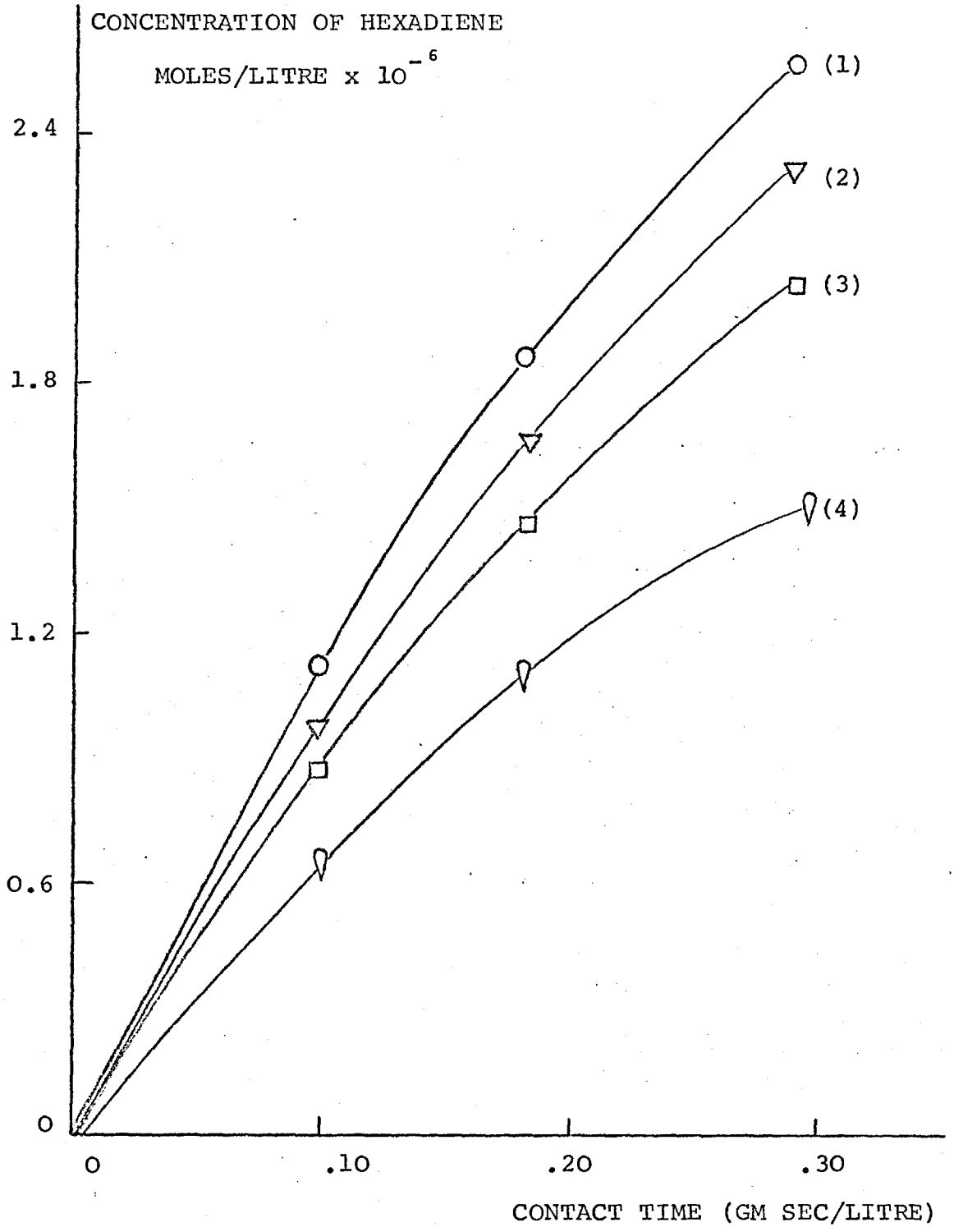

The effect of oxygen concentration on the rate of production of hexadiene.

temperature: 440°C propylene: 8.9×10^{-3} moles/litre

oxygen concentration: (1) 8.9×10^{-3} moles/litre
(2) 6.7×10^{-3} " "
(3) 4.45×10^{-3} " "
(4) $2.23 \times 10^{-}$ " "

FIGURE 66

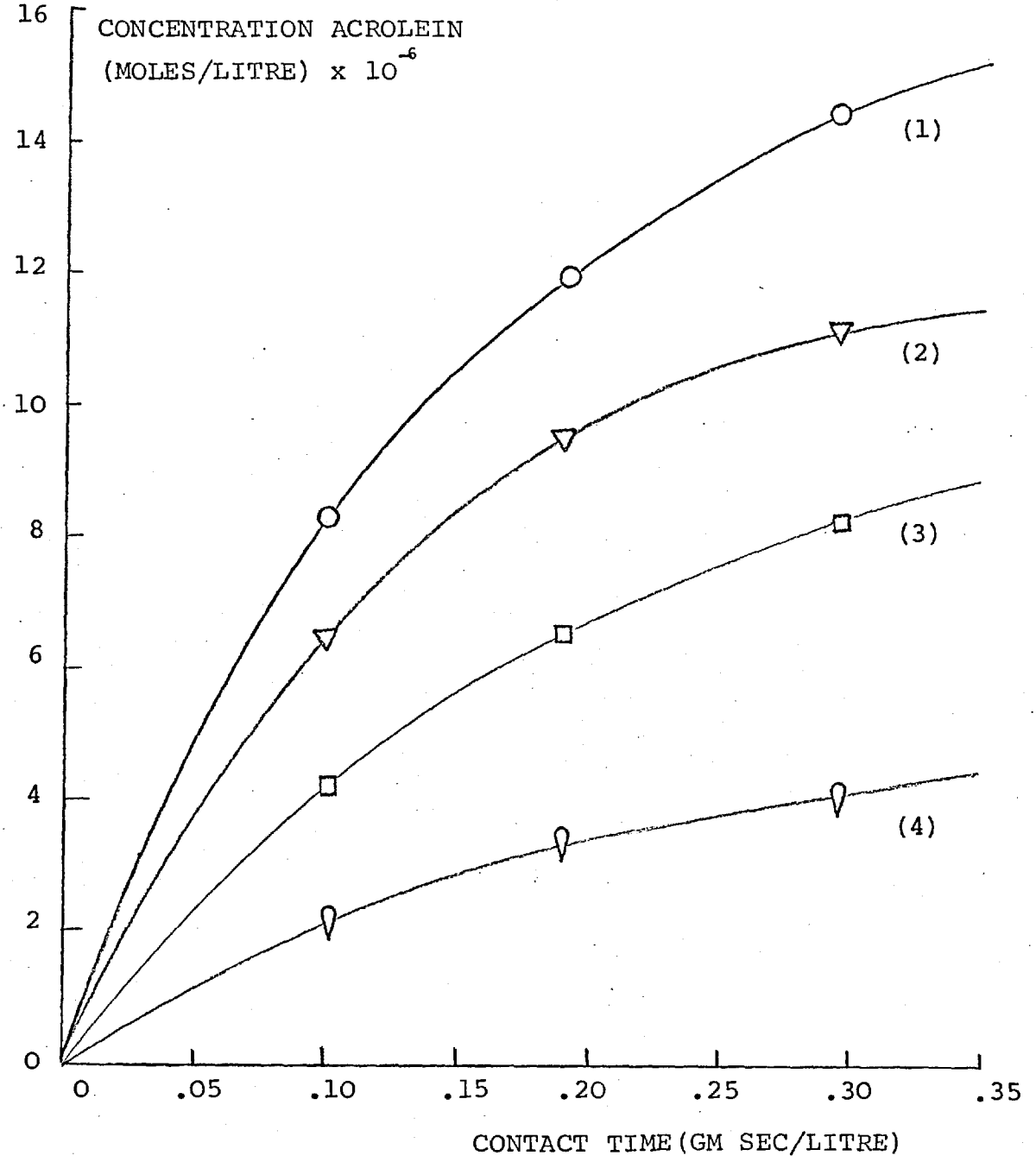

The effect of oxygen concentration on the rate of production of acrolein.

temperature: 440°C propylene: 8.9×10^{-3} moles/litre

oxygen concentration: (1) 8.9×10^{-3} moles/litre
(2) 6.7×10^{-3} " "
(3) 4.45×10^{-3} " "
(4) 2.2×10^{-3} " "

FIGURE 67

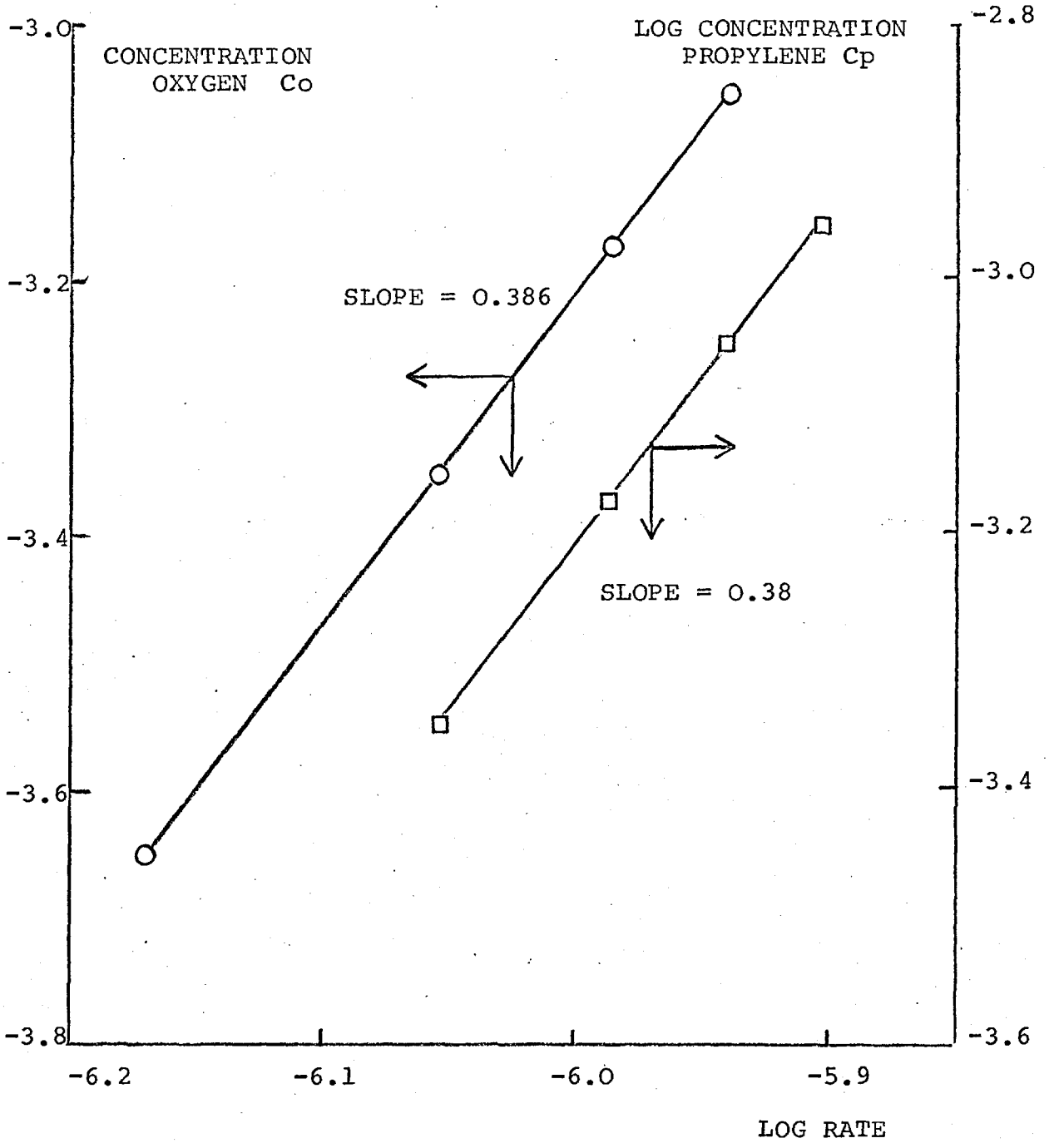

Logarithmic plot of rate versus concentration for the production of hexadiene.

temperature: 440°C

FIGURE 68

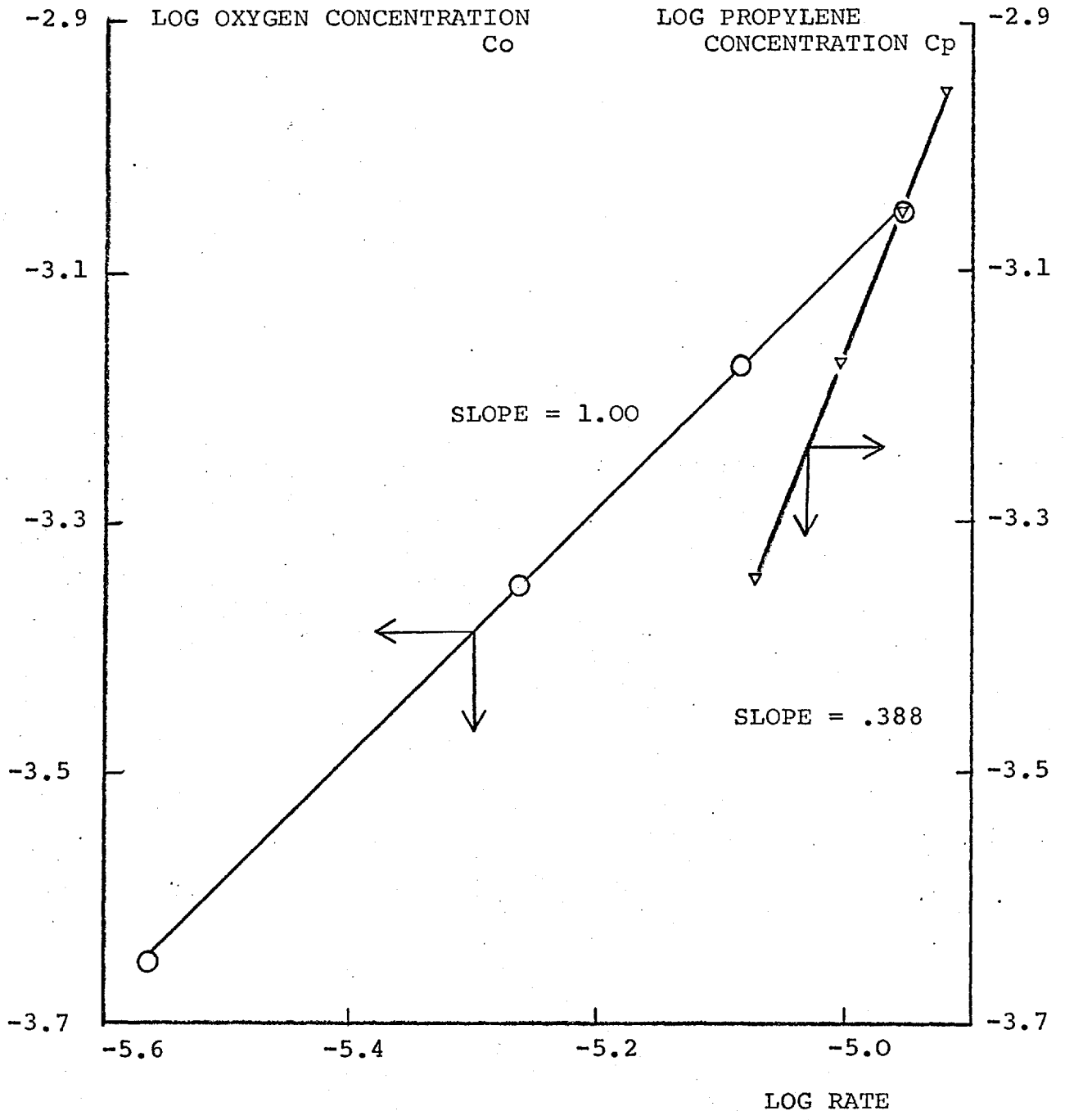

Logarithmic plot of rate versus concentration for the production of acrolein.

temperature: 440°C

to the power 1.0.

The order in propylene was determined in the same way by varying the propylene concentration from 4.45×10^{-3} to 11.1×10^{-3} moles/litre at a constant oxygen concentration of 8.9×10^{-3} moles/litre. The rates of production of hexadiene and acrolein were obtained from Figures 69 and 70 respectively and order plots are shown in Figures 67 and 68 for the production of hexadiene and acrolein respectively. The rate of production of hexadiene was found to depend on the concentration of propylene to the power 0.38, and of acrolein to the power 0.39 . The rate constant was calculated by substituting the concentrations and corresponding rates in the power rate expressions. The full rate expressions at 440°C were found to be

$$\text{rate hexadiene} = 4.4 \times 10^{-4}\ C_p^{0.38} C_o^{0.39}$$

$$\text{rate acrolein} = 0.743\ C_p^{0.38} C_o$$

6B. The determination of activation energies

The rate of reaction was investigated as a function of temperature, over a range from 420°C to 450°C while the concentrations of propylene and oxygen were maintained at 8.9×10^{-3} moles/litre. The temperature was kept within this fairly narrow range to minimise homogeneous reaction. The variation of yield of hexadiene and acrolein with contact time at the different temperatures is shown in Figures 71 and 72. The Arrhenius plot for the production of hexadiene

FIGURE 69

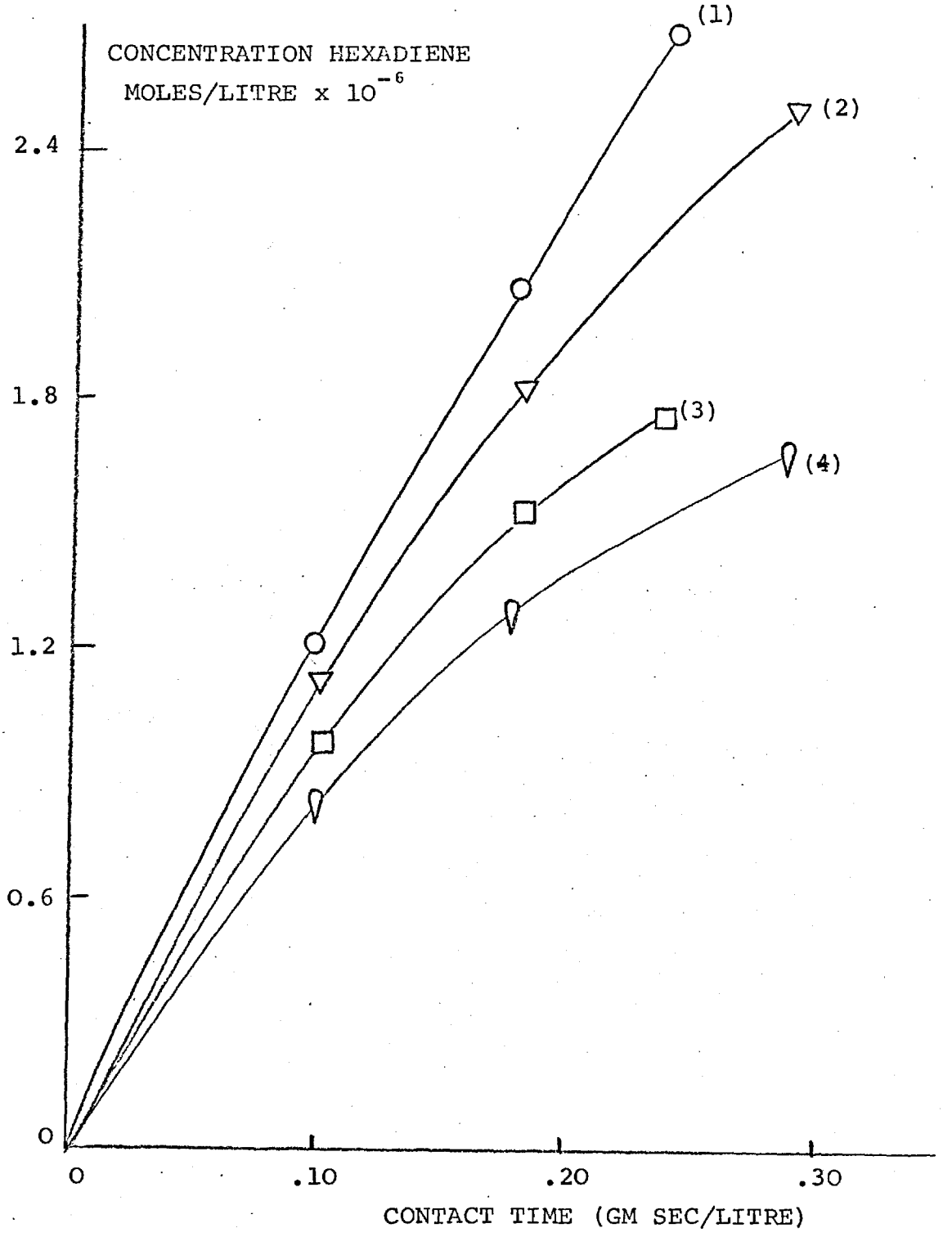

The effect of propylene concentration on the rate of production of hexadiene.

temperature: 440°C

oxygen concentration: 8.9×10^{-3} moles/litre

propylene concentration:
(1) 11.1×10^{-3} moles/litre
(2) 8.9×10^{-3} " "
(3) 6.7×10^{-3} " "
(4) 4.45×10^{-3} " "

FIGURE 70

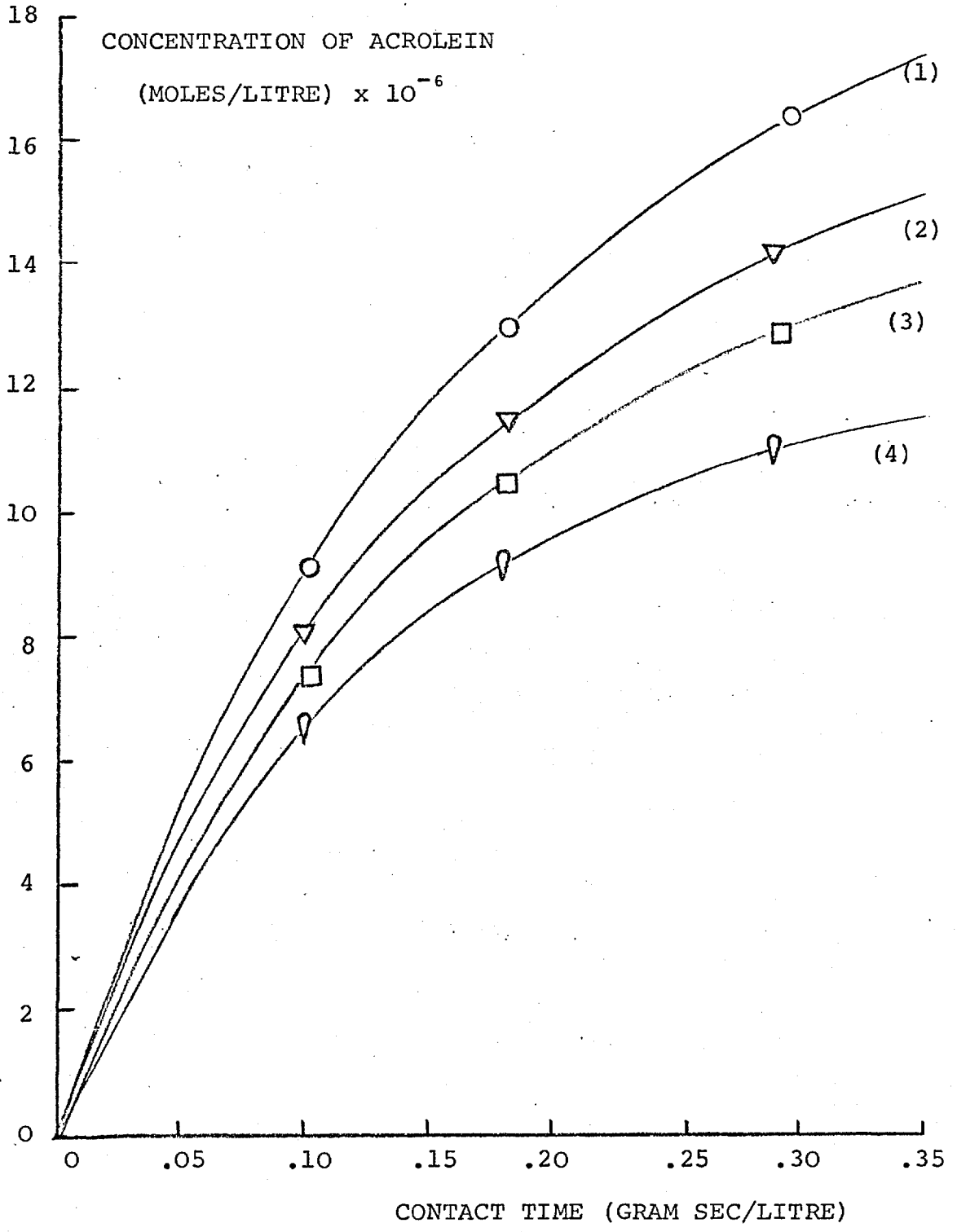

The effect of propylene concentration on the rate of production of acrolein.

temperature: 440°C

oxygen concentration: 8.9×10^{-3} moles/litre

propylene concentration: (1) 11.1×10^{-3} moles/litre
(2) 8.9×10^{-3} " "
(3) 6.7×10^{-3} " "
(4) 4.45×10^{-3} " "

FIGURE 71

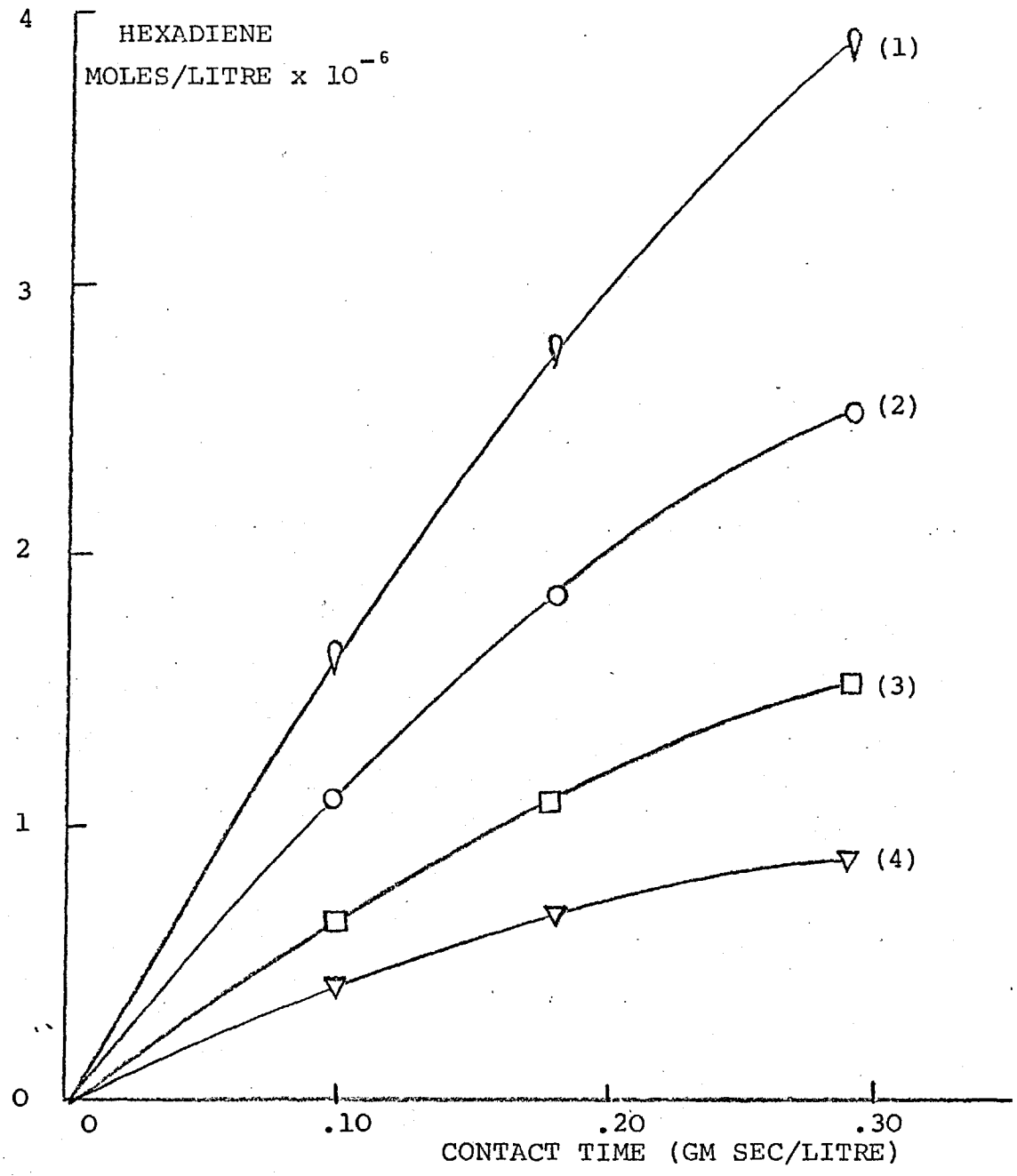

The effect of temperature on the rate of production of hexadiene.

concentrations: 8.9×10^{-3} moles/litre propylene and oxygen

temperature: (1) 450°C
(2) 440°C
(3) 430°C
(4) 420°C

FIGURE 72

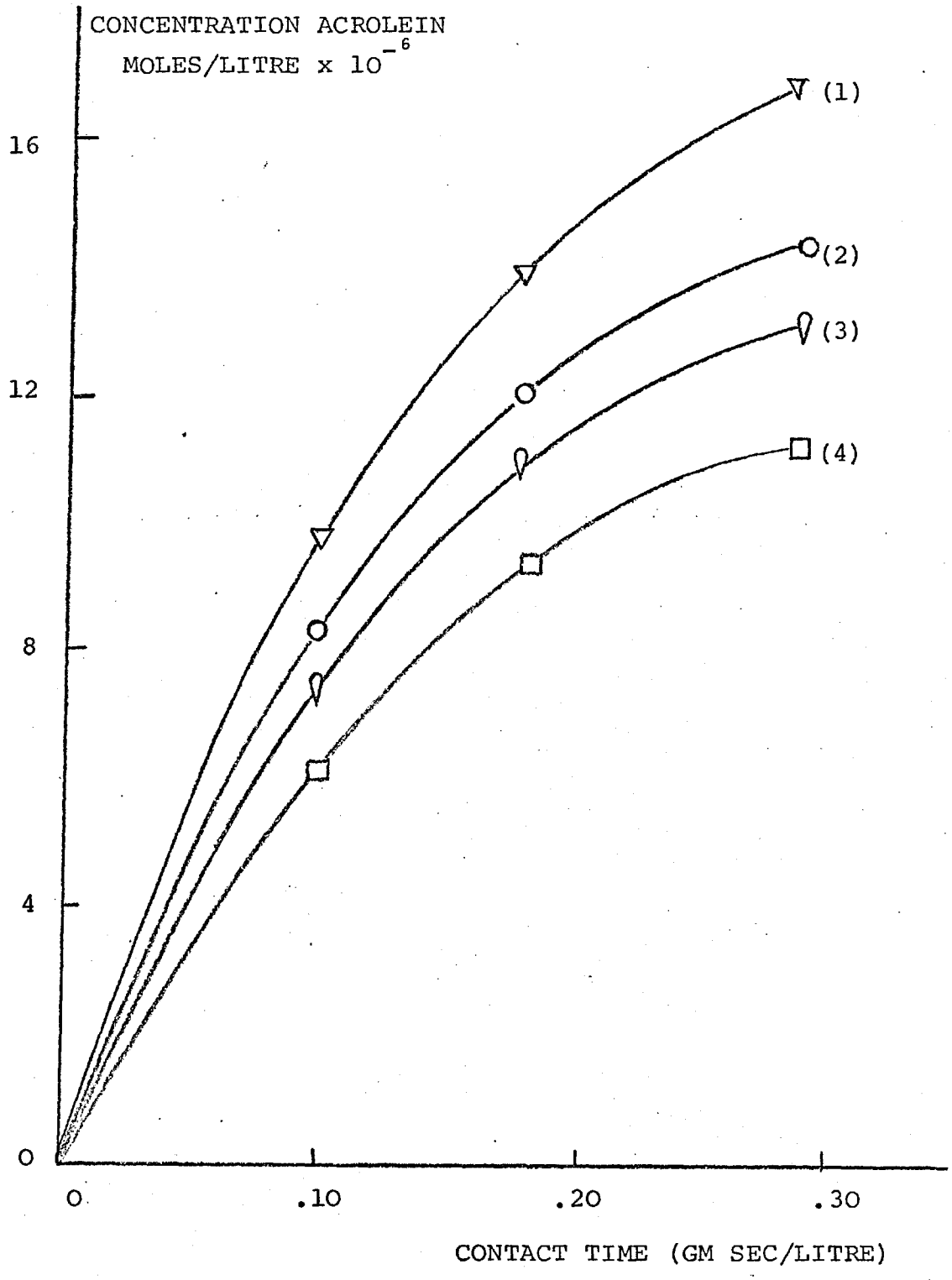

The effect of temperature on the rate of production of acrolein.

concentrations: 8.9×10^{-3} moles/litre propylene and oxygen

temperature: (1) 450°C
(2) 440°C
(3) 430°C
(4) 420°C

is shown in Figure 73 and an activation energy of 45.6 kcal/mole was calculated from the slope. The "frequency factor" was also calculated giving a complete rate expression

$$\text{rate hexadiene} = 1.75 \times 10^{7} \exp(-45.6/RT) C_p^{0.38} C_o^{0.39}$$

The Arrhenius plot for acrolein is also shown in Figure 73 and the calculated activation energy was found to be 16.0 kcal/mole giving a full rate expression

$$\text{rate acrolein} = 5.99 \times 10^{4} \exp(-16.0/RT) C_p^{0.38} C_o$$

6C. Reactions at longer contact times

The contact time was varied from 20 gm sec/litre to 175 gm sec/litre by varying the flow rate at constant composition passing over 12.1 gm of 5.3 wt % In_2O_3 on pumice stone. At these longer contact times two products reappeared that had been previously observed only over the pure catalyst, namely carbon dioxide and benzene. Studies, carried out at four different conditions, are reported in Figures 74, 75, 76 and 77 respectively.

The yield of hexadiene was found to rise relatively quickly but to reach a steady value after ca 50 gm sec/litre. The yield was considerably higher at the higher temperature, and was dependent directly on the concentration of propylene, and oxygen.

The yield of acrolein showed evidence of considerable overoxidation at higher temperatures and longer contact times (Figure 75). The production appeared to be very

FIGURE 73

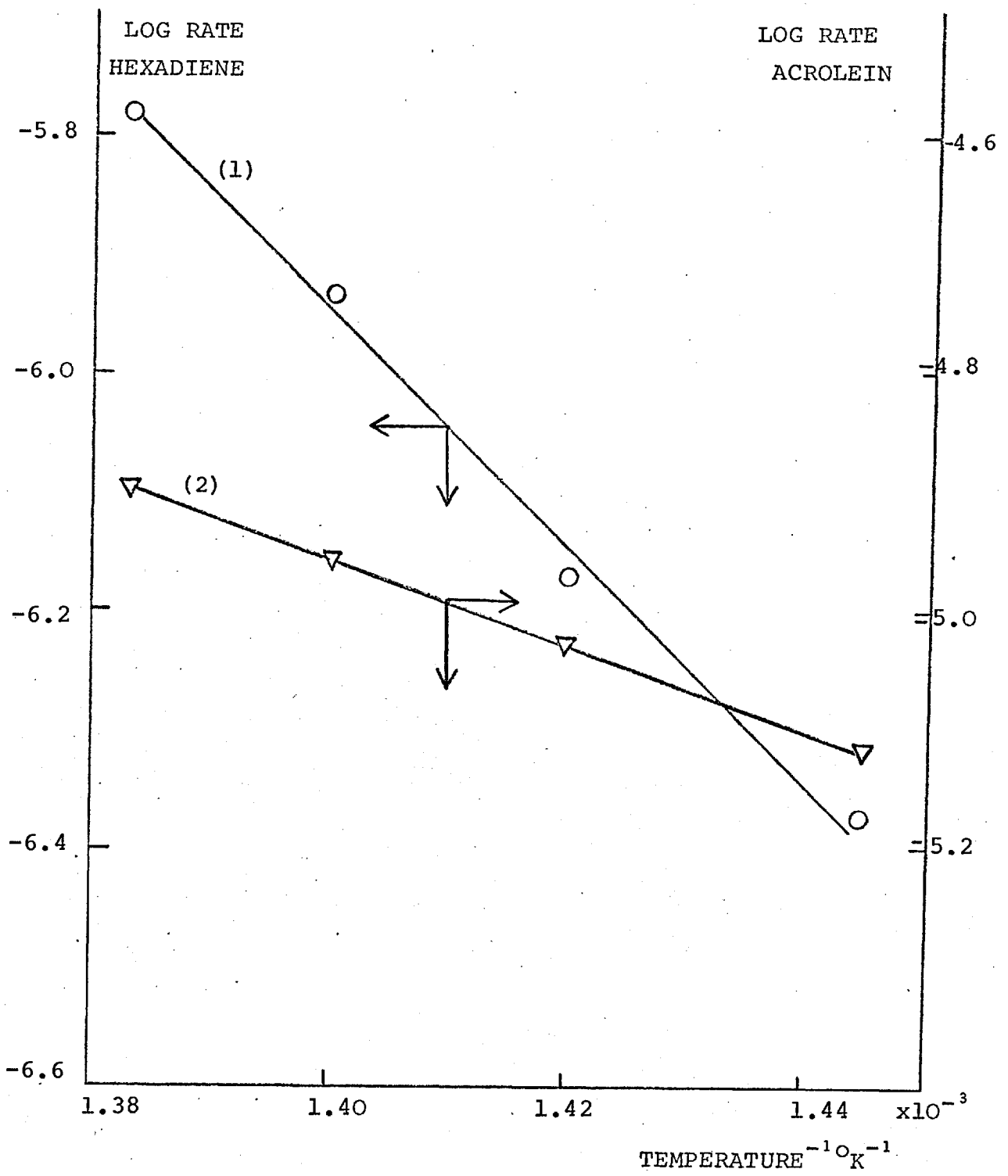

Arrhenius plots over dilute In_2O_3 catalyst.

activation energies: (1) hexadiene 45.6 kcal/mole
(2) acrolein 16.0 kcal/mole

KEY TO FIGURES 74, 75, 76 and 77

	Temperature °C	Propylene moles/litre	Oxygen x 10^{-3}
(1)	460	8.9	8.9
(2)	460	4.5	9.9
(3)	440	9.9	5.0
(4)	440	8.9	8.9

FIGURE 74

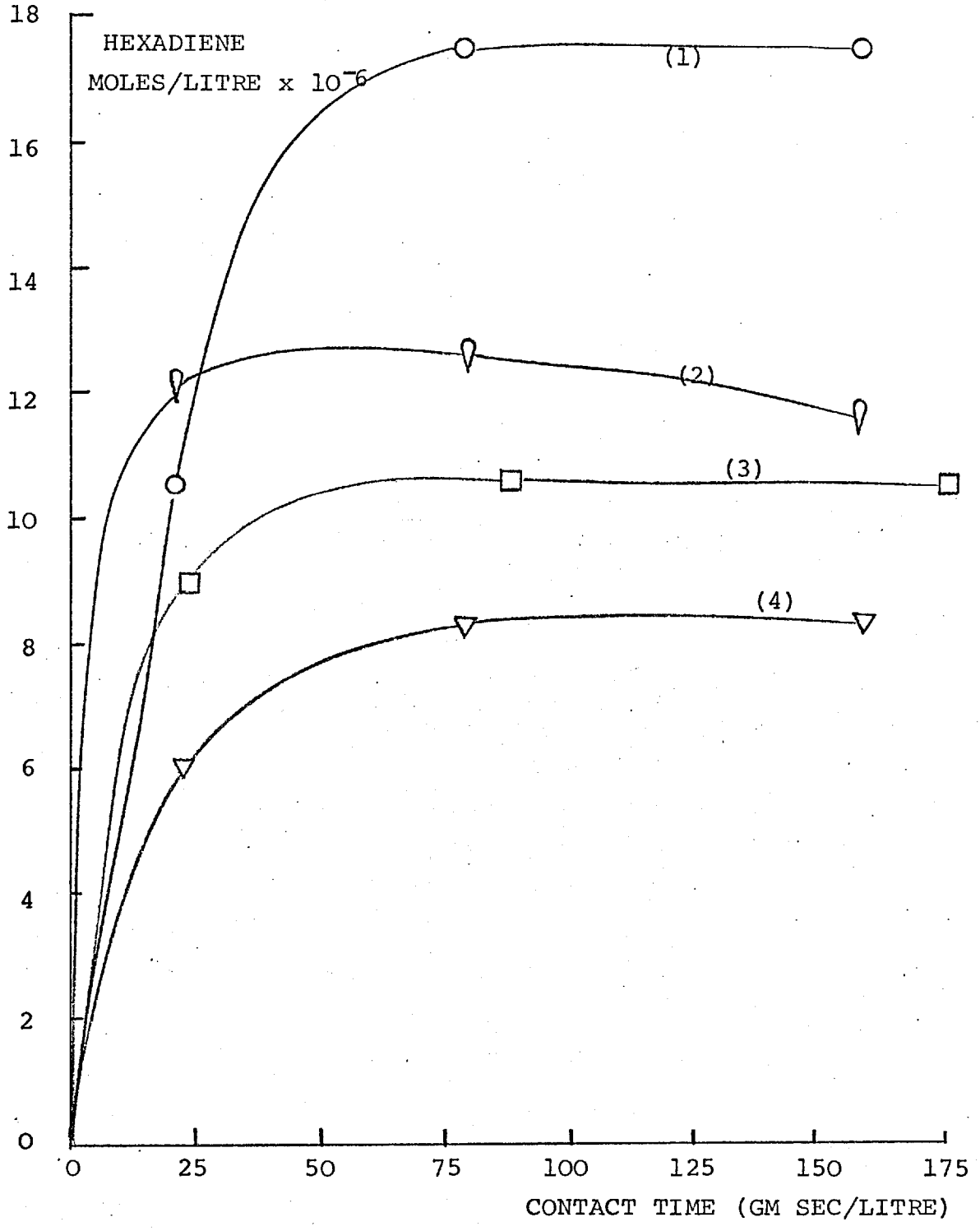

The yield of hexadiene from propylene at longer contact times over In_2O_3 on pumice (2V).

FIGURE 75

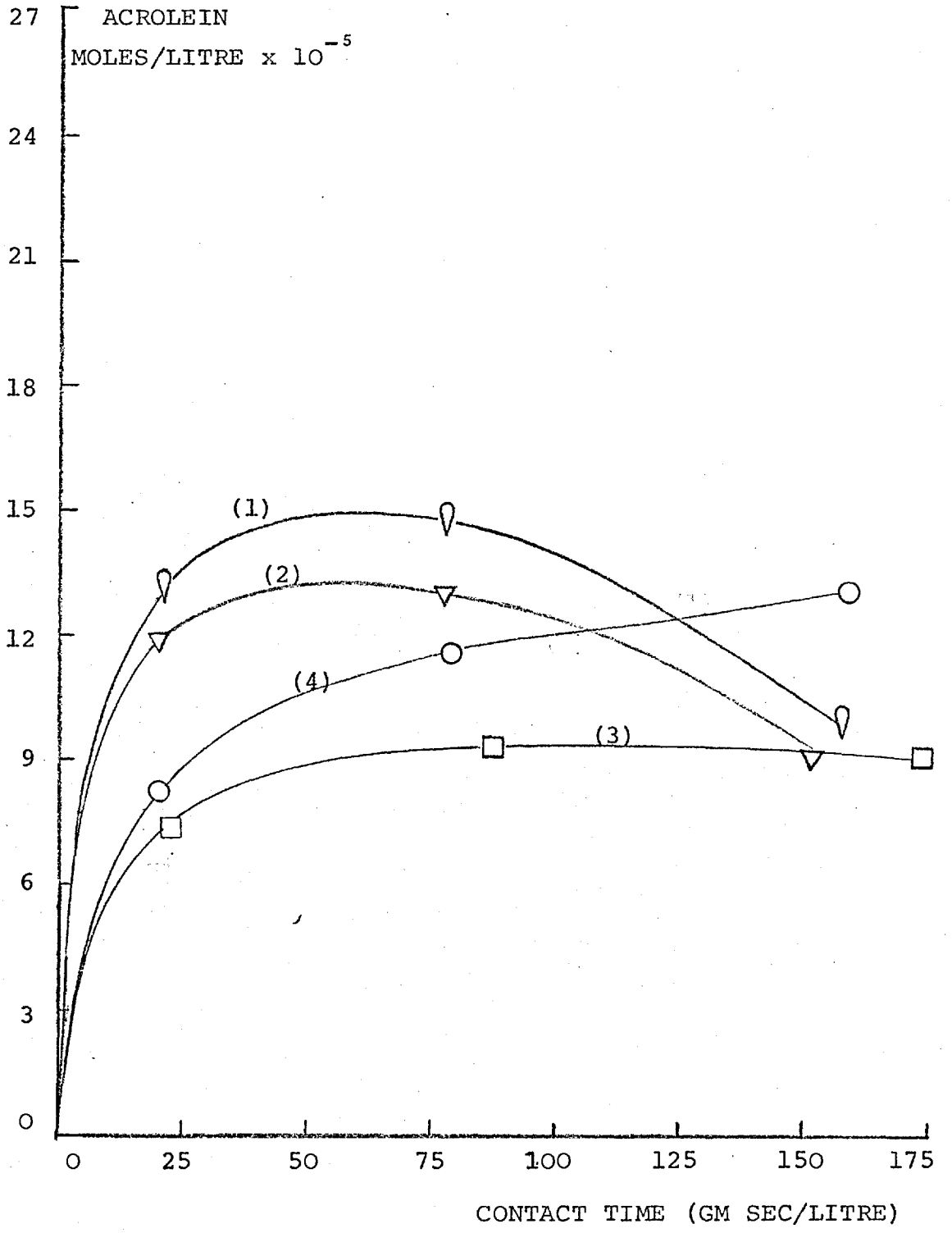

The yield of acrolein from propylene at longer contact times over In_2O_3 on pumice (2V).

See Key Figure 74.

FIGURE 76

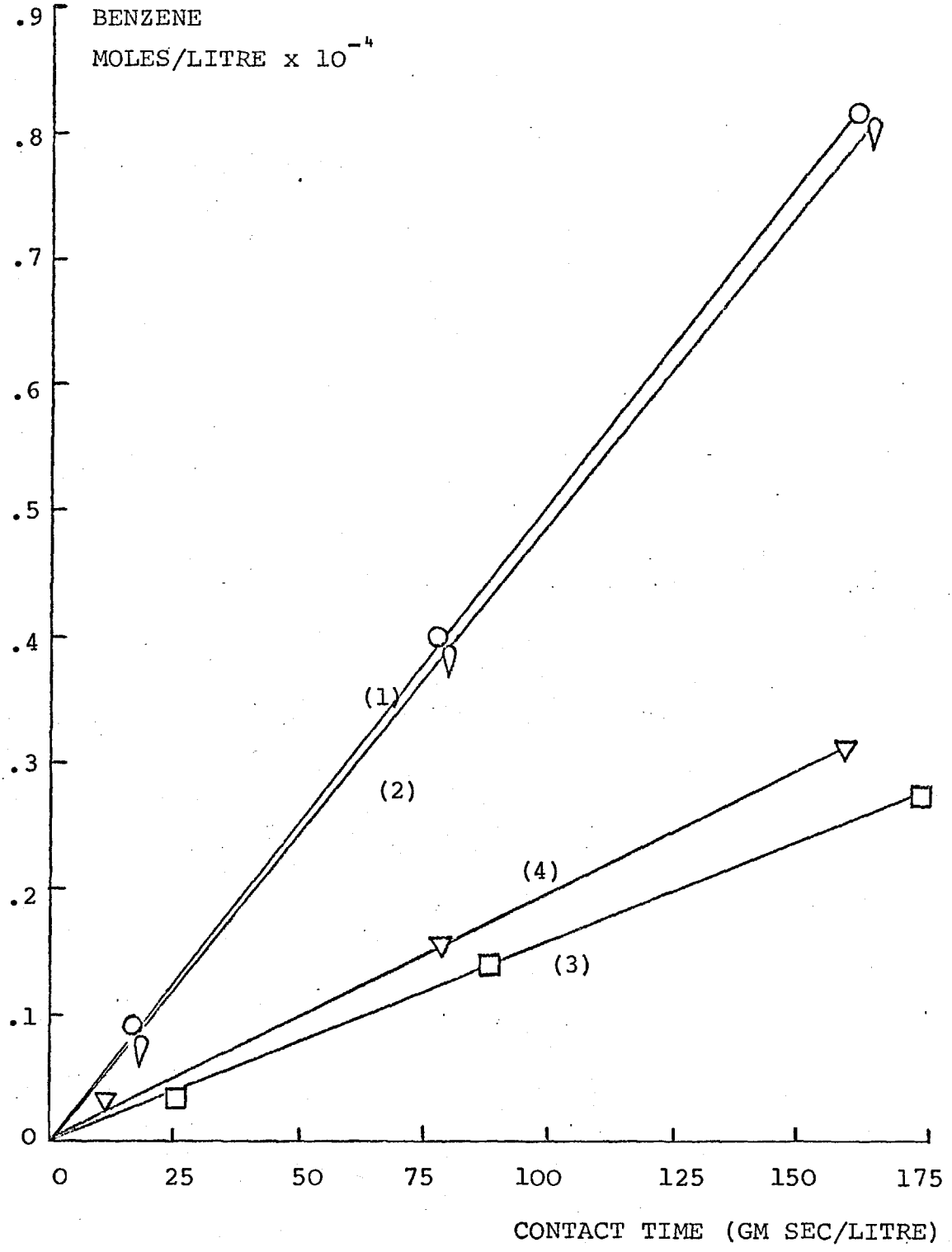

The yield of benzene from propylene at longer contact times over In_2O_3 on pumice (2V).

See Key Figure 74.

FIGURE 77

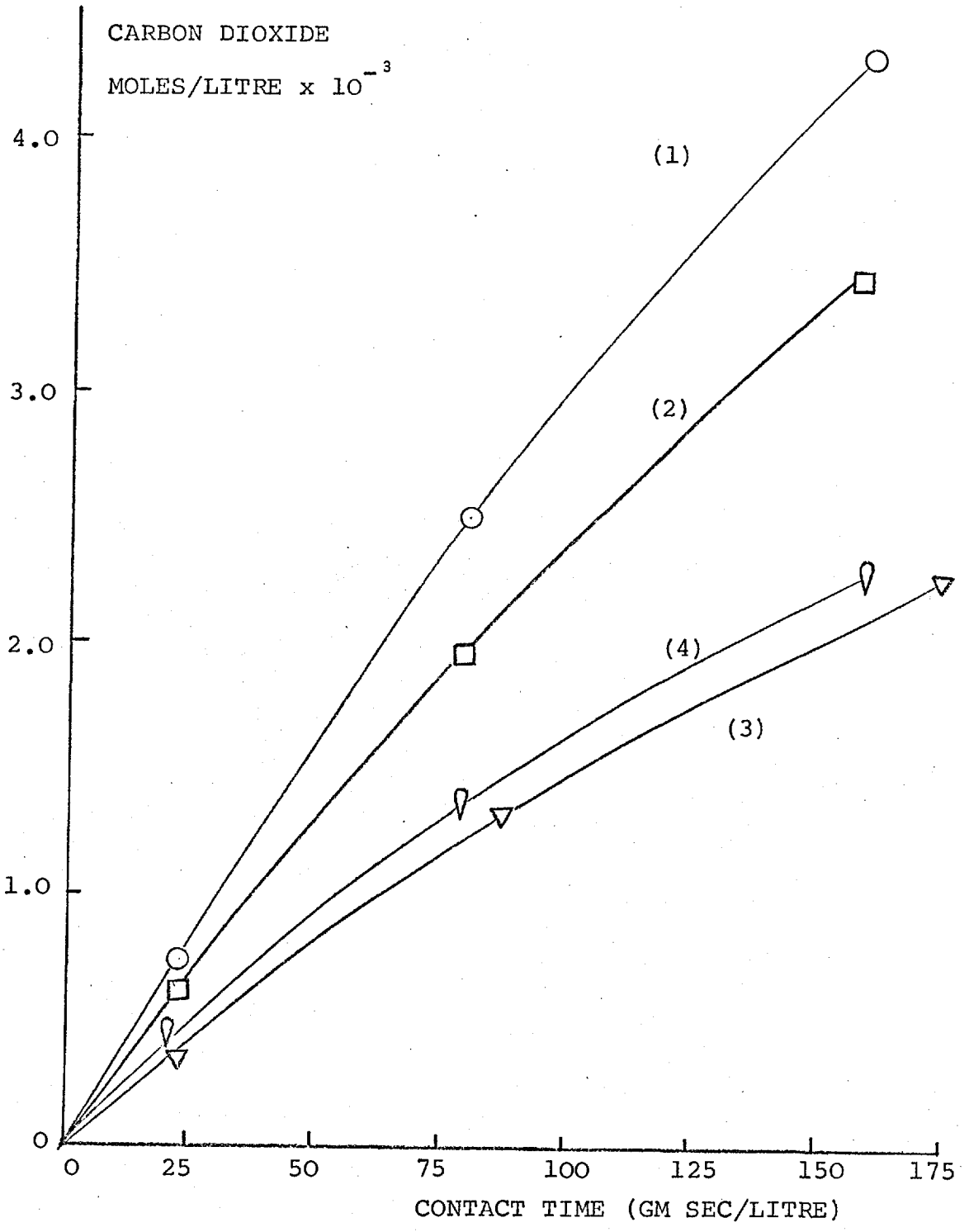

The yield of carbon dioxide from propylene at longer contact times over In_2O_3 on pumice (2V).

See Key Figure 74.

dependent on the concentration of oxygen at 440°C, both the rate of production and the final yield were markedly decreased on decreasing oxygen. The effect of changes in the propylene concentration was considerably smaller.

The yield of benzene at the long contact times was found to increase linearly and was influenced very little by changes in the concentration of propylene or oxygen (Figure 76). An increase in reaction temperature to 460°C from 440°C had a large effect. The yield of carbon dioxide was also very dependent upon temperature (Figure 77) although the production was also dependent upon the concentration of propylene.

6D. The oxidation of benzene

The importance of the overoxidation of benzene was determined by passing a mixture of 4.45×10^{-3} moles/litre oxygen and 2.23×10^{-3} moles/litre benzene over the catalyst at 460°C at a contact time of 79 gm sec/litre. Less than 3% of the benzene was converted to carbon dioxide.

6E. Further reactions of hexadiene

The homogeneous oxidation of hexadiene was studied at 460°C at a contact time of 79 gm sec/litre and a concentration of oxygen and hexadiene of 4.45×10^{-3} moles/litre. The reaction gave approximately 6.0×10^{-5} moles/litre of benzene which was appreciable when compared to the value of 5×10^{-5} moles/litre of benzene produced heterogeneously

using a concentration of 1×10^{-5} moles/litre hexadiene. As a result, the kinetics of the homogeneous disappearance of hexadiene were studied in some detail. Both the rates of production of benzene and of carbon dioxide were found to be approximately first order in hexadiene but both reactions were unimportant being a factor of 500 smaller than the heterogeneous reaction at the normal hexadiene concentration. The sum of the homogeneous reaction plus the heterogeneous reaction (obtained from the contact time curve at the low hexadiene concentrations) equalled the yield of benzene over the catalyst at the high concentration of hexadiene ($6.0 \times 10^{-5} + 5 \times 10^{-5} \simeq 11.5 \times 10^{-5}$). Thus it appeared that although the concentration of hexadiene had increased by a factor of 500 the heterogeneous yield of benzene was approximately the same value as that predicted from the results at the lower concentration of hexadiene, the balance of the reaction being homogeneous reaction.

6F. Product inhibition

One possible explanation of the low yields of hexadiene and acrolein observed at longer contact times is the inhibition by product or products. A qualitative study was undertaken to determine if an increase in the concentration of any product, obtained by feeding that product together with the reagents, inhibited the reaction. A large increase in the concentration of benzene was found to have no effect on the yields of hexadiene and acrolein. Increases

of either hexadiene or acrolein inhibited the reaction by decreasing the other products. Butadiene, which was thought to be relatively inert under the reaction conditions was also passed through the reactor with the normal reaction mixture and it was found that the concentrations of hexadiene and acrolein produced were inversely proportional to the concentration of butadiene.

A quantitative study of the effect of hexadiene concentration on the yield of acrolein was carried out and the results are reported in Table 21. The concentration of acrolein was found to decrease as the concentration of hexadiene was increased. A quantitative study of the effect of acrolein concentration on the reaction was attempted, but the acrolein polymerized in the heated metal vapourizer and no quantitative results could be obtained.

TABLE 21

The inhibition of the production of acrolein by hexadiene

Hexadiene added moles/litre x 10^{-5}	Acrolein produced moles/litre x 10^{-5}
0.475	2.94
0.637	2.86
3.46	2.5
17.25	1.67
23.6	1.37

Catalyst, 0.15 wt. % indium oxide on pumice; temperature, 440°C; contact time, 3 gm. sec/litre; concentration oxygen, 8.9 x 10^{-3} moles/litre; concentration propylene, 8.9 x 10^{-3} moles/litre.

SECTION IV.

DISCUSSION

1. General

Using the reaction of propylene with oxygen to produce hexadiene and benzene as a model, it has been possible to apply a logical sequence of catalyst design to recognise solids that will catalyse the reactions. The design, described fully in the introduction, has been applied to the dimerization of propylene, the cyclization of hexene and the dimerization-cyclization of propylene, all in the presence of oxygen.

Several potential catalysts may be recognised, either from previous reports or by logical deduction. The description of this reasoning is given in the introduction and the results of experimental testing of the solids are presented in chapter 3. It is rewarding, in the light of these results, to consider why these solids are, or are not, good catalysts before discussing the detailed results on the better catalysts in more detail.

It is useful to re-state the findings that were obtained in the introduction. It would seem likely that the initial dimerization would require a catalyst which can exist in two stable valency states two units apart, that can accept two electrons rapidly and that can π bond allylic intermediates. These conditions would appear to favour the production of linear hexene molecules which can be cyclized to benzene.

2. The preliminary selection of catalysts

2A. The dimerization reaction

Experimental testing of the catalysts thought to be active for this reaction showed that only thallium oxides were, in fact, suitable.

Cobalt oxide was originally selected as a catalyst as a result of reports that the solid would catalyse the dimerization of propylene (95). In a proposed mechanism similar to that of hydroformylation, cobalt ions were suggested to π adsorb propylene molecules to give an intermediate in the dimerization reaction.

The reaction thus depends on π complex formation at a free ligand site and the reaction should be strongly inhibited by any compound capable of preferentially adsorbing on the free site. The inactivity of the catalyst under oxidative conditions could then be explained in terms of the presence of carbon monoxide from the oxidation reaction which would complex with the free site and inhibit the reaction.

Alternatively the inactivity of CoO may be due to the oxygen present in the reaction mixture. Even though propylene is present in excess, it could be that the cobalt ion is maintained in the 2+ or 3+ state, on which σ bonding may occur, but π-bonding is impossible (5). As a result, propylene is likely to absorb dissociatively and to undergo destructive oxidation (117).

The lack of dimerization activity of NiO would appear to be related to the fact that the Ni^{2+} state is by

far the most stable (104). Ni^{3+} and Ni^{4+} occur in certain oxide systems but Ni^{O} and Ni^{1+} are very scarce. If a fast transfer of two electrons is necessary for selective dimerization, then the reaction must occur by double electron transfer such as Ni^{4+} to Ni^{2+} or Ni^{3+} to Ni^{1+} or Ni^{2+} to Ni^{O}. The electronic structure of Ni^{4+} (d^6), Ni^{3+} (d^7) are such that only weak octahedral π-complexes (5) can be formed and the formation of π allylic intermediates is unfavourable. If the propylene molecule does π bond with Ni^{2+} (d^8), the required electron transfer is unlikely as Ni^{O} is very unstable. In addition Ni^{O} is capable of π bonding with the product and desorption would probably be slow, resulting in over-reaction.

Conventional cyclization catalysts were also examined for dimerization activity (Chapter 1:section 4A) and found to be inactive. This could be a result of the observation made by McHenry and fellow workers (101) who found during cyclization studies that platinum on alumina when treated with air formed platinum 4+ ions which appeared to be quite stable, having a life of over 10 hours even at hydrogen pressures of over 20 atm.

In the dimerization experiments the same type of catalyst, $Pt-Al_2O_3-Cl$, was treated with air before a run and the Pt^{4+} complex is most likely to be present. The life of the complex should be considerably longer with oxygen present. If adsorption of propylene and electron transfer does occur, then the platinum should be reduced to Pt^{2+}, a stable valency state. However, the Pt^{4+} has a d^6 electronic configuration

which is not able to form the necessary strong π bonds with the propylene. The formation of σ-bonds will lead to complete combustion to carbon dioxide.

Molybdenum salts were found to be inactive, presumably because the more common higher oxidation states ($Mo^{4}+$, $Mo^{5}+$ and $Mo^{6}+$) tend to be stable, particularly if the transfer of two electrons is desired. The most stable states of chromium ($Cr^{2}+$ and $Cr^{3}+$) are only one unit apart, and the transfer of two electrons would not be expected. No other cyclization catalysts were used. From a mechanistic view point, it has been suggested that elements in the groups following the transition elements (namely groups IIIb, IVb and Vb) could form efficient dimerization catalysts (Introduction section 4A). Of these possible catalysts only thallic oxide was tested as a dimerization catalyst and this proved to be very active and selective. The main products of reaction were found to be 1,5 hexadiene and carbon dioxide with up to 75% of the reacted propylene going to 1,5 hexadiene. No trace of further polymerization, dehydrogenation or cyclization reactions could be identified.

The oxygen to fuel ratio and the temperature were varied from 1.0 to 0.1 and 485^{o}C to 560^{o}C respectively. The experimental results, illustrated in Figure 36 indicate that the oxygen to fuel ratio should be maintained at a low value for high selectivity, as the undesired production of carbon dioxide is strongly oxygen dependent. It is also clear that

high temperatures favour the dimerization reaction.

Additional evidence that the mechanistic approach is basically correct comes from a Dutch patent (118). This patent, received only recently, states that oxides of cadmium, lead and thallium, can be used to catalyse the dehydrodimerization of olefins not capable of forming dienes. Cadmium, although not discussed earlier certainly fits the pattern in that a) Cd^{2+} has a d^{10} electronic structure capable of π bonding and b) the only other oxidation state is the element Cd^{o}. Cd^{o} has an electronic configuration of s^2 and π bonds cannot be formed; any intermediates formed at the same time as the Cd^{0} would tend then to combine and to desorb. As with the other groups, the lower oxidation state is more stable with the heavier elements and the transfer of electrons should be quicker with cadmium than zinc.

Lead oxide was considered as a possible catalyst in the introduction but was disregarded because of the instability of the 4+ state. If the patent claims are correct, this would seem to be a more promising catalyst than was at first thought.

No mechanism was postulated in any of the patents.

2B. The cyclization reaction

Various catalysts were tested for their efficiency with respect to oxidative dehydrogenation and cyclization using hexene as a reagent. Conventional cyclization catalysts

showed the same pattern of activity in an oxygen atmosphere as in the normal hydrogen atmosphere. As stated in section 4B. of the Introduction, the rate of dehydrocyclization is controlled by the ability of the catalyst to dehydrogenate and the pattern of selectivity for cyclization follows the dehydrogenation activity pattern

$$Pt > Cr_2O_3 \sim MoO_3 > ThO_2 \quad \ldots.73$$

This same pattern was found under an oxygen atmosphere with the Pt catalyst even more selective than in hydrogen. The rates of the cyclization, cracking and isomerization reactions were all approximately equal in hydrogen, but under a continuous stream of oxygen and hexene, the production of benzene can be the major reaction to organic products (73% selectivity at 450°C and 2:1 oxygen to hexene ratio, Figure 40). The acidity of the catalyst is an important factor in determining the importance of the cracking and isomerization reactions and any further development work must be concerned with this factor.

At the higher temperatures necessary for high cyclization activity over the conventional cyclization catalysts, ThO_2, Cr_2O_3 and MoO_3, side reactions become important and the selectivity is low. Cracking and isomerization reactions, as with the $Pt-Al_2O_3-Cl$ catalyst, are very important and optimization of catalytic cyclization demands further study of the acidities of the system.

Oxidative dehydrogenation catalysts such as

Bi_2O_3-MoO_3 and Sb_2O_5-SnO_2 are also known to be capable of cyclizing hexenes to benzene (87). Comparison of the selectivity (liquid products) of Bi_2O_3-MoO_3 and Sb_2O_5-SnO_2 with conventional cyclization catalysts show that the former catalysts are more selective since they are practically non-acidic. In comparison with previous work over bismuth molybdate (90) the yield of benzene is higher and of hexadiene plus hexatriene is lower in the present studies.

The effect of temperature on the reaction over these two catalysts was as expected from previous studies. For example, the observation that the selectivity was at a maximum at 450°C for the Sb_2O_5-SnO_2 catalyst agrees with results previously reported for the oxidative dehydrogenation of butene to butadiene (119). Only small differences existed between Bi_2O_3-MoO_3 and Sb_2O_5-SnO_2 but in view of the detailed information available for the Bi_2O_3-MoO_3 system further development studies were concentrated on this catalyst.

2C. Summary

Experimental testing of the catalysts thought to be active for dimerization showed that only thallium oxides were suitable. The lack of dimerization activity of CoO, NiO, Pt, Cr_2O_3 and MoO_3 has been shown to be due to the lack of the electronic structure necessary for π bonding propylene and/or of the capability of being reduced or oxidized by two units. The thallium catalyst which had been designed with

the above two constraints in mind selectively produced 1,5 hexadiene with carbon dioxide as the only other product.

In the case of the cyclization studies, all catalysts tested showed activity for benzene production. The selectivity to benzene relative to the other organic products tended to be inversely proportional to the acidity of the catalysts:

$$Bi_2O_3\text{-}MoO_3 \sim SnO_2\text{-}Sb_2O_5 >> Pt\text{-}Al_2O_3 > MoO_3 \sim Cr_2O_3 \quad ....74$$

A decision was taken to examine the bismuth molybdate catalyst in more detail due to its high selectivity (>90%) and to the fact that it has been well documented in the literature.

3. The development of the catalysts

3A. The dimerization reaction over Tl_2O_3

(i) The reaction mechanism

Initial studies of the effect of oxygen showed that the yield of carbon dioxide increased with and the yield of hexadiene was approximately independent of the concentration. The selectivity to hexadiene increased markedly at longer contact times, since the concentration of oxygen was reduced under these conditions. The amount of hexadiene appeared to be maximal at an oxygen concentration of zero (Figure 48) and the sum of the yield of hexadiene plus one-sixth of the carbon dioxide yield was independent of the fuel:oxygen ratio. Taken together all these results indicate that the presence of gas phase oxygen tends to reduce the amount of hexadiene.

In the presence of pure propylene, the catalyst rapidly deactivated (Figure 49), and a similar deactivation could be obtained by reducing the catalyst with hydrogen. The activity could be regenerated by a stream of oxygen, but since only traces of carbon dioxide were evolved, no coke had been deposited on the catalyst. From these results one is forced to the conclusion that the active form of the catalyst is thallic oxide, and that although oxygen must be present to reoxidise thallous oxide (produced during the reaction) the gas also tends to reduce selectivity by over-oxidizing hexadiene. Since the overall rate is independent of the oxygen concentration, the re-oxidation must be fast.

The above conclusions support and extend the mechanism proposed in the Introduction. The lack of other products such as trimers and aldehydes indicates that the dimerization is fast and probably occurs only on one site. This appears to be a Tl^{3+} centre which is reduced to Tl^{1+} by transfer of an electron from each of two intermediates during the reaction. The proposed intermediates are formed via hydrogen abstraction by lattice oxygen and are thought to be allylic species. Oxygen is necessary to reoxidize the Tl^{1+} to Tl^{3+} and to replace some of the lattice oxygen consumed in the reaction.

This proposed mechanism is summarized in Figure 78. The bonding of the two propylene molecules is not known but it seems possible that both could be π bonded to the Tl^{3+} before hydrogen abstraction occurs.

FIGURE 78

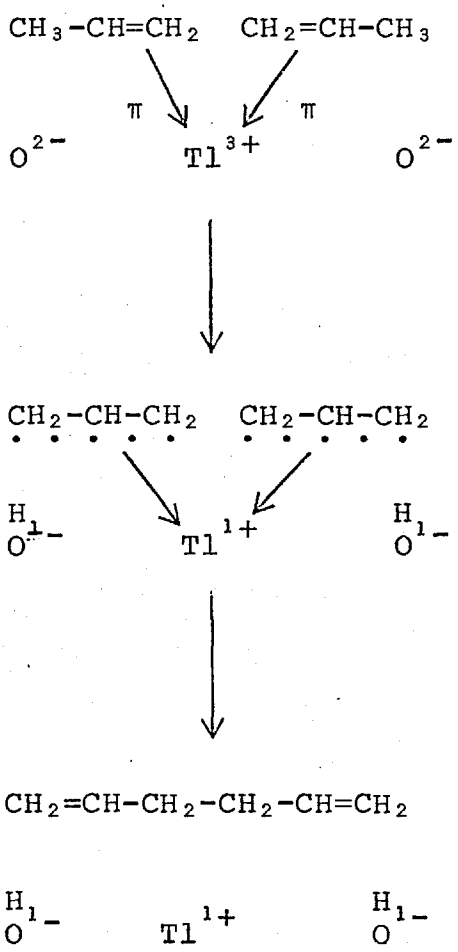

$$Tl^{1+} + \tfrac{1}{2}O_2 \rightarrow Tl^{3+} + O^{2-}$$

$$2OH^{1-} \rightarrow H_2O + O^{2-}$$

A mechanism for the dimerization of propylene over Tl_2O_3.

(ii) Thermal deactivation

Thallium salts tend to distil out of the reactor, and to attack the glass walls at reaction temperatures. Thallic oxide, which fuses at 717°C has a very low vapour pressure in the temperature range examined (120) but thallous oxide melts at 300°C and vaporizes at 506°C (atm pressure). The analysis of the distilled component supports the contention that thallous oxide alone distils out; the tendency can be decreased by lowering the temperature or by increasing the oxygen concentration.

An attempt was made to develop a more stable form of the thallium catalyst. Thallium tungstate was tested as a dimerization catalyst over a range of oxygen to fuel ratios and contact times at a temperature of 500°C, but although the catalyst was active, its selectivity was a good deal less than the thallium oxide (Table 13).

(iii) Optimum conditions

a) Oxygen to propylene ratio

The effect of the oxygen to fuel ratio has been discussed above in connection with the reaction mechanism; an optimum value was approached at an oxygen concentration of zero. The necessity for low oxygen concentration (3-10%) has been recognized for this type of catalyst (118) where the upper concentration is dictated by the loss of selectivity and the lower by the need to maintain an active catalyst. One obvious argument is to pass pure propylene over the catalyst reoxidizing the reduced catalyst when necessary (121). In

the case of Tl_2O_3, if the oxygen concentration is too low, deactivation will occur.

b) Temperature

The reaction to hexadiene occurred at temperatures of 400°C and higher (Figure 43) and the yield and the selectivity to hexadiene, S_α, was found to increase with temperature; a maximum could not be reached due to deactivation at the higher temperatures (Figure 50). The calculated activation energy for the hexadiene production is very high (52 kcal/mole) and over twice that of carbon dioxide (21 kcal/mole). The optimum value again results from balancing the effect of deactivation against the highest selectivity and yield.

3B. The cyclization reaction over Bi_2O_3-MoO_3

The production of benzene over this catalyst was found to be maximized at an oxygen:hexene ratio of ca 1:1 the selectivity decreasing markedly at lower values and over-oxidation becoming increasingly important at higher ratios (Figure 46). The activation energy for benzene formation appeared to be higher than for the production of carbon dioxide, since the selectivity increased with temperature (Table 16).

In agreement with Adams (90) seems likely that the reaction mechanism occurs via the formation of π adsorbed allylic intermediates, as is summarized in Figure 79. The

FIGURE 79

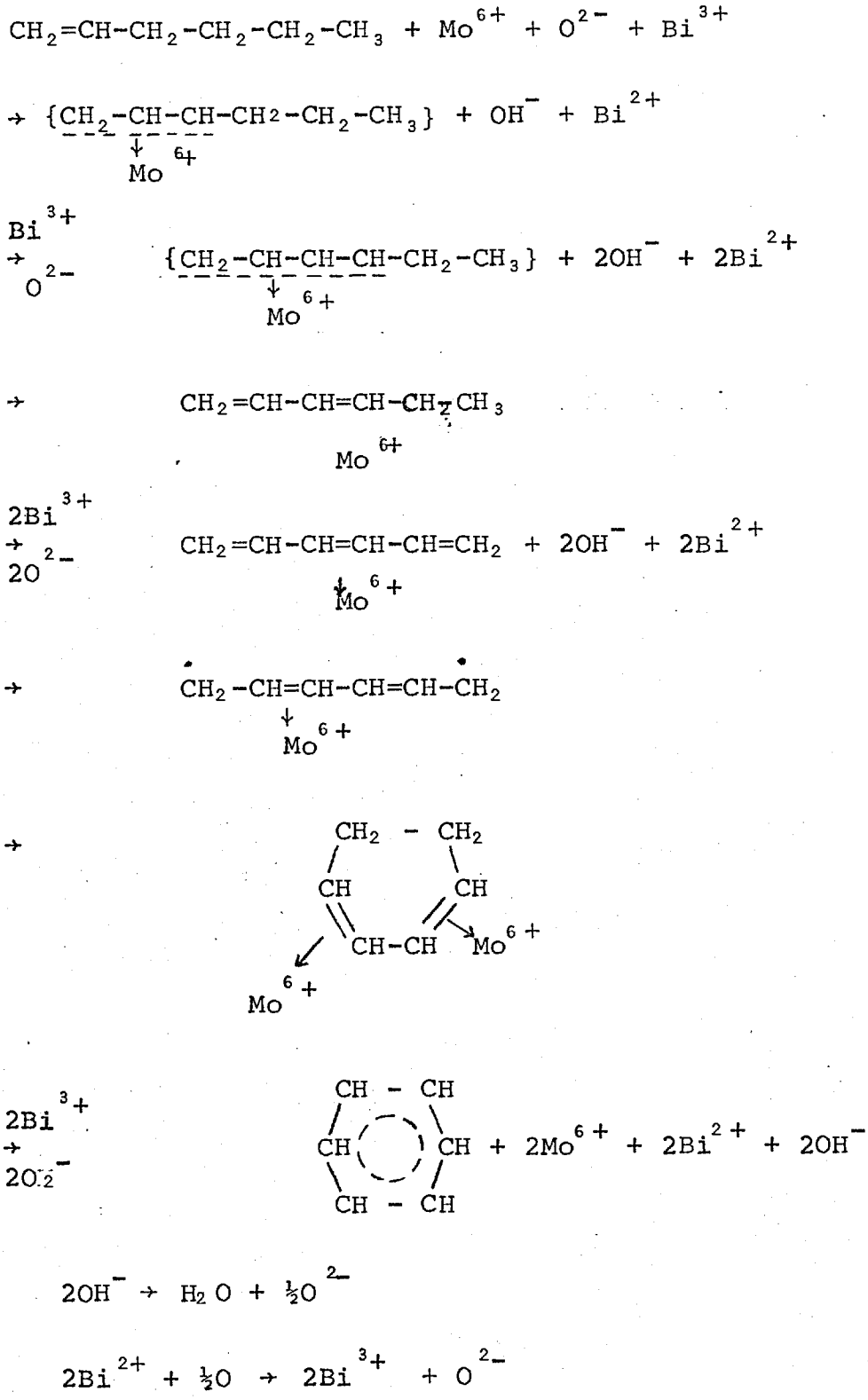

A mechanism for the oxidative dehydrocyclization of hexene to benzene over Bi_2O_3- MoO_3.

formation of hexadiene and hexatriene and the dehydrogenation of cyclohexadiene to benzene occur similarly to the oxidative dehydrogenation of butene to butadiene (104). The cyclization step is very similar to the isomerization of olefins over bismuth molybdate or molybdenum oxide (122)

$$CH_2=CH-CH_2-CH_3+Mo^{6+}+O^{2-} \rightarrow \underset{\underset{Mo^{6+}}{\downarrow}}{CH_2-CH-CH-CH_3}+OH+e^- \rightarrow CH_3-CH=CH-CH_3+Mo^{6+}+O^{2-} \quad \ldots.75$$

3C. The dimerization-cyclization reaction over In_2O_3

Although the thallium oxide catalyst was proved to be active and very selective for dimerization of propylene to hexadiene, the development of the catalyst was not continued since it was not found possible to avoid the permanent deactivation caused by thermal instability. The information gained from the studies over thallium oxide, recycled through the design process (Table 1), not only confirmed the conclusions reached in the initial design, but also extended them.

Thus to the two mechanistic requirements of an electronic structure capable of strong π-bonding and of the correct oxidation states requiring a transfer of two electrons, must be added at least one more, thermal stability. This is particularly important in that the dimerization reaction has been found to possess a high activation energy and that selectivity is particularly high at high temperatures.

Following the arguments outlined in the introduction, further studies were continued on indium oxide. The pure, unsupported catalyst not only catalysed the production of hexadiene but also catalysed the second step to produce benzene. Small amounts of hexatriene and cyclohexadiene were also observed, indicating that the reaction could involve a sequential dehydrogenation/cyclization reaction. The catalytic effect of In_2O_3 was therefore studied under different conditions in order to develop a suitable catalyst for the combined reaction. The effects of the reaction variables, concentration, temperature and contact time, examined over pure In_2O_3, are reported in section 5 of the Results and are discussed below.

(i) The effect of reactant concentration

The yields of hexadiene and benzene (Figure 52) passed through a maximum as the oxygen concentration increased with both products overoxidizing at high oxygen concentration. The asumptotic approach to zero concentration of both yields at low oxygen concentrations was probably caused by heavy coke formation and this was supported by visual inspection of the catalyst.

The lack of reaction in the absence of oxygen, although conflicting with the results over the thallium catalyst, is not unexpected as the high activity of In_2O_3 and the heavy coke formation would result in very fast deactivation. At higher oxygen concentrations, the production

of carbon dioxide consumed over 95% of the oxygen initially available, and it was not unexpected that the yield was directly dependent on the concentration of oxygen.

At the optimum mole fraction of oxygen the conversions of propylene and oxygen were 13% and 97.5% respectively, but the selectivities of reacted propylene and oxygen to hexadiene, benzene and carbon dioxide were 25%, 25% and 50%, and 2.5%, 7.5% and 90% respectively.

The effect of varying the propylene concentration can be best explained in terms of surface concentration. With increasing propylene partial pressure the surface concentration of propylene would be expected to increase, favouring reactions such as the formation of hexadiene (Figure 55). Any increase in the concentration of hexadiene on the surface would probably favour the formation of benzene, although the yield of benzene would be expected to go through a maximum at the higher pressures of propylene as a result of competition between the reagent and hexadiene for surface sites. The increased surface concentration of propylene would also be expected to force the products from the surface, thereby inhibiting the over-oxidation to carbon dioxide. On the other hand, a parallel reaction involving direct oxidation of propylene to carbon dioxide would grow in importance with increasing propylene concentration and the yield of carbon dioxide could well pass through a minimum (Figure 54).

(ii) The effect of temperature

Up to a temperature of 460°C, the yield of hexadiene (Figure 56) responded as would be expected passing through a maximum as the temperature increased. The increase of hexadiene at higher temperatures would appear to result from an increase in the rate of desorption of hexadiene, inferring that the adsorption coefficient for hexadiene is large at the lower temperatures and that a significant surface concentration is present.

The study of the reaction at low conversions and at higher temperatures was complicated by the increasing importance of a homogeneous reaction at temperatures above 500°C (Figure 63). The production of hexadiene could be due, under these conditions, to a pyrolytic reaction since no carbon dioxide or acrolein was detected. Fortunately the importance of the homogeneous reaction declined with increasing conversion; however care was taken that initial rates studies were made at temperatures where the effect of homogeneous reaction was minimal.

The maximum in benzene yield (Figure 56) was probably due either to overreaction or to low hexadiene surface concentration at the high temperatures. The constant yield of carbon dioxide (Figure 57) indicates that the catalyst was converting approximately 100% of the oxygen over the entire temperature range. The calculated conversions are 19% propylene and 98% oxygen while the selectivities of reacted propylene were 52% hexadiene, 13% benzene and 35% carbon dioxide at the optimum temperature of 420°C.

(iii) The effect of contact time

The steep maximum in the benzene yield as a function of contact time apparently results from the deposition of carbon. It is tempting to suggest that over-oxidation occurs, but the amount of oxygen available at the longer times is so small that this is unlikely. In addition, the yield of carbon dioxide is constant at all contact times indicating that nearly all the oxidation occurs in the early stages of the bed or that the reaction is essentially diffusion controlled.

The low yield of hexadiene compared to the benzene was expected at the temperature of 445^{o}C, but the variation of the yield of hexadiene with respect to contact time was unexpected in that an intermediate product normally passes through a maximum. The major part of the oxidation probably occurred in the first part of the bed, consuming a high proportion of the oxygen. The low oxygen concentration would then be expected to affect the production of benzene (removal of 4 hydrogen) more than the hexadiene formation (removal of 2 hydrogen) resulting in increased yields of hexadiene at longer contact time.

(iv) The physical structure of the catalyst

The effect of the porosity of the catalyst on the selectivity of an oxidation reaction may be very important as was discussed in section 2B(iii)a. The fact that the yield of carbon dioxide was constant with temperature and

contact time does suggest that diffusion, and hence catalyst porosity / may be important. Nitrogen adsorption studies (Figure 60) show a steep narrow hysteresis loop indicating that the catalyst is porous, containing a large volume of pores of radius between 50 and 200A^{O}.

The surface area of an In_2O_3 sample activated at 540^{O}C was approximately 60 m^2/gm which decreased at higher temperatures of activation (at 760^{O}C surface area was approximately 25 m^2/gm). Similar effects have been reported for many other catalysts. Studies of the effect of the temperature of activation on the pore size distribution were therefore instigated in order to produce a range of catalysts, containing a characteristic pore radius, over which it would be possible to study the effect of porosity on the selectivity of the reactions. The activation of the catalyst at 240^{O}C rather than 560^{O}C produced a catalyst with closer control on pore size (Figure 61). As the surface area for the 240^{O}C activation (Figure 62) was concentrated in pores with a diameter of 100 to 200A^{O}, the pore size could be well approximated by an average pore radius of 150A^{O}. In fact, events showed that the In_2O_3 was too active a catalyst in the pure form and a supported catalyst with low surface area and porosity had to be developed.

(v) <u>The supported catalyst</u>

The activity of the unsupported In_2O_3 was found to be very high, and large temperature rises, coupled with the complete consumption of oxygen were observed in nearly

all cases tested (Table 18). Although such a catalyst may be useful, it is not possible to obtain a reliable idea of the mechanism or kinetics of the reaction over such a system, and a supported catalyst was prepared.

Preliminary results, using a pumice supported catalyst prepared by the decomposition of $In_2(SO_4)_3$ yielded considerable amounts of carbon dioxide even through the concentration of the oxide was low (Table 20). The catalyst was reddish-brown, compared with In_2O_3 which is yellow. These descrepencies were thought to be due to the high activation temperature (820°C) and another method of preparing an In_2O_3 impregnated catalyst was developed (Experimental, section 2V) which allowed the preparation of catalysts containing as little as 0.009 wt % In_2O_3. Over such catalysts, the homogeneous reaction was found to be unimportant.

The observation that benzene was not produced as an initial product was not unexpected since it was thought that the product originated via hexadiene, but the identification of acrolein as an early product was surprising. Acrolein is easily over-oxidized at higher conversions and at temperatures greater than 400°C to carbon dioxide (123).

Preliminary tests were completed with $InPO_4$, which, by comparison with bismuth molybdate-bismuth phosphomolybdate (102) might have been expected to be more selective but the solid was neither very active or very selective for the reaction.

3D. Summary

(i) Dimerization

The thallic oxide was found to be a selective and active catalyst for the dimerization of propylene to hexadiene with the only other product being carbon dioxide. The proposed mechanism involves the reaction of two propylene over one thallic ion via allylic intermediates. The optimum conditions were found to involve low oxygen concentrations and high temperature; however both optima must be balanced against the rate of thermal deactivation which becomes faster with lower oxygen concentration and higher temperatures.

(ii) Cyclization

Conventional oxidation dehydrogenation catalysts, bismuth molybdate and tin/antimony oxides, were found to be selective for the formation of benzene from hexene. The mechanism put forward for the reaction of hexene over bismuth molybdate is based on the reactions of butene over this catalyst. The oxidative dehydrogenation steps proceeded by initial hydrogen abstraction at the allylic position followed by hydrogen abstraction from the carbon next to the original allylic carbon. The cyclization step was thought to occur in a similar way to butene isomerization over bismuth molybdate. The optima of 1:1 oxygen to hexene ratio and of 450^{o}C are similar to those found for the butene reaction over bismuth molybdate.

(iii) Dimerization-cyclization

Indium oxide was found not only to catalyse the dimerization reaction for which it was developed but also to catalyse the cyclization step resulting in aromatization of propylene to benzene over a single catalyst. Under some conditions the production of carbon dioxide, probably originating in part from the over-oxidation of the initial product acrolein, was an important side reaction. Optimum conditions for selective dimerization-cyclization reaction were found to involve low oxygen and high propylene concentrations and short contact times. Several observations point to the possibility of strong product adsorption and hence product inhibition.

4. Mechanistic aspects of the dimerization/cyclization of propylene

4A. Initial products

Studies of the oxidation reaction over a supported indium oxide catalyst shows that 1,5 hexadiene and acrolein are the only major initial products. Any mechanistic explanation of this must however also satisfy the observations that

(1) fast dimerization to hexadiene occurs even at low catalyst concentration

(2) the selectivity of 1,5 hexadiene is high with respect to other possible hexadienes

(3) production of two different species, acrolein and 1,5 hexadiene, occurs

(4) the double bond is maintained throughout both reactions

(5) the reaction rate depends on propylene to the same extent for the production both of acrolein and 1,5 hexadiene

(6) the order in oxygen is fractional for the production of hexadiene

(7) the order in oxygen is one for the production of acrolein

(8) large differences occur in the activation energies for the production of hexadiene and acrolein.

Any explanation must also take account of the inorganic chemistry of indium oxide.

(i) The reaction mechanism

As was suggested in the introduction (section 3D) the reaction bears many resemblances to oxidative dehydrogenation over catalysts such as bismuth molybdate or tin/antimony oxides. Consequently, it is rewarding to compare and contrast the two reaction systems. In practice, this means comparison mainly with bismuth molybdate in that no substantial studies have been reported on the tin/antimony system (however references 119 and 124 do deal with this system).

On this basis, considerable evidence exists that the reaction over indium oxide involves allylic attack on the propylene via oxygen removal of hydrogen. Dehydrogenation is certainly oxidative, since no free hydrogen could be detected among the reaction products. The reaction tended

to maintain the double bond and on the basis of bond dissociation energies (which indicate that the allylic C-H bond is weaker than most other C-H bonds by 15-20 kcal/mole (125)) attack of oxygen could be expected by H atom removal from the allyl position. Certainly attack on propylene involved a terminal position as neither the oxygen insertion reaction producing acrolein, nor the dimerization to hexadiene produced any evidence of attack in the central position.

Some differences occur in the kinetics of the reaction over indium oxide and bismuth molybdate in that the production of acrolein over indium oxide is fractional order in propylene and first order in oxygen (compared with the production of hexadiene where the rate is 0.38 order with respect to propylene and oxygen) while the rate of acrolein production is first order in propylene and zero in oxygen over bismuth molybdate. These differences can, however, be accounted for in terms of alternative rate determining steps.

Consequently it is reasonable to assume that oxidative attack involves a similar mechanism which - with regard to the extraction of an allylic hydrogen - bears many resemblances to the bismuth molybdate system (126):

$$C_3H_6 + Mo^{6+}O^{2-} + Bi^{3+} \rightarrow \{C_3H_5\text{-}Mo\}^{6+} + OH^- + Bi^{2+} \quad ....76$$

$$\{C_3H_5\text{--}Mo\}^{6+} + OH^- + O^{2-} + 3Bi^{3+} \rightarrow C_3H_4O + Mo^{6+} + H_2O + 3\,Bi^{2+} \quad ....77$$

It appears to be fairly certain that allylic attack is important in the system. A symmetrical molecule is known to be involved as an intermediate since carbon-14

labelling of the terminal group in the molecule showed that the carbonyl could arise equally from both ends of the molecule (127). The alternative route, involving allyl hydroperoxide C_3H_5OOH as an important intermediate (128), cannot involve such a symmetrical intermediate, and has been rejected - at least for the bismuth molybdate system.

It seems probable that allylic intermediates are also involved in the production of hexadiene from propylene over In_2O_3. Indium metal, which possesses 2s and 1p electrons in the outermost shells could possibly adsorb gas if it were present as an ion. With an appropriate gas such as an olefin, In^{3+} (with a d^{10} structure) should be suited for the formation of π bonds

$$CH_2=CH-CH_3$$
$$\downarrow$$
$$-O^{2-}-In^{3+}-O^{2-}- \qquad \ldots.78$$

Now, if π bond formation is followed by abstraction of a hydrogen to give OH^-_{ads}, an allylic species associated with a negative charge remains, and this charge should be transferred to the metal centre.

It seems unlikely, however, that this process will involve only one olefin molecule and therefore, when considering the design of the catalyst attention was directed at compounds that could oxidize or reduce in units of two, the In^{3+}-In^{1+} system fitting into this category. If charge transfer occurs, two possibilities seem tenable. Either two electrons may be transferred from the same molecule leaving

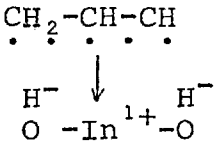

....79

or two molecules may be π bonded on the same centre, each donating one electron

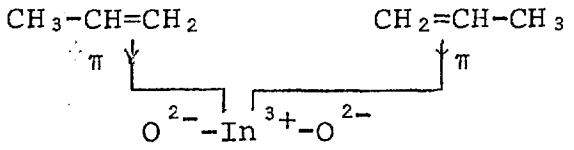

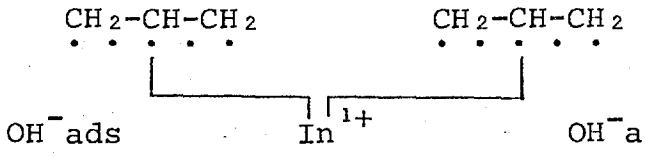

....80

The transfer of the second electron from the same molecule is known to be less easy than the first in the case of the oxidation of propylene to acrolein over bismuth molybdate. In addition it would be expected that the transfer of two electrons to In^{3+} should be fast, as In^{1+} is stable and In^{2+} has never been identified. Under these circumstances it seems plausible that reaction 80 above will be favoured.

If these species are formed in adjacent positions on the same ion, the species could well dimerize to produce 1,5 hexadiene

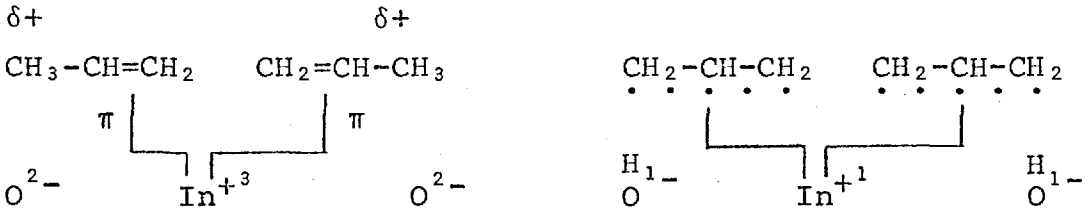

$$CH_2{=}CH{-}CH_2{-}CH_2{-}CH{=}CH_2 + In^{+1} \qquad ....81$$

The other possibility that an allylic intermediate could react with a gas phase propylene molecule does not seem likely in that any such attack would be expected to produce both branched and linear hexadiene.

After dimerization, the product would tend to be released from the In^{1+}-although possibly migrating to another In^{3+} centre - and the ion could be reoxidized.

$$In^{1+} + \tfrac{1}{2}O_2 \rightarrow In^{3+} + O^{2-} \qquad ....82$$

with the adsorbed hydroxyl ions reacting together to give water and an oxide ion.

Some support for this mechanism comes from the kinetic results. The low orders in oxygen and in propylene do show that adsorption of both components is strong, and - as shown in the next section - the results are consistent with the adsorption of two molecules on one site. This is also true of the kinetic results for the production of acrolein, although in this case the dependence of rate upon oxygen indicates that the gas is either weakly or not adsorbed. The energy of activation for the production of hexadiene (45.6 kcal/mole) was found to be higher than for acrolein (16.0 kcal/mole).

Some opposition to the concept that bismuth molybdate and indium oxide react in a similar fashion comes from a Russian study of the catalytic activity of oxides (122). Using patterns of selectivity of oxidative dehydrogenation and isomerization, they were able to characterise different groups of oxides where selective reaction only occurred over catalysts made up of an oxide from each of two groups. One group of oxides which showed no activity for oxidative dehydrogenation was found to be capable of selective isomerization and this was taken to indicate that the formation of the allyl intermediate is fast over these oxides (Mo, Sb, P, W. and V). The other group (oxides of Cd, Co, In, Bi, Cs, Sn and Mn) was apparently not capable of catalysing isomerization but showed a capacity for oxidation although mainly to carbon dioxide. This second group (which contains In_2O_3) possessed some activity for dehydrogenation but the low selectivity and lack of isomerization indicated that the formation of the allylic intermediate was very slow.

Closer inspection does show that these findings are not necessarily in opposition to the present experimental results. The production of hexadiene, which probably involves an allylic mechanism, is not favoured at low temperatures, and the high energy of activation indicates that the reaction is probably slow compared with the production of acrolein. This seems implausible unless acrolein is formed by a mechanism other than allylic abstraction.

There is some evidence to support this in that if the production of acrolein is via an allyl mechanism, the

sequence must involve the rapid donation of two electrons to the In^{3+} (to allow the preferred change to In^{1+}) a sequence which is not normally favoured:

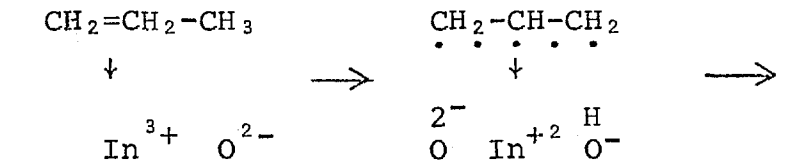

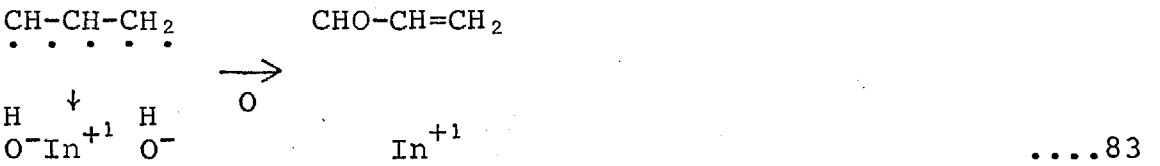

....83

On the other hand, it could be suggested that the acrolein originates via some other intermediate. Thus, for example, if π bonded ~~acrolein~~ propylene can be attacked by molecular oxygen to form an adsorbed hydroperoxide, then the surface complex could rearrange to give acrolein

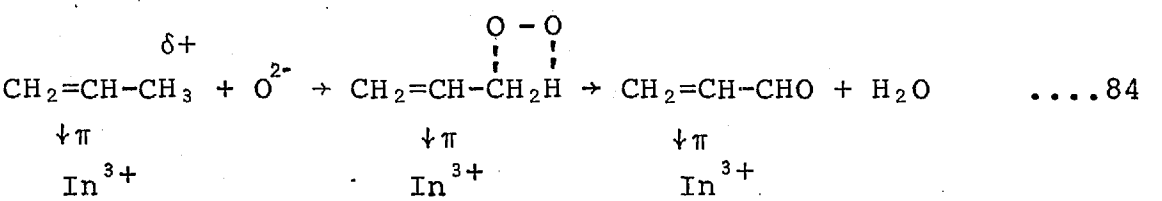

....84

In this case, no charge transfer to the In^{3+} occurs, and no allylic abstraction is involved. The reaction rate should depend upon the coverage of the surface by propylene and the pressure of gaseous oxygen and this is supported by the experimental observations. The activation energy could also be less than that of the unfavourable 2-electron transfer allylic route.

One sure way to test this contention would be by application of radiotracer techniques, as was used to support the allylic mechanism over the hydroperoxy route for bismuth molybdate (90). In the absence of these, the hydroperoxy mechanism does seem to be on balance more satisfactory at least mechanistically for the indium oxide catalyst.

To summarise, then, it seems possible that the mechanisms for acrolein and hexadiene formation involve the following elementary steps:

(1) Hexadiene

a) π adsorption of two propylene molecules at a In^{3+} site

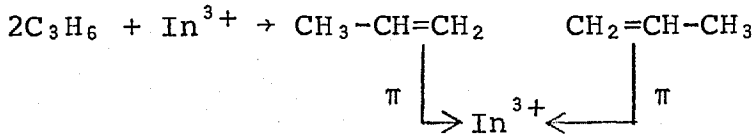

....85

b) initial hydrogen abstraction by oxygen ions produces two allylic species

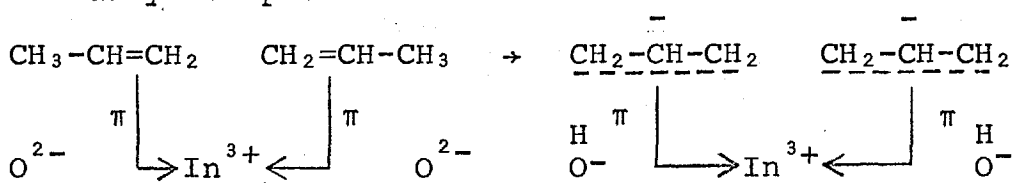

....86

c) the allylic species transfer one electron each to the In^{3+} and interact to form 1,5 hexadiene

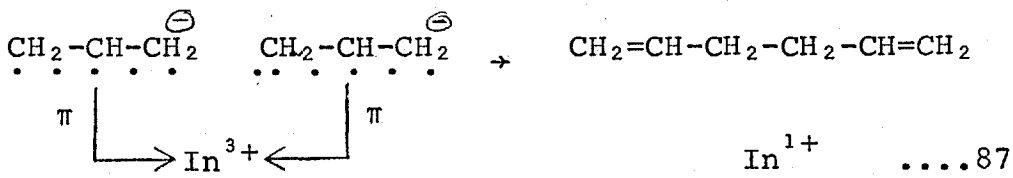

....87

d) the In^{1+} is reoxidized to In^{3+} by reaction with gas phase oxygen

$$2In^{1+} + O_2 \rightarrow 2In^{3+} + 2O^{2-} \quad \text{....88}$$

e) the hydroxyl species react to form water and a lattice oxygen

$$2OH^- \rightarrow H_2O + O^{2-} \quad \text{....89}$$

(2) Acrolein

a) the adsorbed propylene formed in step 1a can react with molecular oxygen to form an intermediate hydroperoxide species

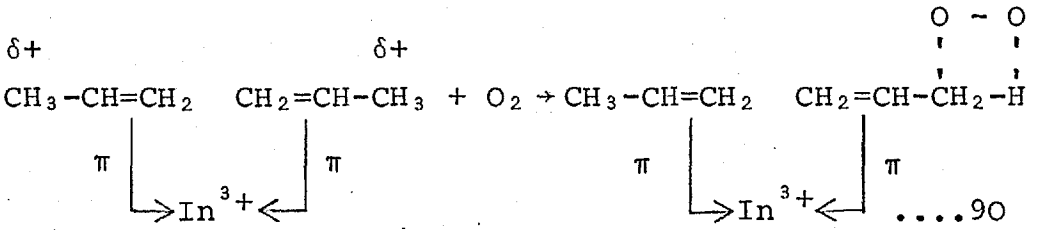

....90

b) this decomposes to form acrolein and water

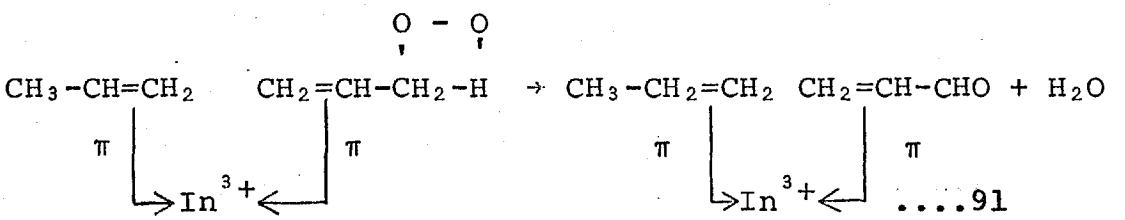

....91

(ii) <u>The chemical mechanism and kinetics</u>

Attempts were then made to ascertain whether the proposed mechanisms could satisfy the experimental observations on the kinetics of the reaction, by developing Langmuir-Hinshelwood expressions on the basis of the mechanisms and comparing the predicted results with experimental values.

Several rate expressions may be developed for a given mechanism, of course, since alternative reactions may be rate controlling.

A first attempt was made on the basis that the formation of the allylic intermediate, Reaction 86, is the slow step, since results available for the butene systems (122) show that this could be rate determining over In_2O_3. The rate of formation of an allylic species will be

$$r = k\ \theta p\ \theta o \qquad \ldots.92$$

However the formation of two allylic intermediates must occur simultaneously because of the electron transfer requirement and the reaction must take place between two propylene molecules and two oxygen monatomic ions; the expected rate expression then becomes:

$$r = k\ \theta p^2\ \theta o^2 \qquad \ldots.93$$

which for surface competition becomes:

$$r = \frac{k(KpCp)^2\ (\sqrt{KoCo})^2}{(1 + KpCp + \sqrt{KoCo})^4} \qquad \ldots.94$$

on application of the full Langmuir Hinshelwood treatment.

This expression is consistent with the results of the hexadiene, but in the case of acrolein the observed rate law was found to be first order in oxygen. If oxygen competes with propylene for the active sites, then a rate expression such as

$$r = \frac{k(KpCp)^x\ Co}{(1 + KpCp + \sqrt{KoCo})^x} \qquad \ldots.95$$

should represent the experimental rates, and this can be rearranged to yield

$$\left[\frac{Co}{r}\right]^{1/x} = \frac{1 + KpCp + \sqrt{KoCo}}{k^{1/x}\ KpCp} \qquad \ldots.96$$

If the above expression represents the results, a plot of $(Co/r)^{1/x}$ versus $\sqrt{Co}$ should yield a straight line and the value of $\sqrt{Ko}$ can be calculated from the expression

$$\text{slope} = \sqrt{Ko}/(k^{1/x}\ KpCp) \qquad \ldots.97$$

However, the division of the oxygen concentration by the experimental rate yields a constant value of 81.0 and, whatever the value of x, the slope is zero showing that Ko is zero. Consequently there was no competition for active sites and the above expression 94 does not hold.

Values of Ko obtained below (Ko = 560 litre/mole) were substituted into equation 97. If the $\sqrt{KoCo}$ term is important then the rates of reaction change by up to 10%. This could easily be seen experimentally if any such effect was important. The conclusion emerges then that oxygen does not compete with propylene for active sites, even though the kinetic results for the production of hexadiene are satisfied by an expression derived on the basis of such competition.

Several alternatives were then examined, including the possibility that propylene and oxygen compete for different sites. Under these circumstances (Introduction section 2Bi) application of Langmuir-Hinshelwood theory to the rate expression 93 above gave the result

$$r\ \text{hexadiene} = \frac{k(KpCp)^2\ \ (\sqrt{KoCo})^2}{(1 + KpCp)^2\ \ (1 + \sqrt{KoCo})^2} \qquad \ldots.98$$

which can be rearranged to give

$$\frac{1}{\sqrt{r}} = \frac{(1 + KpCp)\ (1 + \sqrt{KoCo})}{\sqrt{k}\ (KpCp)\ (1 + \sqrt{KoCo})}$$

Plots of $Cp/\sqrt{r}$ vs Cp at constant Co and $\sqrt{Co}/\sqrt{r}$ vs $\sqrt{Co}$ at constant Cp were found to be linear for the results obtained for hexadiene (Figure 80) and values of the slope and intercept were used to calculate values of $k = 3.42 \times 10^{-5}$ moles/gm sec, Kp = 620 litres/mole and Ko = 560 litres/mole respectively. These large values confirm that both propylene and oxygen are adsorbed on the surface with high surface coverage. From the proposed mechanism over thallium oxide it can be concluded that propylene is adsorbed on an oxidized site (In^{3+}) and oxygen on a reduced site (In^{1+}).

Subsequent attempts have been made to fit a variety of expressions to the results without recourse to chemical arguments. Satisfactory agreement could only be obtained with equations of the type

$$r = \frac{k(KpCp)^x\ (\sqrt{KoCo})^2}{(1 + KpCp)^x\ (1 + \sqrt{KoCo})^2} \qquad \ldots.99$$

where x was 1, 2 or 3. Since this would indicate that the number of propylene entities involved in the rate determining step was 1, 2 or 3, it seems very likely, on chemical grounds, that x = 2 gives the most satisfactory explanation. This is borne out by studies at longer contact times (see below). Langmuir-Hinshelwood expressions, derived on the basis of other reactions in the mechanism proposed for the formation of hexadiene being rate determining did not fit the experimental results.

FIGURE 80

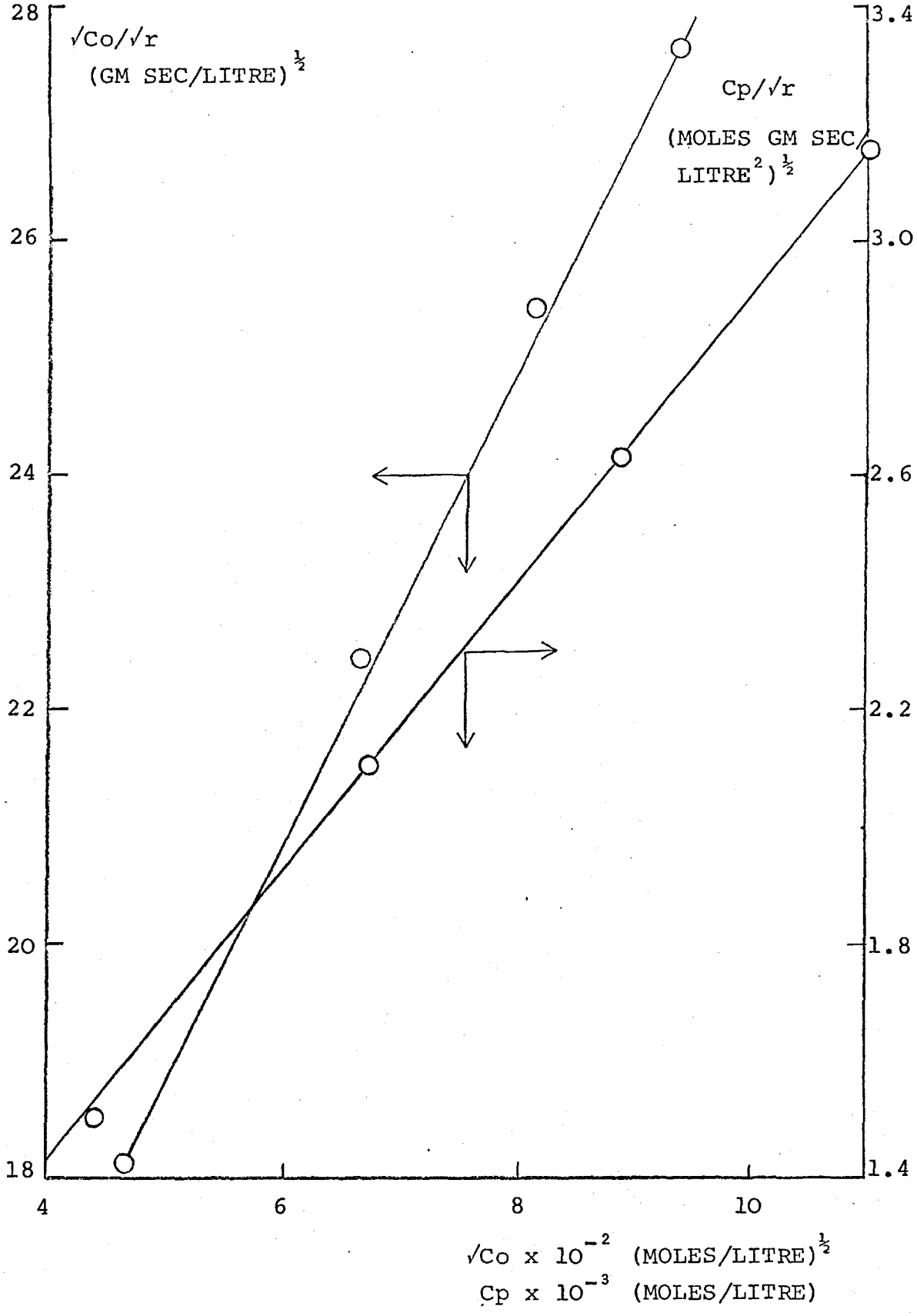

Plots of the Langmuir-Hinshelwood expression

$$r = \frac{k(KpCp)^2 (\sqrt{KoCo})^2}{(1 + KpCp)^2 (1 + \sqrt{KoCo})^2}$$

Similar studies were carried out for the production of acrolein, where the rate expression

$$r = k\ \Theta p\ Po \qquad \ldots.100$$

may be predicted from the hydroperoxide mechanism. In this case, the rate of formation of acrolein should be:

$$\text{rate acrolein} = \frac{k\ KpCp\ Co}{1 + KpCp} \qquad \ldots.101$$

The plot of Cp/r versus Cp at constant Co resulting from rearrangement of equation 101 gives a straight line (Figure 81) and the values of $k = 1.87 \times 10^{-2}$ litre/gm sec and Kp = 225 litre/mole can be calculated. This value of Kp when compared with that calculated for hexadiene appears to indicate that the modes of adsorption of propylene for the two reactions were different, which is not compatible with the proposed reaction mechanism.

Attempts were made to fit the experimental results with other theoretically derived equations. Amongst many expressions, a rate equation

$$r_{acrolein} = k\ \Theta p^2\ Po_2 \qquad \ldots.102$$

was used, which can be resolved to

$$r = \frac{k\ (KpCp)^2\ Co}{(1 + KpCp)^2} \qquad \ldots.103$$

This can be rearranged to give

$$\frac{1}{\sqrt{r}} = \frac{(1 + KpCp)}{\sqrt{k}(KpCp)\ \sqrt{Co}} \qquad \ldots.104$$

FIGURE 81

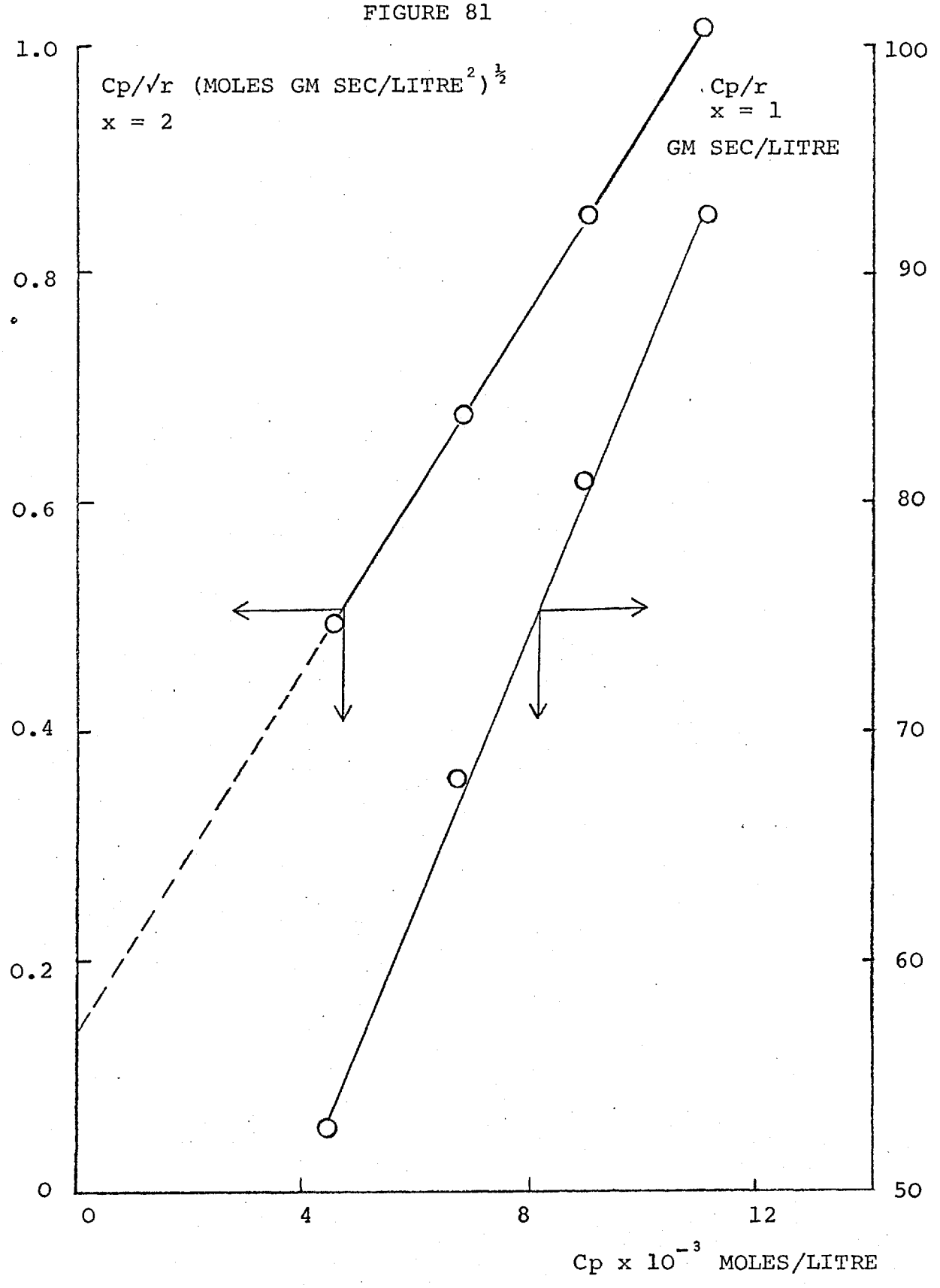

Plots of the Langmuir-Hinshelwood expression

$$r = \frac{k(KpCp)^{x}Co}{(1 + KpCp)^{x}}$$

whence it should be possible to reproduce the experimental results by plotting $Cp/\sqrt{r}$ versus Cp at constant Co. If the equation 103 could represent the reaction kinetics, a straight line plot should and does result (Figure 81). The values of k and Kp are calculated as 1.76×10^{-2} litre/gm sec and 615 litre/mole respectively. This value of Kp is the same as the value calculated from the rate expression representing the hexadiene formation, indicating, if correct, that both reactions occur on the same site and involve the same mode of adsorption of propylene.

The satisfactory application of the Langmuir-Hinshelwood arguments to the proposed mechanism is a necessary but not sufficient condition for acceptance of the mechanism. The arguments can, in certain cases, apply equally well to other mechnaisms, and it is necessary then to consider other information. In this way, other bases for theoretical equations tested and rejected included: adsorption of propylene or oxygen controlling, desorption of acrolein or hexadiene controlling, reaction of gaseous or physically adsorbed propylene with either gaseous or adsorbed oxygen controlling, reaction of dissociated propylene with oxygen controlling and many more, most of which could be eliminated by a quick comparison with the experimental kinetic equations.

To summarise then, the suggestion that the production of hexadiene invòlves the reaction of two allylic adsorbed species satisfies the experimentally observed kinetic

expressions. The production of acrolein appears to be more complex as the kinetic expression developed by Langmuir-Hinshelwood arguments from the proposed hydroperoxy mechanism was shown to be apparently incompatible with the experimental kinetics. The experimental rates agree with a model assuming a θp^2 dependency, and the value of the adsorption coefficient calculated from this comparison show that this is probably correct. This was confirmed by comparison of the kinetic expression with the product inhibition studies, discussed in the following section.

If this kinetic expression is correct then the compatibility of the mechanism and the kinetics may only be explained by the assumption that two propylene molecules are adsorbed on the indium centre. This gives additional support to the proposed hexadiene mechanism, but raises doubts concerning the hydroperoxy mechanism, even though this scheme satisfies the mechanistic observations.

4B. Secondary reactions and product inhibition

At long contact times (up to 175 gm sec/litre) two products reappeared that had been previously observed only over the pure catalyst, namely carbon dioxide and benzene. It is probable that the formation of benzene occurs as a secondary reaction involving hexadiene but carbon dioxide can originate from numerous routes.

The overoxidation of hexadiene was studied under various conditions and found to give benzene and carbon

dioxide. Attempts were made to discover whether the reaction occurred on the catalyst, by studying the homogeneous overoxidation at high concentrations of hexadiene (4.5×10^{-3} moles/litre). 6.0×10^{-5} moles/litre benzene were obtained from the reaction, but the heterogeneous overoxidation of hexadiene, at the same conditions, yielded 11.5×10^{-5} moles/litre benzene. By subtraction, the actual heterogeneous reaction yielded only 5.5×10^{-5} moles/litre of benzene, which is approximately the same yield (5×10^{-5} moles/litre) as obtained from the propylene reaction at the same contact time, even though the hexadiene concentration in the latter case was a factor of 500 smaller. However, if the amount of hexadiene adsorbed on the catalyst is constant, this result is explicable and the rate of formation of benzene is approximately independent of the gas phase concentration of hexadiene.

The rate expression for the formation of benzene, obtained from the studies at long contact times (Figures 74 and 76), was found to be

$$\text{rate benzene} = 1.85 \times 10^{8}\ e^{-\frac{45.5}{RT}}\ C_H^{0.08}\ C_O^{0.37} \qquad \ldots.105$$

The high activation energy, which is the same as for the formation of hexadiene supports the conclusion that benzene comes from hexadiene. The homogeneous rates of formation of benzene and carbon dioxide were actually first order in hexadiene and should not be of significance under normal conditions.

The production of carbon dioxide is much more complex and can originate from several sources. Benzene

was shown to oxidize only to a limited extent (<3%) even under severe conditions (Results: section 6D) and the overoxidation of benzene must contribute very little to the carbon dioxide yield. Several other possibilities may be more important including the direct oxidation of propylene, the overoxidation of acrolein and the combustion of hexadiene.

Considering the direct oxidation from propylene, it is possible to correlate the initial rates of carbon dioxide formation (Figure 77) with the propylene concentration change at 460°C. This yielded an approximate order in propylene of 0.35 which could indicate that the oxidation involved the same bonding for propylene as is involved in the initial reactions. The oxygen order, calculated from the 440°C data, was found to be 0.49 and this would indicate that any such direct oxidation involves a dissociated oxygen species which is weakly adsorbed. Since the results for hexadiene indicated that the dissociatively adsorbed oxygen was strongly bonded to the surface (Ko = 560), the kinetic laws obtained by assuming that all of the carbon dioxide arises by the direct oxidation route from propylene are incorrect.

The observed activation energy of 18 kcal/mole for the production of carbon dioxide supported the assumption that the overoxidation of hexadiene (E_A = 45.6 kcal/mole) led mainly to the production of benzene (E_A = 45.5 kcal/mole) and although combustion to carbon dioxide occurred, the reaction was of secondary importance. On the other hand the present results show that the overoxidation of acrolein

(Figure 75) must be responsible for at least some of the dioxide especially at 460°C. Acrolein is known to oxidise to carbon dioxide, both homogeneously (123) and heterogeneously (129). However, the rate of production of carbon dioxide could not be correlated satisfactorily with either propylene or acrolein in total and the kinetic reaction path must be a combination of both routes.

It is tempting to suggest that an estimate of the importance of overoxidation can be obtained from plots of yield vs time, but an alternative explanation of the shape of these graphs can be advanced in terms of the inhibition of the oxidation of propylene by products. This suggestion was tested by the addition of hexadiene, acrolein and benzene to the reagent stream (section 6F) from which it was found that the two former products, but not the latter, inhibited the oxidation of propylene.

Another diolefin, butadiene, was also shown to have an inhibiting effect on the rates of production of both acrolein and hexadiene. Inhibition of the oxidation of olefins by diolefins and aldehydes has been reported previously (88), the inhibition by the products increasing with an increase in the number of carbon atoms in the molecule. Inhibition is seen mainly as a reduction in the activity, with no essential change in the selectivity of the catalyst.

The results show, then, that benzene arises almost entirely from the overoxidation of hexadiene, that acrolein and hexadiene inhibit the initial reaction and that carbon

dioxide may arise from many sources. A satisfactory reaction network can be proposed

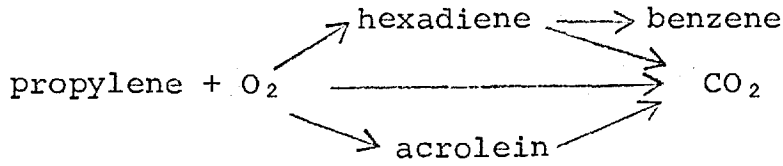

(i) The chemical mechanism and the kinetics

Investigation of the kinetics of such a network represents a major problem in the presence of product inhibition, involving reagent streams consisting of mixtures of propylene, oxygen and products. Attempts were made to do this, even though this is probably not justified at this stage of the catalyst design. This was unsuccessful since it proved impossible to feed accurately known amounts of acrolein to the reactor (Results section 6F). However, considerable advances can be made by the application of the Langmuir-Hinshelwood arguments to the results obtained under various conditions, particularly in the context of the effect of hexadiene concentration on the yield of acrolein (Table 21).

As the hexadiene inhibited the production of acrolein, the hexadiene must compete with the propylene for active sites. The fact that butadiene inhibits both reactions confirms that the products are competing for active sites that adsorb propylene. Under these conditions, the Langmuir-Hinshelwood rate expressions derived previously, may be modified for associative adsorption of products to give

$$r \text{ acrolein} = \frac{k'(KpCp)^2 Co}{(1 + KpCp + K_H C_H + K_A C_A)^2} \quad \ldots.106$$

$$r \text{ hexadiene} = \frac{k(KpCp)^2 (\sqrt{KoCo})^2}{(1 + KpCp + K_H C_H + K_A C_A)^2 (1 + \sqrt{KoCo})^2} \quad \ldots.107$$

The rate expression for acrolein can be rearranged to give:

$$\frac{1}{\sqrt{r}} = \frac{1 + KpCp + K_H C_H + K_A C_A}{\sqrt{k'}(KpCp)\sqrt{Co}} \quad \ldots.108$$

Considering the above expression in the context of the experimental results obtained in the study of the inhibition of acrolein formation by hexadiene, approximate values for the adsorption equilibrium coefficients of acrolein and hexadiene can be calculated if the known values of Kp, Ko, k and k' are inserted.

The rates of production of acrolein were calculated for the highest three concentrations of hexadiene by dividing the yield by the contact time. The effects at the lowest two values of hexadiene were ignored as the concentration of hexadiene produced in the reaction would be appreciable and variant. Then if $1/\sqrt{r}$ is plotted versus C_H, a linear plot is obtained, (Figure 82) whence, by substituting the values of the slope, Kp, k', Cp and Co into the expression a value of 3.28 x 10^4 litre/mole for the adsorption equilibrium coefficient of hexadiene can be calculated. The comparison of this value with the value of 620 litre/mole for propylene indicates the strength of the inhibition by hexadiene.

FIGURE 82

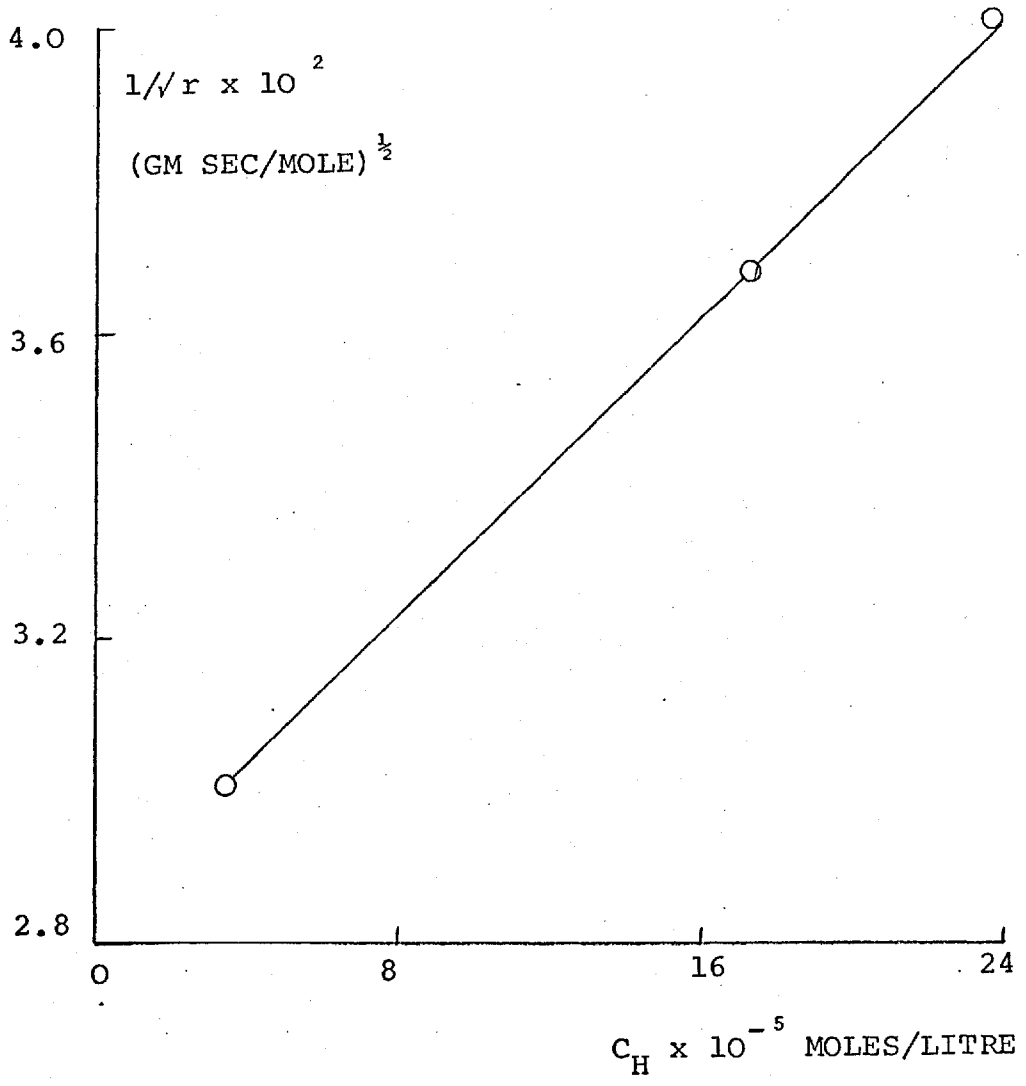

Plot of the Langmuir-Hinshelwood expression

$$r \text{ acrolein} = \frac{k'(KpCp)^2 \, Co}{(1 + KpCp + K_H C_H + K_A C_A)^2}$$

A value of $K_A C_A$ can also be calculated from the expression and if the three sets of data points are plotted in terms of the concentration of acrolein obtained at various values of hexadiene, the approximate value of 2.74×10^{-5} moles/litre acrolein can be determined by extrapolation to a hexadiene concentration of zero. Substituting this value into the value of $K_A C_A$ calculated from equation 108, a value of 4.72×10^{5} litre/mole for the adsorption equilibrium coefficient of acrolein can be calculated. Thus the inhibition by acrolein is apparently even stronger than by hexadiene.

The values of the adsorption equilibrium coefficients for hexadiene and acrolein are, of course, only approximate as (a) C_A was assumed constant when K_H was calculated and (b) the value of C_A at $C_H = o$ had to be estimated for the calculation of K_A. If equation 108 is rearranged to give the following relationships:

$$\sqrt{k(KpCp)}\sqrt{Co}/\sqrt{r} - K_A C_A = 1 + KpCp + K_H C_H \quad \ldots.109$$

$$\sqrt{k(KpCp)}\sqrt{Co}/\sqrt{r} - K_H C_H = 1 + KpCp + K_A C_A \quad \ldots.110$$

a more exact approximation for K_H and K_A may be obtained though an iterative method by successively determining K_H and K_A by plotting the left hand side of equations 109 and 110 against C_H and C_A respectively until both adsorption equilibrium coefficients approach constant values. The final values so obtained were 6.5×10^{4} litre/mole for hexadiene and 5.25×10^{5} litre/mole for acrolein.

Thus, the interpretation of the Langmuir-Hinshelwood equations 106 and 107, which have been shown to fit the

inhibition data, show that the hexadiene and acrolein compete with the propylene for π bonded adsorption on the In^{3+} sites. The strength of adsorption for each varies as:

acrolein > hexadiene >> propylene 111

The expressions for surface coverage:-

$$\theta_p = \frac{620\ C_p}{1 + 620\ C_p + 65000\ C_H + 525000\ C_A} \quad ....112$$

$$\theta_H = \frac{65000\ C_H}{1 + 620\ C_p + 65000\ C_H + 525000\ C_A} \quad ....113$$

$$\theta_A = \frac{525000\ C_A}{1 + 620\ C_p + 65000\ C_H + 525000\ C_A} \quad ....114$$

clearly show how even small amounts of hexadiene and acrolein can decrease the surface concentration of propylene and hence inhibit the overall oxidation. Thus, for example, the surface coverage of propylene at a concentration of 10^{-2} moles/litre in the absence of products is 0.86; in the presence of only 1.4×10^{-5} moles/litre acrolein and hexadiene, the surface coverage of propylene drops to 0.40.

The order of the strength of adsorption (acrolein > hexadiene >> propylene) is similar to observations obtained with oxidative dehydrogenation catalysts where dienes were found to be moderately strong and aldehydes were very strong inhibitors (130). It is well known that the strength of inhibition increases with carbon number which probably accounts for the adsorption equilibrium coefficients for hexadiene and acrolein differing by less than an order of magnitude.

Langmuir-Hinshelwood expressions have been developed for other proposed mechanisms and tested against experimental

results. Particular attention has been paid to possible alternative modes of adsorption of reagents or products. In the first instance an attempt was made to elucidate the kinetics of production of acrolein. Studies of initial rates could not distinguish between rate laws based on a dependency on adsorbed propylene of one or two.

If product inhibition is important, the rate expression for the direct dependence becomes

$$\text{rate acrolein} = \frac{k(KpCp)Co}{1 + KpCp + \Sigma \text{ products}} \qquad \ldots.115$$

and attempts were made to fit this to the results. Satisfactory agreement could not be observed even though the following conditions were used:

(1) acrolein and hexadiene associatively adsorbed

(2) acrolein and hexadiene dissociatively adsorbed

(3) acrolein dissociatively and hexadiene associatively adsorbed

(4) acrolein associatively and hexadiene dissociatively adsorbed

Subsequently, attempts were made to fit the results to a square dependence. In this case, the rate expression becomes

$$r = \frac{K(KpCp)^2 Co}{(1 + KpCp + \Sigma \text{ products})^2} \qquad \ldots.116$$

Consideration of the possibility of the products both dissociatively adsorbed did not give a good fit. However, the Langmuir-Hinshelwood expression for the adsorption of acrolein dissociatively and hexadiene associatively

$$\text{rate acrolein} = \frac{k'(KpCp)^2 Co}{(1 + KpCp + K_H C_H + \sqrt{K_A C_A})^2} \quad \ldots.117$$

gave quite a good fit with the experimental results. By the iterative procedure described above for the associative adsorption of acrolein and hexadiene, values of 5.1×10^4 and 6.0×10^6 litre/mole for K_H and K_A respectively were calculated and the final fit of this expression (equation 117) with respect to acrolein concentration is shown in Figure 83.

A comparison of the quality of this fit with the final fit with respect to acrolein concentration of the expression (equation 106) for associative adsorption of acrolein (Figure 84) shows that the expression arising from associative adsorption of acrolein (equation 106) is possibly a better fit than that obtained for dissociative adsorption. It was not possible to obtain a clear differentiation because of the restricted range of concentration that could be studied.

No other theoretically derived equation gave as good a fit to the experimental results. Chemical reasoning tends to support the concept that both products are adsorbed associatively. Associative π bonding of hexadiene to an In^{3+} site seems highly probable, and the adsorption should be strong since the carbon number of the diolefin is large (130). Since propylene and hexadiene are associatively bonded and acrolein competes with both for the same sites, it seems likely that the acrolein is also associatively adsorbed. In^{3+} is capable only of π complexing and does not tend to form σ bonds (5) and it seems likely that acrolein will be adsorbed associatively via a π bond involving the double bond.

FIGURE 83

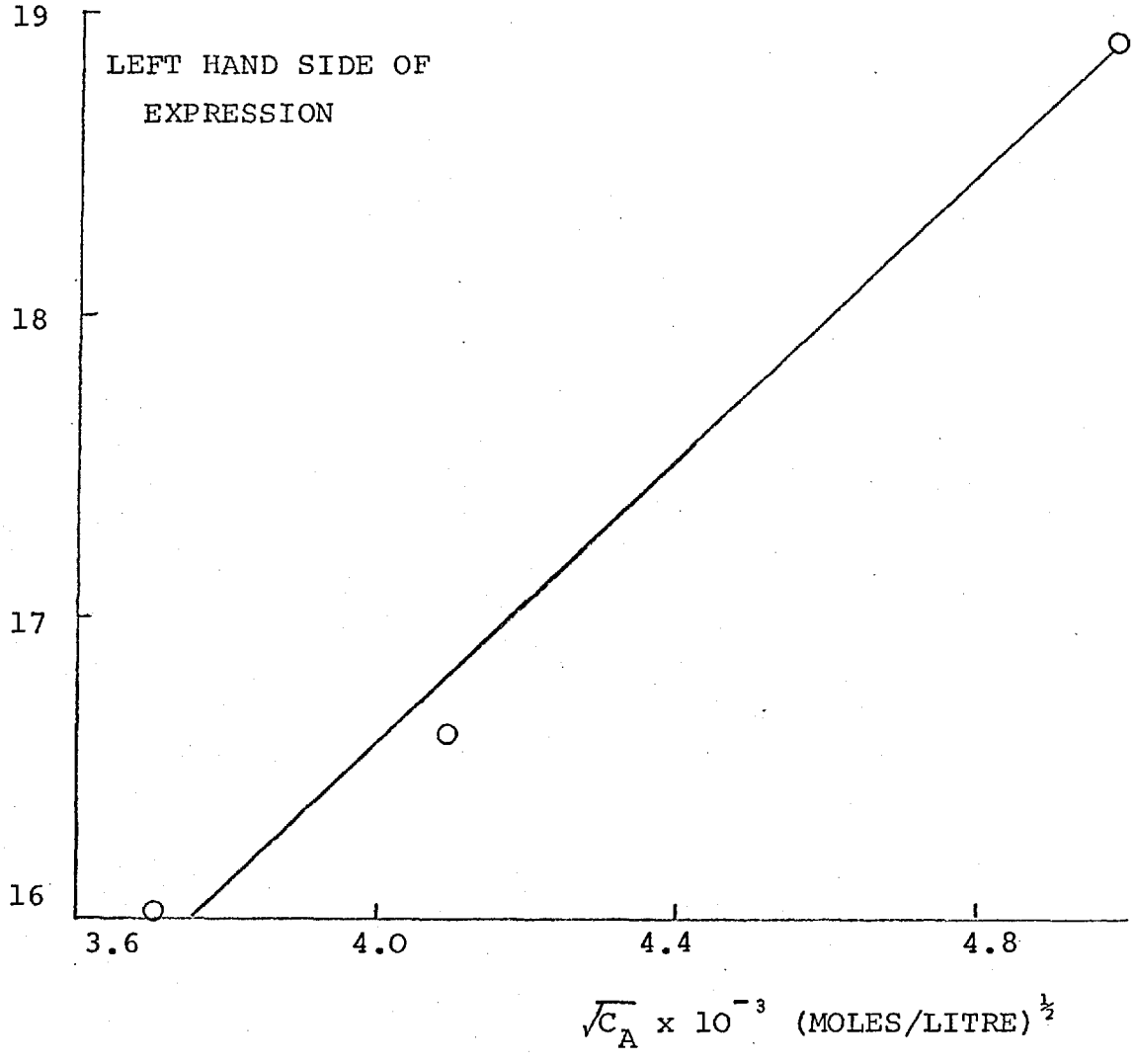

Plot of the left hand side of the expression

$$\frac{(k'(KpCp)^2 Co)^{\frac{1}{2}}}{\sqrt{r}} - K_H C_H = 1 + KpCp + \sqrt{K_A C_A}$$

versus $\sqrt{C_A}$

FIGURE 84

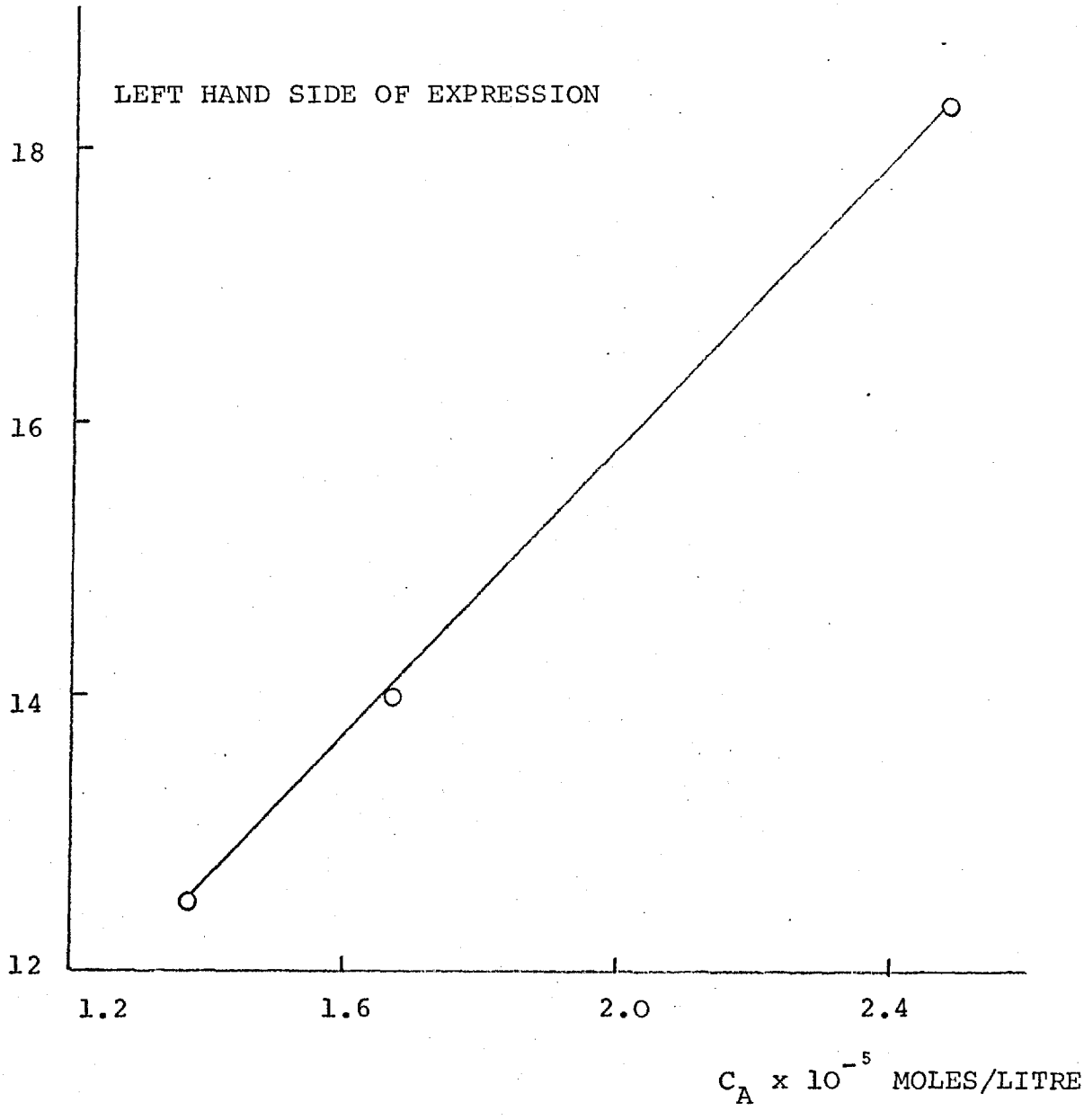

Plot of the left hand side of

$$\frac{(k'(KpCp)^2Co)^{\frac{1}{2}}}{\sqrt{r}} - K_HC_H = 1 + KpCp + K_AC_A$$

versus C_A

The proposed reaction path for the production of benzene via hexadiene appears to be correct. Benzene was not an initial product of any importance and the reaction of hexadiene and oxygen in the absence of propylene produces benzene. Consequently it seems likely that benzene was not produced directly from propylene but via hexadiene. However, the experimentally observed power rate law for benzene was shown to be relatively independent of hexadiene or propylene ($C_H^{0.08}$ or $C_p^{0.04}$) and this kinetic observation must be shown to be compatible with any mechanistic proposal.

A comparison of the dependence on oxygen of the rate of production of hexadiene and benzene showed that the slow step in the benzene formation involves a double monatomic oxygen ion attack. As the slow step must involve two hydrogen abstractions the cyclization step can be arranged reasonably in only three ways:

hexadiene → cyclohexene → cyclohexadiene → benzene

or

hexadiene → hexatriene → cyclohexadiene → benzene

or

hexadiene → cyclohexadiene → benzene

Of the possible intermediates, hexatriene and cyclohexadiene were detected in significant amounts while no cyclohexene has been found. As a result, the first alternative seems unlikely, but either of the other routes seem plausible. In both cases the rate determining step in the reaction must be very early in the sequence. The ratios of the concentration

of hexatriene or cyclohexadiene to hexadiene was not compatible with, for example, fast dehydrogenation to hexatriene. fast cyclization and slow dehydrogenation to benzene.

It is possible to suggest a reasonable chemical mechanism for the reaction via hexatriene. The diolefin is known to be π adsorbed associatively on In^{3+} and hydrogen abstraction may occur quickly at the middle two carbons.

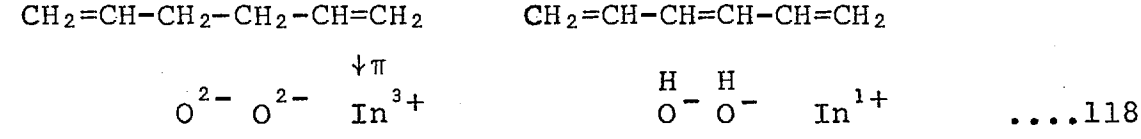

....118

A similar reaction of butene to butadiene has been shown to occur over In_2O_3 (122); although, the reaction was found to be unselective (30% of reacted butene to butadiene).

There are, however, several points of argument with such a scheme. Thus, for example, the selectivity of the hexadiene reaction compared with the butene reaction argues against the sequence. Again, the sequence presupposes that two oxide ions are placed favourably to receive hydrogen ions (which is unlikely) and that sequential transfer of two electrons must occur. As discussed above, this seems unlikely in the In^{3+}-In^{1+} system. Again, there seems no reason why a propylene molecule should not π bond to the spare orbital on the In^{3+}, transfer an electron at the same time as the hexadiene donates its first electron and result in the formation of the trimer. Since no polymer other than the dimer was detected, the conclusion that the mechanism above cannot be correct receives support.

The third alternative does appear to be mechanistically satisfying. It is known that metal ions with a d^{10} electronic

structure are capable of monodentate and bidentate adsorption of olefins (5). It can then be suggested that hexadiene then becomes bidentally π adsorbed on In^{3+}, from which intermediate the rapid donation of two electrons and the formation of observed the experimentally/1,3 cyclohexadiene is possible

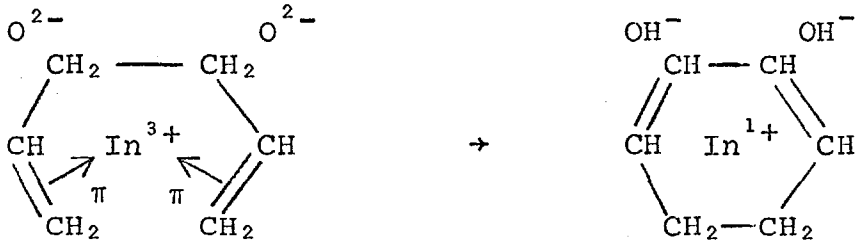

....119

Although this reaction sequence seems most probable on mechanistic grounds, at first glance it is difficult to reconcile the mechanism with the experimental kinetic results. Thus the inhibition studies showed that hexadiene was adsorbed associatively as a monodentate ligand. The most plausible explanation would seem to be that a hexadiene monodentate - bidentate equilibrium exists on the surface. For a sequence such as

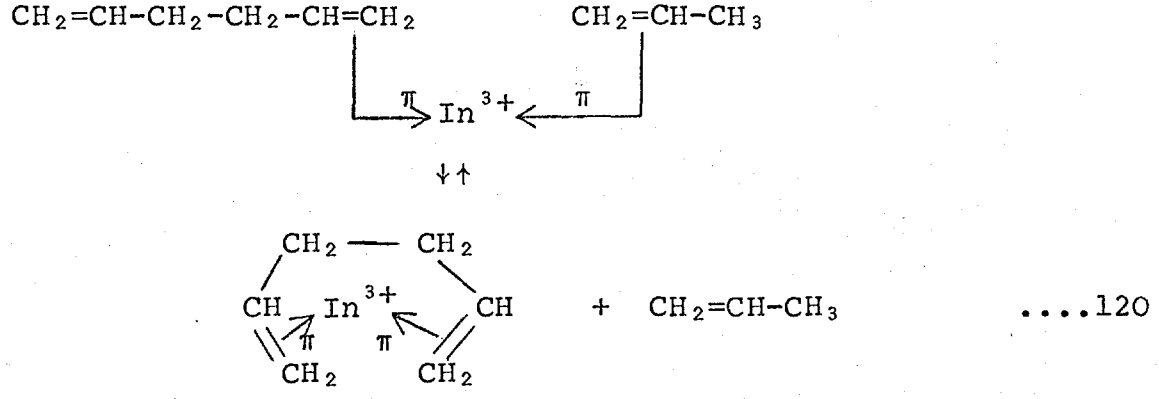

....120

the equilibrium would probably favour the monodentate form as there would be steric hindrance to the formation of the

bidentate. In the dimerization reaction the double bond positions in the two adsorbed propylene have been suggested to be arranged adjacently:

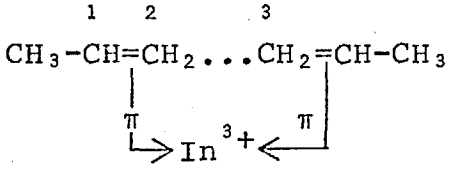

....121

In this case, the 1,5 hexadiene would probably have to form a near circle in order to position the double bonds correctly

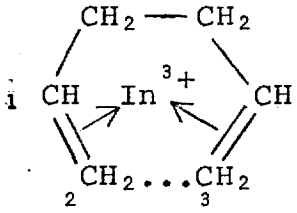

....122

In this event, it would not be unexpected to find that the majority of the hexadiene is present as a monodentate ligand. Once the bidentate ligand was formed, however, the subsequent reaction would appear to be independent of the concentration of hexadiene in the gas phase, since the bidentate ligand should be very firmly adsorbed. In this event, if the formation of the allylic intermediate is rate controlling, the rate of reaction should be independent of the concentration of propylene or hexadiene and should be a function of the concentration of adsorbed oxygen ions, as is observed experimentally. The 1,3 cyclohexadiene should easily re-adsorb on In^{3+} and dual hydrogen abstraction by lattice oxygen could occur. This would be expected to be faster than the first hydrogen abstraction as a result of the energy gained by the stability of the benzene ring.

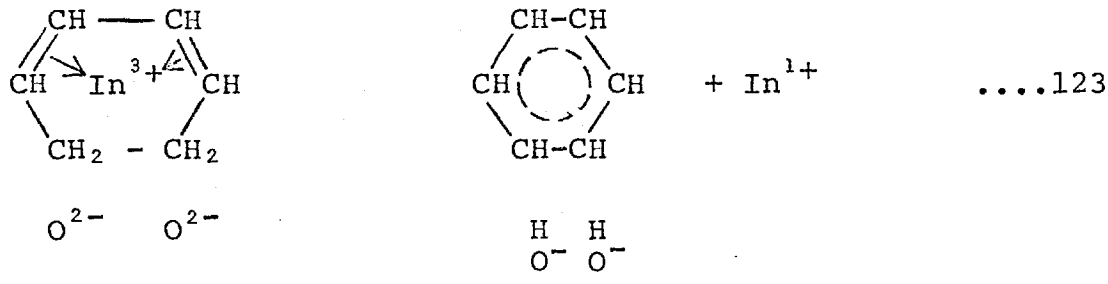

....123

Thus, this mechanism accounts for a) the oxygen dependency of 0.37, b) the fact that the rate is independent of the gas phase concentration of organics, c) the fact that the activation energy of the reaction (45.5 kcal/mole) is very similar to that for the production of hexadiene (45.6 kcal/mole), d) the requirement of two electrons being transferred simultaneously, e) the fast cyclization step and f) the appearance of 1,3 cyclohexadiene as a product.

The determination of the relative importance of the various possible reactions which could produce carbon dioxide becomes more complex in the presence of severe product inhibition. Thus the surface coverage varies between 0.9 and 1.0 during the reaction and the chance of the surface species overoxidising to carbon dioxide is high. Any such reaction of surface adsorbed species is difficult to recognise and very difficult to quantify.

It seems probable that the carbon dioxide is not originating directly from propylene. The conditions of study were necessitated by the importance of homogeneous reactions at higher temperatures and the conversion of propylene was comparatively low. However, at the higher temperatures associated with development studies over pure indium oxide

the reaction was very selective (65% selectivity of reacted propylene to desirable products), and it seems highly unlikely that the homogeneous total oxidation would be important under the milder conditions.

A decrease of selectivity at lower temperatures is not unexpected, however, since under these conditions the adsorption equilibrium coefficients are large and the surface coverage is high, resulting in a large yield of carbon dioxide from overoxidation of adsorbed species. At high temperatures the adsorption equilibrium coefficients would be expected to be smaller and the surface coverage (and inhibition of the reaction) decreases. Consequently, the amount of dioxide produced from adsorbed species should be less, and although some should be produced from the acrolein (probably homogeneously, as no significant yields of acrolein were found) the overall selectivity increases. The instability of acrolein with respect to overoxidation above 400^{o}C has been previously reported (123). The high selectivity to hexadiene and benzene even under the unfavourable condition of a highly porous catalyst is a reflection of the selectivity of the initial reactions in that the activation energies for acrolein and hexadiene are 16.0 and 45.6 kcal/mole respectively.

The kinetics and the mechanism of the reaction are very complicated as a result of severe product inhibition. Ideally, the effect of the inhibition could be determined in more detail by studying the effects of the addition of acrolein and hexadiene to the reagents. The adsorption coefficients (Kp, Ko, K_H, K_A) and rate constants are known

to vary with temperature, and need to be determined before a completely satisfactory model can be developed. It is interesting to note, however, that any such model cannot be based upon the simple power rate laws in that any such model cannot account for effects such as inhibition. However, this situation may change at higher temperatures where the inhibition is not so important.

5. Reaction engineering

5A. Introduction

Further development of the catalytic system requires optimization of the reaction conditions for the production of the desired products and the design of a reactor to achieve these optima. Both of these conditions require a mathematical model which describes the reaction, the validity of which must be tested against the experimental results available. This may conveniently be done by comparing experimental product-time curves, at various conditions with the values obtained by integration on a computer of the rate expressions associated with the reaction network. Of course, the complete design of a reactor should include heat and mass transfer effects, and this is a complex and involved problem which cannot be tackled at this stage of the design. Attention has been focused then on developing an adequate model of the chemical reactions and using any information so obtained to recycle back to earlier stages in the catalyst design.

5B. The original model

A simple mathematical model can be derived from chemical and kinetic studies as discussed above:

hexadiene → benzene
↑
propylene → carbon dioxide
↓
acrolein

where the mathematical expressions for the rates of production of products are related to the gas phase concentrations by the following equations:

$$r_{\text{hexadiene}} = 3.42 \times 10^{-5}\{620\ Cp\ (1-\theta HC)\}^2\{\sqrt{560\ Co}\ (1-\theta OX)\}^2 - 2.9 \times 10^{-6}\ C_H^{0.08} Co^{0.37} \quad \ldots.124$$

$$r_{\text{benzene}} = 2.9 \times 10^{-6}\ C_H^{0.08}\ Co^{0.37} \quad \ldots.125$$

$$r_{\text{acrolein}} = 1.76 \times 10^{-2}\{615Cp(1-\theta HC)\}^2\ Co \quad \ldots.126$$

$$r_{\text{carbon dioxide}} = 5.3 \times 10^{-2}\ CpCo^{0.64} \quad \ldots.127$$

θHC and θOX are the surface concentrations of hydrocarbons and oxygen respectively, with

$$\theta HC = \frac{620\ Cp + 65000\ C_H + 525000\ C_A}{1 + 620\ Cp + 65000\ C_H + 525000\ C_A} \quad \ldots.128$$

and

$$\theta OX = \frac{\sqrt{560\ Co}}{1 + \sqrt{560\ Co}} \quad \ldots.129$$

The relative importance of the different routes to carbon dioxide could not be determined due to the complexity of the reaction and the rates at 440°C were correlated with propylene and oxygen to yield the highest order of oxygen possible (if the oxygen order is greater than 0.64 the propylene order

must be greater than one) in order that the rates will decrease with decreasing oxygen concentration as realized experimentally.

The product time curves obtained on the basis of the original model were obtained by integrating the above rate expressions with respect to time using the Runge-Kutta method. The calculations were done on the 7090 IBM digital computer and the program used is given in the appendix.

The concentrations of oxygen, Co, and propylene, Cp, were computed from a mass balance, assuming the following reactions for the formation of the various products

1. $2C_3H_6 + \frac{1}{2}O_2 \rightarrow C_6H_{10} + H_2O$ 130
2. $2C_3H_6 + 1\frac{1}{2}O_2 \rightarrow C_6H_6 + 3H_2O$ 131
3. $C_3H_6 + O_2 \rightarrow C_6H_4O + H_2O$ 132
4. $C_3H_6 + 4\frac{1}{2}O_2 \rightarrow 3CO_2 + 3H_2O$ 133

The propylene and oxygen concentrations at any time were calculated then as:

$$Cp = B-2C_H-2C_{Bz}-C_A-1/3C_{co_2} \quad ....134$$

$$Co = A-\frac{1}{2}C_H-1\frac{1}{2}C_{Bz}-C_A-1\frac{1}{2}C_{co^2} \quad ....135$$

where A and B were the initial concentrations of oxygen and propylene respectively.

The results of the integration for the production of the major products are shown in Figures 85 to 88 for the two feed compositions experimentally studied at the longer contact times (Results section 6C). The computed results for acrolein exhibit the same trend of response to changes of concentration as the experimental results, but the rate of

KEY TO FIGURES 85 to 95

	Concentrations moles/litre x 10^{-3}	
	Oxygen	Propylene
M1, E1	8.9	8.9
M2, E2	4.95	9.9

M denotes model calculations

E denotes experimental data

FIGURE 85

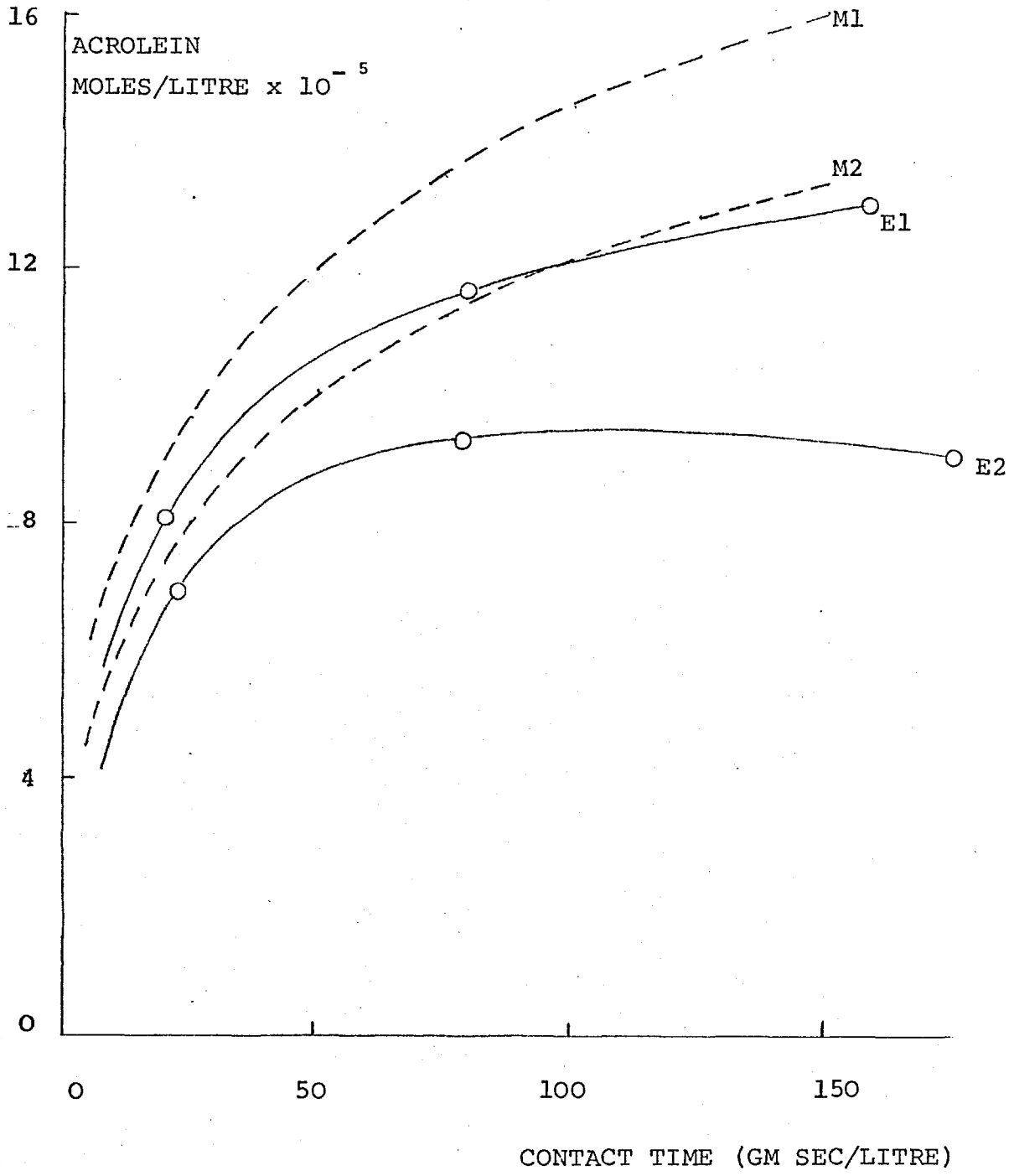

The original model: the production of acrolein at 440°C

FIGURE 86

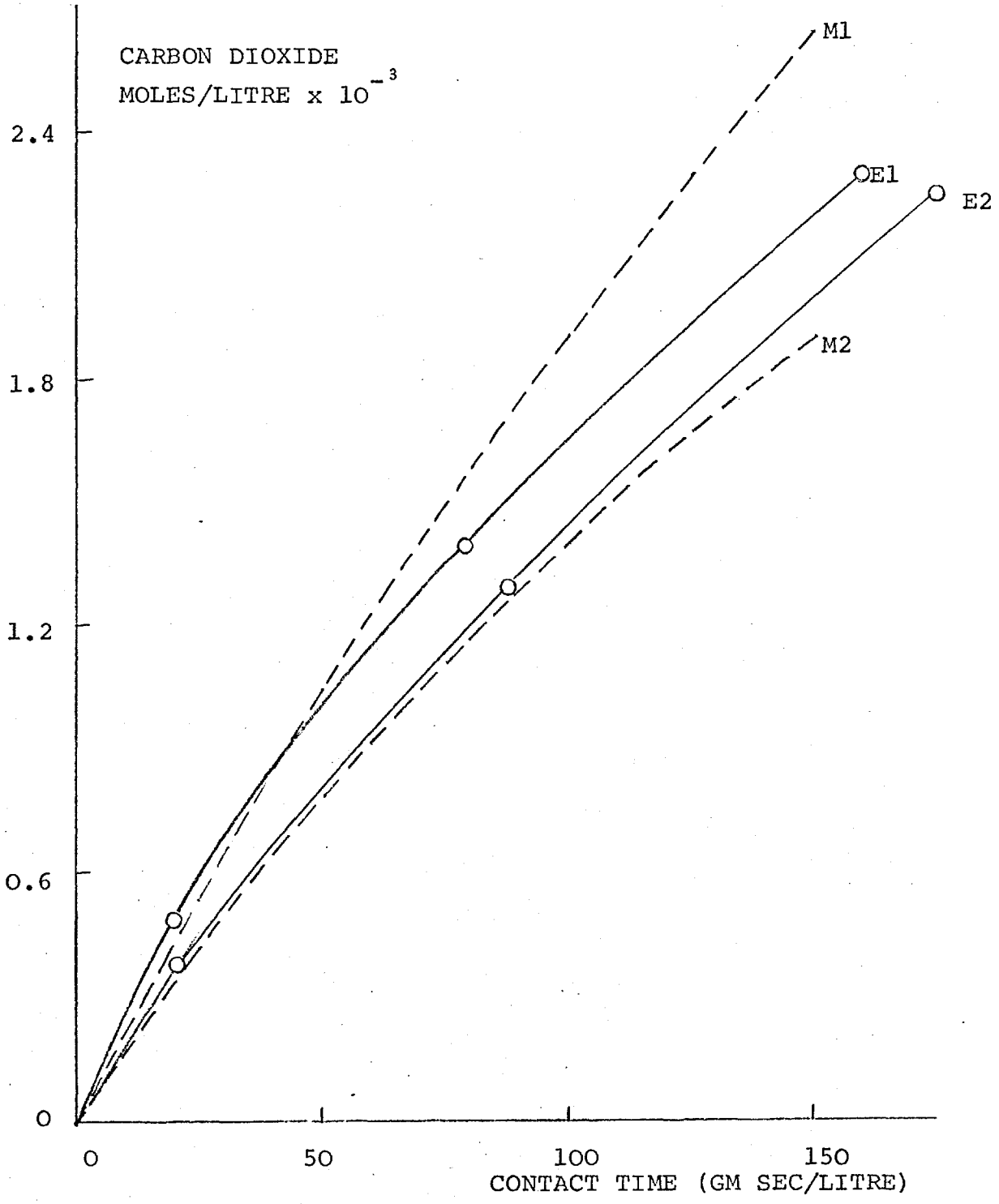

The original model: the production of carbon dioxide at 440°C.

See Key, page 311.

FIGURE 87

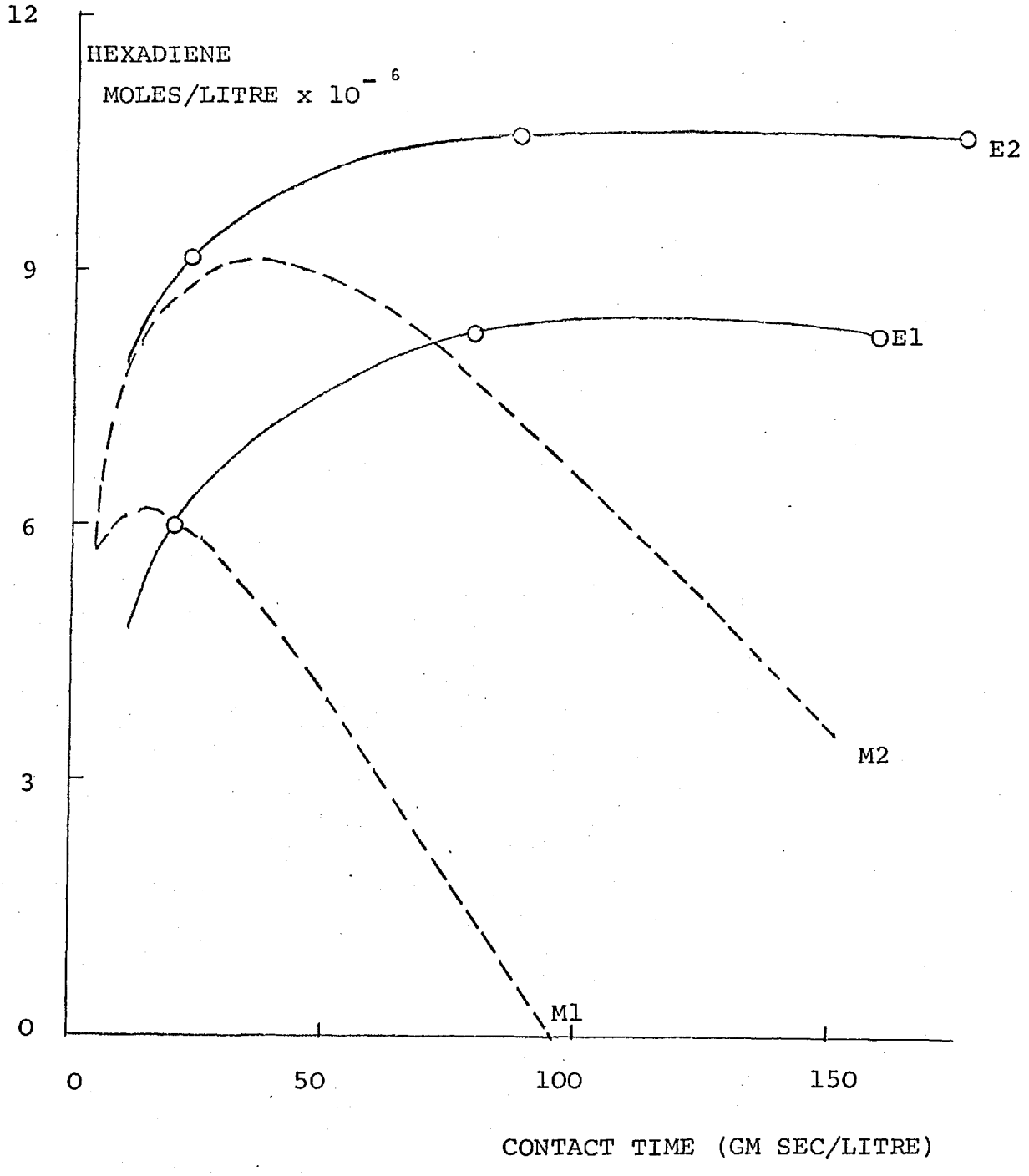

The original model: the production of hexadiene at 440°C.

See Key, page 311.

FIGURE 88

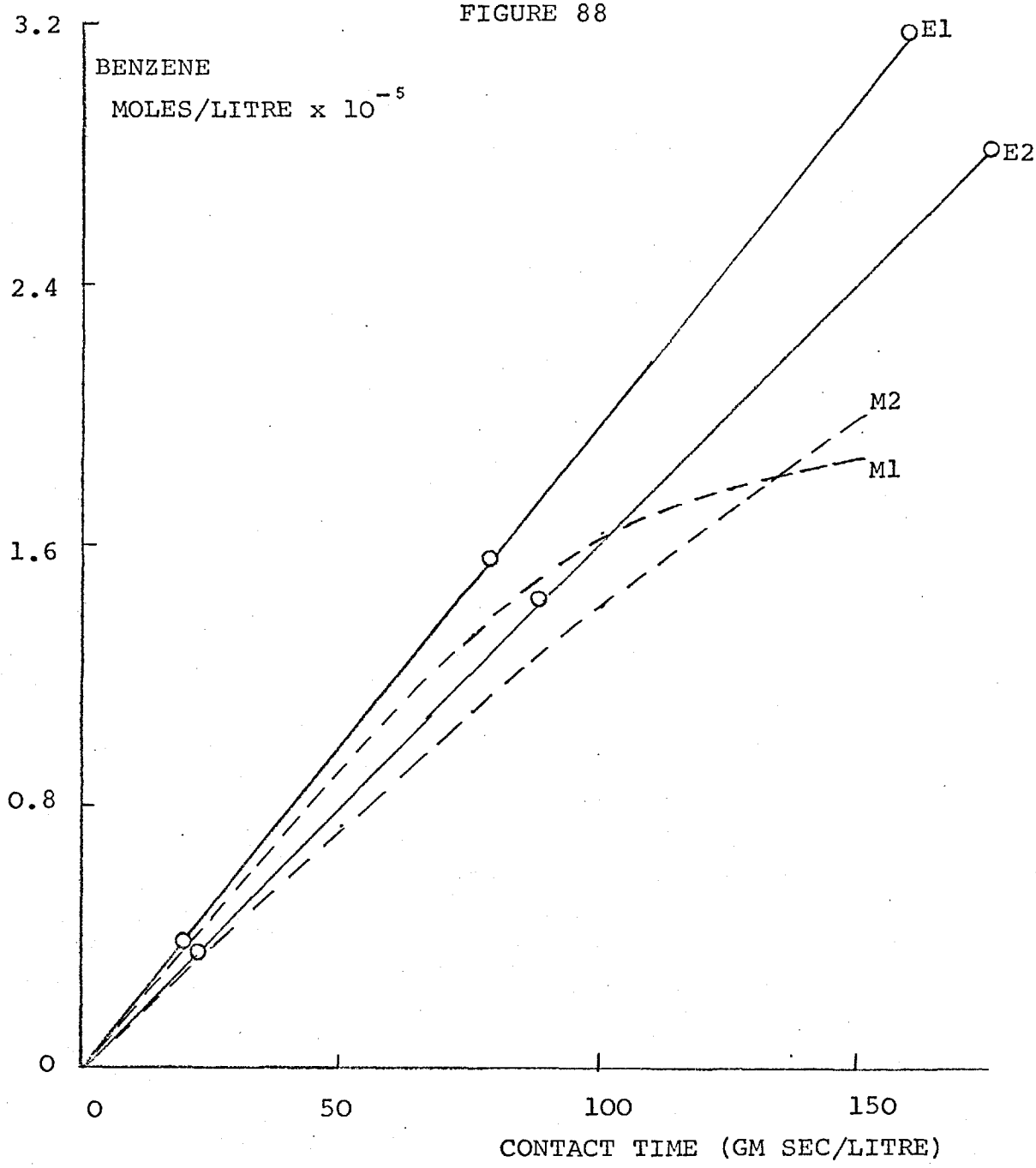

The original model: the production of benzene at 440°C.

See Key, page 311.

production of acrolein does not decrease as fast with time as the experimental data (Figure 85). As a result, the computed values are some 25 to 40% higher at a contact time of 150 gm sec/litre.

It can, however, clearly be seen that the reaction network is approximately correct. Thus, for example, the importance of including inhibition terms in the rate expressions can be seen in the case of acrolein. If the yield is calculated only on the basis of the initial rate expression, the yield at a contact time of 75 gm sec/litre is found to be 3500% higher than the experimental (Figure 89) while the inclusion of the inhibition terms reduces the error to only ca 17%.

The model provides a reasonable fit for the yield of carbon dioxide (Figure 86) except for the one condition at high contact times. The fact that the experimental rate decreases faster with time than the model at this set of conditions is difficult to explain on a chemical basis. It can not be due to a decrease in the oxygen concentration, as the rate at the lower oxygen concentration (E2) does not decrease as fast. The propylene concentration is effectively constant and the only reasonable explanation is that the production of carbon dioxide is not represented accurately by the assumed rate correlation.

The original model gives the worst agreement in the prediction of the hexadiene yield. The model does not give a fast enough rate of production of hexadiene to reproduce the production of benzene and the predicted fall off of the product

FIGURE 89

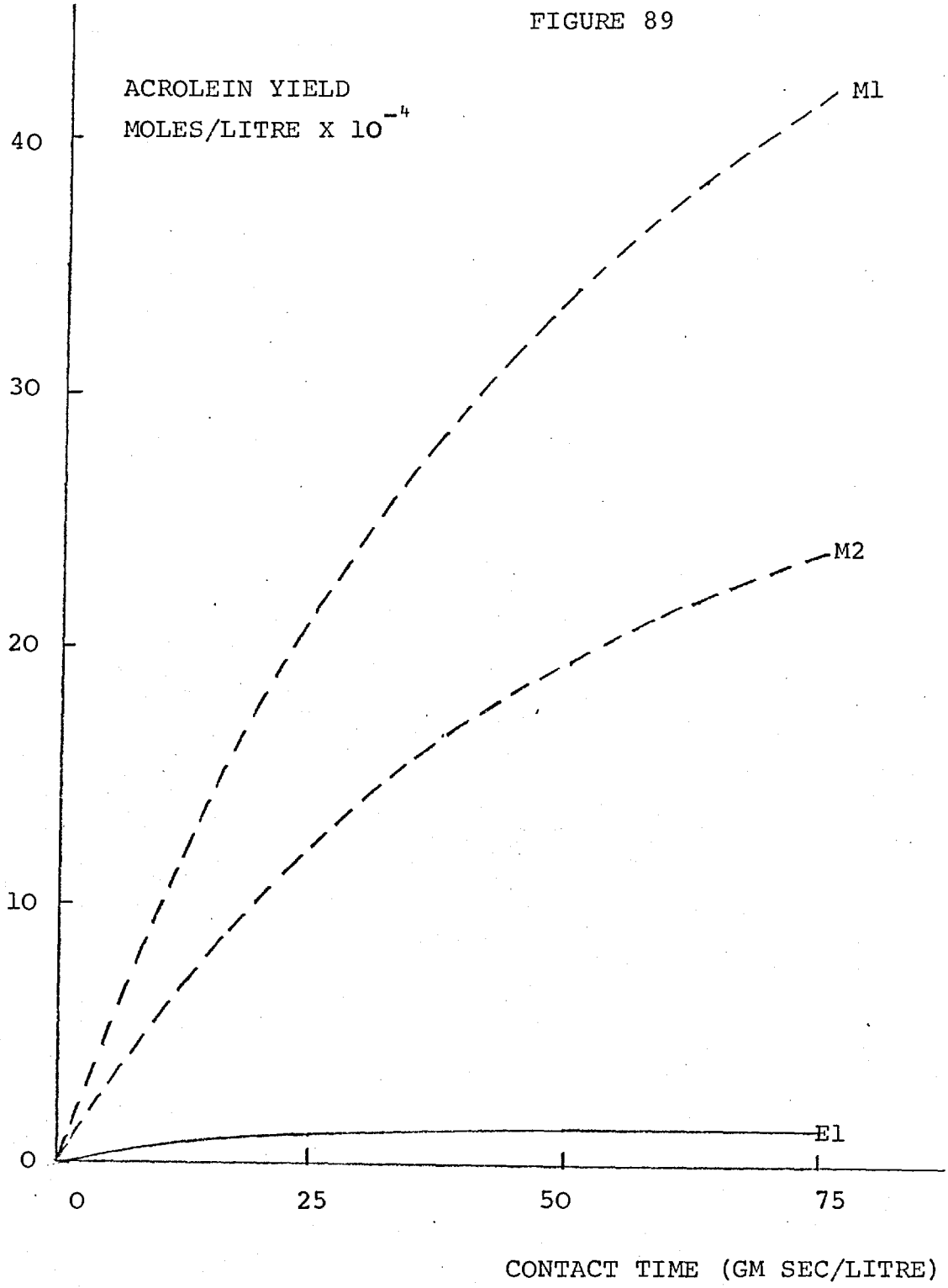

The comparison of the calculated yield of acrolein assuming no product inhibition with the experimental yield at 440°C.

See Key, page 311.

with time is much worse than the experimental value. The first effect could be caused if the inhibition factors used in the calculation were too large or if the benzene could come, possibly only in apparent kinetic terms, from another source. Although the model does not fit the experimental data, it does predict the experimental observation that the yield of hexadiene for the lower oxygen concentration is higher; this observation is contrary to that which would be expected from the initial rate expression.

The predicted benzene yield could not be expected to agree with experiment as it depends on the concentration of hexadiene. However the predicted initial rate, where the predicted hexadiene yield is reasonably good, was in reasonable agreement with experimental results.

It is clear that the model gives a good first approximation to the inhibition effect. However, since the inhibition is strong and depends mainly on the acrolein concentration, the fit of the acrolein yield must be very good in order that the model may provide reasonable agreement for the other products.

5C. Further development of a model for the reaction

It is evident that in order to obtain a better fit for acrolein, the predicted rate of appearance of the product in the gas phase must be decreased more rapidly with increasing time. This can be accomplished by decreasing

the rate of production through assuming stronger inhibition effects or by assuming that acrolein overoxidizes to further products and most probably to carbon dioxide. Stronger inhibition would result in a reduced rate of production of hexadiene, while overoxidation would decrease the acrolein concentration and hence the strength of the inhibition thus increasing the calculated yield of hexadiene.

However, before the acrolein prediction can be adjusted by assuming overoxidation, a good representation of the carbon dioxide yield must be obtained. The model (Figure 86) gave a good fit for only one condition but it would be difficult to adjust the model without knowing what reaction paths may be involved in the production of carbon dioxide. Consequently it is best if an artifical rate which fits the curvature of the experimental data is used:

$$r \text{ carbon dioxide} = 2.0 \times 10^{-3} \text{ Co} \qquad \ldots.136$$

It could be suggested that all the carbon dioxide results from overoxidation of acrolein and the yield-contact time plot calculated on this basis is shown in Figure 90. The concentration of acrolein initially increases quickly but then decreases to a constant value at which the rate of acrolein production equals the rate of overoxidation to carbon dioxide. As this value is considerably lower than the experimental yield, it is evident that the assumption is unjustified.

It is possible to estimate the amount of carbon dioxide produced from acrolein, by calculating the yield of acrolein with respect to time for different percentages

FIGURE 90

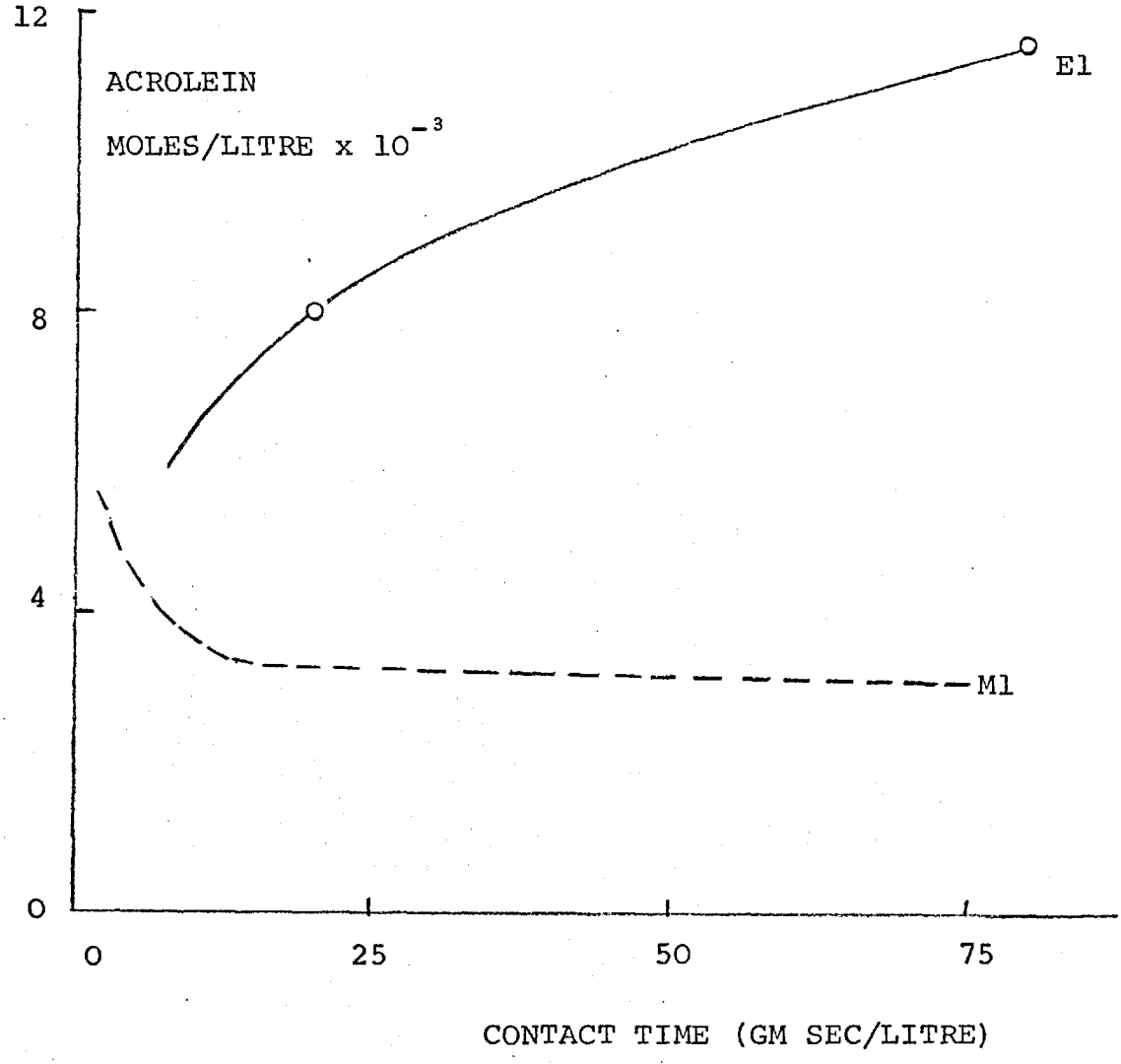

The comparison with experimental yield of the yield calculated by assuming the carbon dioxide at 440°C results from overoxidation of acrolein.

See Key, page 311.

(0 to 100%) of overoxidation of acrolein. The values which yield the best agreement with experimental results (Figure 91) were 9% at a propylene and oxygen concentration of 8.9×10^{-3} moles/litre and 12% at concentrations of 9.9×10^{-3} moles/litre propylene and 4.95×10^{-3} moles/litre oxygen.

Adjusting the acrolein yield in the original model led to decreased inhibition and thereby increased rate of production of hexadiene. However, the resulting rate of production was still not sufficient to account for the production of benzene. The model was then adjusted so that the hexadiene was not overoxidized in order to determine, even under these conditions, whether the calculated rate of production was capable of reproducing the experimental yields. The results, shown in Figure 92, show that this is possible but it is apparent that hexadiene was overoxidized to some extent. The degree of overoxidation was varied from 0 to 100% to determine the best fit, but only an approximate fit could be obtained by assuming a fixed degree of oxidation. The calculated yield at low contact times was higher than the experimental yield indicating that the level of overreaction assumed was too low. However, the calculated yield passed through a maximum crossing the experimental curve (overreaction too high at longer contact times).

It is apparent that the degree of overoxidation of hexadiene must vary with contact time, presumably as a result of the presence of varying amounts on the surface. The effect of varying the rates of overoxidation were

FIGURE 91

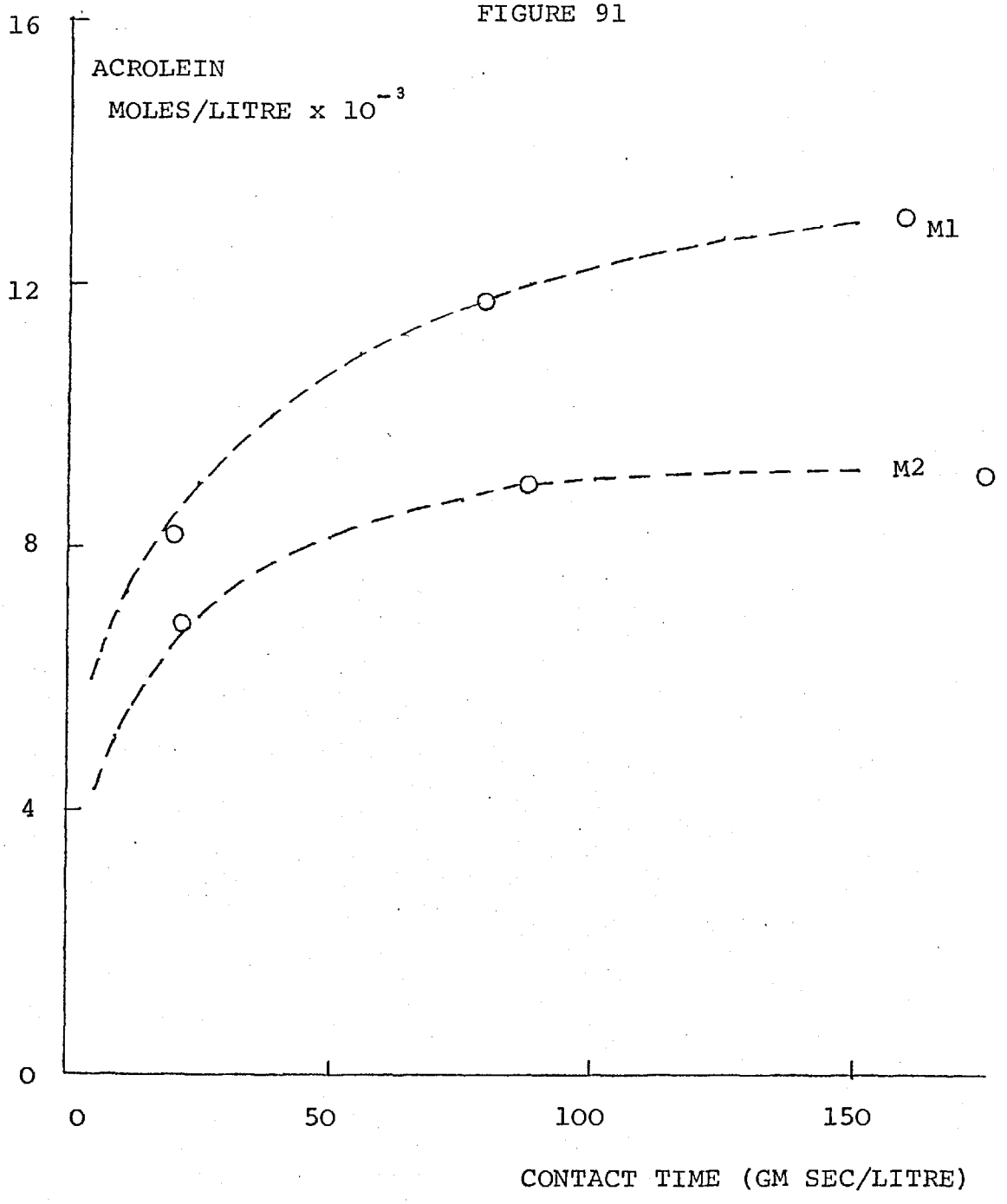

The "best fit" model for the production of acrolein assuming partial overoxidation to carbon dioxide at 440°C.

See Key, page 311.

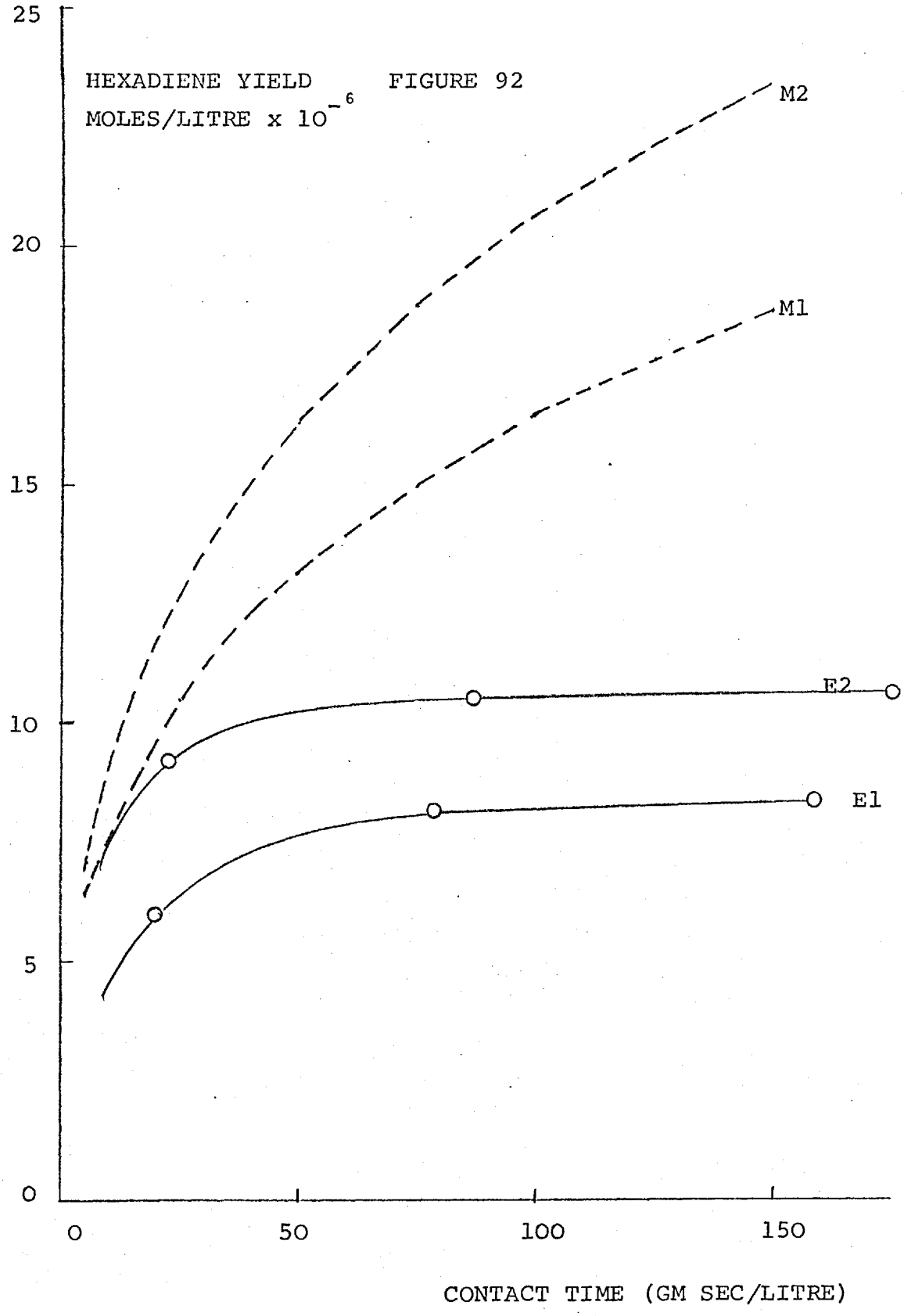

FIGURE 92

The production of hexadiene at 440°C assuming no overoxidation.

See Key, page 311.

examined and the resulting best fits to the experiment data are shown in Figure 93. The variations of the degree of overoxidation (c) which are associated with these calculations are shown in Figure 94.

With a good hexadiene prediction, the calculated yield of benzene gave an excellent fit (Figure 95) if the rate constant was increased by approximately 10%.

5D. Interpretation

The original model did not fit the experimental data to a satisfactory extent and the kinetic scheme had to be modified into order to obtain the "best fit" model. It is interesting to consider these kinetic changes in light of the proposed mechanism.

In the case of acrolein, it was shown that the original model accounted reasonably well for the effect of inhibition, but did not allow for the overoxidation of acrolein. It seemed possible that the overoxidation of acrolein could account for all the production of carbon dioxide formation, but calculations show that only 9-12% of the carbon dioxide resulted from the acrolein.

It seems possible that this finding is, at least in part, an anomaly arising out of the kinetic relationships. On other grounds, it would be expected that the overoxidation should be more important (123), even though this is not apparent from the kinetic results. The anomaly arises in that if propylene reacts on the surface to form acrolein this can

FIGURE 93

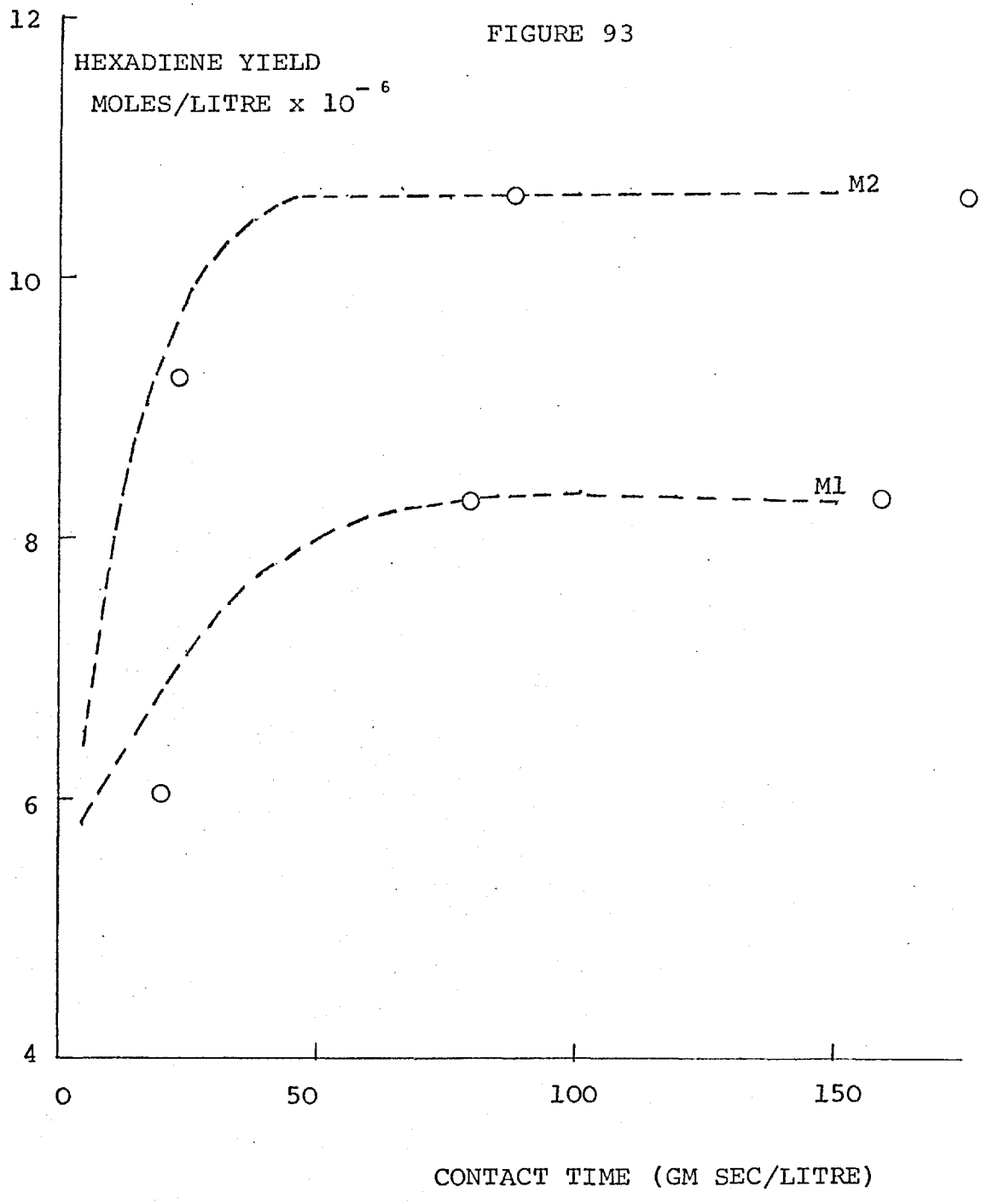

The "best fit" model for the production of hexadiene at 440°C assuming variable partial overoxidation (c) as shown in Figure 94.

See Key, page 311.

FIGURE 94

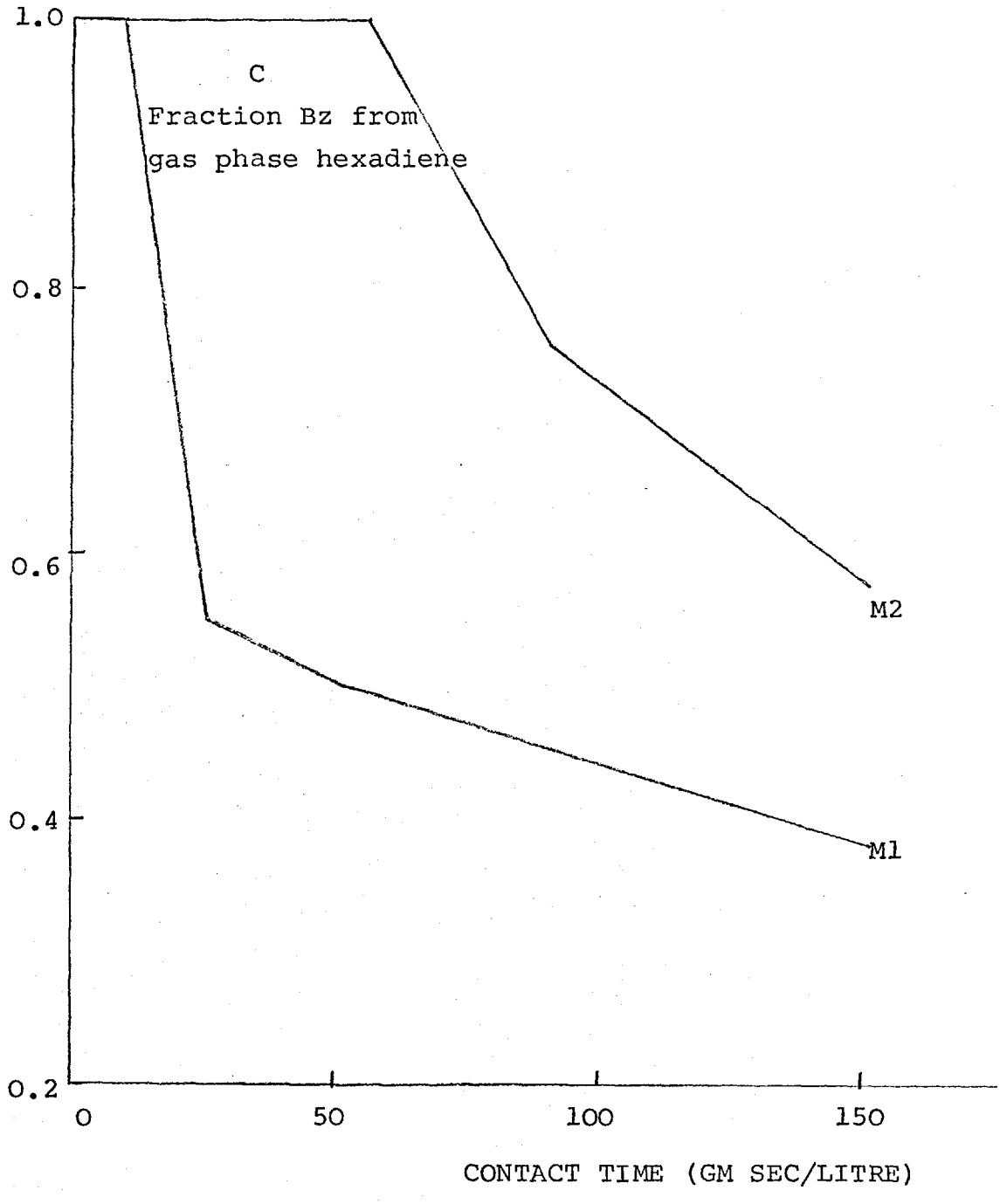

The variation of the degree of partial overoxidation of hexadiene to benzene resulting in the "best fit" of hexadiene yield.

See Key, page 311.

FIGURE 95

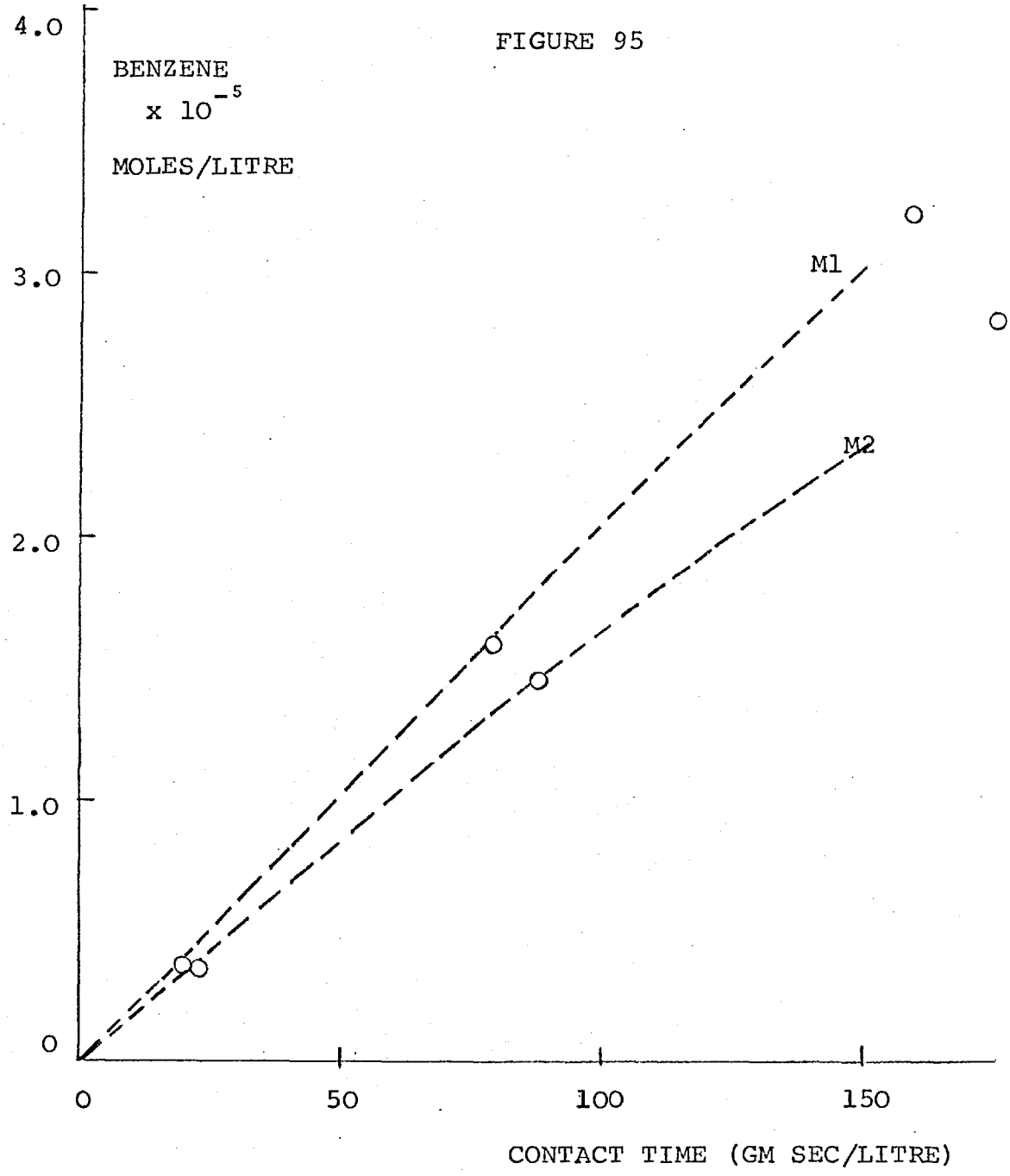

The "best fit" model for the production of benzene at 440°C.

See Key, page 311.

only be analytically determined if it is desorbed. Under normal circumstances acrolein would have to be re-adsorbed to react further to carbon dioxide, but if acrolein is not readily desorbed and can react to carbon dioxide before desorption, then it will appear that the formation of carbon dioxide occurs directly from propylene.

Consequently the kinetic scheme would appear as a consecutive concurrent reaction pattern:

$$\begin{array}{ccccc} & \overset{k_1}{} & & \overset{k_2}{} & \\ C_3H_6 & \rightarrow & C_3H_4O & \rightarrow & CO_2 \\ & \downarrow k_3 & & & \\ & CO_2 & & & \end{array} \qquad \ldots.137$$

This does not, of course, infer that no carbon dioxide can come directly from propylene, but it does show that the amounts apparently produced directly are too large.

For acrolein, it has been experimentally shown that the adsorption equilibrium constant is large (K_A = 5.25×10^5 litre/mole); the possibility of reaction to carbon dioxide before desorption would then be very high.

This receives some support by considering the elementary reactions for a reaction system of A + M → B and B + M → C. If the reactions are first order with respect to A and B and zero order in M, then the consecutive concurrent reaction scheme can be analytically confirmed when B tends to remain on the surface (131, 132). For partial orders in A, B and M the analytical solution is too complex and curve fitting by computer models is necessary to determine the extent of kinetic bypass.

The apparent concurrent reaction path can be suppressed by higher temperatures, a less active catalyst and a lower concentration of oxygen on the catalyst (131). The effect of oxygen concentration was confirmed by the model which yielded a higher k_2/k_3 ratio (0.14 to 0.09) for the lower oxygen concentration.

The results of the original model indicated that kinetically the production of benzene did not result from overoxidation of hexadiene. The modified model showed that the benzene initially results from the overoxidation of hexadiene, but as contact time increases the relative amount of benzene resulting from hexadiene decreases and a direct route from propylene apparently becomes more important.

Thus the kinetic scheme appears to be similar to the acrolein scheme with the final product apparently produced both direct and through an intermediate:

$$\begin{array}{ccccc} \text{propylene} & \rightarrow & \text{hexadiene} & \rightarrow & \text{benzene} \\ \downarrow & & & & \\ \text{benzene} & & & & \end{array} \qquad \ldots.138$$

As in the acrolein case, the chemical and mechanistic observations argue strongly for a consecutive route and the explanation of this apparent anomaly is similar to the acrolein case.

Initially any hexadiene produced is capable of desorbing and readsorbing quickly and the benzene kinetically appeared to be correlated with the gas phase concentration of hexadiene. However, as the contact time increases the surface concentration of acrolein increases inhibiting all reactions

which depend on the concentration of free sites. The rate of adsorption of hexadiene is strongly affected because of its low concentration in the gas phase and if a free space is available, propylene and acrolein can compete more strongly than the hexadiene. Thus the amount of production of benzene resulting from reaction of readsorbed hexadiene will decrease, but the amount of benzene produced from adsorbed hexadiene increases. As a result the direct reaction from propylene apparently will become more important.

5E. Summary

The original model developed from chemical and mechanistic arguments accounted reasonably well for the inhibition of the initial rates but the representation of the overoxidation of the initial products was unsatisfactory. A "best fit" model was developed by assuming a partial degree of overoxidation, fixed in the case of acrolein but variable for hexadiene. The interpretation of this "best fit" model leads to the following conclusions:

a) that the apparent direct oxidation of propylene to carbon dioxide results from a large proportion of the acrolein molecules produced reacting before being desorbed

b) that the variation of the importance of the apparent direct path to benzene from propylene is due to the increasing inhibition of the rate of readsorption of hexadiene by increasing acrolein concentration on the surface

c) that the selectivity of the initial reaction of propylene is unaffected by inhibition

d) that at high temperatures the selectivity to hexadiene and benzene will increase as the production of carbon dioxide which probably originates mainly via acrolein should be less favoured.

6. Conclusions

The main findings arising from the present studies may be summarised:

1) A logical sequence for catalyst design has been developed and applied to the production of benzene from propylene via an oxidative route. Using a postulated reaction mechanism, it has been possible to suggest that some oxides could promote an oxidative dimerization and an oxidative cyclization reaction.

2) Preliminary testing showed that although many of these solids were not useful in the context of the desired reaction, it was possible to identify some potential catalysts.

3) Thallic oxide was found to be a selective and active catalyst for the dimerization of propylene to hexadiene although tending to deactivate. A reaction mechanism proposed, involving the reaction of two propylene over one thallic ion via allylic intermediates, was shown to explain the experimental observations. The highest yields of hexadiene were obtained at low oxygen concentrations and high temperatures but both conditions increased sharply

the rate of thermal deactivation.

4) The oxidative dehydrocyclization of hexene to benzene over bismuth molybdate, first reported by Adams, has been observed. A mechanism for dehydrocyclization was proposed involving an allylic intermediate.

5) Pure indium oxide was found not only to catalyse the dimerization reaction but also to catalyse cyclization resulting in the production of benzene from propylene in a single step. Optimal yields were obtained at low oxygen and high propylene concentrations, at high temperature and at short contact times.

6) The catalyst was thermally stable, although prone to overheat. A supported indium oxide catalyst was found to be satisfactory. The reaction at high temperatures was found to be complicated by homogeneous effects. Detailed studies of the reaction mechanism and kinetics have been completed at 440^{o}C, where these effects were less important.

7) The only initial products that could be detected over this catalyst were 1,5 hexadiene and acrolein. The kinetics of the production of hexadiene were fractional order in both propylene and oxygen while acrolein depended on the concentration of propylene to the same extent, but was first order in oxygen.

8) The proposed mechanism for hexadiene formation involves the simultaneous formation of two allyls from two π adsorbed propylene molecules, which then interact to form

hexadiene. The slow step appears to be the abstraction of the hydrogen by oxygen ions to form the allylic intermediates. This step is energetically unfavourable resulting in a high activation energy for the reaction. The selectivity of the reaction appears to be related to the requirement of two electrons simultaneously by indium 3+. The propylene and the oxygen compete for different sites, the propylene apparently adsorbing on indium 3+ and the oxygen on indium 1+ (where it reoxidizes the ion to indium 3+).

9) The π adsorbed propylene can also react with a gas phase or a weakly adsorbed oxygen molecule to produce acrolein. The mechanism proposed appears to be involve hydroperoxide species as an intermediate.

10) The kinetics of the production of hexadiene were shown to obey the Langmuir-Hinshelwood expression predicted from the mechanism. The kinetics of the formation of acrolein do not obey such an expression predicted directly from the mechanism, but depend on the propylene surface coverage to the second order. This has been explained by the assumption that two propylene molecules must be adsorbed on the indium centre before acrolein formation can take place.

11) As the contact time is increased, two secondary reactions become important: the over-reaction of hexadiene to benzene and the production of carbon dioxide.

12) Inhibition of the initial reactions by the products hexadiene and acrolein was very important, although benzene did not interfere with the reaction. The Langmuir-Hinshelwood expressions for the initial reactions are still valid if terms are included for associatively adsorbed hexadiene

and acrolein. Values of 65,000 and 525,000 litre/mole have been calculated for the adsorption equilibrium coefficients of hexadiene and acrolein respectively and the strength of the inhibition can be noted by comparison with the adsorption equilibrium coefficients of propylene and oxygen (620 and 560 litre/mole respectively).

13) A mechanism was proposed for the formation of benzene from hexadiene in which an equilibrium between monodentate and bidentate adsorbed hexadiene occurs. The less favoured bidentate form then reacts similarly to two propylene molecules, undergoing a cyclization reaction to 1,3 cyclohexadiene. This quickly dehydrogenates to benzene over indium 3+. The close similarity between the cyclization and the dimerization steps results in similar orders with respect to oxygen and similar activation energies for the two cases.

14) The carbon dioxide appears to originate from more than one source.

15) The reaction network could be represented by a mathematical model based on the Langmuir-Hinshelwood expressions developed from the reaction scheme. The model did not give a completely satisfactory fit to the experimental results, but accounted reasonably well for the affect of inhibition. A "best fit" model was developed by assuming that the amount of overoxidation of the initial products could vary. The fit of the model was good if it was assumed

that the inhibition of acrolein caused both hexadiene and acrolein molecules to react to benzene and carbon dioxide respectively before desorption. This result could well be consistent with the experimental results.

16) The design sequence has reached the stage where the reaction mechanisms are well understood, the optimum conditions can be approximated, the kinetics are known at 440^{o}C, the yields and selectivities can be approximated and the desired physical properties of the catalyst are known. The reaction should now be examined at higher temperatures, where inhibition by products is expected to be less important, but homogeneous effects may complicate the system. Extension of the present mathematical model to account for these effects should lead to the recognition of optimal operating conditions, and make possible an economic evaluation of the potential of the process on a commerical scale.

APPENDIX

```
C       INTEGRATION OF KINETIC  EQUATIONS.
C       DEFINITIONS.
C       ALL CINCENTRATIONS ARE MEASURE IN MOLES/LITRE
C       THE CONTACT TIME X I S MEASURED IN  GRAMS.SECONDS/LITRE
C       EQUATIONS ARE INTEGRATED USING THE RKINT SUBROUTINE.
C       Y(1)= HEXADIENE.
C       Y(2)= BENZENE.
C       Y(3)= ACROLEIN.
C       Y(4)= CARBON DIOXIDE.
C       O = OXYGEN CONCENTRATION
C       P = PROPYLENE CONCENTRATION
C       A = INITIAL OXYGEN CONCENTRATION
C       B = INITIAL PROPYLENE CONCENTRATION
C       OHC = SURFACE COVERAGE OF HYDROCARBON
C       OOX = SURFACE COVERAGE OF OXYGEN
        REAL Y,YG,YH,O,P
        DIMENSION Y(4),YG(4),YH(4),YD(4)
        DIMENSION RESULT(8,30)
        COMMON A,O,B,P
        N=4
        H=1.
        MX=2
        DO8 M=1,MX
        READ(5,3)A,B
        WRITE(6,2)A,B
        X=0.
        Y(1)=0.0
        Y(2)=0.0
        Y(3)=0.0
        Y(4)=0.0
        DO 4 I=1,N
      4 YD(I)=Y(I)
        DO5I=1,30
        DO6 J=1,5
        CALL RKINT(X,H,N,Y,YG,YH,YD)
      6 CONTINUE
        DO7 K=1,4
      7 RESULT(K,I)=Y(K)
        RESULT(5,I)=O
        RESULT(6,I)=P
        RESULT(7,I)=X
        RESULT(8,I)=OHC
      5 CONTINUE
        WRITE(6,100) RESULT
      8 CONTINUE
        STOP
      3 FORMAT(2F10.8)
      2 FORMAT(1H1,2F15.9)
    100 FORMAT(1HO,8E12.4)
        END
```

```
      SUBROUTINE YGRD(X,N,Y,YG)
      REAL Y(N),YG(N)
      COMMON A,O,B,P
      O=A-0.5*Y(1)-1.5*Y(2)-Y(3)-1.5*Y(4)
      P=B-2.0*Y(1)-2.0*Y(2)-Y(3)-Y(4)/3.0
      IF(O.LT.0.) O=0.
      IF(P.LT.0.) P=0.
      S = 620.0*P+65000.0*Y(1)+525000.0*Y(3)
      OHC=S/(1.0+S)
      OOX=23.6*O**0.5/(1.0+23.6*O**0.5)
      DO1 I=1,N
      IF(Y(I).LT.0.) Y(I)=0.
    1 CONTINUE
      YG(1)=0.0000342*(620.0*P*(1.0-OHC))**2.0*560.0*O*(1.0-OOX)**2.0
     X-0.0000029*Y(1)**0.08*O**0.37
      YG(2)=0.000CC29*Y(1)**0.08*O**0.37
      YG(3)=0.0176*(615.0*P*(1.0-OHC))**2.0*O
      YG(4)=0.0530*P*O**0.64
      RETURN
      END
```

```
**O**     RKINT COMPILED FROM DISK


**O**     EXECUTION
```

REFERENCES

1. Hydrocarbon Processing, 48, 11, 135 (1969).

2. British Patent 906, 215.

3. Button, E.C., Dietzler, A.J. and Noddings, C.R., Ind. Eng. Chem., 43, 2871 (1951).

4. American Petroleum Institute, Research Project 45, Sixteenth Annual Report (1954).

5. Dowden, D.A., Chem. Eng. Prog. Symposium Series, 63, no. 73, 90 (1967).

6. Thomson, S.J. and Webb, G., "Heterogeneous Catalysis" (Oliver & Boyd) page 9 (1962).

7. Lennard-Jones, J.E., Trans. Faraday Soc., 28, 333 (1962).

8. Eley, D.D., and Rossington, D.R., "Chemisorption", ed. by W.E. Garner, (Butterworths) page 152 (1957).

9. Langon, M.A.H. and Trapnell, B.M.W., Proc. Roy. Soc., A227, 387 (1955).

10. Bond, G.C. "Catalysis by Metals" (Academic Press) page 98 (1962).

11. Gundry, P.M. and Tompkins, F.C., Trans. Faraday Soc., 52, 1607 (1956).

12. Dowden, D.A., "Chemisorption", ed. by W.E. Garner, (Butterworths) page 3 (1958).

13. Fahrenfort, J., van Reijen, L.L. and Sachtler, W.M.H., "The Mechanism of Heterogeneous Catalysis" ed. by J.H. de Boer et al., (Elsevier) page 23 (1960).

14. Pauling, L., J. Am. Chem. Soc., 69, 542 (1947).

15. Reference 10, page 21.

16. Thomas, J.M. and Thomas, W.J., "Introduction to the Principles of Heterogeneous Catalysis" (Academic Press) page 308 (1967).

17. Reference 10, page 17.

18. Hayward, D.O. and Trapnell, B.M.W., "Chemisorption" (Butterworths) pages 7 and 226 (1964).

19. Stone, F.S., "Chemisorption", ed. W.E. Garner, (Butterworths) page 182 (1957).

20. Stone, F.S., "Chemistry of the Solid State", ed. W.E. Garner, (Butterworths) page 367 (1955).

21. Reference 18, page 261.

22. Garner, W.E., Gray, T.J. and Stone, F.S., Proc. Roy. Soc., A197, 294 (1949).

23. Kubokawa, Y. and Toyama, O., J. Phys. Chem. 60, 883 (1956).

24. Wolkenstein, T., Adv. in Catalysis, 12, 189 (1960).

25. Beeck, O., Disc. Faraday Soc., 8, 118 (1950).

26. Dowden, D.A., MacKenzie, N. and Trapnell, B.M.W., Proc. Roy. Soc., A237, 245 (1956).

27. Sherman, A. and Eyring, H., J. Am. Chem. Soc., 54, 2661 (1932).

28. Beeck, O., Smith, A.E. and Wheeler, A., Proc. Roy. Soc. A177, 62 (1940).

29. Reference 16, page 307.

30. ibid, page 308.

31. Balandin, A.A., Z. Phys. Chem., 132, 289 (1929).

32. Batist, Ph.A., der Kinderen, A.H.W.M., Leeuwenburgh, Y., Metz, F.A.M.G., and Schuit, G.C.A., J. Cat., 12, 45 (1968).

33. Wells, A.F., "Structural Inorganic Chemistry" (Clarendon Press) (1962).

34. Germain, J.E., "Catalytic Conversion of Hydrocarbons" (Academic Press) page 7, (1969).

35. Morozova, I.D. and Popovsky, V.V., Kinetics and Catalysis, 3, 489 (1962).

36. Boreskov, G.K., Kinetics and Catalysis, 8, 878 (1967).

37. Sazonova, I.S. and Keier, N.P., Kinetics and Catalysis 6, 448 (1965).

38. Keier, N.P., Mikhailova, I.L. and Sazonova, I.S., Kinetics and Catalysis, 5, 1086 (1964).

39. Balandin, A.A., Klabunovskii, E.I. and Tolstopyatova, A.A., Preprint Paper 41, 4th Inter. Cong. on Catalysis, Moscow (1968).

40. Makishima, S., Joneda, J. and Saito, J., Actes du II congrés Intern de Catalyse, 1, 617 (Technip), Paris (1961).

41. Sachtler, W. and Fahrenfort, I., ibid, 831, (1961).

42. Temkin, M.I., Zh. Fiz. Khimii., 31, 3 (1957).

43. Roiter, V.A. and Golodets, G.I., Inter. Chem. Eng., 4, 632 (1964).

44. Tanaka, K. and Tamaru, K., J. Cat., 2, 366 (1963).

45. Boreskov, G.K., Popovsky, V.V. and Sazonov, V.A., Preprint Paper 33, 4th Inter. Cong. on Cat., Moscow (1968).

46. Boreskov, G.K., Kinetics and Catalysis, 8, 878 (1967).

47. Boreskov, G.K., Disc. Farad. Soc., 41, 263 (1966).

48. Hinshelwood, C.N., "Kinetics of Chemical Change" (Oxford University Press) (1941).

49. Langmuir, I., J. Am. Chem. Soc., 38, 2221 (1916).

50. Eley, D.D. and Rideal, E.K., Proc. Roy. Soc., A178, 429 (1941).

51. Laidler, K.J., "Catalysis" ed. P.H. Emmett, (Reinhold Publ. Co.) 1, page 75 (1954).

52. Reference 16, pages 458 and 459.

53. Walas, M.W., "Reaction Kinetics for Chemical Engineers" (Mcgraw-Hill) page 160 (1959).

54. Hougen, O.A. and Watson, K.M., "Chemical Process Principles", (Wiley) part 3 (1947).

55. Corrigan, T.E., Chem. Eng., Refreshers Series, part 5 and 6, (Nov. 1954-July 1955).

56. Feigelman, S. and O"Connor, C.B., Hydrocarbon Processing, 45, May 140 (1966).
Weiss, A.H., Hydrocarbon Processing 48, 10, 125 (1969).

57. Smith, J.M., "Chemical Engineering Kinetics" (Mcgraw-Hill) pages 234-240 (1956).

58. Hougen, O.A. and Wilkie, C.R., Trans. Am. Inst. Chem. Engrs., 45, 445 (1945).

59. Cited from Levenspiel, O., "Chemical Reaction Engineering" (Wiley) pages 350-352 (1965).

60. Satterfield, C.N. and Sherwood, T.K., "The Role of Diffusion in Catalysis" (Addison-Wesley) pages 12-20 (1963).

60a. Reference 16, page 213.

61. Gillilard, E.R., Baddour, R.F., and Russel, J.L., A.I.Ch.E. J., 4, 90 (1958).

62. Kammermeyer, K.A. and Rutz, Chem. Eng. Prog., Symposium Series, 55, No. 24, 163 (1959).

63. Thiele, E.W., Ind. Eng. Chem. 31, 916 (1939).

64. Wheeler, A. "Catalysis" P.H. Emmett ed., (Reinhold) 2 (1955).

65. Weisz, P.B. and Prater, C.D., Adv. in Catalysis, 6, 143 (1954).

66. Reference 60, pages 56-67.

67. Wheeler, A., Adv. in Catalysis, 3, 250 (1950).

68. de Acetis, J. and Thodos, G., Ind. Eng. Chem., 52, 1003 (1960).

69. Tinkler, J.D. and Metzner, A.B., Ind. Eng. Chem., 53, 663 (1961).

70. Weisz, P.B. and Hicks, J.S., Chem. Eng. Sci., 17, 265 (1962).

71. Carberry, J.J., A.I.Ch.E. J., 7, 350 (1961).

72. Aris, R., Chem. Eng. Sci., 6, 262 (1957).

73. Reference 59, page 441.

74. Reference 16, page 235.

75. Kilpatrick, J.E., Prosen, E.J., Pitzer, K.S. and Rossini, F.D., J. Research Natl. Bur. Standards, 36, 559 (1946).

76. Oblad, A.G., Mills, G.A. and Heinemann, H., "Catalysis" ed. P.H. Emmett, VI, p. 341 (Reinhold) 6, 341 (1958).

77. Karlinszki, L., Zoellner, G. and Matolcsy-Szabo, G., Acta Chim. Hung. 40, 445 (1964). Chem. Abstr, 62, 1552 (1965).

78. Shaw, A.W., Bittner, C.W., Bush, W.V. and Hobzman, G., J. Org. Chem., 30, 3286 (1965).

79. U.S. Patent 3, 201, 493: Chem. Abstr. 63, 13,072 (1965).

80. Ziegler, K., Angew. Chem. 72, 829 (1952).

81. Bell, E.R., Vaughan, W.E. and Rust, F.F., J. Am. Chem. Soc., 79, 3997 (1957).

82. Feighan, J.A. and Davis, B.H., J. Cat. 4, 594 (1965).

83. Hettinger, W.P., Keith, C.D., Gring, J.L. and Teter, J.W., Ind. Eng. Chem., 47, 719 (1955).

84. Steiner, H., "Catalysis", ed. by Emmett, P.H., (Reinhold) 4, 558 (1956).

85. Chambers, R.P. and Boudart, M., J.Cat. 5, 517 (1966).

86. Jouy, M. and Balaceanu, J.C., Actes du II Congrès Inter. de Catalyse (Paris) 645 (1960).

87. Adams, C.R., Proceeding of the Third Intern. Congress on Catalysis, (Amsterdam) 240 (1964).

88. Skarchenko, V.K., Inter. Chem. Eng., 9, 1 (1969).

89. Sampson, R.J. and Shooter, D., "Oxidation and Combustion Reviews" Vol. 1 (Elsevier Publ. Co.) 1, 255 (1965).

90. Voge, H.H. and Adams, C.R., Adv. in Catalysis, 17, 151 (1967).

91. Voge, H.H., Wagner, C.D. and Stevenson, D.P., J. Cat., 2, 58 (1963).

92. Adams, C.R. and Jenning, T.J., J. Cat. 2, 63 (1963).

93. Adams, C.R. and Jenning, T.J., J. Cat. 3, 549 (1964).

94. Adams, C.R., Voge, H.H., Morgan, C.Z. and Armstrong, W.E., J. Cat., 3, 379 (1964).

95. Schultz, R.G., Schuck, J.M. and Wildi, B.S., J. Cat., 6, 385 (1966).

96. Reference 6, page 18.

97. Private Communication, Dowden, D.A.

98. Herington, E.F.G. and Rideal, E.K., Proc. Roy. Soc., A184, 434, 447 (1945).

99. Enikeev, E. Kh., Isaev, O.V. and Margolis, L. Ya., Kinetics and Catalysis 1, 431 (1960).

100. Cotton, F.A. and Wilkinson, G., "Adv. Inorg. Chem." (Interscience) page 435 (1967).

101. McHenry, K.W., Bertolacini, R.J., Brennan, H. M., Wilson, J.L. and Seeling, H.S., Actes du II Inter. Cong. Cat. (Paris) page 2295 (1960).

102. British Patent 945,707.

103. British Patent 932,046.

104. Batist, P.A., der Kinderin, A.H.W.M., Leeuwenburgh, Y., Metz, F.A.M.G. and Schuit, G.C.A., J. Cat., 12, 45 (1968).

105. Japanese Patent 66-11971.

106. Handbook of Chemistry and Physics (Chemical Rubber Publ.) 47th Edition (1962).

107. Sidgwick, N.V., "The Chemical Elements and their Compounds" (Oxford University Press) 1, 467 (1950).

108. Gmelins Handbuck Der Anorganischen Chemie. System number 37, Indium (Verlag Chemie) page 100 (1936).

109. Littlewood, A.B., "Gas Chromatograpy" (Academic Press) page 302 (1962).

110. Kaiser, R., "Gas Phase Chromatograpy", translated by P.H. Scott, (Butterwosrths) 1, 112 (1963).

111. Kyryacos, G. and Boord, C.E., Analyt. Chem., 29, 787 (1957).

112. Reference 109, page 381.

113. Smith, R., Ohlson, R. and Larson, G., Acta. Chem. Scand., 17, 436 (1963).

114. Smith, R. and Ohlson, R., Acat. Chem. Scand., 16, 351 (1962).

115. Gregg, S.J. and Sing, K.S.W., "Adsorption, Surface Area and Porosity" (Academic Press) page 160 (1967).

116. Emmett, P.H. "Catalysis" (Reinhold) 1, 32 (1954).

117. Rubanik, M. Ya, Kholyavenko, K.M., Gershingorina, A.V., and Lazukin, V.I., Kinetics and Catalysis 5, 666 (1964).

118. Dutch Patent 66-04526.

119. Gabbay, D.S., Ph.D. thesis, University of London (1969).

120. Gmelins Handbuck Der Anorganischem Chemie, System number 36, Thallium (Verlag Chemie) (1936).

121. United States Patent 3,435,089.

122. Alkhazov, T.G., Belenky, M.S., Alekseyeva, R.I. and Azizbekov, M. 4th Inter. Cong. on Cat., Moscow, preprint paper no. 17 (1968).

123. Popova, N.I. and Latyshev, V.P. Dokl. Akad. Nauk., S.S.S.R., 147, 1382 (1962).

124. Godin, G.W., McCain, C.C. and Porter, E.A., 4th Inter. Congr. on Cat., Moscow, Preprint of paper 20 (1968).

125. Noller, C.R. "Chemistry of Organic Compounds" (Saunders) page 993 (1965).

126. Peacock, J.M., Sharp, M.J., Parker, A.J., Ashmore, P.G. and Hockey, J.A., J. Cat., 15, 379 (1969).

127. Sachtler, W.M.H. and de Boer, J.H., "Proc. 3rd Intern. Congr. Catalysis, Amsterdam" (North-Holland Publ.) 1, 252 (1965).

128. Margolis, L. Ya., Adv. in Catalysis, 14, 429 (1963).

129. McCain, C.C. and Godin, G.W., Nature 202, 692 (1964).

130. Adams, C.R., Ind. Eng. Chem., 61, 6, 31, (1969).

131. de Boer, J.H. and Van der Borg, R.J.A.M., Actes du II Congres Intern. de Catalyse, Paris (Technip) 1, 617 (1961).

132. Reference 16, page 324.